Beatrice Offshore Wind Farm

Year 2 Post-construction Ornithological Monitoring Report

Date:	25/07/2023
Tel:	0141 342 5404
Web:	www.macarthurgreen.com
Address:	93 South Woodside Road |Glasgow | G20 6NT

Document Quality Record

Version	Status	Person Responsible	Date
0.1	Draft	Dr Mark Trinder	19.09.2022
0.2	Reviewed	Prof Bob Furness	20.09.2022
0.3	Updated	Dr Mark Trinder	29.09.2022
1	Internal Approval	Dr Mark Trinder	29.09.2022
1.1	Updated following stakeholder review	Dr Mark Trinder	30.03.2023
1.2	Updated following stakeholder review	Dr Mark Trinder	23.05.2023
1.3	Final revisions following stakeholder review	Dr Mark Trinder	25.07.2023

CONTENTS

EXECUTIVE SUMMARY

The Beatrice Offshore Wind Farm has been fully operational since May 2019, shortly after which the first year of post-construction digital aerial surveys were conducted as a key component of the ornithological monitoring of the wind farm. These surveys were undertaken in an identical manner to pre-construction surveys flown in 2015, and in 2021 a second year of post-construction surveys were flown. This report focusses on the results of the most recent (2021) surveys, but also provides analysis and comparison with the results from previous years in order to highlight changes in the abundance and distribution of the seabirds recorded. The survey area is approximately 1,100km^2 and extends from the Caithness coast to the far side of the wind farm (plus a 4km buffer) and by 10km to the north-east and south-west along the coast.

The abundance and distributions of the seabird species of interest (gannet, kittiwake, guillemot, razorbill, puffin, great black-backed gull and herring gull) have been estimated using design-based and model-based (MRSea) methods, and within wind farm distributions have been analysed using a randomisation method developed for this monitoring programme.

There do not appear to have been any consistent trends in the overall abundance of these species in the survey area across the span of years (2015/2019/2021), with some species increasing across the period (guillemot, kittiwake and puffin), others peaking in the second year (razorbill and large gulls) while the gannet abundance was lowest in the second year. Similarly, the within wind farm abundances have shown no clear trends, with the exception of gannet for which there does appear to have been a consistent decline in abundance in the wind farm following construction.

Spatial modelling has been used to compare the distributions across the survey area between years. For gannet these results indicate avoidance of the wind farm. However, for the other species modelled (guillemot, razorbill, puffin and kittiwake), while there have been significant changes in their distributions between years, there is little to indicate these are responses to the wind farm, with varying areas of increase and decrease for each species located throughout the survey area.

Analysis was also conducted of the distribution of seabirds (guillemot, razorbill, puffin, kittiwake and herring gull) within the wind farm, comparing the observed bird densities around turbines with randomised alternative turbine locations, to determine if the observed bird locations are related to turbine locations. Seabird distributions can show considerable variation between years, which can confound between year comparisons, but a key strength of the method developed for this analysis is that it does not rely on between year comparisons, thereby avoiding such effects. The results of this analysis, which took rotor speed into account and were conducted independently on the data from both post-construction years (2019 and 2021), showed that these species did not avoid turbines, irrespective of the turbine operational status (however, confidence in this conclusion is lower for herring gulls as very few were recorded in the wind farm).

Overall, the only species which appears to have responded negatively to the wind farm is gannet, with reduced abundance in the vicinity of the wind farm. However, this species' ecology (large foraging range and wide range of prey species) means connected populations are unlikely to be affected by such avoidance behaviour. For the remaining species, which are qualifying features of the large seabird breeding colonies within the East Caithness Cliffs SPA, the results show that the wind farm is very unlikely to have had any detrimental effects on their populations.

1 INTRODUCTION

The Beatrice Offshore Wind Farm is located in the Moray Firth, at its closest 13.5 km from the Caithness coast (Figure 2-1). Construction of the offshore elements began in April 2017, the first turbine was installed and operational by July 2018 and the final turbine was installed on the 14th May 2019.

The potential ornithological impacts which were considered of greatest concern during the application process were collision risk to large gulls (great black-backed gull and herring gull) and displacement of foraging auks (guillemots, razorbills and puffins). All these species breed at colonies which comprise the East Caithness Cliffs SPA and some of the birds present at the Wind Farm during the breeding season are likely to be from this SPA population. Through discussion with the Moray Firth Regional Advisory Group Ornithology Subgroup (MFRAG-O), the potential for the above impacts to affect these breeding populations was identified as the focus of ornithological monitoring for the Wind Farm.

A survey area, approximately rectangular in shape aligned parallel to the Caithness coast, was defined and surveyed in 2015 to provide pre-construction data. The surveys follow transects extending from the Caithness coast to 4 km beyond the seaward edge of the Wind Farm site boundary which measure approximately 40 km from north-east to south-west (Figure 2-1).

In 2019, following installation of all turbines, the first post-construction survey was conducted. The results from the first year of monitoring were reported in MacArthur Green (2021). In 2021 a second year of post-construction monitoring surveys was undertaken. In both cases the same survey design and aerial survey contractor (HiDef) were used to ensure data comparability.

This report provides results from the 2021 surveys and comparisons with the results from both the pre-construction surveys (2015) and the year one post-construction surveys (2019). Thus, the purpose of this monitoring report was two-fold: a second year of comparisons with the pre-construction results and a comparison between the two years of post-construction monitoring. These pairwise comparisons allow consideration of whether changes in seabird distribution following wind farm construction are consistent.

All seabirds were recorded during the surveys, however the targets for monitoring (hereafter, focal species) agreed by MFRAG-O were great black-backed gull, herring gull, puffin, common guillemot, razorbill, kittiwake and gannet. Therefore, this report only discusses these species.

The primary aims of the aerial surveys as originally defined are:

- To collect seabird distribution data during the breeding season to enable comparisons of seabird abundance distributions before and after construction and estimate the magnitude (if any) of displacement resulting from avoidance of the Wind Farm (with a particular emphasis on puffin);
- Estimate the extent of connectivity between the Wind Farm and the East Caithness Cliffs SPA through analysis of flight directions; and
- Investigate the robustness of flight heights calculated from digital aerial data.

The aerial survey data are most suitable for considering spatial distributions and therefore most of the analyses and reporting presented here focus on this element of potential wind farm impacts.

Two independent analyses have been conducted. The first uses spatial models to compare the before (pre-construction) and after (post-construction) distributions using the MRSea R package (Scott-Hayward *et al.* 2013). With the two years of post-construction data now available, this has been extended to include a comparison of the distributions in the two post-construction periods (2019 and 2021), as well as a second pre- and post- comparison (2015 and 2021). Thus, the following spatial analyses of the whole survey area are presented:

- Pre-construction (2015) vs post-construction year 1 (2019; NB, these were also presented in MacArthur Green 2021)
- Pre-construction (2015) vs post-construction year 2 (2021)
- Post-construction year 1 (2019) vs post-construction year 2 (2021)

To simplify notation, the monitored years will be referred as pre, post-1 and post-2 in this report.

The second analysis method uses a bespoke turbine avoidance method, developed specifically for this monitoring study. This method, focused on data collected within the wind farm area itself, compares the observed range of seabird densities around turbines with those that might be observed by chance. This provides an indication of whether birds are either avoiding, or attracted to, the turbines. One of the strengths of this analysis is that, because it is not based on before-after comparisons (in contrast with the spatial analysis described above), the results are not affected by potential inter-annual variations.

The analysis was trialed with the pre-construction data, however since there were no structures for birds to react to at that time this could only consider if the method was expected to work (i.e. would be able to detect turbine avoidance if present). The method was used for the first time for data collected at an operational wind farm in the analysis of the year 1 post-construction data (MacArthur Green 2021). The results provided strong indications that the species assessed, which were those present in the wind farm in sufficient numbers to be analysed (guillemot, razorbill, puffin, kittiwake and herring gull) showed little evidence of negative spatial responses to the turbines, with distributions no different from those expected by chance (and in some cases there were suggestions of a preference for areas closer to turbines). This report provides a second year of this analysis using the same methods. Following minor revisions to the methods to improve the precision and accuracy of the densities calculated from the aerial survey images, the data collected in 2019 have been re-analysed and are provided alongside the 2021 results.

2 METHODS

The area of interest for surveying was identified as a region extending from the East Caithness coast to beyond the eastern Wind Farm boundary and extending to the north-east and south-west beyond the limits of the Wind Farm (Figure 2-1). Following discussions with MFRAG-O the finalised design of the aerial surveys was submitted to Marine Scotland on 29th May 2015 (Doc Ref: LF000005-SOW-05). Following the successful use of this survey design for the pre-construction surveys this design was used for the post-construction surveys in 2019 (MacArthur Green 2021) and 2021, the results from the latter surveys being the focus of the current report.

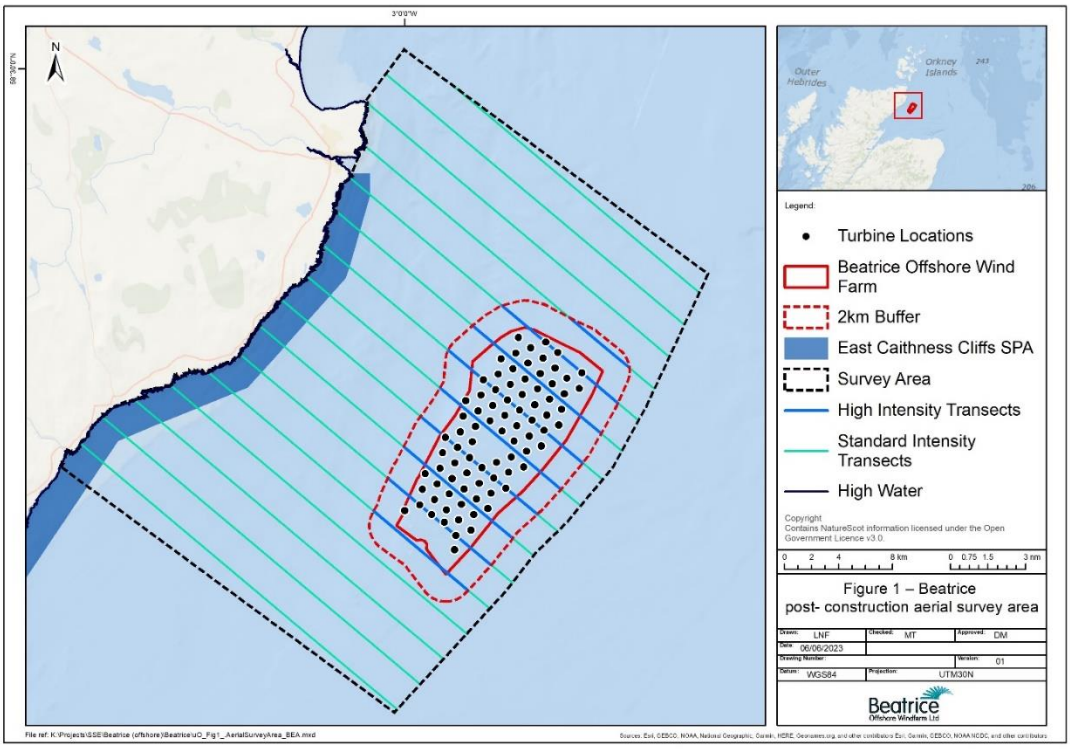

Figure 2-1. Survey area (light blue boundary) for aerial survey coverage of the Beatrice Offshore Wind Farm and the region of sea between the Wind Farm and the Caithness coast. Transects shown in green/blue (as they cross the 2km buffer), Wind Farm boundary (solid red), 2 km buffer (dashed red) and turbine locations (black dots) shown. The 2km seaward extension of the East Caithness Cliffs SPA also shown (dark blue shading).

The survey area measures approximately 40 km south-west to north-east and 26 km to 30 km north-west to south-east with 16 transects oriented approximately perpendicular to the coast and strictly parallel to each other. The seaward boundary follows a 4 km buffer from the Wind Farm boundary to match the site characterisation boat survey buffer. The transects which cross the Wind Farm were aligned to ensure that alternate ones crossed rows of turbines, with spacing of the remaining transects taken from this requirement. Hence the transects are separated by 2.5 km, and are between 24.2 and 31.7 km in length, giving a total transect length of 456 km. Approximately 60 km of this crosses the Wind Farm area (i.e. the area within the red line boundary shown in (Figure 2-1 and Figure 2-2). All surveys have been conducted by HiDef using high definition video cameras which record data continuously, generating strip transect data, with the entire area surveyed within a single day on each occasion. Use of the same contractor ensured the datasets were comparable for analysis.

HiDef utilise up to four cameras mounted in parallel to give a total transect width of up to 500 m (125 m for each camera). For transects within the Wind Farm and 2 km buffer area, data were provided from all four cameras, giving a coverage of 20% (hereafter 'high intensity survey'). These data were used for the turbine avoidance analysis. For the remainder of the survey area, data were provided from the two central cameras (250 m), giving coverage of 10% (hereafter 'standard

intensity survey'). The high intensity transects were positioned so that alternate ones crossed rows of planned (in 2015) and subsequently constructed turbine locations (Figure 2-2). The total area surveyed was approximately 1,142 km², within which the wind farm area plus buffer covers an area of 383 km² and the wind farm covers an area of 131 km².

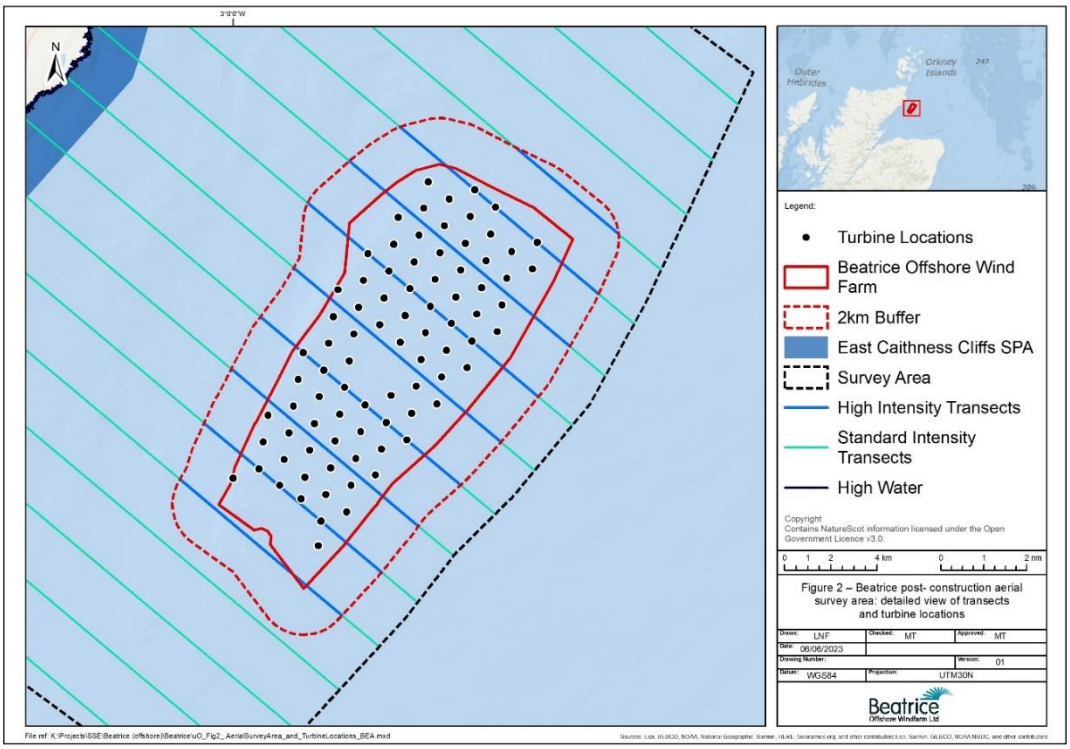

Figure 2-2. Detail of transects for aerial surveys over the Beatrice Wind Farm showing transect alignment in relation to turbine rows. Transects shown in green/blue (as they cross the 2km buffer), Wind Farm boundary (solid red), 2 km buffer (dashed red) and turbine locations (black dots) shown. The 2km seaward extension of the East Caithness Cliffs SPA also shown (dark blue shading).

Following image processing and transcription by HiDef the data collected during each survey were supplied as spreadsheets and GIS shapefiles. Each bird observed was identified using a hierarchical classification, down to species level wherever possible, with an associated confidence level. The following data were supplied following the surveys:

- Locations for all individuals observed; and,
- Flight heights for selected species (great black-backed gull, herring gull, gannet and kittiwake).

Additional data which were collected include behaviour (e.g. flying, sitting, etc.), age and sex (if possible).

2.1 Data analysis

The survey data were categorised spatially for different aspects of the analysis into the following regions:

- Total survey area – this was the entire survey region within the survey boundary (i.e. 1,142 km^2) making use of the standard intensity survey data;
- Wind Farm and 2 km buffer – this was the area within the 2 km buffer of the Wind Farm and used the high intensity survey data;
- Wind Farm and 500 m buffer – this was a subset of the Wind Farm and 2 km (high intensity) data; and
- Wind Farm – this was the area within the Wind Farm site boundary only.

Data analysis was split into the following components:

1. Assessment of the 2021 distribution and abundance of great black-backed gull, herring gull, puffin, common guillemot, razorbill, kittiwake and gannet across the entire surveyed area using the standard intensity data. Birds on the water and in flight were analysed separately; spatial models were used for birds on the water (if seen in sufficient numbers), permitting the use of explanatory variables to improve model precision; birds seen in lower numbers (on the water) and birds recorded in flight were analysed using design-based methods (further details are provided below). Spatial modelling outputs were used to generate density surface maps for the total survey area and estimates of the population abundance in the total survey area and the Wind Farm area;
2. Comparison of the pre-construction and post-construction (post-1 and post-2) model distributions using MRSea. Three comparisons are provided:
    a. Pre and post-1 (these were presented previously in MacArthur Green 2021);
    b. Pre and post-2; and
    c. Post-1 and post-2.
3. For each analysis, the two datasets in question were combined and modelled with explanatory covariates (as above) and additional factor covariates of survey number and impact (defined as before/after the wind farm or year 1 and year 2 for the post-construction analysis). To test for a redistribution effect, an interaction term for impact and spatial location was included. Outputs from the models are provided as difference surfaces (i.e. the spatially explicit difference in abundance for the before and after surveys);
4. Analysis of seabird distributions within the Wind Farm and 500 m buffer in relation to planned turbine locations. A method to assess within Wind Farm avoidance of turbines was developed using these data and the results of this approach are included (note that this aspect was focused on the potential to detect displacement of foraging birds from areas around turbine bases rather than estimation of collision avoidance rates); and,
5. Analysis of flight height data for collision risk species (great black-backed gull, herring gull, kittiwake and gannet), to explore relationships between height and proximity to the turbines.

2.2 Spatial modelling and design-based analysis of birds on the water

The distributions of the focal species across the survey area were analysed using the MRSea Package for R, developed by Scott-Hayward *et al.* (2013). This package was developed under

contract to Marine Scotland for analysis of data collected for marine renewable developments and is therefore directly applicable to the current study.

Spatial modelling permits the use of explanatory variables to be included in the analysis to identify significant relationships between the variables and the recorded distributions. Any significant covariates identified can then be used to predict distributions in areas not surveyed, either between transects or to areas beyond the surveyed area (in the current analysis only the former was undertaken). Thus, the observations made along transects can be used to estimate the density between transects and thereby to derive predictive maps and abundance estimates for the whole survey area.

Spatial analysis was conducted using only birds recorded on the sea surface since the explanatory covariates were selected on the basis of potential relationships with foraging locations, and hence these would not be expected to show strong correlations with the distribution of flying birds (particularly auks). Analysis of the density and abundance of flying birds was conducted separately (see Section 2.3).

The candidate covariates used in the analysis were sea depth (obtained from EMODnet, 13/12/2019) and distance to coast, together with a spatial term (a combined x-y position), which captures additional spatial patterns not explained by the other covariates. To conduct this analysis the transect data were divided into 500 m long segments. Segment width for analysis of the total survey area was 250 m, and for the data collected on the Wind Farm and 2 km buffer was 500 m. Covariate values for use in the modelling (e.g. distance to coast and depth) were obtained for the midpoint of each segment. The depth value was the average value for the 90x90 m cell in which the segment midpoint was located.

Spatial model fitting followed the methods set out in Scott-Hayward *et al.* (2013). To generate maps of spatial distributions, each survey was analysed independently, using the smoothed x-y spatial term with depth and minimum distance to coast as additive terms. The MRSea functions automatically test relationships and retain only significant covariates in the final model. The outputs from these models are provided primarily for illustration.

If modelling was unsuccessful (i.e. the model failed to converge, usually due to sample size limitations) for a particular species on a survey, maps of the observed bird locations are provided without an underlying density surface.

To test for a Wind Farm effect the data from each pair of before-after years (2015–2019 and 2015-2021) were analysed with the inclusion of a wind farm term (0/1) included as a categorical variable. The two post-construction years (2019-2021) were also compared, with a 'year' term used in place of wind farm. To accommodate autocorrelation (e.g. along transects) a blocking structure was included in the analysis. This was a composite of survey ID (1 to 6) and transect ID (1 to 16) and allowed for spatial and temporal autocorrelation and also for testing for influential blocks within the data.

The initial model formulation was as follows:

$$y \sim \text{wind farm} + s(\text{depth}) + s(\text{dist.to.coast}) + s(x.y, \text{wind farm})$$

with only significant terms (at $p < 0.05$) retained in the final model.

As well as wind farm (0/1) this model included smoothed, one-dimensional terms for depth and distance to coast, a two dimensional spatial smooth term (x,y) and an interaction between the spatial smoother and wind farm (or year) to test for a redistribution effect (i.e. rather than simply an overall change in number). It is not possible to determine from the model coefficients what the spatial nature of the changes are. Thus, while a significant interaction between the wind farm and spatial terms indicates a before-after re-distribution effect, this does not on its own indicate where the change has occurred. To visualise the changes to the spatial distribution, the models were used to make predictions across a grid of cells covering the study area. To ensure the outputs are robust, MRSea employs a bootstrap routine, thereby incorporating parameter uncertainty. The median differences between the pre- and post- surfaces were plotted as maps which indicate where changes in distribution have occurred. Cells which have changed significantly are identified with symbols that also denoted the direction of change (increase or decrease in abundance).

The spatially explicit abundance predictions were made across a prediction grid of 500 m cells covering the entire survey area, each cell of which had a covariate parameter value for depth, distance to coast and the spatial term (i.e. coordinate). The abundance of each species in any spatial subset of cells was obtained by summing the cells within that region (e.g. those in the Wind Farm). By including covariate values for the wind farm and survey number terms in the model, the abundance for all combinations of survey and wind farm could also be obtained.

Comparison of the values predicted in each cell, for example of the pre and post datasets, allows spatially explicit differences to be derived (i.e. subtracting one from the other to obtain cell by cell differences).

To check the extent to which the before-after results were influenced by individual surveys the *runInfluence* function in MRSea was used to obtain the covratio and press statistics. The summary results are provided in the results section, with the plotted outputs in ANNEX E.

While the spatial modelling repeated and updated the pre-construction analysis originally presented in BOWL (2016), it should be noted that in some cases the pre-construction abundances derived from the spatial models presented in the current report differ slightly from those in the pre-construction report. This is a result of methodological revisions (e.g. to the MRSea library), changes in the orientation of the grid of prediction cells used and the consequent small changes in some of the covariate estimates (see ANNEX A for a comparison of abundance estimates).

In addition to spatial modelling, the abundances of birds in the survey area and the wind farm were calculated in each year using design-based methods. Although design-based estimates are less robust than model-based ones, for species observed in smaller numbers it was not possible to successfully fit models and therefore it was necessary to use design-based methods to obtain abundance estimates. To derive an estimate of the uncertainty around the design-based abundances, each transect was split into 500m segments which were resampled 1,000 times using a bootstrap method. From the resulting, resampled dataset the 95% confidence intervals were obtained. As this method has been repeated here for previous years, the results presented differ slightly compared with those in previous monitoring reports.

For those species for which availability bias may lead to underestimation of absolute abundance (e.g. diving species such as auks), abundance estimates can be multiplied by correction factors to obtain an estimate of the total abundance allowing for birds which were underwater when the

images were recorded. This is useful for comparisons with previous estimates and sites elsewhere (assuming those have also been corrected for potential bias), however since the correction factor is applied as a constant rate for each species, there is no benefit in terms of comparing distributions between surveys or between the spatial modelling and design-based estimates. Correction factors for guillemot, razorbill and puffin were taken from Thaxter *et al.* (2010) and Burton *et al.* (2013). The values used were: guillemot, 1.237; razorbill, 1.174; puffin, 1.202. Note that these adjustments were only made to the design-based abundance estimates (as it was considered less appropriate to adjust the model-based ones), and therefore partly explain differences between the two sets of abundance estimates for these species.

2.3 Abundance of birds in flight

The abundance of birds in flight was estimated using design-based methods, with the density of birds in each transect calculated as the number observed divided by the area surveyed. To estimate abundance across the total survey area the standard intensity data were used, while for the estimated abundance in the Wind Farm area the high intensity data were used, thereby maximising use of the data. The average density across transects was multiplied by the relevant area to obtain estimates of the abundance of birds in flight. The locations recorded on each survey were plotted and are provided in ANNEX B.

2.4 Seabird distributions in relation to turbine locations

The high intensity data from the post-construction surveys were analysed using the method developed to investigate within wind farm seabird distributions. For each species (guillemot, puffin, razorbill, kittiwake and herring gull; note that there were insufficient observations within the wind farm for gannet or great black-backed gull) the analysis used the locations of each observed individual within 400 m of turbines.

The analysis was focused on seabird usage of habitat within the wind farm. Therefore, since birds recorded in flight may have been passing through the wind farm, rather than utilizing the area, only birds recorded on the sea surface were included in the analysis.

To reduce glare from the sun in the recorded imagery the cameras used by HiDef are pointed forwards (or backwards, depending on the flight direction relative to the sun) at an angle of 30° from the vertical. This introduces an offset in the estimated bird locations relative to the plane's location. Since the observation data included turbine positions (i.e. turbines were reported in the same manner as birds), it was possible to calculate the average offset distance (along the transect line) using the actual turbine locations as reference points. The part of the turbine observed was not recorded in the data, but could include a rotor blade or the tower, and therefore the distance between the 'turbine' position recorded in the survey data and the actual turbine (tower) position varied between observations. The offset was estimated to be an average of 69.7m (s.d. 25.5m) in the 2019 data and 57.3m (s.d. 18.9m) in the 2021 data. The mean offset values were subtracted from the bird locations in each year of data prior to running the turbine avoidance analysis.

The density of birds within nested 100m radius circles (0-100, 0-200, 0-300 and 0-400m) around each turbine was calculated to provide the observed estimates. The turbines were then randomly relocated, using the same x and y offset values for all turbines (i.e. all turbines are moved for this calculation by the same distance and in the same direction) and the densities recalculated. The x

and y turbine offset values were selected from uniform distributions, within a range of +/-510 m (x) and +/-550 m (y), with an angular offset to ensure the random locations generated by this method were within adjacent parallelograms around each turbine location (see Figure 2-3). This approach ensured turbines were relocated within discrete parallelograms up to half the distance to the next turbine. To avoid bias in the densities estimated around randomised turbine positions which fall partially or completely outside the areas covered by the transect data (i.e. regions for which no aerial data were collected), the area of each circle used to calculate density was adjusted to only include the portion which overlapped the transects. As this aspect was omitted in the post-1 analysis (MacArthur Green 2021) the data for that year have been re-analysed and are presented with this adjustment incorporated in ANNEX G.

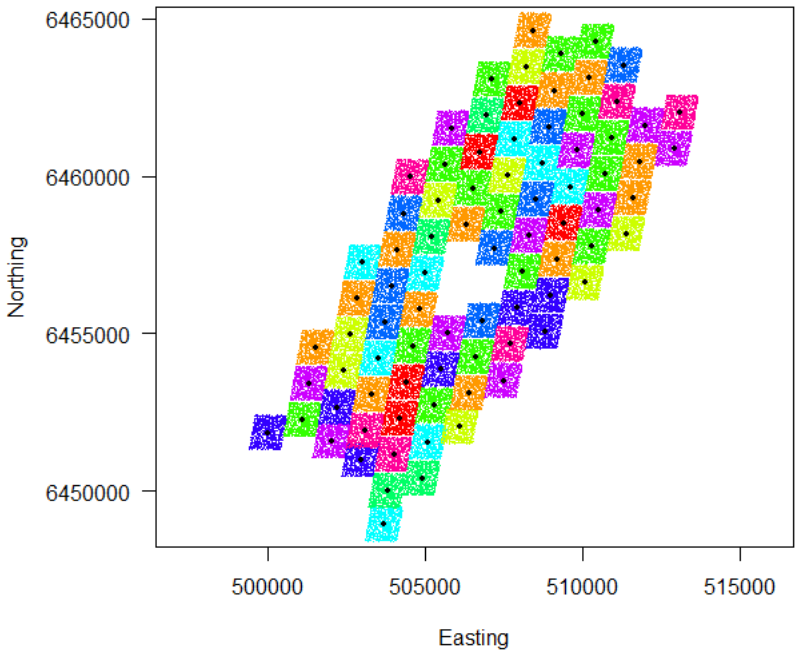

Figure 2-3. Illustration of randomised turbine positions used in the turbine avoidance analysis. Each coloured parallelogram contains 1,000 dots, each one a single realization of the randomized turbine location around the actual turbine locations (black dots).

Two sets of analysis were conducted for each year's dataset. The first combined the data across all six surveys within each post-construction dataset, on the assumption that bird responses to turbines were consistent irrespective of the survey or turbine operation status. For the second, the data collected in each year were divided into subsets based on turbine RPM (revolutions per minute), in order to investigate for any variations in density around turbines in relation to their operation. Each bird observation was assigned the RPM value from the nearest turbine recorded at the closest time (to the nearest 10 minutes). The turbine avoidance analysis was run on four RPM data subsets[1]:

- <2.5,

[1] In MacArthur Green (2021) the data were divided into five categories, 0-2, 2-4, 4-6, 6-8, 8+, which have been reduced to the four discussed in this report to improve clarity.

- >=2.5 & <5.0,
- >=5.0 & <7.5, and
- >=7.5 & <12.

2.5 Flight heights

HiDef provided size-based flight height estimates, derived by comparing the body length of birds observed on the surveys with baseline body length information obtained and analysed by HiDef from surveys conducted across multiple sites. The baseline data, containing what is referred to hereafter as known height body lengths, have been measured from birds that show reflection on the sea surface, which calculation has shown to comprise only birds within 3 m of the sea surface.

The body lengths of birds recorded during the surveys were measured in the same way during processing of the reflection data, with the maximum bird length (across multiple frames) used as the value for that record. For each maximum body length, a range of possible heights was calculated using the upper and lower 95% body lengths of the known height birds.

The minimum height of each record is calculated using the equation:

$$\text{Bird height} = \text{Aeroplane height} \times (1 - (l_{r\ min}/l_{s\ max})$$

Where:

$l_{r\ min}$ = lower 95% CI of birds with reflection; and,

$l_{s\ max}$ = maximum length of the bird from available frames.

The maximum height of each record is calculated using the equation:

$$\text{Bird height} = \text{Aeroplane height} \times (1 - (l_{r\ max}/l_{s\ max})$$

Where:

$l_{r\ max}$ = upper 95% CI of birds with reflection

This provided a minimum and maximum height value for each individual. In some cases, for birds recorded close to the sea surface, this calculation resulted in an estimate of height less than sea level, due to uncertainties in the body length measurements. These birds were assigned a height of zero, on the basis that they were definitely below rotor height but could not be assigned a reliable estimate. While inclusion of these in estimates of flight height would clearly bias the results, they could be included in estimates of the proportions at and below rotor height. Thus, height was analysed as a binomial response variable with respect to the lower rotor tip height (32.7 m; below/above), using the maximum estimated value (including the zero values as noted above in the below category). Data were filtered on distance from shore (selecting birds the same distance offshore as the wind farm) with inside/outside the wind farm as an explanatory variable.

It should be stressed however that estimates of bird flight height calculated from aerial imagery in the manner described include a large degree of uncertainty, due to several sources of potential error (e.g. the orientation of the bird relative to the camera, the comparatively small size of the

bird image) and this is evidenced by negative height estimates (i.e. below sea level). Thus, the height data should be considered to provide a guide rather than definitive estimates.

3 RESULTS

3.1 Surveys

The survey design was based on six evenly spaced surveys with two in each of May, June and July. In each year, although six surveys have been conducted, weather conditions have prevented the even spacing of surveys across the period. Thus, in both 2015 and 2019 only one survey could be completed in May. In 2015 an additional survey was conducted in the first week of August (in agreement with MFRAG-O) and in 2019 an extra survey was completed in June (i.e. there were three surveys in that month). In 2021, two surveys were successfully completed in May and June, but only one was conducted in July, with the final one taking place at the beginning of August.

The dates of the six surveys in each year are provided in Table 3-1.

Table 3-1. Survey dates, start and end times in 2015, 2019 and 2021.

Survey no.	2015		2019		2021	
	Date	Time	Date	Time	Date	Time
1	30/05/2015	17:43 – 20:12	28/05/2019	10:49 – 12:22	22/05/2021	10:05 – 12:53
2	10/06/2015	09:40 – 12:09	10/06/2019	11:09 – 12:27	31/05/2021	08:35 – 11:04
3	29/06/2015	13:18 – 15:48	22/06/2019	10:52 – 12:13	08/06/2021	08:21 – 11:01
4	15/07/2015	10:28 – 13:19	29/06/2019	10:25 – 11:48	20/06/2021	08:15 – 10:46
5	22/07/2015	08:10 – 11:25	19/07/2019	08:16 – 09:49	01/07/2021	08:56 – 11:30
6	05/08/2015	09:31 – 11:58	25/07/2019	11:55 – 13:26	04/08/2021	07:35 – 10:13

As can be seen in Table 3-1, the 2021 surveys were conducted between 0730 and 1300. Breeding seabird activity levels may vary through the day, and it is therefore possible that these survey times omitted peaks in activity (e.g. if these occur around dawn and dusk). However, not all seabirds appear to exhibit marked variations during the day (e.g. Furness et al. 2018 reported relatively constant levels of gannet activity throughout the day) and indeed recording average levels (e.g. during the middle of the day) could be considered more appropriate for characterizing usage levels. There was also considerable between-survey variation in seabird abundance, despite the surveys having been flown at similar times, suggesting that factors other than time of day are also important in determining activity levels (e.g. factors such as tide state might influence activity patterns). In addition, given the remote location of the wind farm it is also important to acknowledge that practical aspects need to be considered (e.g. periods of suitable weather and in accordance with safe flying practices), and these also impose limits on when surveys can be undertaken.

The raw count of the number seen in the survey area and in the wind farm, on the sea ('sitting'), in flight ('flying') and combined ('all') are provided in Table 3-2.

Table 3-2. Raw counts of birds recorded on the sea ('sitting'), in flight ('flying') and combined ('all') on each survey in 2021. The first value in each cell is the number recorded in the whole survey area and the second value is the number recorded in the wind farm.

Species	Observation	Raw counts in survey area / wind farm on each survey					
		1	2	3	4	5	6
Gannet	All	16 / 0	83 / 3	76 / 5	24 / 0	20 / 0	18 / 1
	Sitting	5 / 0	53 / 0	43 / 4	2 / 0	4 / 0	14 / 1
	Flying	11 / 0	30 / 3	33 / 1	22 / 0	16 / 0	4 / 0
Guillemot	All	7022 / 345	13625 / 95	13378 / 938	4524 / 261	6270 / 275	3246 / 691
	Sitting	6665 / 331	13234 / 73	12527 / 817	3504 / 113	5140 / 180	3232 / 691
	Flying	357 / 14	391 / 22	851 / 121	1020 / 148	1130 / 95	14 / 0
Kittiwake	All	668 / 14	740 / 14	2446 / 216	628 / 170	1129 / 182	1049 / 252
	Sitting	141 / 0	239 / 0	1478 / 105	43 / 35	618 / 130	441 / 149
	Flying	527 / 14	501 / 14	968 / 111	585 / 135	511 / 52	608 / 103
Puffin	All	100 / 4	274 / 2	312 / 14	142 / 3	202 / 6	1889 / 87
	Sitting	98 / 4	267 / 2	309 / 13	116 / 3	190 / 6	1885 / 87
	Flying	2 / 0	7 / 0	3 / 1	26 / 0	12 / 0	4 / 0
Razorbill	All	621 / 45	517 / 4	704 / 83	1009 / 36	481 / 32	397 / 63
	Sitting	571 / 42	505 / 3	662 / 80	765 / 23	370 / 23	395 / 62
	Flying	50 / 3	12 / 1	42 / 3	244 / 13	111 / 9	2 / 1
Herring gull	All	30 / 1	50 / 1	174 / 10	104 / 15	163 / 14	23 / 1
	Sitting	6 / 0	11 / 0	64 / 0	7 / 0	6 / 2	9 / 0
	Flying	24 / 1	39 / 1	110 / 10	97 / 15	157 / 12	14 / 1
Great black-backed gull	All	12 / 1	15 / 0	13 / 0	10 / 1	10 / 0	21 / 9
	Sitting	2 / 0	9 / 0	5 / 0	3 / 0	2 / 0	11 / 8
	Flying	10 / 1	6 / 0	8 / 0	7 / 1	8 / 0	10 / 1

3.2 Spatial modelling and design-based analysis of birds on the water

To obtain model-based estimates of each species' abundance in the 2021 surveys, where possible the data for each survey were analysed independently in order to avoid outputs being constrained by the need to fit a shared model to distributions that vary between surveys (this is achieved by inclusion of an interaction between survey and spatial smoother). However, flexible models of this type require a reasonably high number of records in each survey, and there were insufficient data for gannet, herring gull and great black-backed gull to be able to fit these flexible models. For gannet and herring gull it was possible to fit models averaged over all surveys. Consequently, these share the same spatial distribution but different cell values in each month (i.e. omitting the interaction term makes these a form of additive model). For great black-backed gull it was not possible to fit even these simplified models and therefore only design-based estimates are presented.

The predicted population abundances from the best-fit models are provided in Table 3-3 and for comparison the design-based population estimates are provided in Table 3-4. The figures for 2015 and 2019 are those previously presented (MacArthur Green 2021).

Figures 3-1 to 3-7 provide the fitted density surfaces for 2021 where these were obtained, with the observation locations indicated, or just plain figures with the observation locations for less abundant species.

Table 3-3. Model-derived population abundance estimates of numbers of birds on the water in the total survey area (shaded) and within the Wind Farm boundary for each species in each survey in 2015, 2019 and 2021. Entries marked with '-' indicate instances when small sample sizes prevented model fitting or unreliable estimates were obtained due to edge effects. Values for 2015 and 2019 taken from MacArthur Green (2021).

Species	Year	Region	Population abundance on each survey						Peak
			1	2	3	4	5	6	
Gannet	2015	Total survey area	174.1 (68.7-560.1)	461 (144.7-1663.8)	708.6 (253.7-2304.5)	182.6 (53.6-735.1)	17.5 (4-88.8)	8.9 (1.2-99.7)	709
		Wind Farm	56.4 (25.7-135.6)	149.3 (58.6-382.4)	229.4 (77.3-697.2)	59.1 (20.3-169.8)	5.7 (1.4-25.4)	2.9 (0.4-23)	229
	2019	Total survey area	49 (11.9-231.5)	397.5 (116.4-2146.7)	19.9 (4.3-90.5)	20 (3.8-128.9)	49.9 (15.5-190.9)	159.3 (45-713.7)	397
		Wind Farm	15.9 (4.2-54.5)	128.7 (46.5-428.4)	6.4 (1.4-23)	6.5 (1.3-32.7)	16.2 (5.5-51.6)	51.6 (16.3-179.9)	129
	2021	Total survey area	49.6 (11.4-240120.8)	481.9 (102.4-862301.4)	397.5 (137.7-1436425.8)	19.8 (4.1-182568.9)	39.5 (10.4-209743.2)	109.3 (39.2-564645.1)	482
		Wind Farm	2.4 (0.6-12.9)	23.1 (8.1-75.6)	19.1 (6.4-68.9)	0.9 (0.2-5.4)	1.9 (0.4-8.9)	5.2 (1.9-19.2)	23
Guillemot	2015	Total survey area	39760.1 (20689.1-79196.5)	36561 (20289.5-67384)	15487.5 (7806.2-33179.9)	51036.9 (18376.3-181745.8)	7642.7 (2917.3-22387.1)	4063.5 (2531.3-6572.3)	51,037
		Wind Farm	5819.9 (3862.2-8494.5)	1421.2 (726.9-3277.2)	2060.1 (671.1-5699.7)	7015.9 (2874.1-18580.8)	1452 (597.6-4140)	902.2 (571.5-1371.5)	7,016
	2019	Total survey area	25525.3 (13044.3-55685.9)	86819.9 (51048.5-154260.6)	54556.2 (26481.7-124613)	41419.2 (27175.9-65578.8)	25857.3 (14639.1-51179.3)	9845 (4332-28441.8)	86,820
		Wind Farm	987.6 (378.3-3829)	10859 (6527-19028.2)	4129.7 (2560.5-7088.9)	2768 (1754-5172.8)	1306.5 (824.1-2301.7)	456.8 (206.1-1152.6)	10,859
	2021	Total survey area	57446.7 (29897.8-110798.1)	103710.1 (57252.6-256659.4)	100231.4 (56583.9-195453.6)	27498.4 (15573.1-52030.5)	41069.4 (23598.4-79192.6)	20977.3 (12851-39792.5)	103,710
		Wind Farm	2340.5 (1151.8-4724.4)	33.6 (2.3-1610.2)	6683.2 (2705.7-17434.8)	578.8 (266-1857.8)	1256.9 (628.5-3000.3)	5571.4 (3549.1-9810.7)	6,683
Kittiwake	2015	Total survey area	1443.4 (240.6-Inf.)	3639.1 (1006.2-18202.8)	3376 (1287.4-42182.8)	3707.1 (1300.7-14844.8)	1666.9 (665.7- Inf.)	352.2 (119.9-2094.1)	3,707
		Wind Farm	37.7 (4.7-Inf.)	246.8 (41.9-1796.3)	62.5 (17.5-1292)	1290.7 (468.6-5478.9)	174 (49.2-532.6)	63.1 (22.3-273.7)	1,291

Species	Year	Region	Population abundance on each survey						Peak
			1	2	3	4	5	6	
	2019	Total survey area	716.7 (224.8-3084.7)	4610.2 (1247.5-25631.6)	3394.1 (1572.5-9227.7)	3910.3 (1590.9-12892.6)	2176.3 (573.7-10062.3)	1440.1 (456.1-11148.5)	4,610
		Wind Farm	15 (2.3-108.3)	1648.4 (455-6363.4)	1005.4 (498-2368.6)	304.6 (76.6-1224.4)	353.4 (91.7-1729.7)	148.3 (46.7-476.5)	1,648
	2021	Total survey area	1207.5 (222.6-492192.1)	1738.5 (694.6-15707)	14774.3 (7472.4-87620.8)	82.9 (21.7-538.7)	4651.1 (1247.9-21249.6)	1855.3 (687.9-6611.1)	14,774
		Wind Farm	0.1 (0-83034)	0.1 (0-82.1)	509.7 (56.7-4656.8)	0.7 (0-49)	294.1 (53.1-1483.8)	873.9 (338.6-2206.5)	874
Puffin	2015	Total survey area	1960 (1045.3-3909.2)	1409.8 (709.4-2834.9)	479.3 (274.2-894.5)	532.2 (307.8-1506.8)	214 (68.7-2470.4)	3133.1 (1847.2-5478.7)	3,133
		Wind Farm	193.2 (92.5-390.7)	72.9 (23.8-176.2)	19.8 (6.5-69.8)	2.7 (0.2-135.2)	2.6 (0.1-1017.9)	1027.5 (677.1-1489.5)	1,027
	2019	Total survey area	335.7 (132.4-975.7)	1170.6 (703.2-2115.3)	523.3 (252.3-1167)	520.6 (274.4-971.1)	310.5 (128.3-826.9)	509.7 (279.1 – Inf.)	1,171
		Wind Farm	16.8 (5.6-64.2)	38.7 (16.9-95)	15.6 (4.3-57.2)	2.8 (0.5-15.6)	9.9 (2.3-51.5)	0.1 (0 – Inf.)	39
	2021	Total survey area	949.8 (511-1859.8)	2339.9 (1231.6-5257.4)	2652.2 (1724.3-4173.7)	1100.8 (645-2158.1)	1792.5 (950.5-3388.2)	16577.8 (11109.9-24826.5)	16,578
		Wind Farm	54 (27.1-119.1)	43.3 (19.8-110.3)	70.3 (33-158.5)	22.9 (11.6-48.7)	37.7 (15.6-87.6)	959.6 (668.7-1381.7)	960
Razorbill	2015	Total survey area	817.8 (378.7-1807.1)	2034.5 (1068.4-3815.1)	3527.9 (2435.7-5279.5)	1674.8 (710.3-3628.8)	37.7 (15.3-94.8)	9.6 (1.6-80.9)	3,528
		Wind Farm	49.3 (20.6-107.9)	122.6 (62.5-222.1)	212.6 (146.2-295.3)	100.9 (44.2-219.9)	2.3 (0.9-5.7)	0.6 (0.1-4.9)	213
	2019	Total survey area	2048 (1167.7-3514.6)	10407.7 (6957.6-16843.1)	4197.7 (2887.7-6092.9)	11246.8 (8048.7-16336.4)	3631.8 (2419.7-5716)	1289.6 (568.9-3499.7)	11,249
		Wind Farm	123.4 (74.3-224.7)	627.3 (426.8-963.7)	253 (171.6-378.9)	677.8 (486.8-967.7)	218.9 (143.6-365.1)	77.7 (34.6-216.6)	678
	2021	Total survey area	4987.9 (2798.8-9588.9)	4358.3 (2008.2-12375.6)	4644.9 (2909.3-7916.0)	6395.4 (3793.4-11204.6)	2963.3 (1537.6-5890.5)	3050.7 (1665.9-5929.1)	6,395
		Wind Farm	90.9 (47.3-191.1)	5.3 (1.2-23.6)	308.4 (178.4-592.6)	138.4 (70.8-270.3)	116.9 (58.9-286.5)	454.2 (262.5-827.5)	454

Species	Year	Region	Population abundance on each survey						Peak
			1	2	3	4	5	6	
Great black-backed gull	2019	Total survey area	-	-	-	127.5 (36.4-833)	-	-	127
		Wind Farm	-	-	-	1 (0.3-10.8)	-	-	1
	2021	Total survey area	-	-	-	-	-	-	-
		Wind Farm	-	-	-	-	-	-	-
Herring gull	2019	Total survey area	-	5072.8 (1338.8-19979.2)	804.8 (260.8-3554.7)	533 (207.9-2030.8)	-	-	5,073
		Wind Farm	-	1298.2 (383.7-4431.9)	39.4 (8.9-231.5)	12 (2.2-112.4)	-	-	1,298
	2021	Total survey area	57.8 (14.5-251.4)	103 (24.9-513.4)	627.1 (249.3-2040.5)	67.2 (17.3-231)	38.7 (10.4-146.3)	76.8 (16.5-556.4)	627
		Wind Farm	0 (0-0.8)	0.1 (0-1.1)	0.5 (0.1-4.3)	0.1 (0-0.5)	0 (0-0.4)	0.1 (0-1.1)	0.5

Table 3-4. Design-based population abundance estimates (and 95% confidence intervals) in the total survey area and within the Wind Farm boundary for each species in each survey in 2015, 2019 and 2021, calculated for birds recorded on the sea surface. Values for 2015 and 2019 taken from MacArthur Green (2021). Abundance across the total survey area was estimated using the standard intensity data, Wind Farm abundance was estimated using the high intensity data. Confidence intervals estimated using a bootstrap resampling method (see text for details).

Species	Year	Area	Population abundance on each survey						Peak
			1	2	3	4	5	6	
Gannet	2015	Total survey area	266.6 (110.6-492.5)	543.3 (180.9-1126.1)	810 (422.2-1286.9)	211.3 (90.5-371.9)	29.6 (0-60.6)	9.8 (0-30.2)	810
		Wind Farm	25.2 (5-50.3)	64.8 (10.1-130.8)	536.4 (266.3-834.4)	20.1 (5-40.2)	24.6 (5-50.4)	0 (0-0)	536
	2019	Total survey area	60.8 (20.1-110.6)	566.9 (281.2-924.8)	20.4 (0-50.3)	30.2 (0-70.4)	50 (9.8-110.6)	177.2 (60.3-351.8)	567
		Wind Farm	0 (0-0)	0 (0-0)	0 (0-0)	0 (0-0)	5.3 (0-15.1)	0 (0-0)	5
	2021	Total survey area	46.4 (0-120.5)	503.9 (133.1-1102.9)	384.6 (192.3-634.8)	19.1 (0-47.7)	38.1 (9.5-85.8)	111.5 (55.7-185.8)	504
		Wind Farm	0 (0-0)	0 (0-0)	20.6 (0-61.9)	0 (0-0)	0 (0-0)	5.2 (0-15.5)	21
Guillemot	2015	Total survey area	67486.7 (48838.3-93543.4)	68431.6 (49699.1-90366.4)	24508.3 (18886.8-30563.9)	77502 (47309.8-123530.3)	18220.9 (11111-27219.7)	5841.4 (4649.5-7187.4)	77,502
		Wind Farm	7794.9 (5620.2-10326.7)	2286.2 (1398.9-3345.3)	6243.9 (2168.9-12516.9)	9425.8 (5676.1-13833.7)	4750.2 (1485.9-8983.8)	971.2 (671.3-1318)	9,426
	2019	Total survey area	47705.2 (29811-71541.5)	143361.4 (106507.4-190991.8)	79641.7 (50488.3-118429.8)	61415.9 (51848.6-72706)	40754.1 (29792-52734.6)	12900.5 (8517.2-18166.9)	143,361
		Wind Farm	1258.8 (578.2-2406.4)	24570.4 (19214.9-30459.3)	6720.9 (4686.5-9314.1)	1986.6 (1454.7-2592.7)	1091.8 (652.8-1647.7)	232.5 (105.5-404.1)	24,570
	2021	Total survey area	58488 (41615-81540.4)	124978.7 (78006.4-180285.5)	101887.5 (80746.2-124656.7)	31863.1 (21127.5-44913.9)	47105.8 (31151.1-69011.4)	22118.5 (18939.1-25595.1)	124,979
		Wind Farm	1701.7 (1249.2-2241.7)	374.5 (256.5-507.9)	4213.7 (1763.5-8596.3)	582.1 (303.8-999.3)	925.3 (668.3-1208.1)	3566.8 (2529.1-4857.8)	4214
Kittiwake	2015	Total survey area	1575.9 (210.8-4165)	3791.2 (1336.9-7498.8)	3451.5 (1407-5941)	3806.4 (1868.9-6192)	3759.2 (1557.3-6605.2)	424.3 (130.4-814.2)	3,806

Species	Year	Area	Population abundance on each survey						Peak
			1	2	3	4	5	6	
		Wind Farm	70.4 (30.2-120.6)	25.2 (0-75.4)	384.8 (5-1106)	2334.7 (643.3-4986.8)	556.7 (140.7-1141)	78.9 (0-201)	2,335
	2019	Total survey area	571.3 (130.4-1176.6)	7918.5 (3445.8-13510.4)	3841.7 (2090.3-5941.2)	5204.2 (1999.6-9651.2)	2350.1 (995.1-4081.6)	1376.7 (532.8-2392.6)	7,919
		Wind Farm	10 (0-25.1)	4072.9 (2090.7-6654.7)	1862.6 (713.6-3181.7)	1167.9 (45.2-2825.5)	64.7 (0-160.8)	72.4 (0-216.1)	4,073
	2021	Total survey area	1307.4 (333.8-2549.8)	2272.3 (66.6-4935.7)	14084.3 (7911.7-21575.1)	85.8 (28.6-152.5)	4672.4 (2422-7582.2)	1746.4 (872.8-2787.1)	14,084
		Wind Farm	0 (0-0)	0 (0-0)	541.5 (5.2-1593.9)	180.3 (0-530.6)	668.3 (41.1-1609)	769.1 (355.8-1259.5)	769
Puffin	2015	Total survey area	2614 (2053.4-3213.9)	2206.8 (1534.5-3032.7)	738.4 (483.3-1002.8)	1236.6 (374.6-2888)	377.8 (145-664.8)	4112.4 (3346.9-4917.6)	4,112
		Wind Farm	247.4 (108.7-453.1)	77.9 (24.2-138.9)	61.1 (18.1-120.8)	36.9 (6-78.5)	11.7 (0-30.2)	1543.5 (1135.6-2017.8)	1,543
	2019	Total survey area	459.4 (290-664.5)	1600.4 (1014.9-2319.8)	721.5 (495.4-966.6)	698.4 (447.1-978.7)	397.6 (229.6-567.9)	875.8 (422.6-1426.3)	1,600
		Wind Farm	6.2 (0-18.1)	156.7 (90.6-223.5)	54.8 (18.1-102.7)	18.2 (0-48.3)	6 (0-18.1)	0 (0-0)	157
	2021	Total survey area	862.3 (593.4-1177.8)	2453 (1568.5-3784.3)	2615 (2076.6-3249.5)	1096.1 (667.2-1592)	1773.6 (1353.8-2298.1)	15996.7 (14295.7-17780.3)	15,997
		Wind Farm	20.6 (0-46.3)	10.3 (0-30.8)	67 (25.8-113.5)	15.5 (0-36.1)	30.8 (5.1-66.8)	449.1 (289.1-660.8)	449
Razorbill	2015	Total survey area	1034.2 (519.2-1829.2)	2635 (1746.3-3799.9)	4457.7 (3209.9-5853.6)	2140.6 (1132.9-3622.9)	83.2 (23.6-153.4)	11.9 (0-35.4)	4,458
		Wind Farm	47.5 (17.7-88.5)	17.6 (0-47.2)	278.1 (76.7-525.1)	153.9 (23.6-336.5)	18.5 (0-53.1)	11.6 (0-29.5)	278
	2019	Total survey area	2680.1 (1793.8-3729.1)	12542.8 (9157.3-16605.5)	4668.5 (3658.3-5841.5)	12938.5 (10785.6-15542)	4026.3 (3020.5-5240)	1305.5 (672.4-2077)	12,938
		Wind Farm	71.1 (17.7-141.6)	1344.3 (1002.9-1705.3)	475.5 (283.2-690.4)	447.3 (277.3-619.7)	222.6 (47.2-477.9)	47.5 (11.8-94.4)	1,344
	2021	Total survey area	4969.8 (3486.1-6805.9)	4763.4 (2661.4-7254.8)	4585.8 (3730.2-5518.6)	6853 (5375.2-8331.1)	3184.9 (2498.3-3900.1)	3093.4 (2303.8-4031.7)	6,853

Species	Year	Area	Population abundance on each survey						Peak
			1	2	3	4	5	6	
		Wind Farm	215.9 (118.2-313.6)	15.4 (0-41)	412.6 (180.5-727.5)	118.5 (20.6-257.5)	118.2 (51.4-200.5)	320 (154.7-521.5)	413
Great black-backed gull	2015	Total survey area	19.2 (0-50.3)	30.2 (0-70.4)	29.7 (0-70.6)	51.4 (10.1-110.6)	28.9 (0-80.4)	10.5 (0-30.2)	51
		Wind Farm	0 (0-0)	4.9 (0-15.1)	0 (0-0)	15.1 (0-45.2)	5.4 (0-15.1)	0 (0-0)	15
	2019	Total survey area	0 (0-0)	141.4 (0-321.7)	9.5 (0-30.2)	171.4 (60.3-321.9)	319.4 (0-954.9)	41.4 (0-110.6)	319
		Wind Farm	0 (0-0)	41.4 (0-115.6)	0 (0-0)	4.9 (0-15.1)	0 (0-0)	0 (0-0)	41
	2021	Total survey area	18.5 (0-55.6)	85.6 (0-199.7)	48.1 (0-115.4)	28.6 (0-76.3)	19.1 (0-47.7)	46.4 (0-120.8)	86
		Wind Farm	0 (0-0)	0 (0-0)	0 (0-0)	0 (0-0)	0 (0-0)	41.3 (0-123.9)	41
Herring gull	2015	Total survey area	70.2 (10.1-170.9)	70.7 (10.1-160.8)	10.6 (0-40.2)	414.4 (0-1176.1)	125.6 (0-371.9)	20.5 (0-50.3)	414
		Wind Farm	0 (0-0)	5 (0-15.1)	0 (0-0)	0 (0-0)	0 (0-0)	0 (0-0)	5
	2019	Total survey area	49.9 (10.1-90.7)	5370.6 (623-12022.7)	1040 (351.8-1920.2)	778.1 (291.5-1367.6)	0 (0-0)	743.6 (10.1-2221.7)	5,371
		Wind Farm	0 (0-0)	1578.4 (25.1-4161.5)	525 (50.1-1332)	0 (0-0)	0 (0-0)	0 (0-0)	1,578
	2021	Total survey area	55.6 (0-129.8)	104.6 (28.5-218.9)	605.7 (125-1375)	66.7 (19.1-123.9)	38.1 (9.5-85.8)	83.6 (9.3-195.1)	606
		Wind Farm	0 (0-0)	0 (0-0)	0 (0-0)	0 (0-0)	10.3 (0-30.8)	0 (0-0)	10

3.3 Results of 2021 surveys and comparison with previous years

In all years the most abundant species recorded was guillemot. In 2015 the peak modelled abundance was estimated as 51,000 individuals within the total survey area (late July), while in 2019 the peak modelled abundance estimate was 87,000 (early June). In 2021 the peak modelled abundance was 104,000 (late May). Within the wind farm, the 2015 modelled peak was 7,000 (in July), the 2019 peak was 11,000 (June) and the 2021 peak was 6,700 (June).

In all years the main guillemot concentrations have been recorded along the Caithness coast, and this was especially marked in the 2021 surveys. Nonetheless, as can be seen from the 2021 survey plots (Figure 3-1), this species was recorded throughout the survey area.

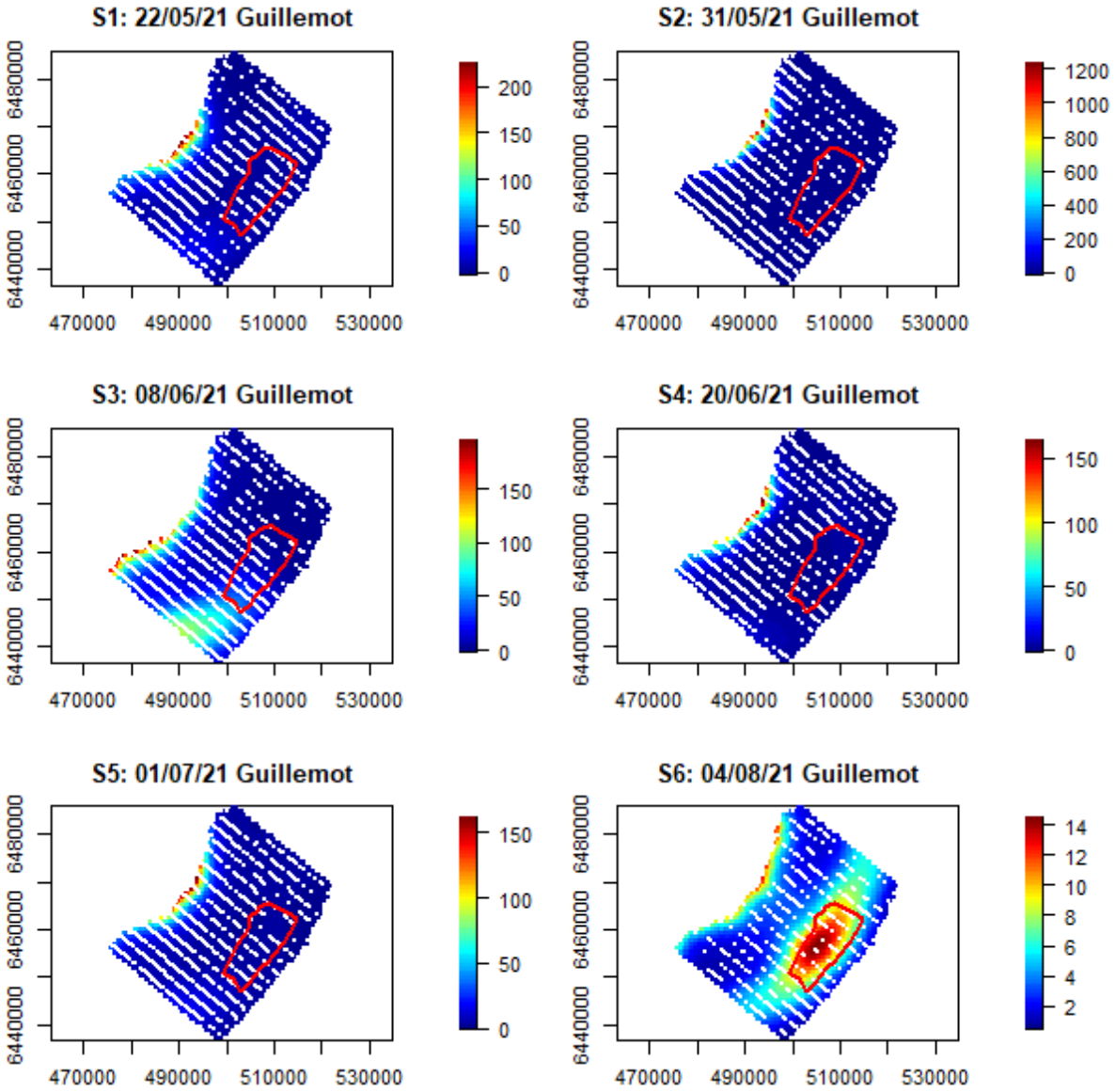

Figure 3-1. Guillemot distributions in 2021 (scale bars indicate birds/km²). Density surfaces generated using the best fit spatial model for each survey (note the scale differs for each survey). White dots are birds recorded on the water (standard intensity data only).

In 2015 the Kittiwake abundance peaked at just under 4,000 in the total survey area in June and July and 1,300 in the Wind Farm in July. Similar levels were recorded in 2019, with a peak abundance in the total survey area of approximately 4,600 in June and a wind farm peak of 1,600. In 2021 a higher overall abundance was recorded, with a peak in the survey area of 14,800 although the wind farm peak was a little lower than previous years at 870.

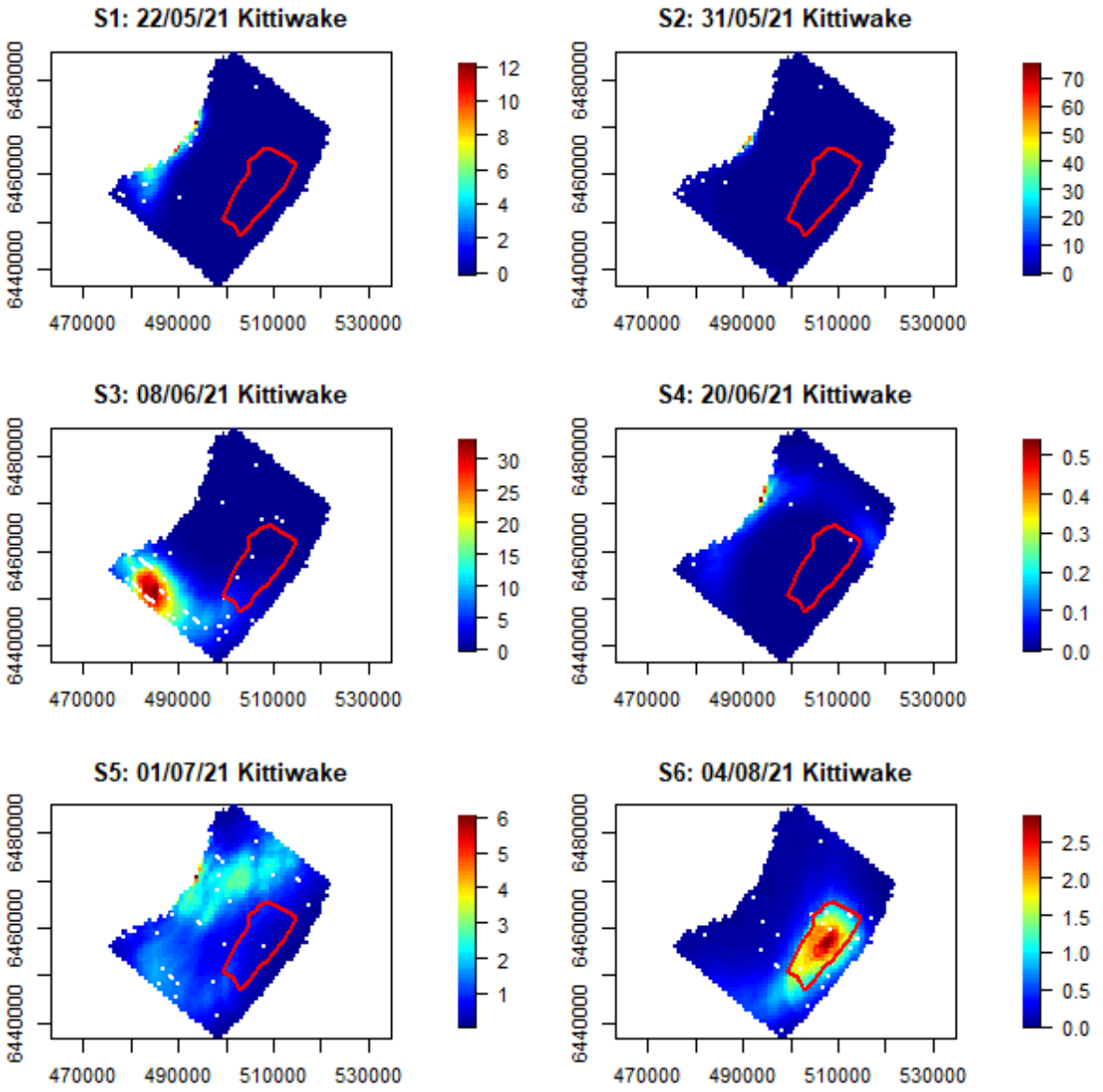

Figure 3-2. Kittiwake distributions in 2021 (scale bars indicate birds/km²). Density surfaces generated using the best fit spatial model for each survey (note the scale differs for each survey). White dots are birds recorded on the water (standard intensity data only).

In 2015, puffin abundance peaked in August at 3,100 in the total survey area and 1,000 in the wind farm. The August 2015 survey (which was outside the intended survey window due to weather delays) was considered likely to have recorded the beginning of post-breeding dispersal. No surveys were conducted in August in 2019, and it was considered that comparison of the 2015 peak with the 2019 one was potentially unreliable as a result. The June and July surveys recorded similar

numbers in both years with around 200-2,000 in 2015 and 300-1,200 in 2019 across the whole area and up to 200 in the wind farm in 2015 and up to 40 in 2019. The abundance estimated from the 2021 surveys were within a similar range, albeit higher, with May and June estimates of around 2,500 in the survey area. Due to weather constraints it was again necessary to conduct the final 2021 survey in August, and this yielded the highest puffin abundance to date of 16,600, with 960 in the wind farm. As with 2015, this seems very likely to have captured post-breeding movements.

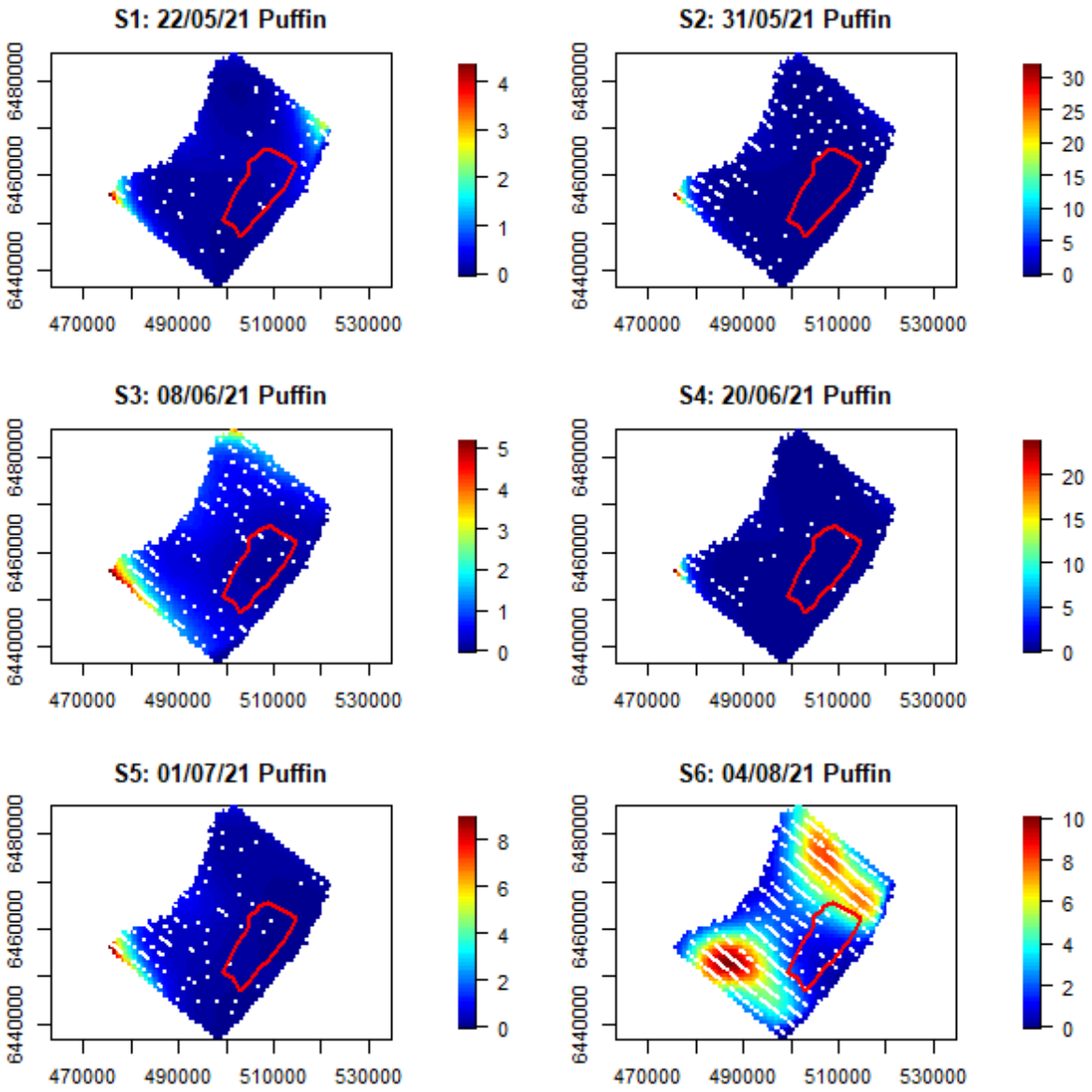

Figure 3-3. Puffin distributions in 2021 (scale bars indicate birds/km^2). Density surfaces generated using the best fit spatial model for each survey (note the scale differs for each survey). White dots are birds recorded on the water (standard intensity data only).

In 2015, razorbill was present in highest numbers in early July with a peak abundance of nearly 3,500 in the total survey area and around 200 in the Wind Farm. Numbers were overall higher in 2019, with up to 11,250 in total and 680 in the wind farm. The 2021 abundance estimates across the whole survey area were intermediate between these, with 4,000 to 5,000 recorded in May and

early June and 6,400 in July. Numbers in the wind farm in 2021 were similar to previous years, with peaks of 300 in July and 450 in August.

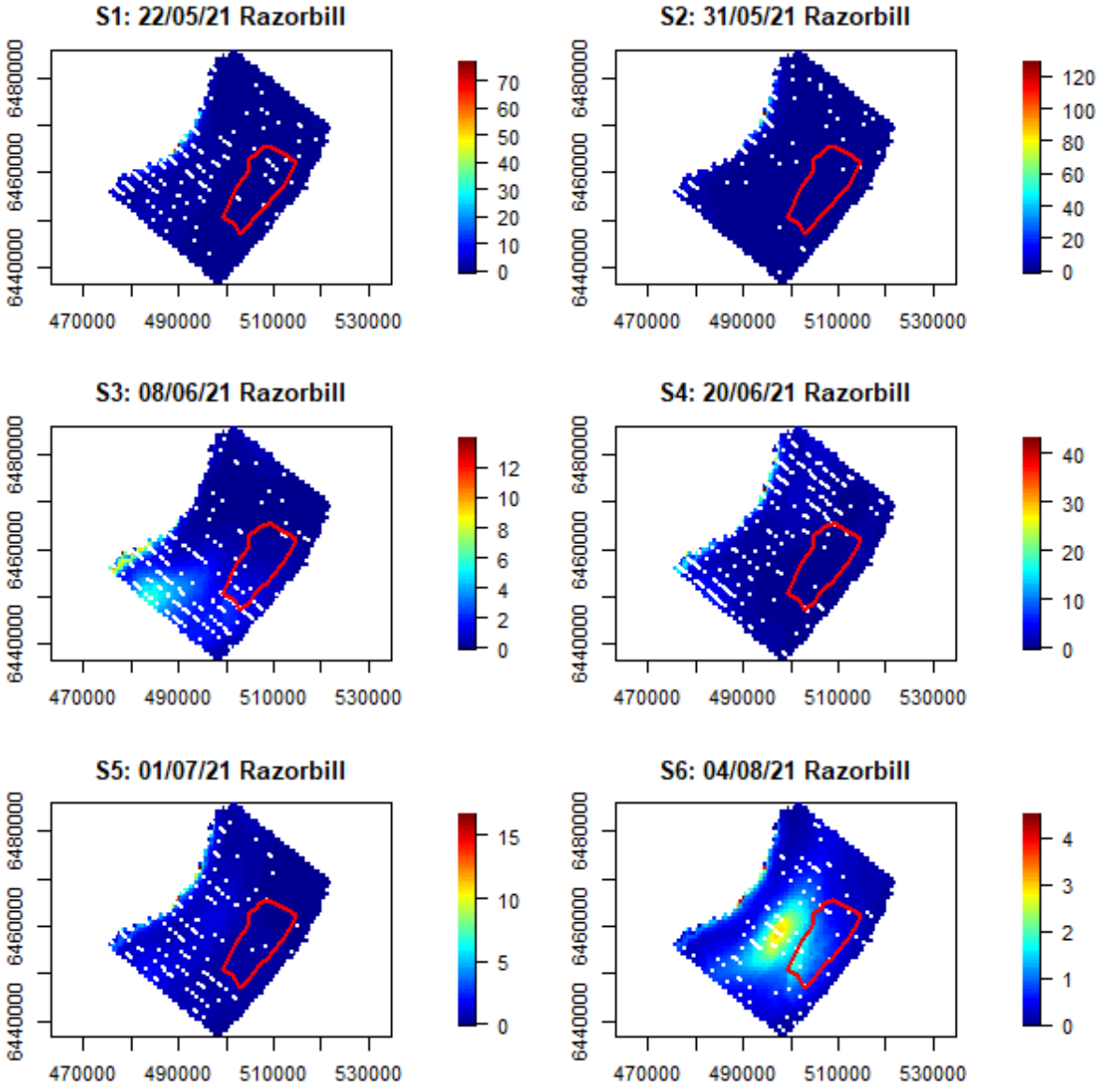

Figure 3-4. Razorbill distributions in 2021 (scale bars indicate birds/km²). Density surfaces generated using the best fit spatial model for each survey (note the scale differs for each survey). White dots are birds recorded on the water (standard intensity data only).

In 2015 the peak gannet estimate was 700 in the total survey area in early July, of which 230 were estimated to be present within the Wind Farm. In 2019 numbers recorded were generally lower, with an estimate for the early June 2019 survey of 400 in the total area and 130 in the wind farm. The 2021 estimates are very similar, with peaks of nearly 500 in the survey area, but lower in the wind farm with a peak of only 23.

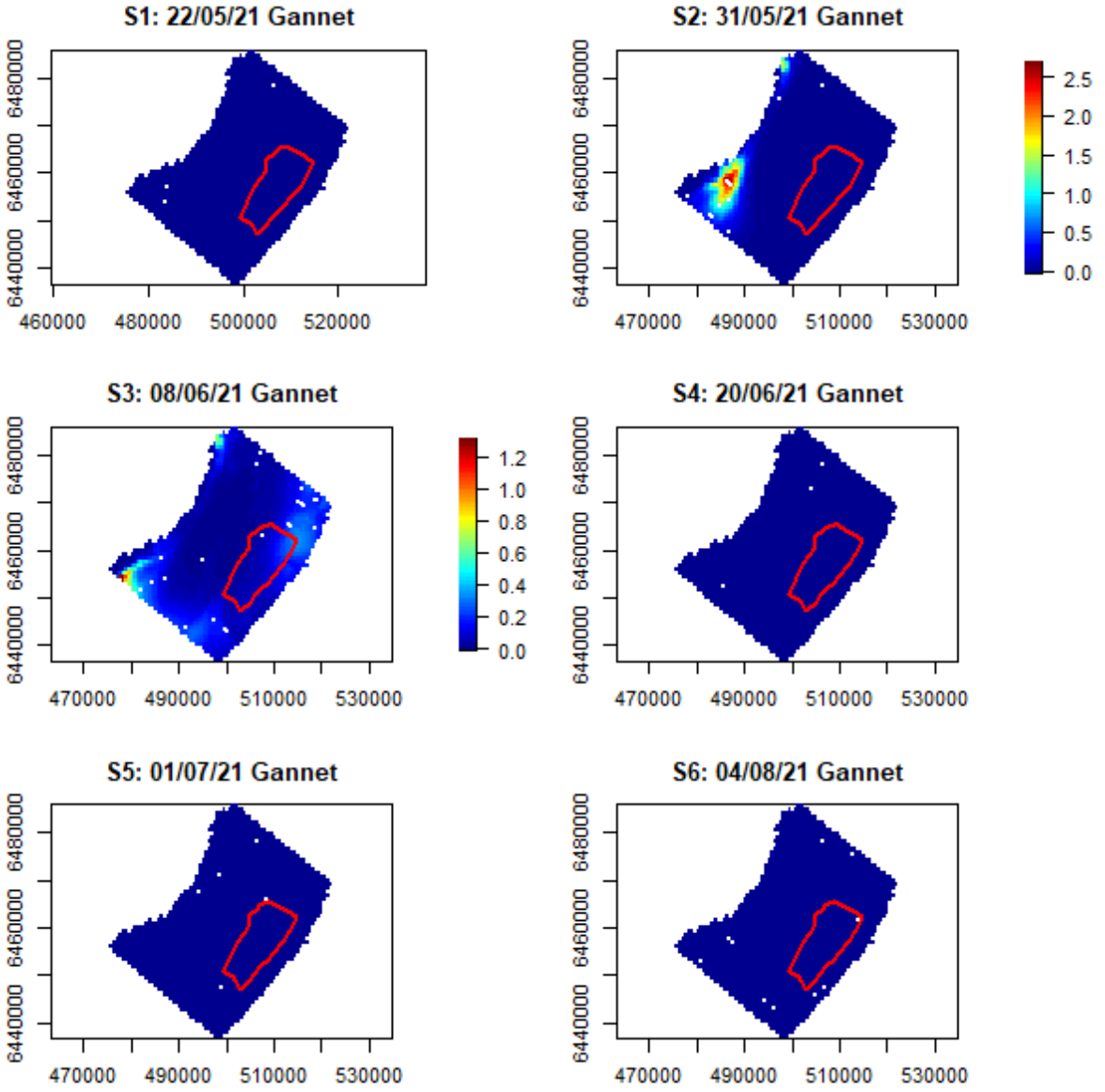

Figure 3-5. Gannet distributions in 2021 (scale bars indicate birds/km²). Density surfaces (surveys 2 and 3) generated using the best fit spatial models (note the scale differs for each survey). White dots are birds recorded on the water (standard intensity data only). Note, too few birds were recorded to permit model fitting on surveys 1,4,5 and 6.

Herring gull and great black-backed gull have been generally recorded in much smaller numbers than the other species, with the consequence that model fitting has generally been much less reliable. Thus, comparisons for these species are based on the design-based estimates.

Herring gulls were recorded in low numbers in 2015, with a peak estimate in the survey area of 400 (July) and only 5 in the wind farm, recorded on a single survey (June). In 2019 a peak estimate of over 5,000 was obtained, of which 1,600 were in the wind farm. The 2021 surveys were similar to the 2015 results, with a peak of 600 in the survey area, and none recorded in the wind farm on all but one survey, when a wind farm estimate of 10 was obtained.

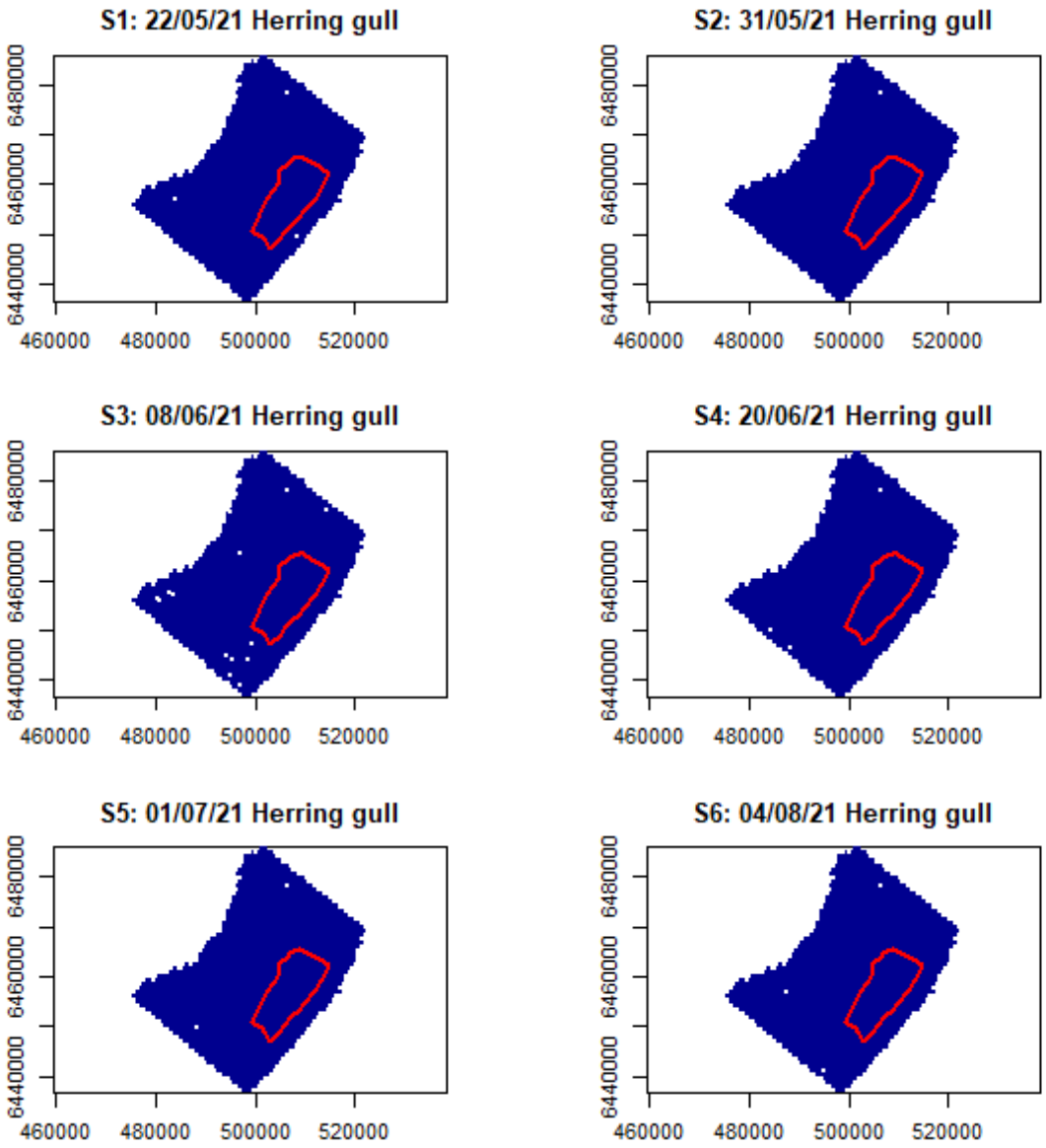

Figure 3-6. Herring gull distributions in 2021. No density surfaces could be fitted to the data due to small sample sizes. White dots are birds recorded on the water (standard intensity data only).

Great black-backed gull is the least abundant of the focal species, with a 2015 peak in the survey area of 50 and in the wind farm of 15 and in 2019 equivalent figures of 319 and 41, respectively. The 2021 estimates were closer to the 2015 ones, with a survey area peak of 86 and a wind farm one of 41.

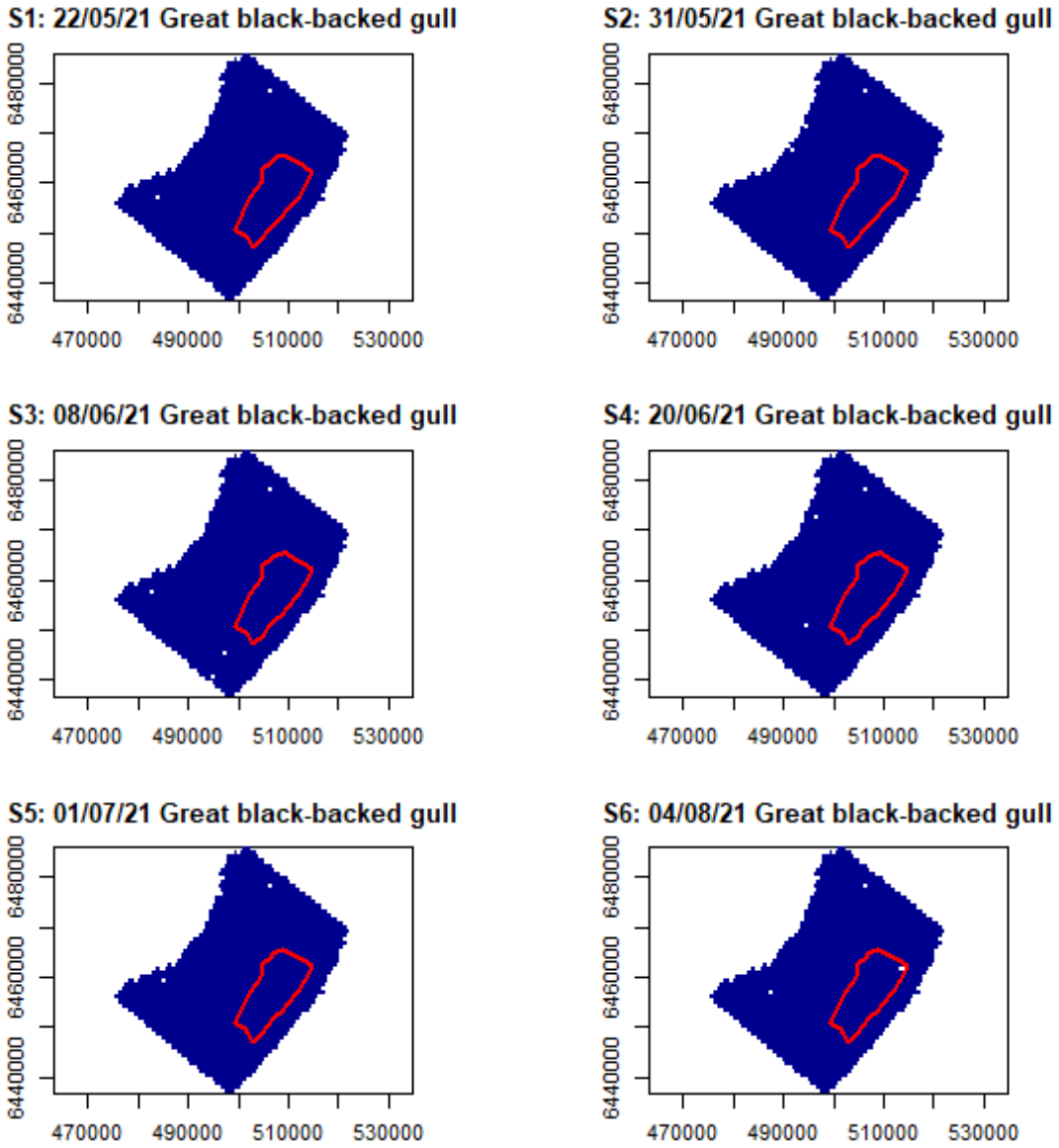

Figure 3-7. Great black-backed gull distributions in 2021. No density surfaces could be fitted to the data due to small sample sizes. White dots are birds recorded on the water (standard intensity data only).

3.4 Spatial modelling comparisons: pre vs post-1, pre vs. post-2 and post-1 vs post-2

Three pair-wise spatial models were fitted to the data for gannet, guillemot, razorbill, puffin and kittiwake. These provided two before-after comparisons and an additional one comparing the two post construction survey years. The expectation from these analyses, for a species which avoids the wind farm, would be to observe reduced densities in the wind farm in the second surveys of the two before-after models and no apparent difference in the pattern in distributions for the

comparison of the two post-construction datasets. The full tables of model coefficients are provided in ANNEX C and the model partial plots are provided in ANNEX D.

3.4.1 Gannet

The chi-squared spatial model terms are provided in Table 3-5 and discussed below.

Table 3-5. Gannet spatial model anova tables. Only terms retained in the final model are presented. The spatial term is denoted as 's(x,y)' and the interaction between that and wind farm or year as 's(x,y) : wind farm' or 's(x,y) : year'. Significance is indicated as follows: non-significant '-', 0.05-0.01 '*', 0.01-0.001 '', <0.001 '***'. Significant terms marked in bold.**

Comparison	Parameter	d.f.	Chisq.	P (>Chisq)	Significance
Pre - Post1	**Wind farm**	1	3.835	0.050	.
	Depth	3	5.051	0.168	-
	Distance to coast	3	14.174	0.003	**
	s(x,y)	5	25.818	0.000	***
	s(x,y) : wind farm	5	15.616	0.008	***
Pre - Post2	Wind farm	1	1.775	0.183	-
	Depth	3	4.294	0.231	-
	Distance to coast	3	11.804	0.008	**
	s(x,y)	4	13.502	0.009	**
	s(x,y) : wind farm	4	20.988	0.000	***
Post1 - Post2	Year	1	0.833	0.361	-
	Depth	3	5.458	0.141	-
	Distance to coast	3	10.801	0.013	*
	s(x,y)	4	9.744	0.045	*
	s(x,y) : year	4	2.835	0.586	-

3.4.1.1 Pre vs. Post-1

There was an overall decline in abundance between 2015 and 2019, which was marginally significant with the wind farm term having a value of 3.58 (p=0.05) and also a highly significant interaction between wind farm and the spatial smoother with a value of 15.62 (p<0.01). Plotting of the spatially explicit differences indicated a significant decrease in the middle of the survey area which included the wind farm and extended towards the coast (Figure 3-8, top row), with areas of significant increase around the edges of the survey area.

3.4.1.2 Pre vs. Post-2

There was no overall difference in abundance between 2015 and 2021, with the wind farm term having a value of 1.77 (p=0.18), but there was a highly significant interaction between wind farm and spatial smoother with a value of 20.99 (p<0.001). Plotting of the spatially explicit differences indicated a significant decrease in the middle of the survey area centred on the wind farm and an area of significant increase in the south-west corner of the survey area (Figure 3-8, middle row).

3.4.1.3 Post-1 vs. Post-2

There was no overall difference in abundance between 2019 and 2021, with the year term having a value of 0.83 (p=0.36), and there was also no significant interaction between year and spatial smoother with a value of 2.83 (p=0.58). Plotting of the spatially explicit differences indicated no areas of significant decrease or increase across the survey area (Figure 3-8, bottom row).

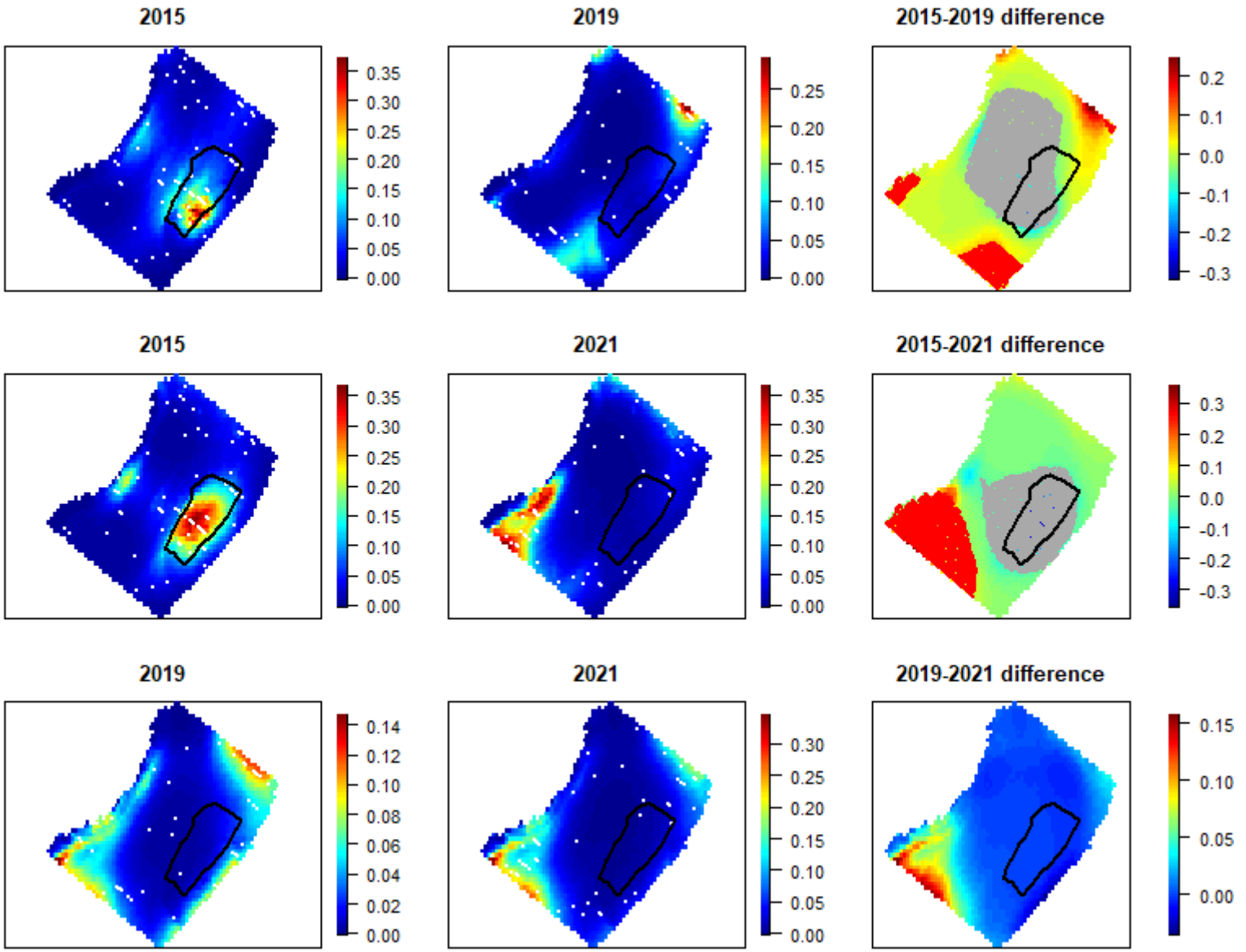

Figure 3-8. Gannet before-after plots for all pair-wise comparisons. Areas of significant increase in abundance are marked on the right-hand column with red symbols, significant reductions in grey.

3.4.2 Guillemot

The chi-squared spatial model terms are provided in Table 3-6 and discussed below.

Table 3-6. Guillemot spatial model anova tables. Only terms retained in the final model are presented. The spatial term is denoted as 's(x,y)' and the interaction between that and wind farm or year as 's(x,y) : wind farm' or 's(x,y) : year'. Significance is indicated as follows: non-significant '-', 0.05-0.01 '*', 0.01-0.001 '', <0.001 '***'. Significant terms marked in bold.**

Comparison	Parameter	d.f.	Chisq.	P(>Chisq)	Significance
Pre - Post1	**Wind farm**	1	20.880	0.000	***
	Depth	3	8.171	0.043	*
	Distance to coast	3	65.235	0.000	***
	s(x,y)	5	24.054	0.000	***
	s(x,y) : wind farm	5	17.860	0.003	**
Pre - Post2	**Wind farm**	1	9.899	0.002	**
	Depth	3	33.953	0.000	***
	Distance to coast	4	53.932	0.000	***
	s(x,y)	4	21.578	0.000	***
	s(x,y) : wind farm	4	17.831	0.001	**
Post1 - Post2	Year	1	1.469	0.226	-
	Distance to coast	4	96.088	0.000	***
	s(x,y)	5	34.933	0.000	***
	s(x,y) : year	5	10.262	0.068	-

3.4.2.1 Pre vs. Post-1

There was an overall increase in abundance between 2015 and 2019, which was highly significant with the wind farm term having a value of 20.88 ($p<0.001$) and also a significant interaction between wind farm and spatial smoother with a value of 17.86 ($p<0.01$). Plotting of the spatially explicit differences indicated a small area of significant decrease in the north-west corner of the survey area and large areas of significant increase across the southern and northern edges of the survey area (Figure 3-9, top row). Over the wind farm itself there was no indication of any change in abundance.

3.4.2.2 Pre vs. Post-2

There was an overall increase in abundance between 2015 and 2021, which was significant with the impact term having a value of 9.89 ($p<0.01$) and also a highly significant interaction between impact and spatial smoother with a value of 17.83 ($p<0.001$). Plotting of the spatially explicit differences indicated a small area of significant decrease in the centre of the survey area which overlapped the western edge of the wind farm (Figure 3-9, middle row). There was a large area of significant increase in abundance across the lower half and western and eastern edges of the survey area. Across the remainder of the wind farm there was little indication of any change in abundance.

3.4.2.3 Post-1 vs. Post-2

There was no overall difference in abundance between 2019 and 2021, with the year term having a value of 1.47 (p=0.23), and there was also no significant interaction between year and spatial smoother with a value of 10.26 (p=0.068). Plotting of the spatially explicit differences indicated an area of significant decrease in the centre of the survey area which partially overlapped the wind farm (Figure 3-9, bottom row), with small areas of increase near the coast and in the southern corner of the survey area.

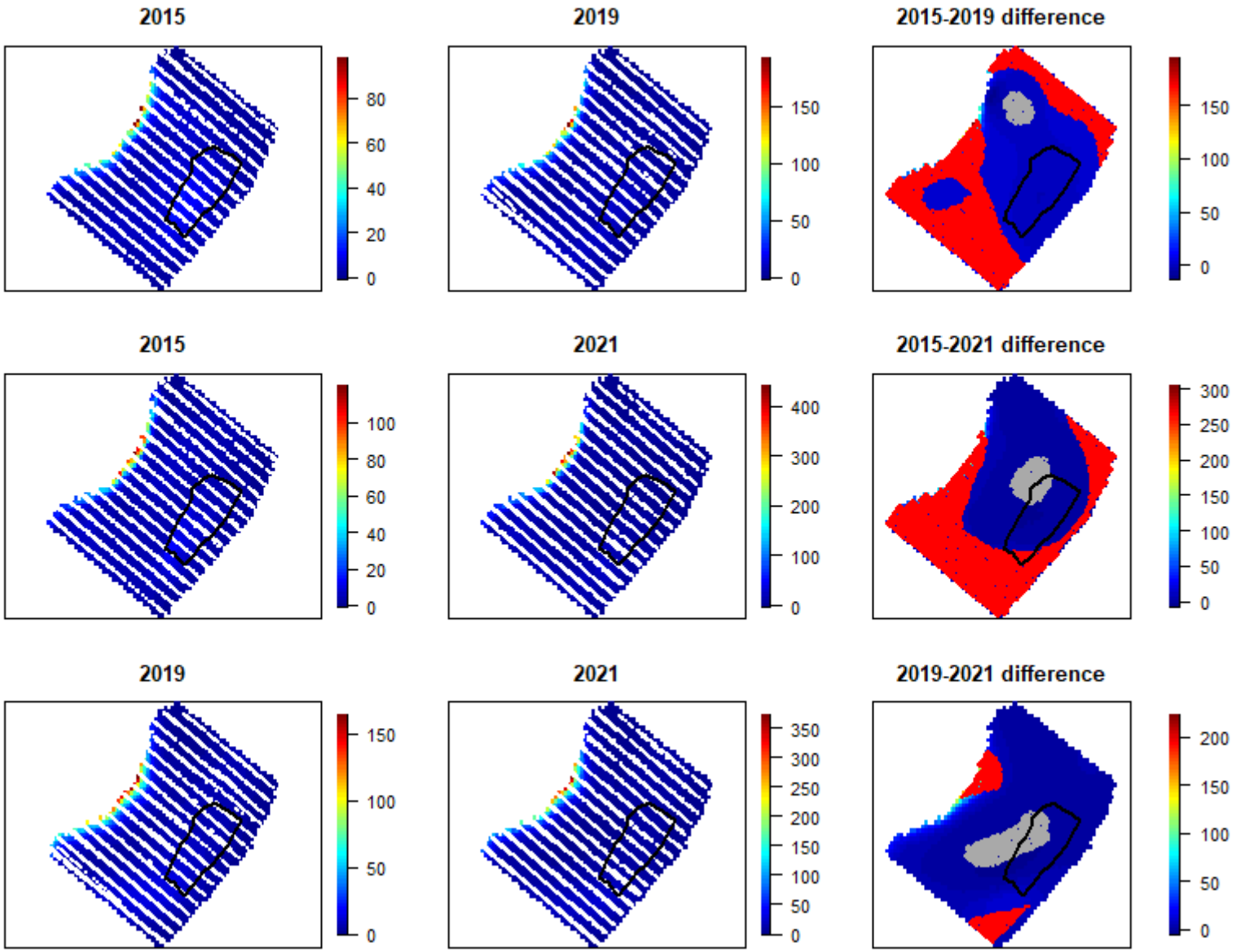

Figure 3-9. Guillemot before-after plots for all pair-wise comparisons. Areas of significant increase in abundance are marked on the right-hand column with red symbols, significant reductions in grey.

3.4.3 Kittiwake

The chi-squared spatial model terms are provided in Table 3-7 and discussed below.

Table 3-7. Kittiwake spatial model anova tables. Only terms retained in the final model are presented. The spatial term is denoted as 's(x,y)' and the interaction between that and wind farm or year as 's(x,y) : wind farm' or 's(x,y) : year'. Significance is indicated as follows: non-significant '-', 0.05-0.01 '*', 0.01-0.001 '', <0.001 '***'. Significant terms marked in bold.**

Comparison	Parameter	d.f.	Chisq.	P(>Chisq)	Significance
Pre - Post1	Wind farm	1	3.421	0.064	-
	Depth	3	17.233	0.001	**
	Distance to coast	5	24.010	0.000	***
	s(x,y)	5	19.749	0.001	**
	s(x,y) : wind farm	5	13.313	0.021	*
Pre - Post2	Wind farm	1	3.517	0.061	-
	Depth	5	18.280	0.003	**
	Distance to coast	3	13.191	0.004	**
	s(x,y)	4	9.178	0.057	*
	s(x,y) : wind farm	4	2.578	0.631	-
Post1 - Post2	Year	1	0.013	0.910	-
	Depth	4	9.263	0.055	-
	Distance to coast	4	15.261	0.004	*
	s(x,y)	5	7.233	0.204	-
	s(x,y) : year	5	22.818	0.000	***

3.4.3.1 *Pre vs. Post-1*

There was no overall change in abundance between 2015 and 2019, with the impact term having a value of 3.42 (p=0.06), although there was a significant interaction between wind farm and spatial smoother with a value of 13.31 (p=0.02). Plotting of the spatially explicit differences indicated areas of significant increase along the western edge of the wind farm and to the north-east of the survey area, with a decrease along the coast (Figure 3-10, top row). Over the remainder of the wind farm itself there was an indication of a small increase in abundance (albeit not significant).

3.4.3.2 *Pre vs. Post-2*

There was an overall increase in abundance between 2015 and 2021, although this was not significant with the wind farm term having a value of 3.52 (p=0.06), and there was no interaction between wind farm and spatial smoother with a value of 2.58 (p=0.63). Plotting of the spatially explicit differences indicated small areas of significant increase in the south-western part of the survey area (Figure 3-10, middle row). There was no indication of any change in abundance across the rest of the survey area, including the wind farm.

3.4.3.3 Post-1 vs. Post-2

There was no overall difference in abundance between 2019 and 2021, with the year term having a value of 0.013 ($p=0.9$), but there was a highly significant interaction between year and spatial smoother with a value of 22.82 ($p<0.001$). Plotting of the spatially explicit differences indicated an area of significant decrease which included the northern half of the wind farm, and an area of significant increase near the coast (Figure 3-10, bottom row).

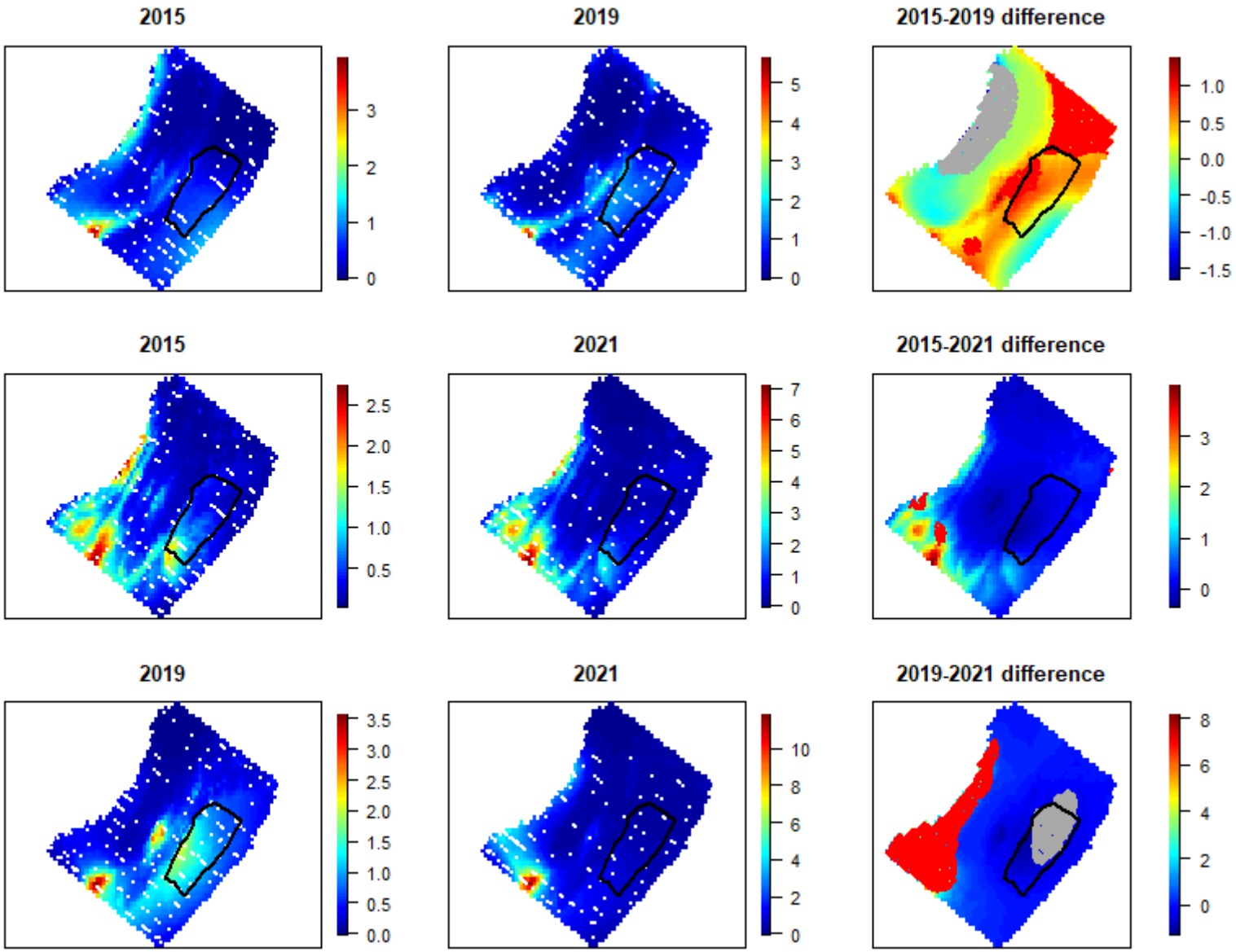

Figure 3-10. Kittiwake before-after plots for all pair-wise comparisons. Areas of significant increase in abundance are marked on the right-hand column with red symbols, significant reductions in grey.

3.4.4 Razorbill

The chi-squared spatial model terms are provided in Table 3-8 and discussed below.

Table 3-8. Razorbill spatial model anova tables. Only terms retained in the final model are presented. The spatial term is denoted as 's(x,y)' and the interaction between that and wind farm or year as 's(x,y) : wind farm' or 's(x,y) : year'. Significance is indicated as follows: non-significant '-', 0.05-0.01 '*', 0.01-0.001 '', <0.001 '***'. Significant terms marked in bold.**

Comparison	Parameter	d.f.	Chisq.	P(>Chisq)	Significance
Pre - Post1	**Wind farm**	1	15.541	0.000	***
	Distance to coast	3	86.192	0.000	***
	s(x,y)	4	12.094	0.017	*
	s(x,y) : wind farm	4	9.613	0.047	*
Pre - Post2	**Wind farm**	1	8.243	0.004	**
	Depth	6	40.682	0.000	***
	Distance to coast	6	84.379	0.000	***
	s(x,y)	5	21.483	0.001	**
	s(x,y) : wind farm	5	10.181	0.070	-
Post1 - Post2	Year	1	0.092	0.762	-
	Distance to coast	3	182.909	0.000	***
	s(x,y)	4	48.047	0.000	***
	s(x,y) : year	4	1.880	0.758	-

3.4.4.1 Pre vs. Post-1

There was an overall increase in abundance between 2015 and 2019, which was highly significant with the wind farm term having a value of 15.5 ($p<0.001$) and also a significant interaction between wind farm and spatial smoother with a value of 9.61 ($p=0.047$). Plotting of the spatially explicit differences indicated large areas of significant increase extending across most of the survey area, including the wind farm, and no areas of significant decrease (Figure 3-11, top row).

3.4.4.2 Pre vs. Post-2

There was an overall increase in abundance between 2015 and 2021, which was significant with the wind farm term having a value of 8.24 ($p<0.01$) but there was no interaction between wind farm and spatial smoother with a value of 10.18 ($p=0.07$). Plotting of the spatially explicit differences indicated large areas of significant increase extending across most of the survey area, including the southern half of the wind farm, and no areas of significant decrease (Figure 3-11, middle row).

3.4.4.3 Post-1 vs. Post-2

There was no overall difference in abundance between 2019 and 2021, with the year term having a value of 0.092 ($p=0.76$), and there was also no significant interaction between year and spatial smoother with a value of 1.88 ($p=0.76$). Plotting of the spatially explicit differences indicated no areas of significant increase or decrease across the survey area (Figure 3-11, bottom row).

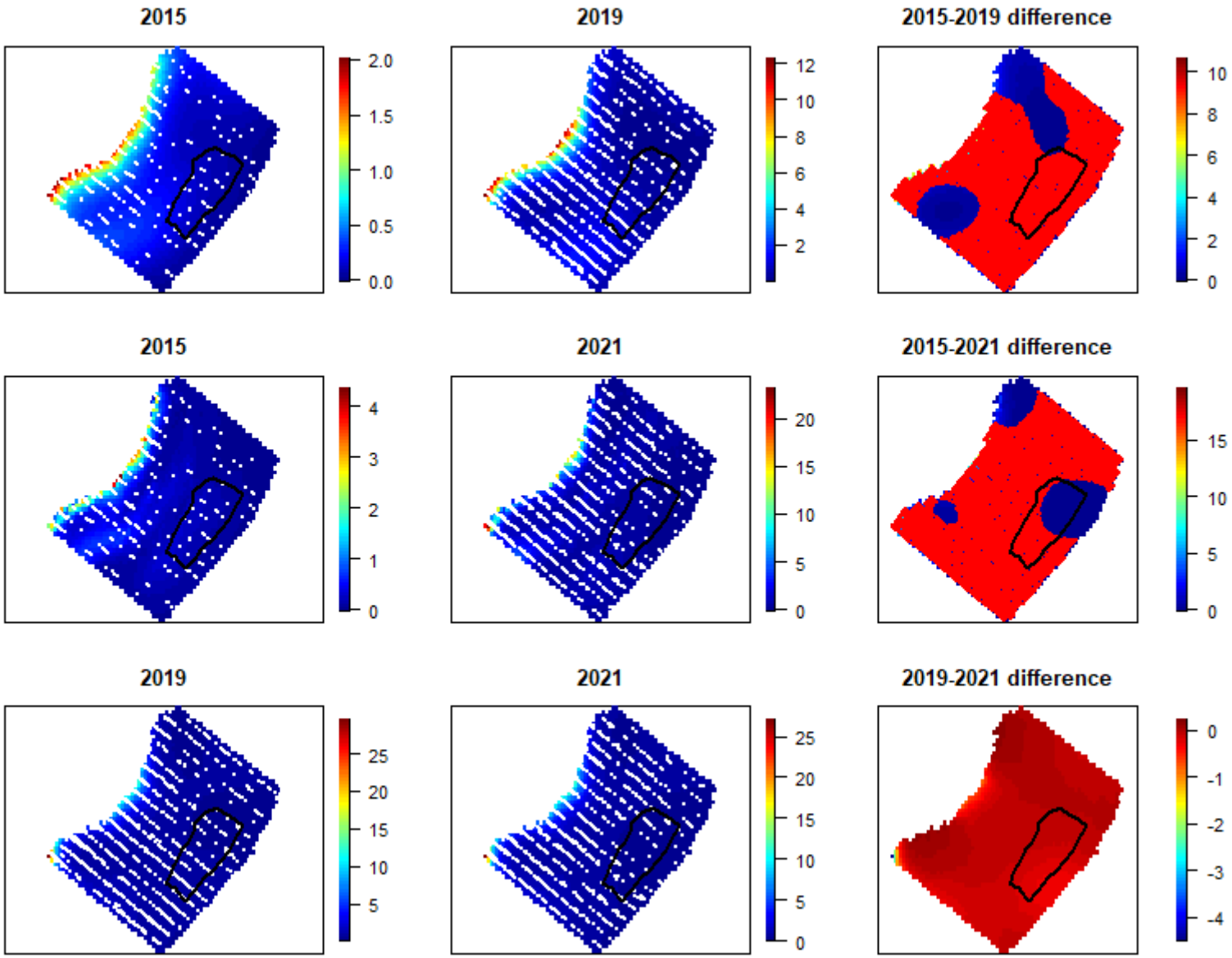

Figure 3-11. Razorbill before-after plots for all pair-wise comparisons. Areas of significant increase in abundance are marked on the right-hand column with red symbols, significant reductions in grey.

3.4.5 Puffin

The chi-squared spatial model terms are provided in Table 3-9 and discussed below.

Table 3-9. Puffin spatial model anova tables. Only terms retained in the final model are presented. The spatial term is denoted as 's(x,y)' and the interaction between that and wind farm or year as 's(x,y) : wind farm' or 's(x,y) : year'. Significance is indicated as follows: non-significant '-', 0.05-0.01 '*', 0.01-0.001 '', <0.001 '***'**

Comparison	Parameter	d.f.	Chisq.	P(>Chisq)	Significance
Pre - Post1	Wind farm	1	0.901	0.343	-
	Depth	1	73.148	0.000	***
	Distance to coast	1	15.591	0.000	***
	s(x,y)	5	27.249	0.000	***
	s(x,y) : wind farm	5	57.766	0.000	***
Pre - Post2	Wind farm	1	0.438	0.508	-
	Depth	1	3.670	0.055	-
	Distance to coast	6	881.958	0.000	***
	s(x,y)	5	18.411	0.002	**
	s(x,y) : wind farm	5	11.420	0.044	*
Post1 - Post2	**Year**	1	38.381	0.000	***
	Depth	5	8.876	0.114	-
	Distance to coast	3	20.363	0.000	***
	s(x,y)	5	21.196	0.001	**
	s(x,y) : year	5	27.120	0.000	***

3.4.5.1 Pre vs. Post-1

There was no overall change in abundance between 2015 and 2019, with the wind farm term having a value of 0.90 ($p=0.34$), but there was a significant interaction between wind farm and spatial smoother with a value of 57.77 ($p<0.001$). Plotting of the spatially explicit differences indicated large areas of significant decrease extending across approximately half of the survey area away from the coast and including the wind farm (Figure 3-12, top row).

3.4.5.2 Pre vs. Post-2

There was an overall increase in abundance between 2015 and 2021, but this was not significant with the wind farm term having a value of 0.44 ($p=0.51$) however there was a significant interaction between wind farm and spatial smoother with a value of 11.42 ($p<0.04$). Plotting of the spatially explicit differences indicated large areas of significant increase extending across most of the survey area (Figure 3-12, middle row).

3.4.5.3 Post-1 vs. Post-2

There was a significant increase in the overall abundance between 2019 and 2021, with the year term having a value of 38.38 ($p<0.001$), and there was also a significant interaction between year and spatial smoother with a value of 27.12 ($p<0.001$). Plotting of the spatially explicit differences

indicated that this increase had occurred across almost the entire survey area (Figure 3-12, bottom row), with a small area along the coast with no significant change.

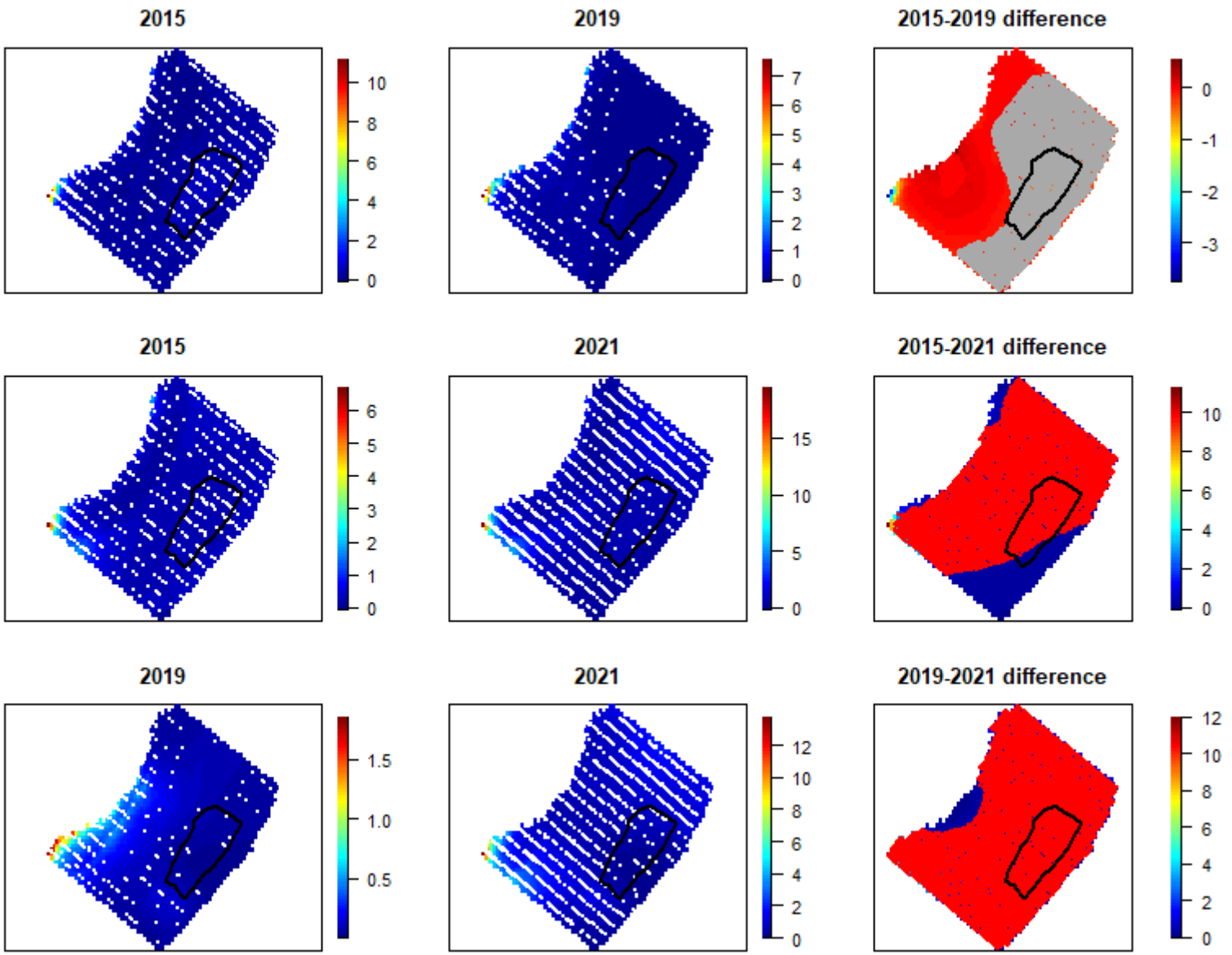

Figure 3-12. Puffin before-after plots for all pair-wise comparisons. Areas of significant increase in abundance are marked on the right-hand column with red symbols, significant reductions in grey.

3.5 Model diagnostics

The potential for the spatial modelling results to be strongly influenced by individual surveys was tested using the *runInfluence* function in MRSea (see ANNEX E for results). This was considered at the level of individual surveys (i.e. 1 – 18). While these tests did indicate the presence of outliers in the data since the values were calculated as quantiles by definition there will be points outside the 95% confidence interval. However, these outliers were not a large distance outside the range of the remaining data, and the analysis revealed that outliers were recorded across multiple surveys in all years. Therefore, these tests did not find evidence that the combined distributions as presented above were driven by particular surveys and the observed redistributions are considered robust.

3.6 Abundance of birds in flight

The abundances of birds recorded in flight across the total survey area and within the Wind Farm are presented in Table 3-10. Comparison of the design-based estimates for birds on the water (Table 3-4) and birds in flight (Table 3-10) across all years reveals a split between gannet and the gull species (kittiwake, herring gull and great black-backed gull) and the auks. When looked at across all the surveys, the former species were recorded as often, or more often, in flight as on the water (in-flight: gannet 45%, kittiwake 56%, great black-backed gull 51% and herring gull 51%), while the latter were recorded much more often on the water (in flight: guillemot 8%, puffin 3% and razorbill 10%). These differences were consistent within each year with little apparent variation between the overall survey area and the wind farm. This presumably reflects differences in the species' foraging ecology, with gannets and gulls foraging on the wing, whereas auks forage from the sea surface and predominantly fly only between foraging locations or between foraging locations and the colony if they are breeding birds. Thus, gulls are equally likely to be recorded in flight as on the sea leading to a high degree of correlation, whereas auks are much more likely to be recorded on the sea surface than in flight and with no particular reason for the two estimates to be correlated.

Table 3-10. Design-based population abundance estimates of birds in flight in the total survey area and within the Wind Farm boundary for each species in each survey in 2015, 2019 and 2021. Abundance across the total survey area was estimated using the standard intensity data, Wind Farm abundance was estimated using the high intensity data.

Species	Year	Area	Population abundance on each survey					
			1	2	3	4	5	6
Gannet	2015	Total survey area	764.4 (512.7-1015.5)	148.9 (70.4-231.2)	169.4 (90.5-261.4)	120.1 (50.3-191)	81 (20.1-150.8)	140.6 (60.3-251.3)
		Wind Farm	66.3 (20.1-130.7)	20.6 (0-45.2)	60.8 (25.1-100.5)	10.2 (0-25.1)	20 (0-50.3)	0 (0-0)
	2019	Total survey area	61 (20.1-110.6)	570.7 (140.7-1226.6)	20 (0-50.3)	81 (30.2-140.7)	19.1 (0-60.3)	49.8 (10.1-100.5)
		Wind Farm	0 (0-0)	0 (0-0)	0 (0-0)	0 (0-0)	0 (0-0)	4.9 (0-15.1)
	2021	Total survey area	83.4 (27.8-157.6)	266.2 (38-656)	259.6 (144.2-384.6)	209.7 (85.8-371.7)	152.6 (57.2-276.5)	27.9 (0-74.3)
		Wind Farm	0 (0-0)	15.4 (0-41)	5.2 (0-15.6)	0 (0-0)	0 (0-0)	0 (0-0)

Species	Year	Area	Population abundance on each survey					
			1	2	3	4	5	6
Guillemot	2015	Total survey area	4903.1 (3759.2-6081.5)	5900.7 (4935.5-6956.2)	3802.6 (3025.7-4613.9)	2450.7 (1859.6-3137)	923.1 (442.3-1558.1)	19.9 (0-50.3)
		Wind Farm	182.1 (90.5-291.6)	814.1 (537.7-1146.1)	494 (276.4-789.2)	296.9 (170.9-422.3)	281.4 (55.3-623.2)	0 (0-0)
	2019	Total survey area	3635.5 (2724.1-4674.7)	5766.6 (4644-7026.3)	8175.7 (6614-10094)	6741.9 (5548.7-8011.4)	2420.5 (1809.4-3116.4)	510.6 (291.5-774)
		Wind Farm	153.1 (55.3-286.5)	329.8 (205.9-472.4)	535.9 (281.5-889.6)	445.5 (256.2-653.4)	232.4 (90.5-407.2)	5 (0-15.1)
	2021	Total survey area	3032 (2243.8-3903.8)	3565.4 (2376.9-5067.8)	6672 (5335.2-8162.2)	7615.5 (6185.6-9245.4)	9840.7 (8048-12130.2)	120.8 (55.7-185.8)
		Wind Farm	72 (30.8-123.4)	112.9 (46.2-200.1)	624.1 (257.7-1181.3)	762.3 (432.7-1107.7)	488.3 (282.6-729.9)	0 (0-0)
Kittiwake	2015	Total survey area	3844.2 (2110.9-6021.9)	5014.8 (2934.9-7771.2)	5304.9 (4201.5-6604.7)	5117.2 (4111-6333)	6236.4 (4220.8-8826.7)	811.2 (552.9-1095.7)
		Wind Farm	120.5 (75.4-175.9)	256.4 (130.7-392.2)	1032 (562.8-1613.7)	1253.8 (683.3-1915)	1090.2 (537.8-1814.8)	51 (20.1-85.4)
	2019	Total survey area	5194.9 (3155.8-8102.2)	10412.1 (7950.9-14329.4)	3472.6 (2864.8-4111.3)	4663.8 (3699.1-5719.6)	5848.7 (4533.2-7509.3)	4376.8 (2713.5-6504.1)
		Wind Farm	144.3 (45.2-301.6)	1793.3 (1241.3-2432.6)	556.2 (296.5-879.7)	491 (286.5-723.7)	407 (276.4-562.9)	414.6 (120.6-934.8)
	2021	Total survey area	4747.3 (3347-6462.6)	4630.2 (1473.5-10212.5)	7739.1 (5297-10710.1)	4184.2 (3192.5-5337.8)	4415 (3423.3-5626.7)	4449.7 (3845.7-5146.4)
		Wind Farm	72 (36-118.4)	71.8 (30.8-123.1)	572.5 (304.2-892.2)	695.4 (231.7-1386)	267.3 (113.1-488.3)	531.7 (361.3-707.2)
Puffin	2015	Total survey area	0 (0-0)	193.8 (100.5-301.6)	112.3 (40.2-191)	29.3 (0-70.4)	30.8 (0-90.5)	0 (0-0)
		Wind Farm	0 (0-0)	5.1 (0-15.1)	36.1 (5-75.4)	0 (0-0)	0 (0-0)	0 (0-0)
	2019	Total survey area	20.1 (0-50.3)	159.8 (60.3-271.4)	61.2 (0-160.8)	9.9 (0-30.2)	10 (0-30.2)	19.7 (0-50.3)
		Wind Farm	4.9 (0-15.1)	15 (0-40.2)	5.1 (0-15.1)	0 (0-0)	0 (0-0)	0 (0-0)
	2021	Total survey area	18.5 (0-46.4)	66.6 (19-142.6)	28.8 (0-67.3)	228.8 (104.8-381.3)	114.4 (47.7-190.7)	37.2 (0-102.2)
		Wind Farm	0 (0-0)	0 (0-0)	5.2 (0-15.5)	0 (0-0)	0 (0-0)	0 (0-0)

Species	Year	Area	Population abundance on each survey					
			1	2	3	4	5	6
Razorbill	2015	Total survey area	69 (20.1-120.6)	231.8 (120.6-351.8)	326.1 (180.9-502.6)	40 (10.1-80.4)	19.9 (0-50.3)	0 (0-0)
		Wind Farm	5.1 (0-15.1)	43.7 (9.9-95.5)	19.9 (5-40.2)	0 (0-0)	4.9 (0-15.1)	0 (0-0)
	2019	Total survey area	229.3 (110.6-361.9)	923.1 (613.2-1296.7)	1118.8 (814.2-1457.5)	1316 (965-1678.9)	151.9 (80.2-241.5)	0 (0-0)
		Wind Farm	0 (0-0)	39.9 (15.1-75.4)	35.6 (10.1-70.4)	89.5 (40.2-150.8)	15.1 (0-45.2)	0 (0-0)
	2021	Total survey area	454.3 (241.1-723.2)	104.6 (28.5-190.4)	230.7 (115.4-365.3)	1944.4 (1515.5-2344.7)	953.6 (648.4-1278)	9.3 (0-27.9)
		Wind Farm	15.4 (0-41.1)	5.1 (0-15.4)	15.5 (0-36.1)	67 (20.6-123.8)	46.3 (10.3-87.4)	5.2 (0-15.5)
Great black-backed gull	2015	Total survey area	79.2 (20.1-151)	70 (20.1-130.7)	50.7 (10.1-110.6)	20.1 (0-50.3)	80.3 (30.2-150.8)	60.8 (0-150.8)
		Wind Farm	0 (0-0)	0 (0-0)	0 (0-0)	0 (0-0)	0 (0-0)	10.2 (0-25.1)
	2019	Total survey area	91.3 (30.2-180.9)	91 (40.2-160.8)	70.8 (10.1-160.8)	110.8 (50.3-180.9)	19.9 (0-50.3)	51.1 (10.1-100.5)
		Wind Farm	0 (0-0)	15.5 (0-35.2)	5 (0-15.1)	5.1 (0-15.1)	0 (0-0)	0 (0-0)
	2021	Total survey area	83.4 (27.8-157.9)	57 (19-114.1)	76.9 (28.8-134.6)	57.2 (9.5-114.4)	76.3 (28.6-133.5)	92.9 (37.2-157.9)
		Wind Farm	5.1 (0-15.4)	0 (0-0)	0 (0-0)	5.2 (0-15.5)	0 (0-0)	5.2 (0-15.5)
Herring gull	2015	Total survey area	457.4 (180.9-834.3)	273.5 (150.8-442.3)	321.7 (100.5-663.7)	482.7 (251.3-774)	122.3 (20.1-271.4)	101.8 (20.1-221.1)
		Wind Farm	0 (0-0)	5.3 (0-15.1)	5 (0-15.1)	0 (0-0)	0 (0-0)	0 (0-0)
	2019	Total survey area	692.7 (251.3-1307)	1786.8 (1256.5-2422.8)	886.8 (572.7-1347)	709.1 (341.8-1316.8)	119.8 (30.2-231.2)	151.2 (0-442.3)
		Wind Farm	0 (0-0)	669.2 (266.3-1181.1)	35.3 (10.1-65.3)	35.3 (10.1-70.4)	0 (0-0)	0 (0-0)
	2021	Total survey area	213.3 (92.7-352.3)	361.3 (161.6-627.5)	903.7 (567.2-1249.8)	800.6 (552.8-1077)	1449.4 (762.6-2536.9)	120.8 (46.4-213.7)
		Wind Farm	5.1 (0-15.4)	5.1 (0-15.4)	51.6 (15.5-93)	77.3 (30.9-133.9)	61.7 (10.3-128.5)	5.2 (0-15.5)

3.7 Seabird distributions in relation to turbine locations

The pooled densities of birds within circles of radius 100, 200, 300 and 400m around the turbine locations for each species analysed are summarised in Table 3-11 and plotted for both 2019 and 2021 in Figure 3-13 to Figure 3-17, overlaid on histograms of the densities obtained for 1,000 randomly offset turbine layouts. Across all species, the observed densities (red lines) on the graphs fall within the range of the bootstrapped distributions, typically within the middle of the range. This analysis

therefore strongly indicates these species are not avoiding turbines. In the contrasting situation, if such avoidance behaviour was occurring, the observed densities would be expected to be lower than the resampled ones, which would mean the red lines would be to the left of the histogram peaks.

Empirical p-values were calculated for each species at each radial distance in each year, with both one-sided and two-sided values calculated. The latter (two-sided) makes no assumptions about whether observed responses are avoidance or attraction, while the former provides a stronger test of either response. The one-sided empirical p-values were derived as the number of bootstrap densities less than, and greater than, the observed density respectively (i.e. tests for attraction and avoidance respectively). The two-sided p-values were obtained as the minimum of the one-sided values multiplied by two.

Guillemot, the most numerous species in the surveys, showed no indication of response to the turbines in either 2019 or 2021. However, the overall densities in the wind farm were higher in 2019 (40 to 48 birds/km^2) than 2021 (10 to 15 birds/km^2).

Puffin densities in the wind farm were slightly higher in 2021 than 2019, but there was no indication of any significant responses, either avoidance or attraction in either year.

Razorbills were observed in lower densities in the wind farm in 2021, with around 3 to 5 birds/km^2 in 2019 and between 0.3 and 1.3 birds/km^2 in 2021. There was some indication of attraction in 2019 (p=0.04 within 100m and p=0.03 within 300m) but no significant responses in 2021.

Kittiwake densities were variable in both years and overall slightly higher in 2021, but there was no indication of any significant responses, either avoidance or attraction in either year.

Herring gulls were recorded in the wind farm in larger numbers in 2019, but were almost absent in 2021. In 2019 there was an indication of avoidance within 100m (p<0.01), with higher densities from 300m.

Table 3-11. Densities recorded within 400m of turbines in 2019 and 2021.

Species	Year	Observed density (birds/km^2)				Sample size
		<100m	<200m	<300m	<400m	
Guillemot	2019	47.6	41.3	40.7	41.6	6941
	2021	13.07	14.56	11.32	10.51	4297
Puffin	2019	0.0	0.20	0.31	0.31	44
	2021	0.57	0.50	0.81	0.71	197
Razorbill	2019	5.41	3.26	3.20	2.86	557
	2021	0.28	1.07	1.36	1.31	385
Kittiwake	2019	1.35	3.87	4.93	6.66	1733
	2021	9.38	5.04	3.40	2.58	869
Herring gull	2019	0	13.91	10.25	6.15	465
	2021	0	0	0	0	2

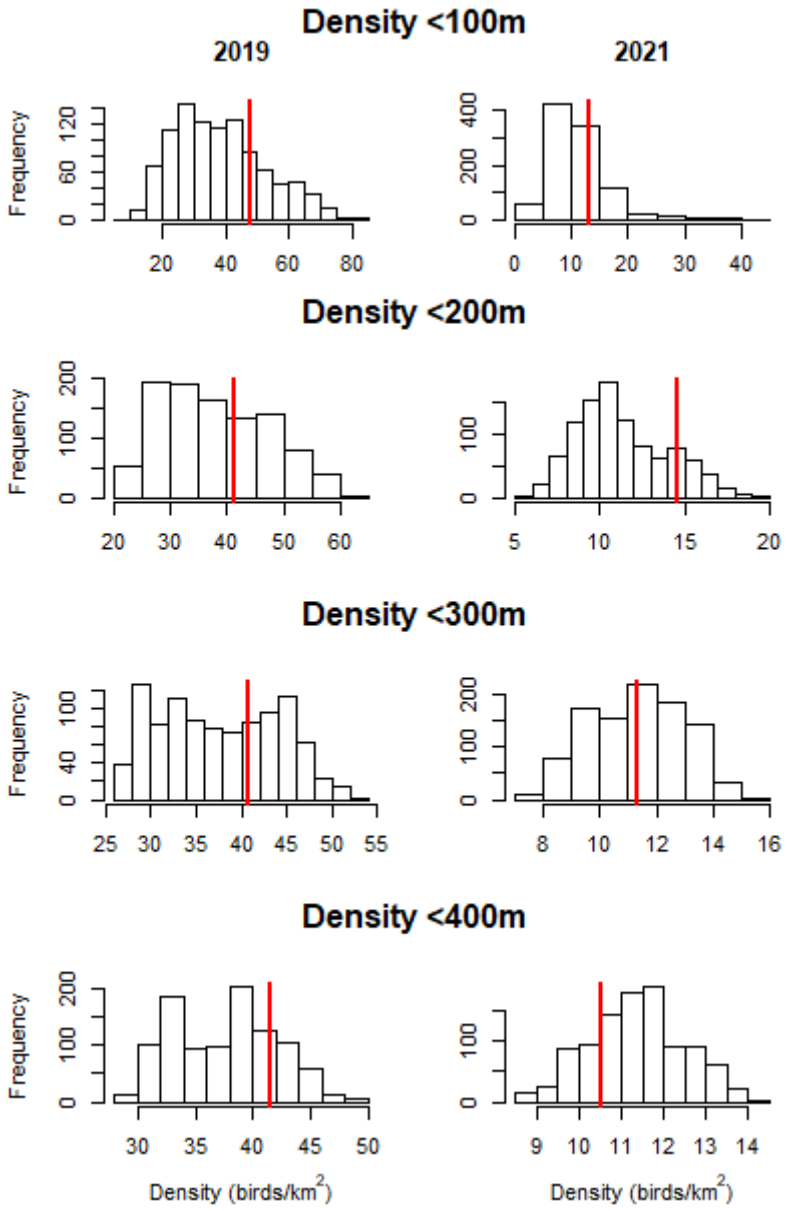

Figure 3-13. Guillemot densities in 2019 (left) and 2021 (right) within 100/200/300/400m of turbine locations (red lines) and distribution of densities estimated for 1,000 simulations with randomly re-positioned turbines (relative turbine positions maintained). Data combined across all six surveys.

Table 3-12. Guillemot empirical p-values of likelihood that observed densities around turbines would be obtained by chance. Significant (<0.05) values highlighted in bold.

Test	Year	<100m	<200m	<300m	<400m
1-sided (avoidance)	2019	0.76	0.64	0.62	0.79
1-sided (attraction)		0.24	0.36	0.38	0.21
2-sided		0.49	0.71	0.76	0.42
1-sided (avoidance)	2021	0.72	0.85	0.47	0.22
1-sided (attraction)		0.28	0.15	0.53	0.78
2-sided		0.56	0.31	0.95	0.44

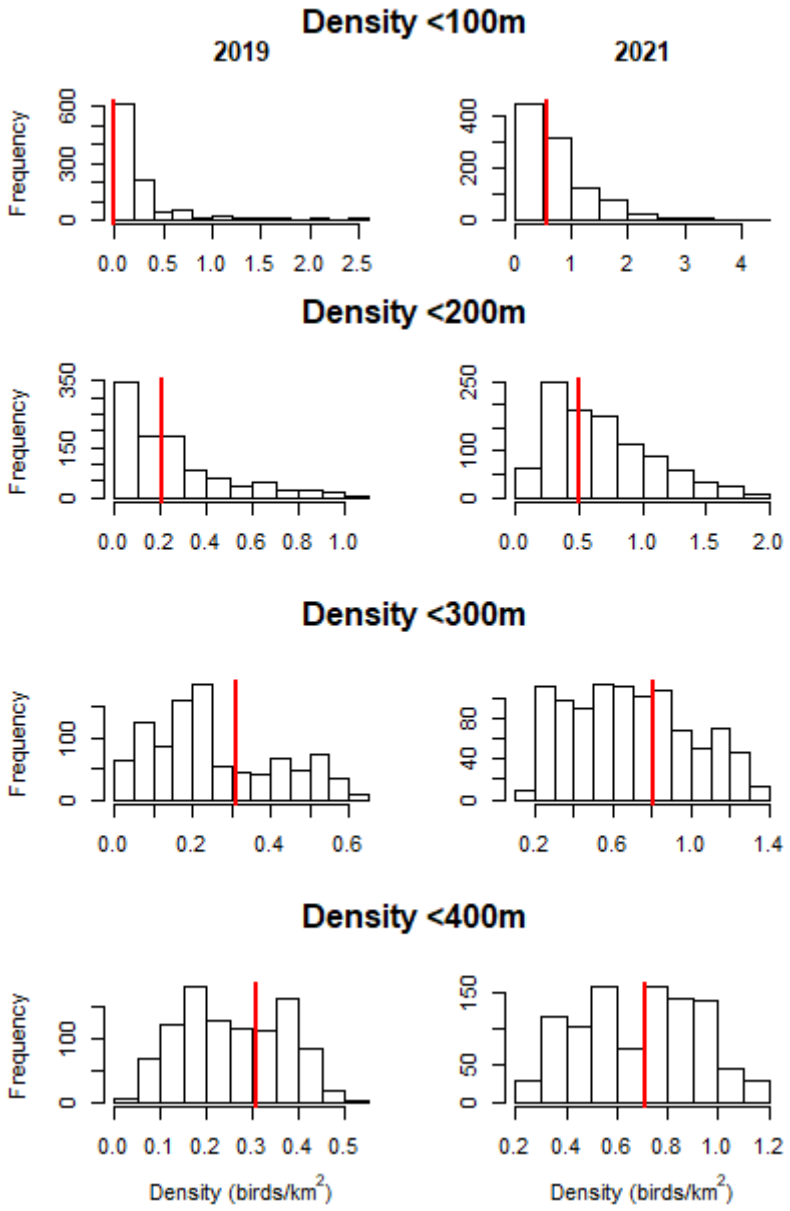

Figure 3-14. Puffin densities in 2019 (left) and 2021 (right) within 100/200/300/400m of turbine locations (red lines) and distribution of densities estimated for 1,000 simulations with randomly re-positioned turbines (relative turbine positions maintained). Data combined across all six surveys.

Table 3-13. Puffin empirical p-values of likelihood that observed densities around turbines would be obtained by chance. Significant (<0.05) values highlighted in bold.

Test	Year	<100m	<200m	<300m	<400m
1-sided (avoidance)	2019	0	0.55	0.70	0.64
1-sided (attraction)		0.39	0.45	0.30	0.36
2-sided		0	0.90	0.61	0.73
1-sided (avoidance)	2021	0.47	0.42	0.65	0.50
1-sided (attraction)		0.53	0.58	0.35	0.50
2-sided		0.95	0.84	0.70	0.99

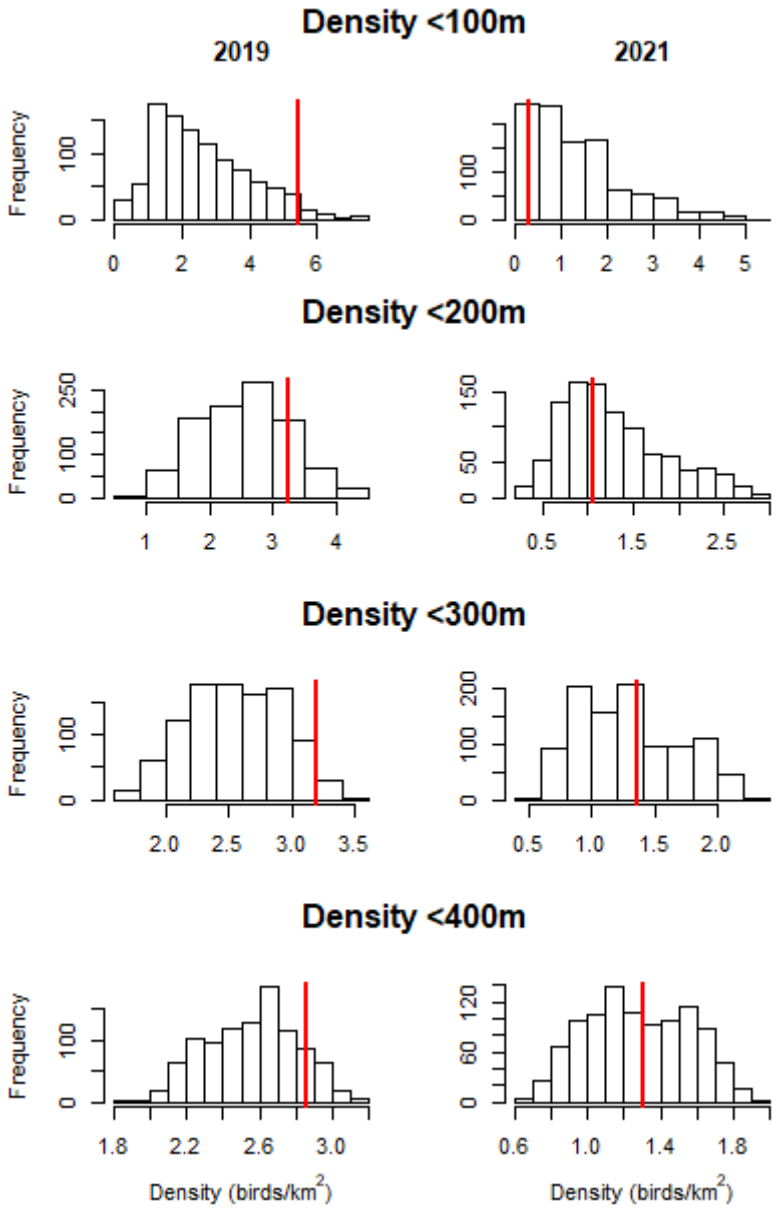

Figure 3-15. Razorbill densities in 2019 (left) and 2021 (right) within 100/200/300/400m of turbine locations (red lines) and distribution of densities estimated for 1,000 simulations with randomly re-positioned turbines (relative turbine positions maintained). Data combined across all six surveys.

Table 3-14. Razorbill empirical p-values of likelihood that observed densities around turbines would be obtained by chance. Significant (<0.05) values highlighted in bold.

Test	Year	<100m	<200m	<300m	<400m
1-sided (avoidance)	2019	0.96	0.84	0.97	0.88
1-sided (attraction)		**0.04**	0.16	**0.03**	0.12
2-sided		0.07	0.32	0.06	0.25
1-sided (avoidance)	2021	0.16	0.42	0.61	0.55
1-sided (attraction)		0.84	0.58	0.39	0.45
2-sided		0.32	0.84	0.77	0.89

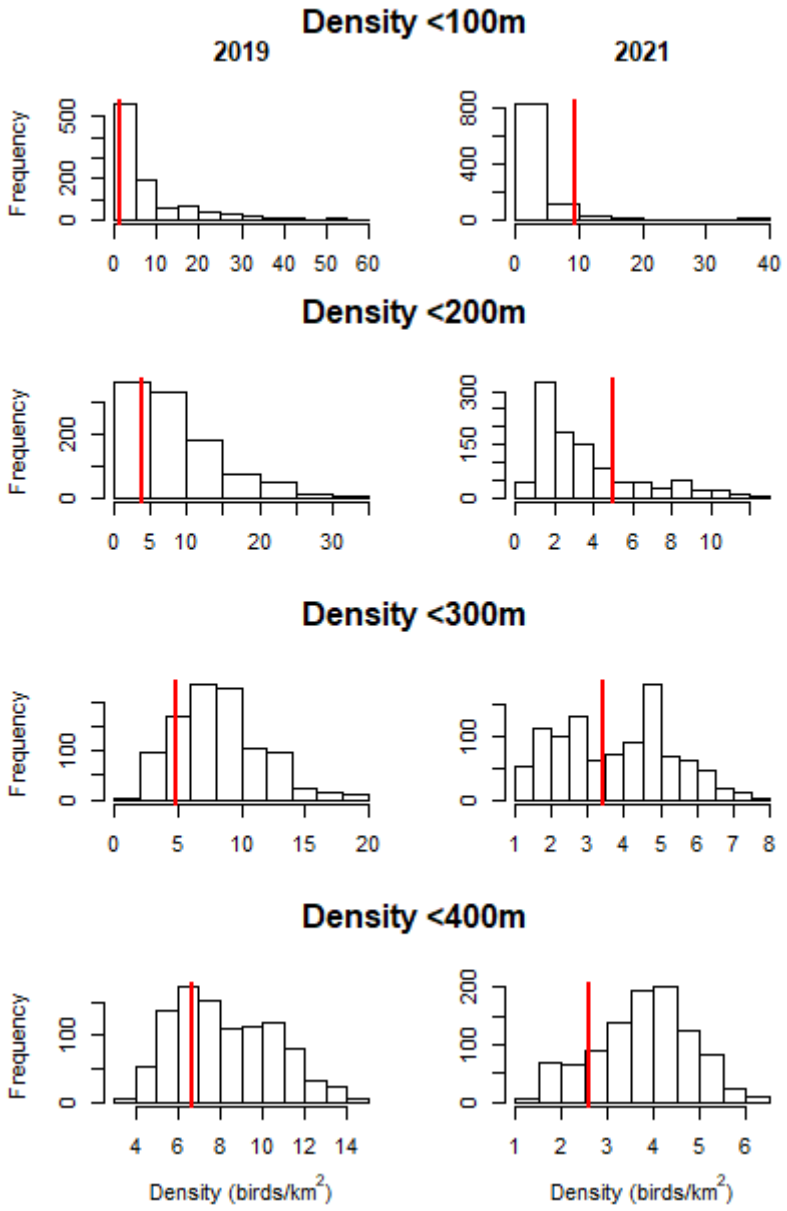

Figure 3-16. Kittiwake densities in 2019 (left) and 2021 (right) within 100/200/300/400m of turbine locations (red lines) and distribution of densities estimated for 1,000 simulations with randomly re-positioned turbines (relative turbine positions maintained). Data combined across all six surveys.

Table 3-15. Kittiwake empirical p-values of likelihood that observed densities around turbines would be obtained by chance. Significant (<0.05) values highlighted in bold.

Test	Year	<100m	<200m	<300m	<400m
1-sided (avoidance)	2019	0.27	0.24	0.16	0.31
1-sided (attraction)		0.73	0.76	0.84	0.69
2-sided		0.54	0.48	0.33	0.62
1-sided (avoidance)	2021	0.91	0.79	0.45	0.15
1-sided (attraction)		0.09	0.21	0.55	0.85
2-sided		0.17	0.43	0.90	0.31

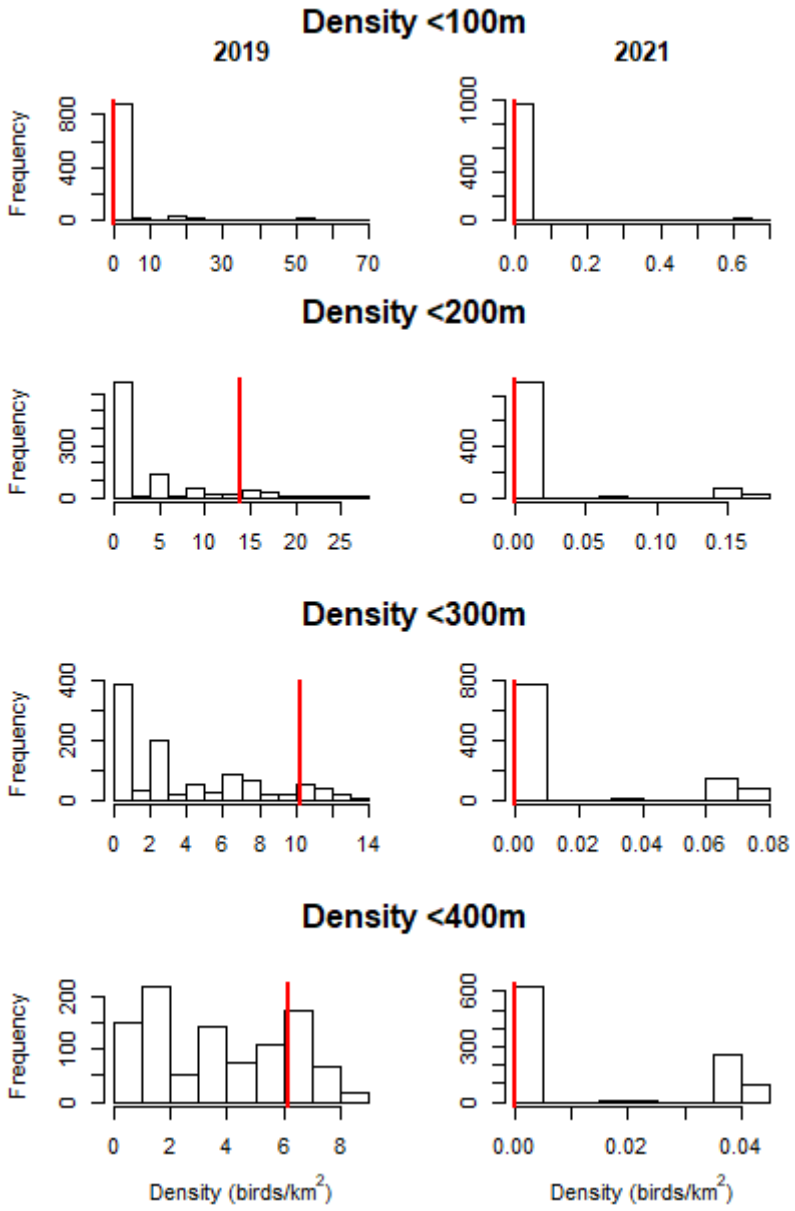

Figure 3-17. Herring gull densities in 2019 (left) and 2021 (right) within 100/200/300/400m of turbine locations (red lines) and distribution of densities estimated for 1,000 simulations with randomly re-positioned turbines (relative turbine positions maintained). Data combined across all six surveys.

Table 3-16. Herring gull empirical p-values of likelihood that observed densities around turbines would be obtained by chance. Significant (<0.05) values highlighted in bold. Note that only two individuals were recorded in the wind farm in 2021 so this year was not tested.

Test	Year	<100m	<200m	<300m	<400m
1-sided (avoidance)	2019	0	0.90	0.91	0.80
1-sided (attraction)		0.28	0.10	0.09	0.20
2-sided		0	0.20	0.19	0.41

3.7.1 Turbine avoidance in relation to turbine RPM

To investigate whether the density of birds around turbines was related to their operational status the data were split into subsets using the average RPM of the closest turbine to each bird recorded during the 10-minute period when each bird observation was recorded. Four RPM subsets were analysed, 0 - 2.5, 2.5 - 5, 5 – 7.5, 7.5+ (the highest RPM recorded in 2019 was 10.3 and in 2021 was 10.0). The graphed outputs for each species and RPM subset are provided in ANNEX G, and a summary table is provided below. To provide context, it is useful to consider how frequently a rotor blade will approach the sea surface at these RPM values: 2 RPM = 1 blade approach to the sea every 10 seconds; 4 RPM = 1 blade approach every 5 secs; 6 RPM = 1 every 3.33 secs; 8 RPM = 1 every 2.5 secs.

Table 3-17. Summary of turbine avoidance outputs for subsets of turbine RPM. Sample sizes are provided in brackets. The turbine response is presented as 4 characters representing indications for attraction (+), avoidance (-) or neither (0) in sequential nested 100 m areas around the turbines (>100m, >200m, >300m and >400m). For example, '-/-/0/+ (50)' would indicate avoidance up to 100m and 200m, neither attraction nor avoidance when measured up to 300m and attraction when considered up to 400m, with a sample size of 50. Attraction or avoidance were assigned if the observed density was higher or lower (respectively) than the peak of the resampled densities. NA = not applicable.

Species	RPM (sample size)					
	Year	0 – 2.5	2.5 – 5.0	5.0 – 7.5	7.5+	all RPM
Guillemot	2019	0/0/0/0 (2817)	+/0/0/0 (2387)	+/+/+/0 (1352)	0/0/+/+ (385)	0/0/0/0 (6941)
	2021	+/0/0/0 (81)	+/0/0/0 (582)	0/0/0/0 (2746)	+/0/0/0 (888)	0/0/0/0 (4297)
Puffin	2019	0/0/0/0 (18)	0/0/0/- (11)	0/0/+/+ (15)	NA (0)	0/0/0/0 (44)
	2021	0/0/0/0 (16)	0/0/+/0 (78)	+/0/0/0 (93)	0/0/0/0 (10)	0/0/0/0 (197)
Razorbill	2019	+/+/+/0 (132)	0/0/0/0 (229)	0/0/0/0 (155)	0/0/0/0 (41)	+/0/0/+ (557)
	2021	0/0/0/0 (14)	0/+/0/0 (55)	0/0/0/0 (194)	0/0/0/0 (122)	0/0/0/0 (385)
Kittiwake	2019	0/0/0/0 (638)	0/0/0/0 (464)	0/0/0/0 (558)	0/0/0/0 (73)	0/0/0/0 (1733)
	2021	0/0/0/0 (37)	+/+/+/0 (257)	+/+/++0 (370)	0/0/+/+ (205)	+/+/0/0 (869)
Herring gull	2019	0/+/+/+ (255)	0/0/0/0 (64)	0/0/+/+ (145)	NA (1)	0/+/+/0 (465)
	2021	NA (0)	NA (0)	NA (2)	NA (0)	NA (2)

Sample sizes varied across the RPM subsets and were small for puffin in both years and there were only two herring gulls in 2021, both recorded in the 5 to 7.5 RPM band. Among the species recorded in higher numbers (guillemot, razorbill and kittiwake), in 2019 abundance was higher at lower RPM, while in 2021 the largest samples sizes were for RPM between 5 and 7.5.

There was little consistent evidence that avoidance or attraction to turbines was related to rotor RPM for any species in either year, with observed densities typically located within the range of the randomized samples irrespective of the rotor RPM.

The relationship between the sample sizes for each species (taken here as a proxy for abundance in the wind farm) and the turbine RPM data show opposite patterns in 2019 and 2021. In 2019, as RPM increased (which was mirrored by an increase in the number of RPM samples) the number of birds

in the wind farm decreased. However, in 2021 the opposite was found: as RPM increased the number of birds in the wind farm increased (peaking in the 5 - 7.5 RPM band). Thus, in 2019 the data could be interpreted as indicating a broad preference for entering the wind farm at low turbine RPM, while in 2021 the data indicate a preference for moderate to high turbine RPM. This would appear to be further support that the presence of these species in the wind farm is not related to turbine RPM, and also does not exert a strong effect on the distance that the species are willing to approach turbines.

3.8 Flight heights

The proportion of birds flying below rotor height (defined as 32.7 m above MSL) was compared between birds recorded inside the wind farm and those outside, having first filtered by distance to obtain a subset of birds recorded more than 13km offshore (i.e. approximately the same minimum distance offshore as the wind farm). A binomial GLM was fitted to the data with the response variable (below/above lower rotor height) modelled in relation to birds recorded inside or outside the wind farm. Bird heights were estimated with uncertainty with a mean, minimum and maximum value (see HiDef methods, section 2.5). All birds with a height estimate were considered in this analysis, although as noted above this focused on birds more than 13km offshore.

Models were fitted using both the mean height and maximum height as the dependent variable, the latter providing a more precautionary estimate. A summary of the height data is provided in Table 3-18.

Table 3-18. Summary of flight height data recorded in 2021.

Species	Total	Mean height relative to rotor height				No. with no minimum height	No. with no mean height
		Height estimate < PCH		Height estimate at PCH			
		In wind farm	Outside wind farm	In wind farm	Outside wind farm		
Gannet	29	1	12	2	14	7	6
Kittiwake	1137	213	434	121	369	420	288
Great black-backed gull	4	0	1	2	1	1	1
Herring gull	108	4	10	26	68	8	2

Using mean height estimates, for gannet, great black-backed gull and herring gull there were no significant differences in the proportion recorded above/below rotor height inside or outside the wind farm (gannet p=0.67; great black-backed gull p=0.99 and herring gull p=0.94). A significant difference was obtained for kittiwake (p<0.01), with the percentage at rotor height estimated to be lower in the wind farm (36.2%, n=647) than outside (46.0%, n=490). The average kittiwake height estimates were 27.5m and 35.4m (inside and outside the wind farm respectively) using the individual mean estimates.

The same picture across species was obtained using the maximum height estimates (gannet p=0.81, great black-backed gull p=0.99, herring gull p=0.9, kittiwake p=0.034) with the percentage of kittiwake at rotor height estimated to be lower in the wind farm (58.1%, n=334) than outside (64.7%, n=803). The average of the kittiwake maximum height estimates were 49.5m and 52.2m (inside and

outside the wind farm respectively). Thus, with the exception of kittiwake, there was no evidence for differences in flight height in relation to turbines. In contrast, kittiwakes recorded in the wind farm flew lower. However, for the other species this may also be related to the very small sample sizes available. These results also appear to be consistent, with the same effects obtained in 2019.

Using all data recorded more than 13km offshore (i.e. the minimum distance from the coast to the wind farm) and the mean height estimate, the overall proportion of gannets at rotor height was estimated as 55.1% (n=29), for kittiwake as 43.1% (n=1,137), for great black-backed gull as 75.0% (n=4) and for herring gull as 87.0% (n=108). Using the maximum height estimate these increased to: gannet 72.4%, kittiwake 62.7%, great black-backed gull 75% (unchanged) and herring gull 96.2%.

4 DISCUSSION

4.1 Evidence for broad scale wind farm effects on seabird distributions and abundance

The total population sizes for each species recorded within the survey area have varied quite widely across the three years. For example, the guillemot abundance estimates have increased from 51,000 in 2015, to 87,000 in 2019 and 104,000 in 2021. Kittiwakes had similar abundance estimates in 2015 and 2019 (3,700 and 4,600 respectively) but much higher in 2021 with 14,700. A similar pattern was observed in puffin, with a 2021 estimate of 16,600, the highest estimate across all three years, compared with 1,000 to 3,000 estimated previously. Razorbill abundance peaked in 2019, with 11,250, compared to 3,500 in 2015 and 6,400 in 2021. Gannet abundance was highest in 2015 (700), with 400 (2019) and 500 (2021) recorded subsequently. Herring gull and great black-backed gull had lower estimates in 2015 and 2021, with peak estimates in 2019. Herring gull estimates were 400, 5,000 and 600 across the three years and great black-backed gull estimates were 50, 319 and 86.

Thus, there has been considerable variation in the overall abundances recorded in the surveys, and no consistent trends across the species. Similar variations in abundance with no clear trends have also been observed within the wind farm, with the exception of gannet which has been recorded in consistently lower numbers in the wind farm following construction.

The spatial distribution of gannet, guillemot, razorbill, puffin and kittiwake (species with sufficient data to fit models) compared across each pair of years, reveals more detail about how these species have responded to the wind farm.

Gannets have shown the most consistent and clear pattern in response to the wind farm. The pre vs. post-1 and pre vs. post-2 show very similar reductions in abundance covering the wind farm with increases in abundance elsewhere, while there was no apparent difference in the comparison between the two post-construction surveys (there were no areas of significant increase or decrease). Other studies have reported high levels of gannet avoidance of wind farms (Leopold et al. 2013, Vanermen et al. 2013, APEM 2014, Dierschke et al. 2016, Vanermen et al. 2016, Garthe et al. 2017a,b).

No significant changes were found in the guillemot distribution within the wind farm area between the pre and post-1 surveys, although there was an area of significant decrease in the north-west of the survey area, and large areas of significant increase in the north and south of the survey area. A similar pattern was found between pre and post-2, with an area of significantly increased abundance across the southern third of the survey area, although there was also an area of significant decline in the centre of the survey area which overlapped the north-west corner of the wind farm. The post-1 vs post-2 also found a significant decline within the centre of the survey area. This suggests that the area of decreased abundance which overlaps the wind farm is no more than partially related to the wind farm (and only in the pre-post-1 comparison), and is either linked to other changes in the area such as moving prey hotspots, or may simply be due to chance.

Comparison of the kittiwake distribution between pre and post-1 found an increase in abundance across the wind farm, which included some areas of significant increase. The pre vs post-2 comparison found areas of increase around the margins of the survey area, but no changes in the centre, including the wind farm. Between post-1 and post-2 there was an area of significant increase along the coast and an area of significant decrease overlapping the northern half of the wind farm.

Neither of the pre vs post comparisons indicated any decreases across the wind farm, and the differences between the two post surveys would therefore appear to be unrelated to the wind farm.

There were large areas of significant increase in razorbill abundance across the survey area in both of the pre vs post comparisons, which included the wind farm. There were no significant changes between the two post years. Given these results it seems unlikely that there has been any negative effect of the wind farm on razorbill distributions.

Between the pre and post-1 surveys there was a large area of decreased puffin abundance across much of the survey area, including the wind farm, while the opposite was found in the pre vs post-2 comparison, with a large area of significant increase across the western part of the survey area, and no areas of decrease. Comparison of the two post surveys found a significant increase across almost all of the survey area.

It was not possible to fit spatial models to the great black-backed gull and herring gull data so no further exploration of these species in relation to wind farm avoidance was conducted.

Consideration was given to the potential that construction activity at the adjacent Moray East Wind Farm could have influenced the distribution of birds. ANNEX F provides a plot of the locations where turbines were installed during the survey period (May 22nd to 5th August, inclusive). Two turbines were installed on the day prior to surveys 4 and 5 (19th June and 30th June) and two were installed on the day of these two surveys (20th June and 1st July). However, the closest of these was over 12km from the wind farm, which is almost the same distance that the Beatrice wind farm is from the coast. Therefore, this activity is not considered likely to have had any effect on the distribution of seabirds within our study area in the 2021 surveys.

4.2 Evidence for fine scale turbine effects on seabird distributions and abundance

The analysis of the 2019 monitoring data provided the first outputs for an operational wind farm of an analysis designed to identify if seabird distributions around turbines differ from those expected by chance. The 2019 results strongly indicated that, for the species assessed (auks, kittiwake and herring gull), there was no evidence of small-scale avoidance of individual turbines, and this result was unrelated to how fast the turbine rotors were spinning.

The analysis method has been slightly revised following the original analysis, and the 2019 data have been re-analysed alongside the 2021 data for this report (the revision ensured that the correct areas of overlap between the aerial transects and turbine radii were applied in the density estimates). This revision has not affected the conclusions for the 2019 data and the analysis of the 2021 data has found the same effects, using data both pooled across all surveys and also when subsetted by RPM. Overall there is no evidence that these species avoid turbines (however it must be acknowledged that there were very few herring gull records, so conclusions for this species are less robust).

4.3 Synthesis of wind farm and turbine responses

A key aspect of the Beatrice ornithology monitoring is the collection of data to permit analysis designed to detect both large scale and fine scale responses to the wind farm. The driver for adopting this approach was to be able to derive a mechanistic understanding of seabird responses to wind farms. Armed with the improved understanding obtained from such a study, the goal is to

be able to make predictions for how seabirds will respond at other wind farms which may have different design characteristics (e.g. closer or more widely spaced turbines).

4.3.1 Gannet

Gannet has been found to exhibit high levels of wind farm avoidance in other studies (e.g. APEM 2014, Dierschke *et al*. 2016, Leopold *et al*. 2013, Vanermen *et al*. 2013, Vanermen *et al*. 2016, Garthe *et al*. 2017a,b). The results of the current study are in agreement with these previous studies and provide a clear indication that gannets avoid wind farms. This overall avoidance was sufficiently marked that it was not possible to consider turbine avoidance as virtually no gannets were recorded within the wind farm (e.g. only 12 gannets were recorded in the wind farm in 2021). A key conclusion from this is that displacement is likely to be a greater potential source of impact for this species than collision risk, with the former potentially needing to be assessed with higher rates of displacement than the current 60-80%. Conversely, the current collision avoidance rate of 98.9% may well be an underestimate of the level of avoidance this species exhibits. However, the consequences of displacement are generally considered to be minimal for this species due to the wide range of prey species taken, the long potential foraging range and the low-energy flight costs in this species.

4.3.2 Puffin

The spatial modelling has indicated that there may have been some avoidance of the wind farm, although that conclusion is made with low confidence due to the fact the apparent avoidance has varied quite markedly between years and only covered part of the wind farm site in the most recent comparison. However, analysis of the individuals which did enter the wind farm provided no indication that turbines were avoided. Taken together, there does not appear to be a notable response of puffin to the presence of the wind farm. The displacement rates currently applied for this species are 30-70%, and the current results would indicate that the lower end of this range is likely to be more appropriate for similarly located wind farms. There are no other known studies of puffin responses to wind farms, so it is unclear if these results are typical for this species.

4.3.3 Guillemot

There is very little indication from either the spatial modelling or the turbine avoidance analysis that guillemots are responding to the presence of the wind farm either negatively or positively. No data on prey distributions are available, however underwater structures are known to aggregate fish, so it is possible that guillemots have been attracted to the enhanced foraging opportunities thus presented. However, it is also plausible that the main change to the fish populations around the turbine structures is an increase in larger fish which are also predators of the forage fish prey of auks, thereby increasing competition, at least locally. Thus, it is difficult to make statements with any confidence about the reasons for the observed guillemot distributions. It certainly would appear that the upper end of the displacement rates of 30-70% currently used in assessment are considerably over-estimating the extent to which this species is likely to be displaced from operational wind farms, and even the lower end of this range is probably precautionary. Dierschke *et al.* (2016) reviewed the evidence for seabird displacement across a range of taxa, and reported variable findings for guillemot: at different wind farms numbers were reported to have increased, decreased and remained unchanged. Notably the sites included in the review were predominantly in the southern North Sea, and probably reflect wintering distributions, rather than breeding ones, and it is possible that the birds will respond differently at different times of year.

4.3.4 Razorbill

The spatial modelling and turbine avoidance analysis lead to similar conclusions for razorbill as for guillemot. The pooled analysis of turbine avoidance found no indication of systematic avoidance of the wind farm or individual turbines, and some evidence of higher densities in proximity to the turbines. Thus, it is considered that the current 30-70% displacement rates used in assessment likely over-estimate the extent to which this species is displaced from operational wind farms. Dierschke *et al.* (2016) reviewed the evidence for seabird displacement across a range of taxa, and reported variable findings for razorbill: at different wind farms numbers were reported to have increased, decreased and remained unchanged. Notably the sites included in the review were predominantly in the southern North Sea, and probably reflect wintering distributions, rather than breeding ones, and it is possible that the birds will respond differently at different times of year.

4.3.5 Kittiwake

The distribution of kittiwakes across the survey area has varied across each year, although there appears to have been a consistent area of higher density on the south-western edge of the survey area. The spatial modelling has not indicated any consistent differences between years, and the analysis of locations within the wind farm has found no indication that kittiwakes avoid turbines. This corresponds to the results of the review by Dierschke *et al.* (2016) which found no indication for wind farm responses in this species.

Kittiwake was the only species for which a significant difference in flight height was detected for birds recorded within the wind farm compared with those recorded outside, but at equivalent distances offshore. Birds in the wind farm were estimated to fly around 8m lower on average than those outside. However, there remains a large degree of uncertainty associated with aerial survey derived flight height estimates and therefore these results should be considered indicative of trends rather than definitive.

4.3.6 Great black-backed gull

Great black-backed gulls were recorded in low numbers in both the pre-construction and post-construction surveys. Given these low numbers it is difficult to draw conclusions on how, if at all, the wind farm is affecting the species. Birds were only rarely recorded within the wind farm in any year: 2015 (24 individuals), 2019 (60 individuals) and 2021 (12 individuals). Therefore, while it is difficult to draw any conclusions on how this species may be affected by the wind farm, it would seem that any such effects will most likely be minor. On the basis of their review of studies, Dierschke *et al.* (2016) classed this species as weakly attracted to wind farms, although this reflected a range of responses including weak avoidance, no response and weak attraction.

While further understanding of this species' behaviour and possible wind farm interactions would be gained from undertaking tracking studies, there are no current plans to undertake such work due to welfare concerns (this species has been found to be sensitive to handling and tag attachment) and also the current avian influenza outbreak has put severe restrictions on handling wild birds. In lieu of tracking, an observational study was conducted at the ECC SPA during the 2022 breeding season which found little evidence that great black-backed gulls breeding at colonies within ECC SPA foraged offshore at distances greater than 3km (Furness 2022).

4.3.7 Herring gull

Herring gulls were recorded in considerably larger numbers in 2019, with a peak overall abundance more than 10 times that seen in 2015 and within the wind farm of over 124 times higher. In 2021 herring gull numbers were much lower again, with a peak abundance of 500 which was similar to the 2015 results. It is not apparent why the numbers for this species have varied so widely. The turbine avoidance analysis found no evidence for this species avoiding turbines although the relatively small sample sizes, particularly in 2021, limits the degree of confidence in these results. However, this would correspond to previous observations that large gull species are not displaced to an appreciable extent by offshore wind farms (Dierschke *et al*. 2016).

5 REFERENCES

APEM (2014) Assessing northern gannet avoidance of offshore windfarms. APEM ref: 512775.

BOWL (2016) Pre-construction aerial survey report. http://marine.gov.scot/sites/default/files/bowl_pre-construction_aerial_surveys_report-redacted.pdf

Burton, N.H.K., Thaxter, C.B., Cook, A.S.C.P., Austin, G.E., Humphreys, E.M., Johnston, A., Morrison, C.A., & Wright, L.J. (2013). Ornithology Technical Report for the Proposed Dogger Bank Creyke Beck Offshore Wind Farm Projects. A report carried out by the British Trust for Ornithology under contract to Forewind Ltd BTO Research Report No. 630

Dierschke, V., Furness, R.W. and Garthe, S. (2016). Seabirds and offshore wind farms in European waters: Avoidance and attraction. Biological Conservation 202: 59-68.

Furness, R.W., Garthe, S., Trinder, M., Matthiopoulos, J., Wanless, S. & Jeglinski, J. (2018). Nocturnal flight activity of northern gannets *Morus bassanus* and implications for modelling collision risk at offshore wind farms. Environmental Impact Assessment Review, 73, https://doi.org/10.1016/j.eiar.2018.06.006

Furness, R. (2022) Observed flight directions and inferred foraging by breeding great black-backed gulls at East Caithness Cliffs SPA. Unpubl. Report for the Moray Offshore Wind Farms.

Garthe, S., Peschko, V., Kubetzki, U. and Corman, A-M. (2017a) Seabirds as samplers of the marine environment – a case study of northern gannets. Ocean Science, 13, 337-347.

Garthe, S., Markones, N. and Corman, A.M. (2017b) Possible impacts of offshore wind farms on seabirds: a pilot study in northern gannets in the southern North Sea. Journal of Ornithology, 158, 345-349.

Leopold, M. F., van Bemmelen, R. S. A. and Zuur, A. (2013) Responses of local birds to the offshore wind farms PAWP and OWEZ off the Dutch mainland coast. Report C151/12, Imares, Texel.

MacArthur Green (2021) Beatrice Offshore Wind Farm. Year 1 Post-construction Ornithological Monitoring Report 2019 [https://www.google.com/url?sa=t&rct=j&q=&esrc=s&source=web&cd=&cad=rja&uact=8&ved=2ahUKEwiO28mJh7z6AhUEhFwKHZdWBYcQFnoECBgQAQ&url=https%3A%2F%2Fmarine.gov.scot%2Fsites%2Fdefault%2Ffiles%2Fbowl_2019_post-con_monitoring_report_v2.2_30042021.pdf&usg=AOvVaw2uESeLU5tYtfYIM5nDKYuq]

Scott-Hayward, L.A.S., C.S. Oedekoven, M.L. Mackenzie, C.G. Walker, and E. Rexstad. (2013). User Guide for the Mrsea Package V0.1.2: Statistical Modelling of Bird and Cetacean Distributions in Offshore Renewables Development Areas. University of St. Andrews Contract for Marine Scotland; Sb9 (Cr/2012/05). University of St Andrews.

Thaxter, C. B., Wanless, S., Daunt, F., Harris, M.P., Benvenuti, S., Watanuki, Y., Grémillet, D. and Hamer, K.C. (2010). Influence of wing loading on the trade-off between pursuit-diving and flight in common guillemots and razorbills. The Journal of Experimental Biology, 213, 1018-1025.

Vanermen, N., Courtens, W., Van de walle, M., Verstraete, H. and Stienen, E.W.M. (2016) Seabird monitoring at offshore wind farms in the Belgian part of the North Sea: Updated results for the Bligh Bank and first results for Thorntonbank. Rapporten van het Instituut voor Natuur- en Bosonderzoek 2016 (INBO.R.2016.11861538). Instituut voor Natuur- en Bosonderzoek, Brussels.

Vanermen, N., Stienen, E.W.M., Courtens, W., Onkelinx, T., Van de walle, M. and Verstraete, H. (2013) Bird monitoring at offshore wind farms in the Belgian part of the North Sea - Assessing seabird displacement effects. Rapporten van het Instituut voor Natuur- en Bosonderzoek 2013 (INBO.R.2013.755887). Instituut voor Natuur- en Bosonderzoek, Brussels.

ANNEX A. COMPARISON OF MODEL BASED ESTIMATES FROM 2015 ANALYSIS AND 2019 ANALYSIS

Following the pre-construction surveys, BOWL (2016) presented abundance estimates obtained from spatial modelling. Following the 2019 post-construction surveys (reported here) the spatial models included both sets of survey data with the inclusion of a before/after categorical model term with the aim of identifying wind farm effects. In the period between the two analyses there were minor updates made to the spatial modelling method used (i.e. the MRSea packages was revised) and the spatial grid used for the model was slightly different (in order to accommodate both datasets). As a consequence the abundance estimates for the pre-construction surveys presented in the current report are slightly different from those in BOWL (2016). For clarity the two sets of abundance estimates are presented below.

Pre-construction results from BOWL (2016)

Table 4*. Model derived population abundance estimates in the total survey area and within the Wind Farm boundary for each species in each survey. Estimates were generated as predictions from the best-fit models identified in Table 3 using appropriate covariate values for the total survey area and within the Wind Farm boundary respectively. Entries marked with '-' indicate instances when small sample sizes prevented model fitting.*

Species	***Area***	***Population abundance on each survey***					
		1	***2***	***3***	***4***	***5***	***6***
Gannet	*Total survey area*	*198.3*	*520.6*	*816.6*	*206.1*	-	-
	Wind Farm	*21.9*	*207.9*	*458.5*	*4.1*	-	-
Guillemot	*Total survey area*	*48494.2*	*50252.9*	*20176.8*	*61625.6*	*8457.8*	*4501.4*
	Wind Farm	*5410.1*	*2720.5*	*6056.7*	*7630.5*	*680.5*	*803.1*
Kittiwake	*Total survey area*	*1689.6*	*3708.1*	*3415.1*	*3801.5*	*1683.2*	*377.9*
	Wind Farm	*13.3*	*196.6*	*62.0*	*1616.6*	*86.2*	*101.3*
Puffin	*Total survey area*	*1738.2*	*1315.5*	*566.5*	*930.9*	*261.6*	*3413.7*
	Wind Farm	*209.7*	*60.6*	*50.3*	*33.9*	*5.5*	*938.2*
Razorbill	*Total survey area*	*798.6*	*1686.7*	*3692.1*	*1750.2*	-	-
	Wind Farm	*68.3*	*122.5*	*177.0*	*229.4*	-	-

2015 spatial model abundance estimates re-calculated for this report.

Species	**Area**	**Population abundance on each survey**					
		1	**2**	**3**	**4**	**5**	**6**
Gannet	Total survey area	174.14	461	708.6	182.6	17.5	8.9
	Wind Farm	56.38	149.3	229.4	59.1	5.7	2.9
Guillemot	Total survey area	39760.1	36561.0	15487.5	51036.9	7642.7	4063.5
	Wind Farm	5819.9	1421.3	2060.1	7015.9	1452.0	902.1
Kittiwake	Total survey area	1443.4	3639.1	3375.9	3707.1	1666.9	352.2
	Wind Farm	37.7	246.7	62.5	1290.7	174.0	63.0
Puffin	Total survey area	1959.9	1409.8	479.2	532.2	214.0	3133.1
	Wind Farm	193.2	72.9	19.7	2.7	2.6	1027.5
Razorbill	Total survey area	817.8	2034.5	3527.9	1674.8	37.7	9.6
	Wind Farm	49.3	122.6	212.6	100.94	2.3	0.6

ANNEX B. DISTRIBUTION OF BIRDS IN FLIGHT IN 2015, 2019 AND 2021

The locations of birds recorded in flight on each survey in each year are plotted in figures B1 to B21 (note that the plots are provided for each species in turn, 2015, 2019 and 2021). These were not analysed using spatial models on the basis that physical covariates (e.g. depth and distance to coast) are unlikely to explain the observed distributions.

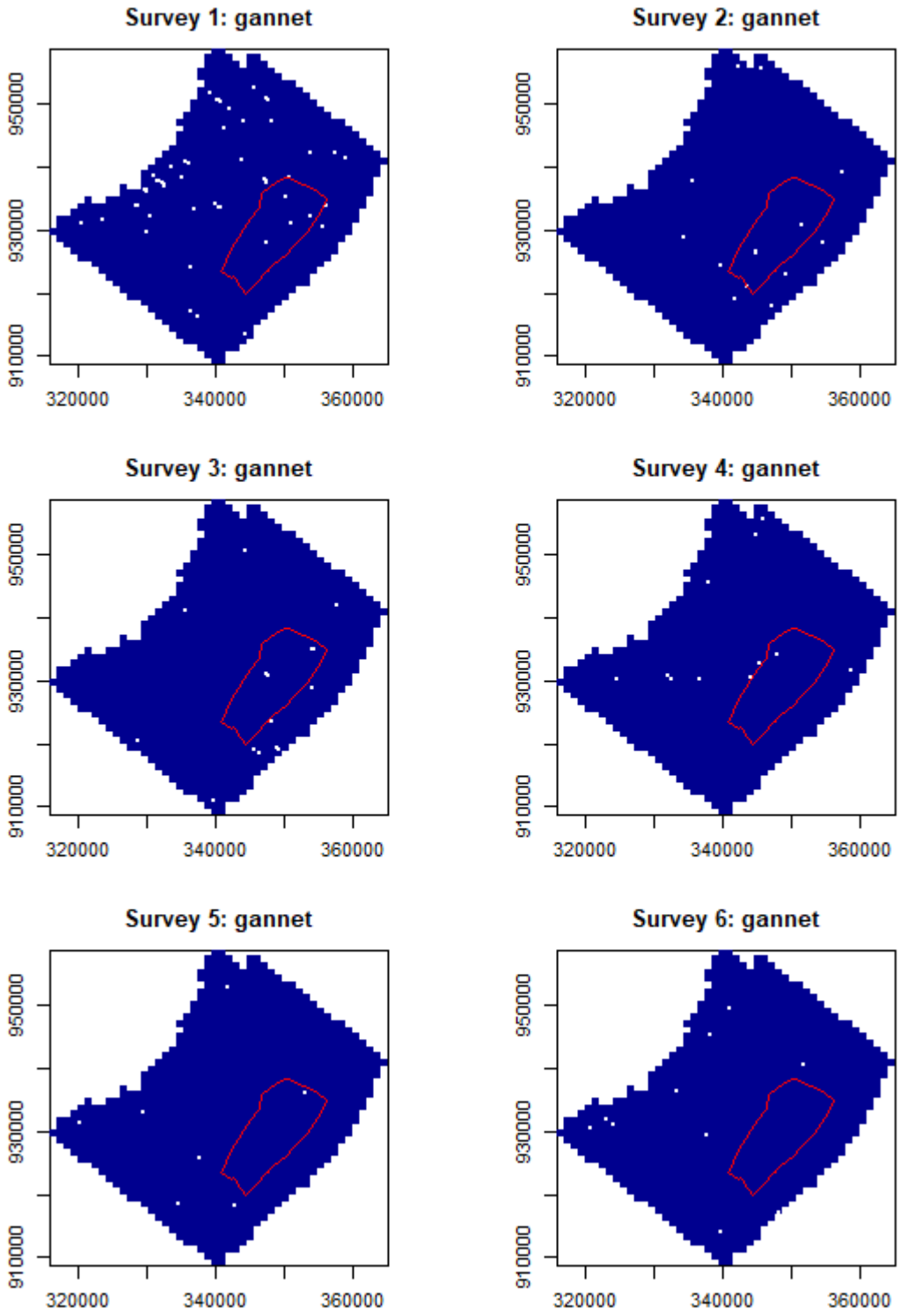

Figure B1. Locations of gannets recorded in flight during 2015 surveys.

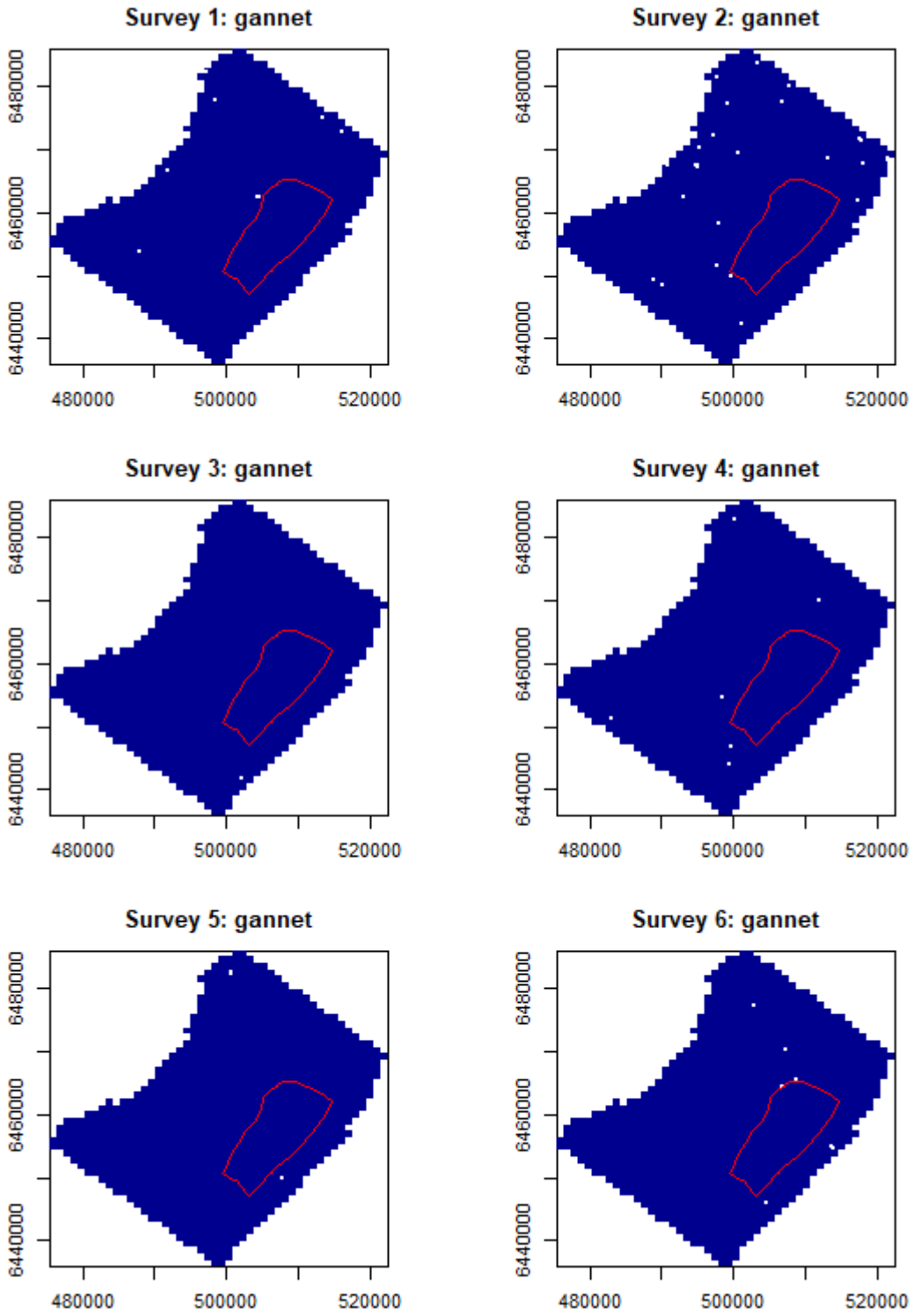

Figure B2. Locations of gannets recorded in flight during 2019 surveys.

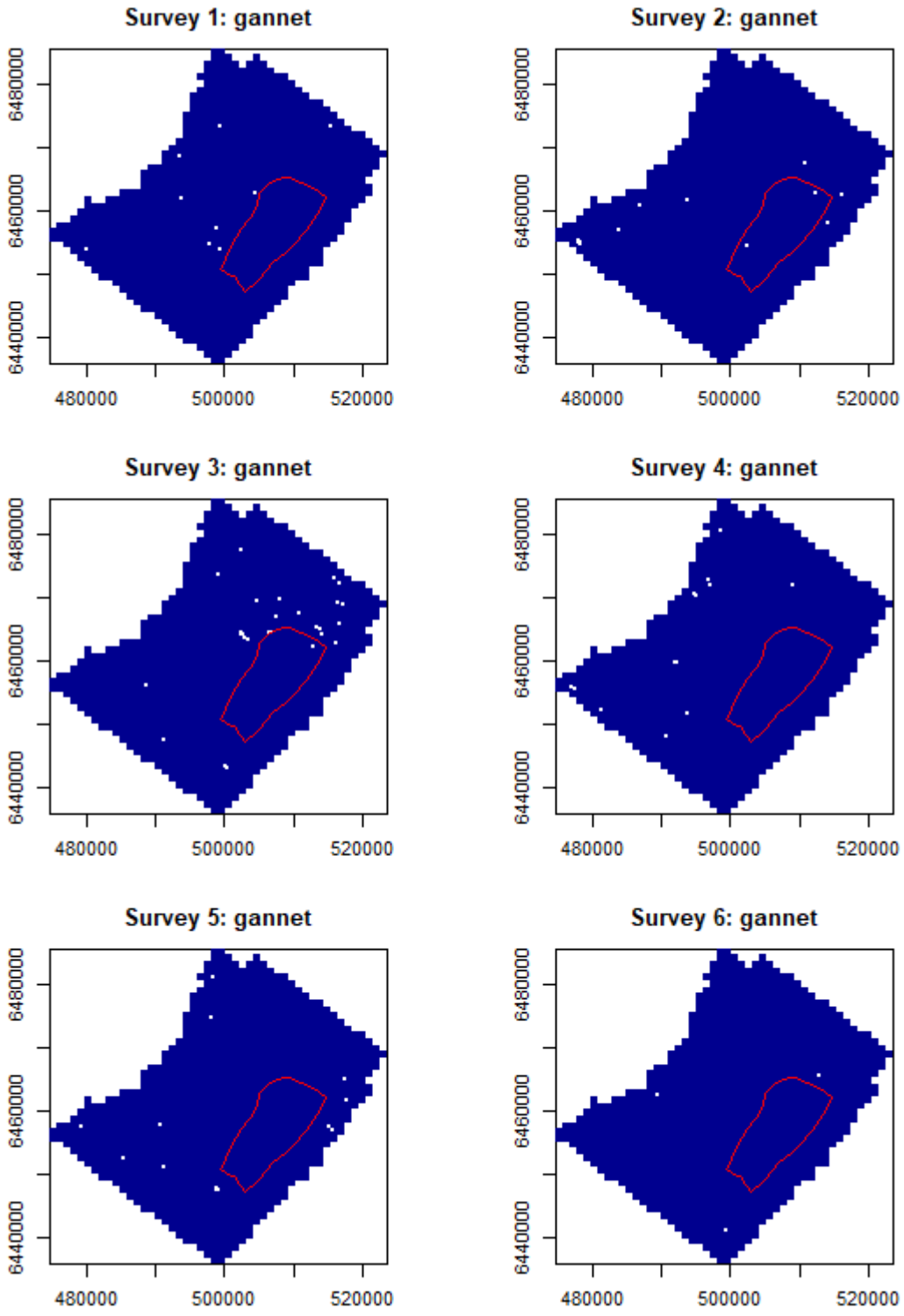

Figure B3. Locations of gannets recorded in flight during 2021 surveys.

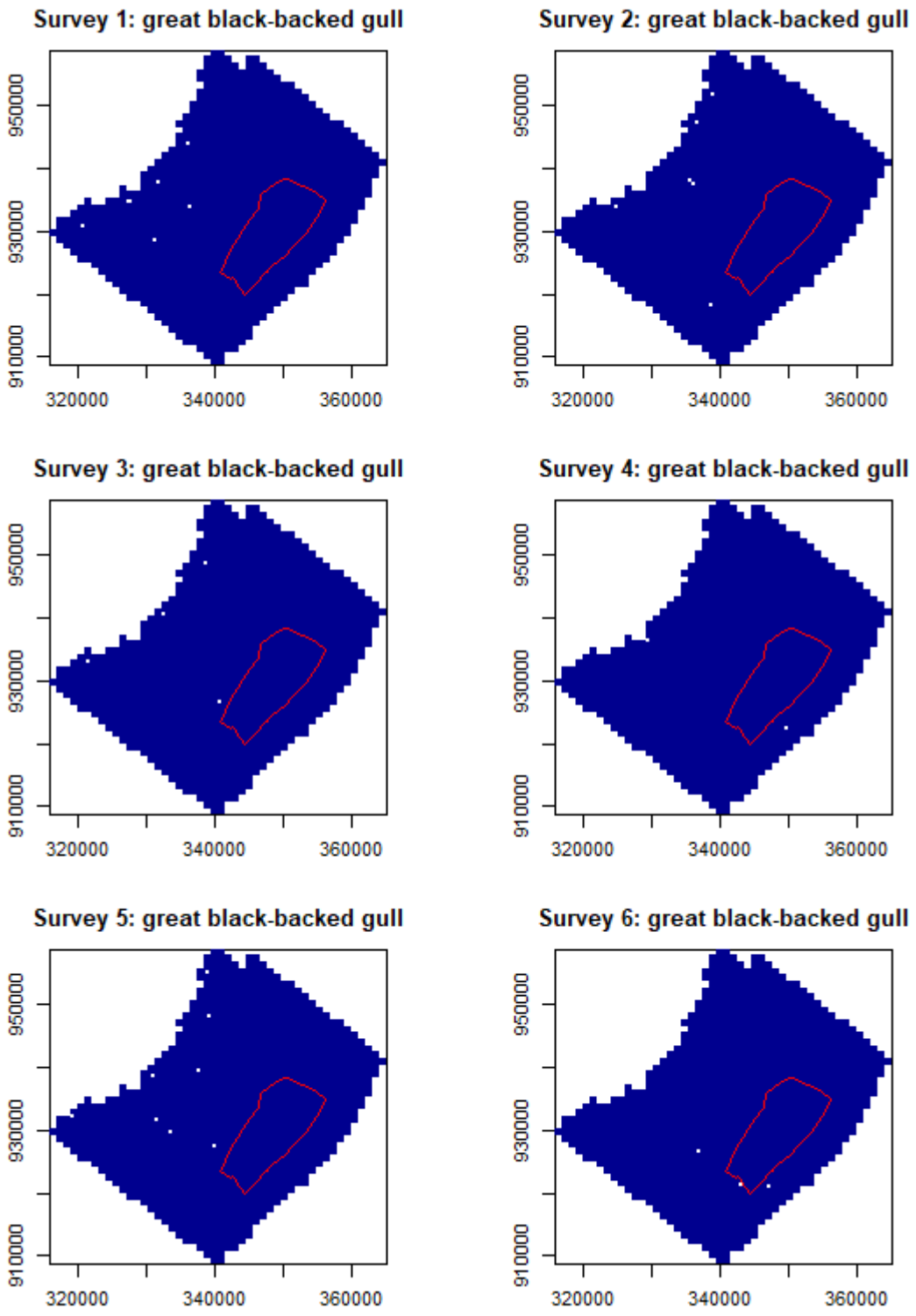

Figure B4. Locations of great black-backed gulls recorded in flight during 2015 surveys.

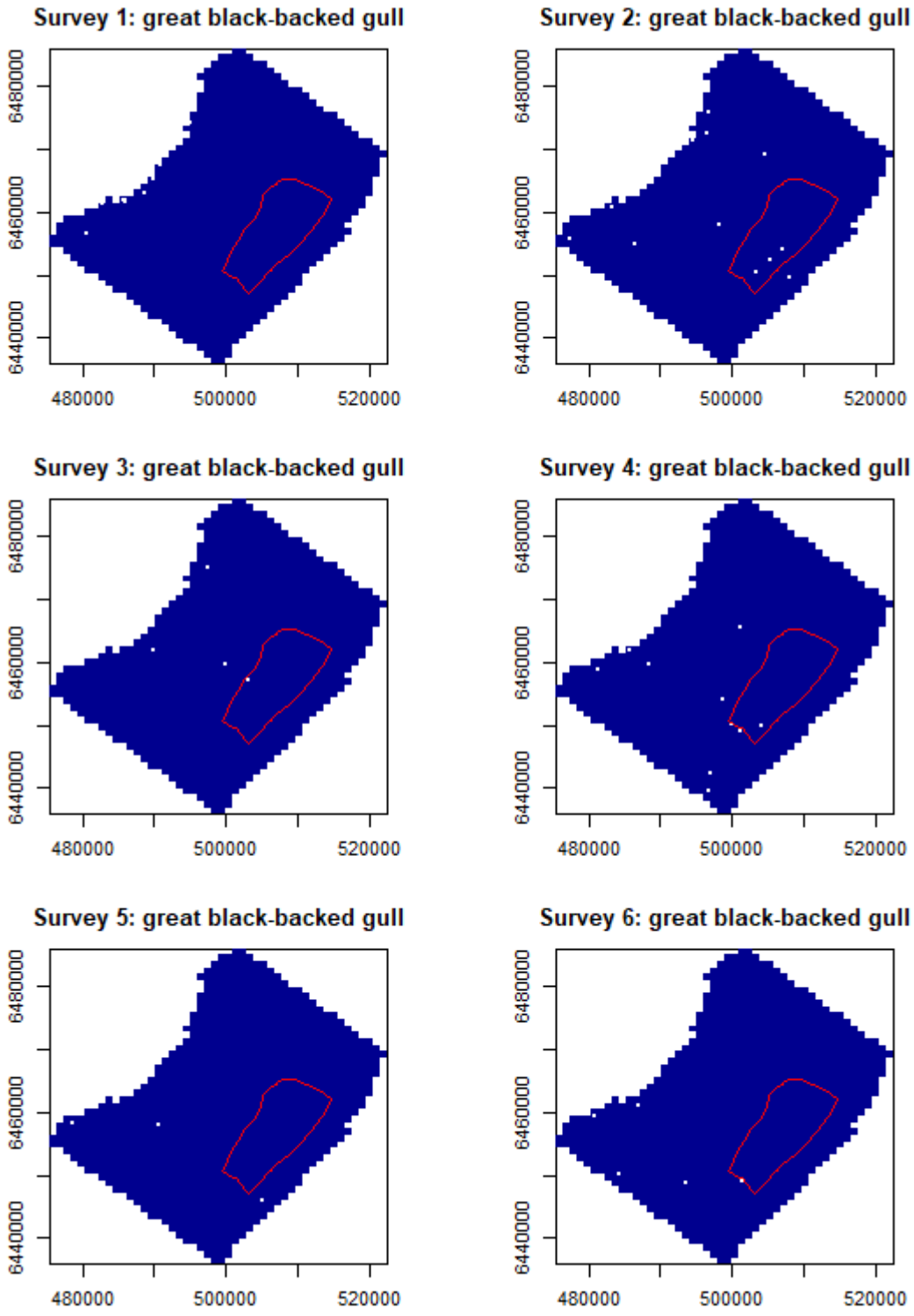

Figure B5. Locations of great black-backed gulls recorded in flight during 2019 surveys.

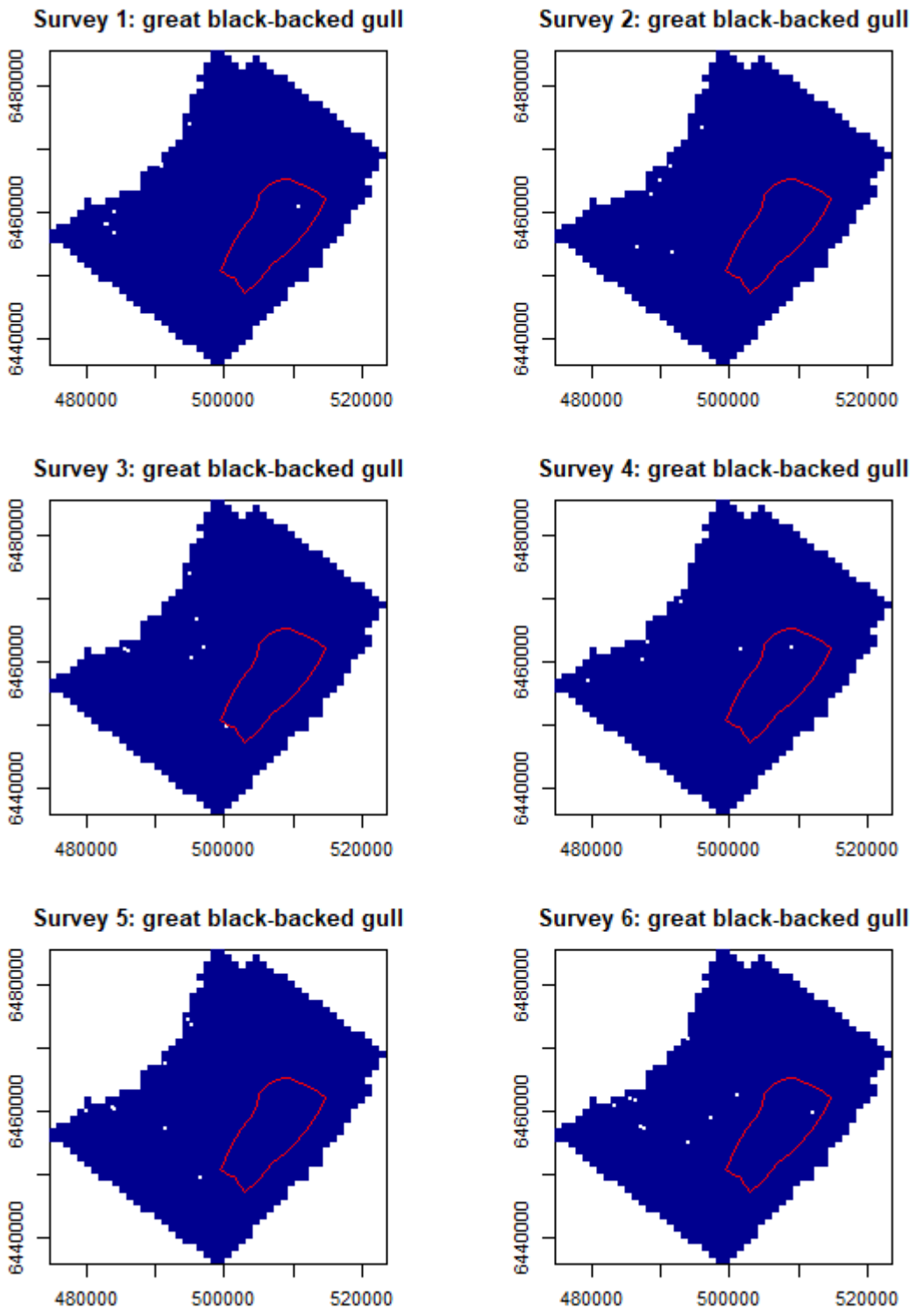

Figure B6. Locations of great black-backed gulls recorded in flight during 2021 surveys.

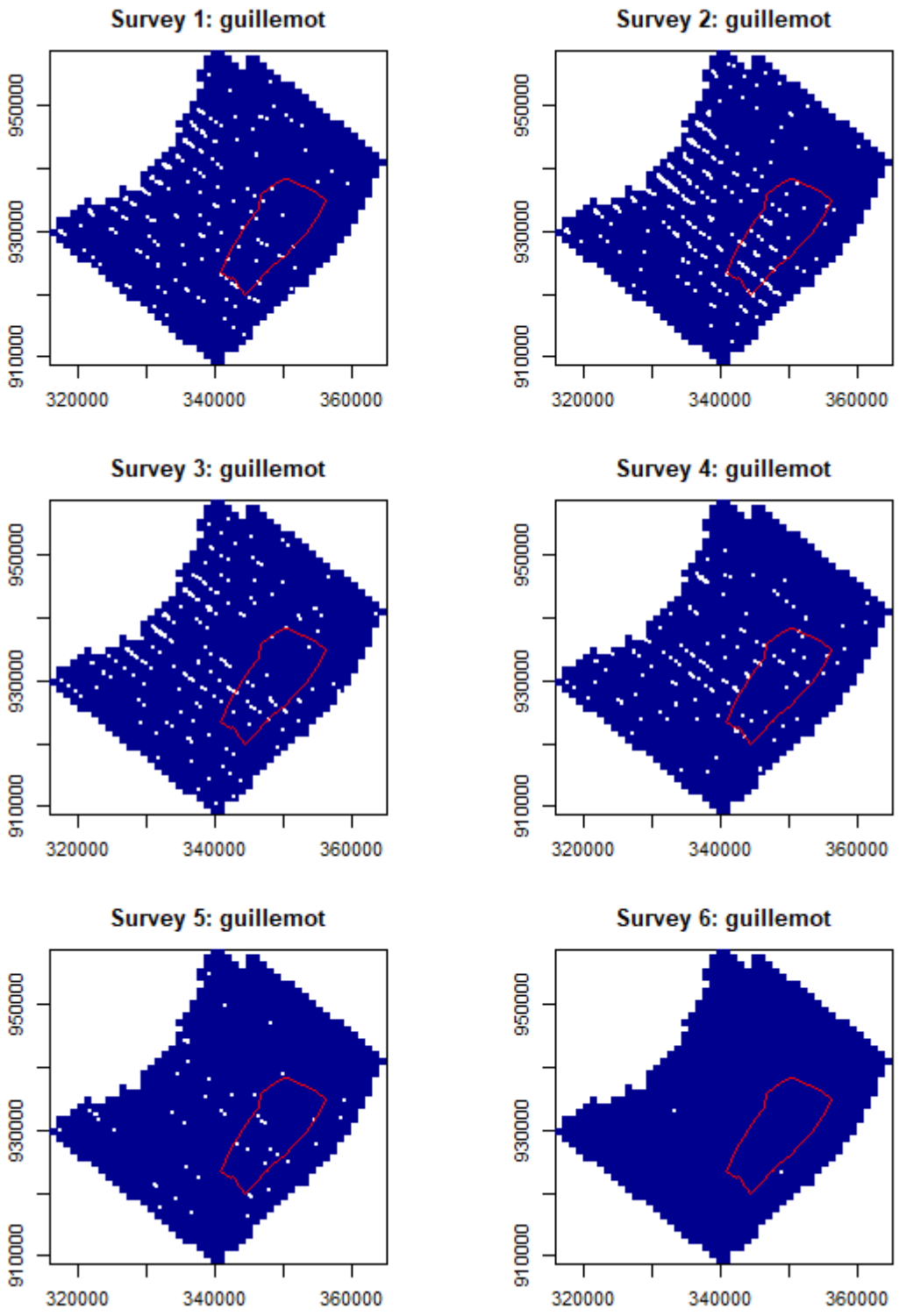

Figure B7. Locations of guillemots recorded in flight during 2015 surveys.

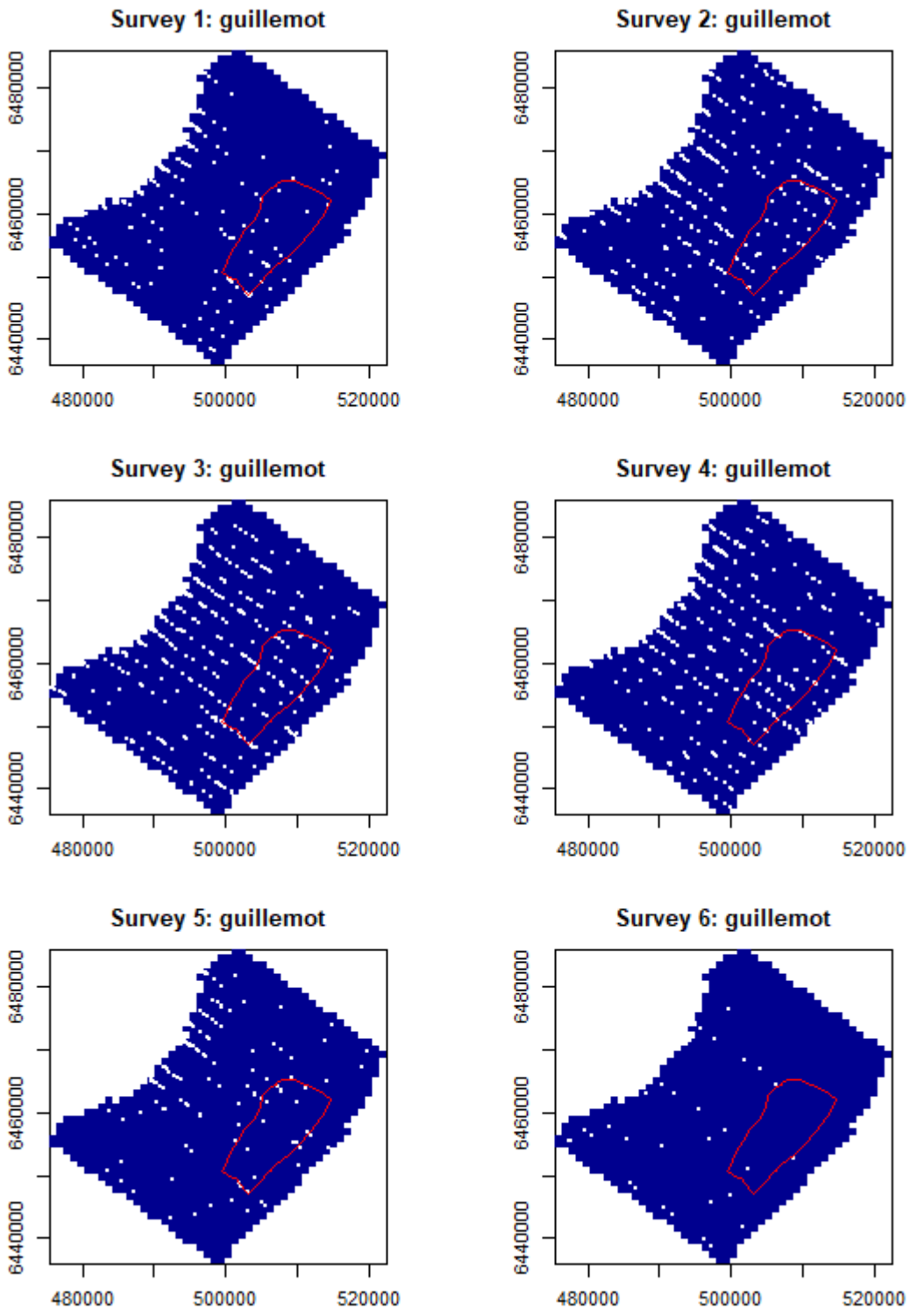

Figure B8. Locations of guillemots recorded in flight during 2019 surveys.

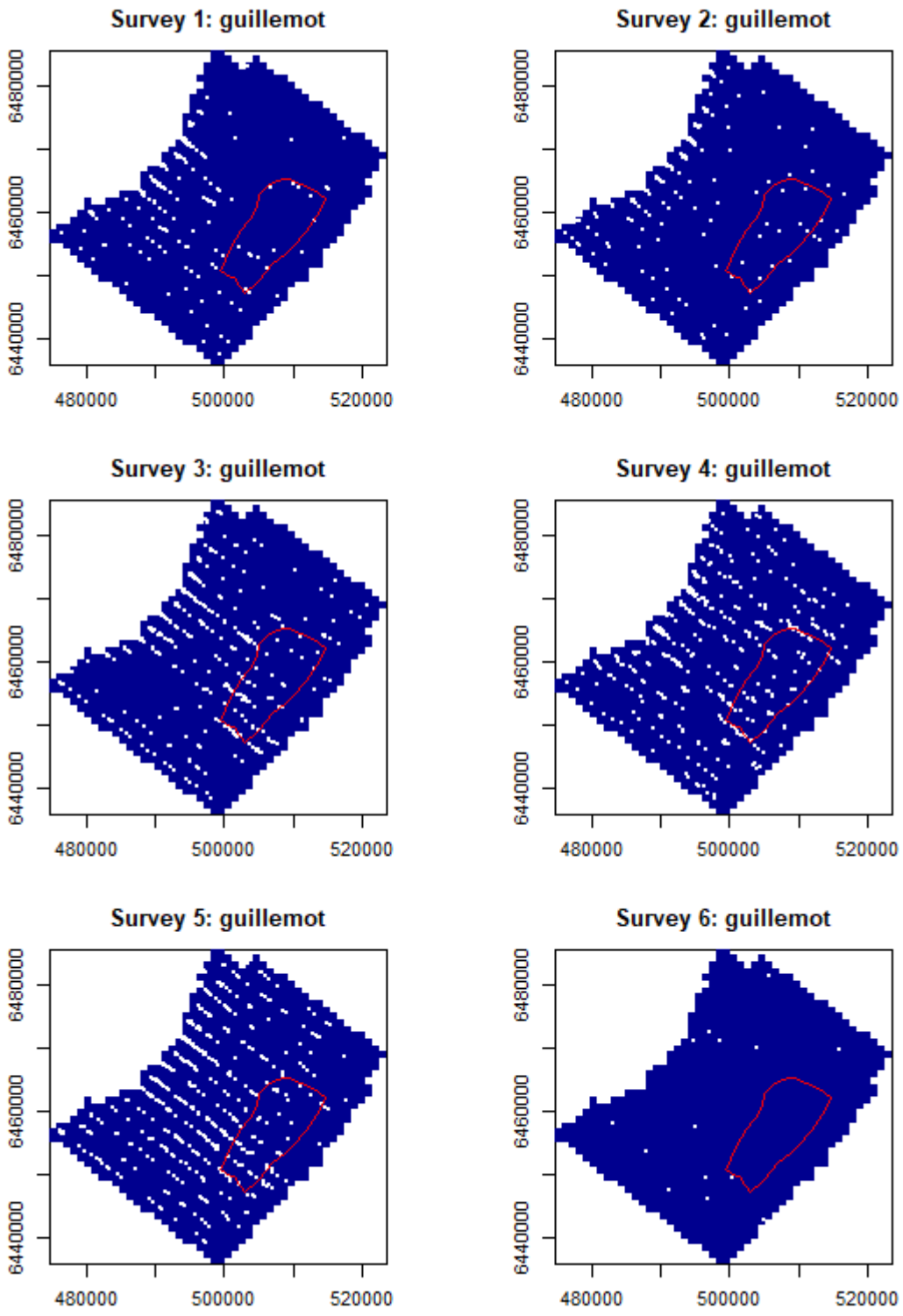

Figure B9. Locations of guillemots recorded in flight during 2021 surveys.

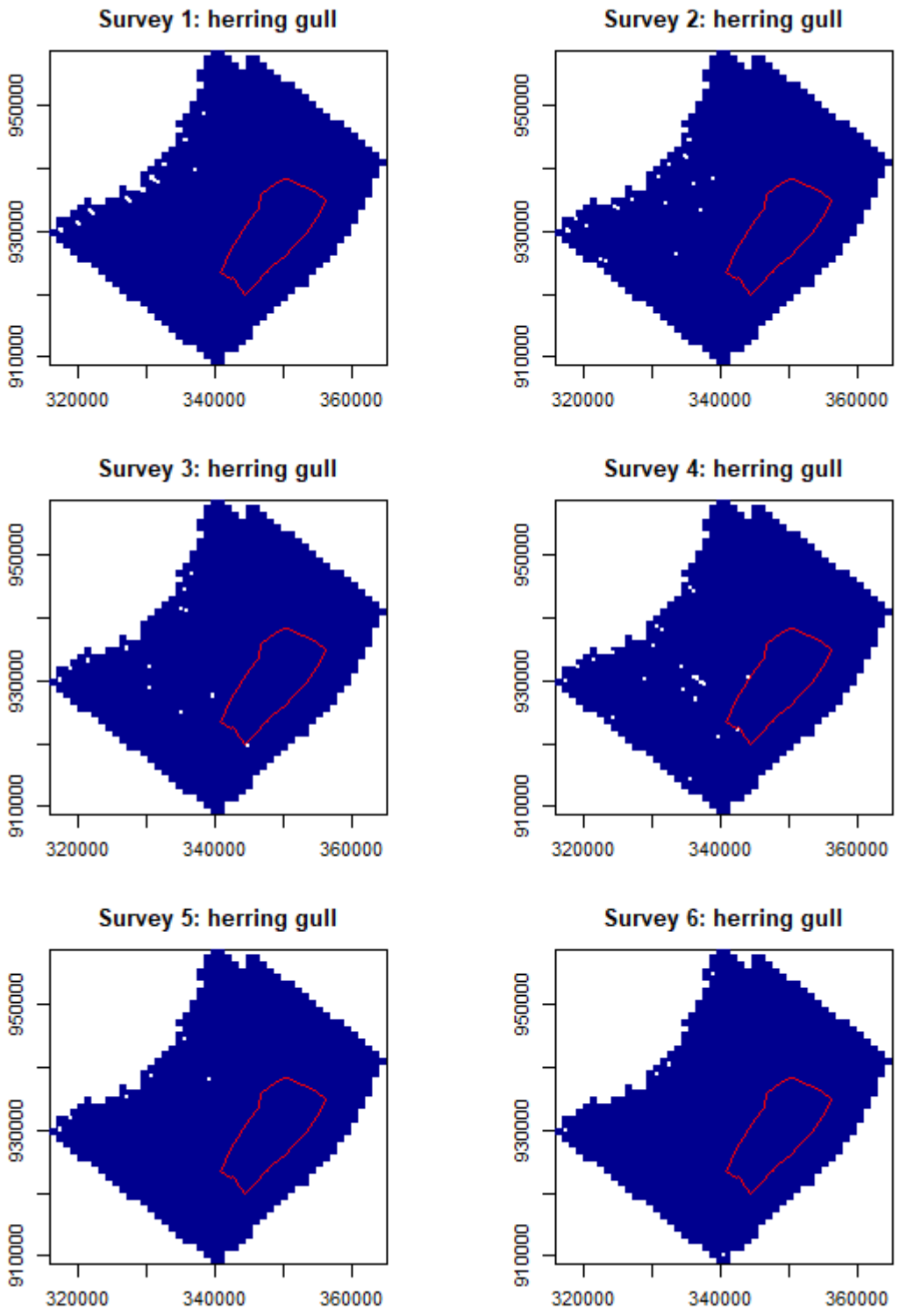

Figure B10 Locations of herring gulls recorded in flight during 2015 surveys.

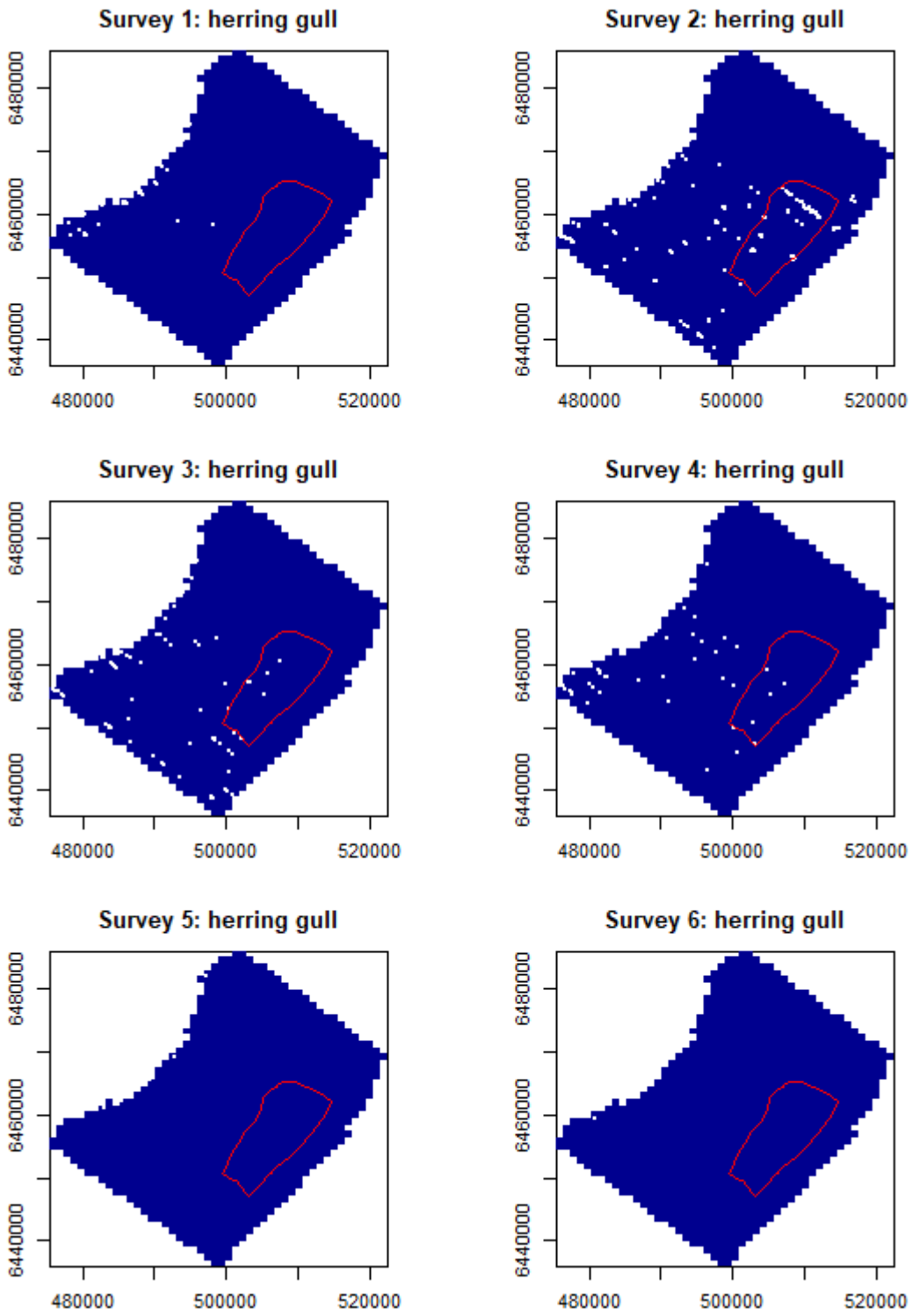

Figure B11. Locations of herring gulls recorded in flight during 2019 surveys.

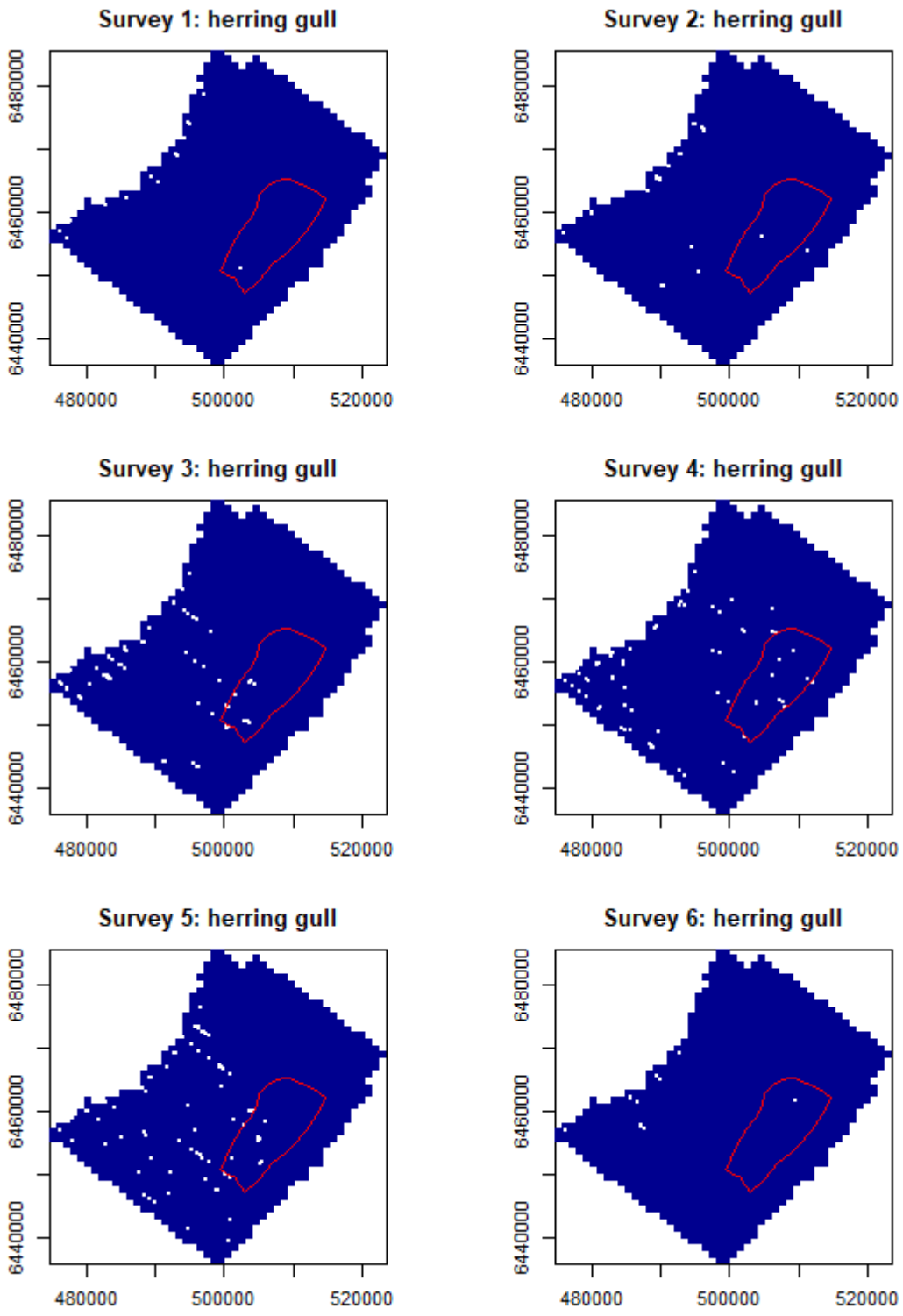

Figure B12. Locations of herring gulls recorded in flight during 2021 surveys.

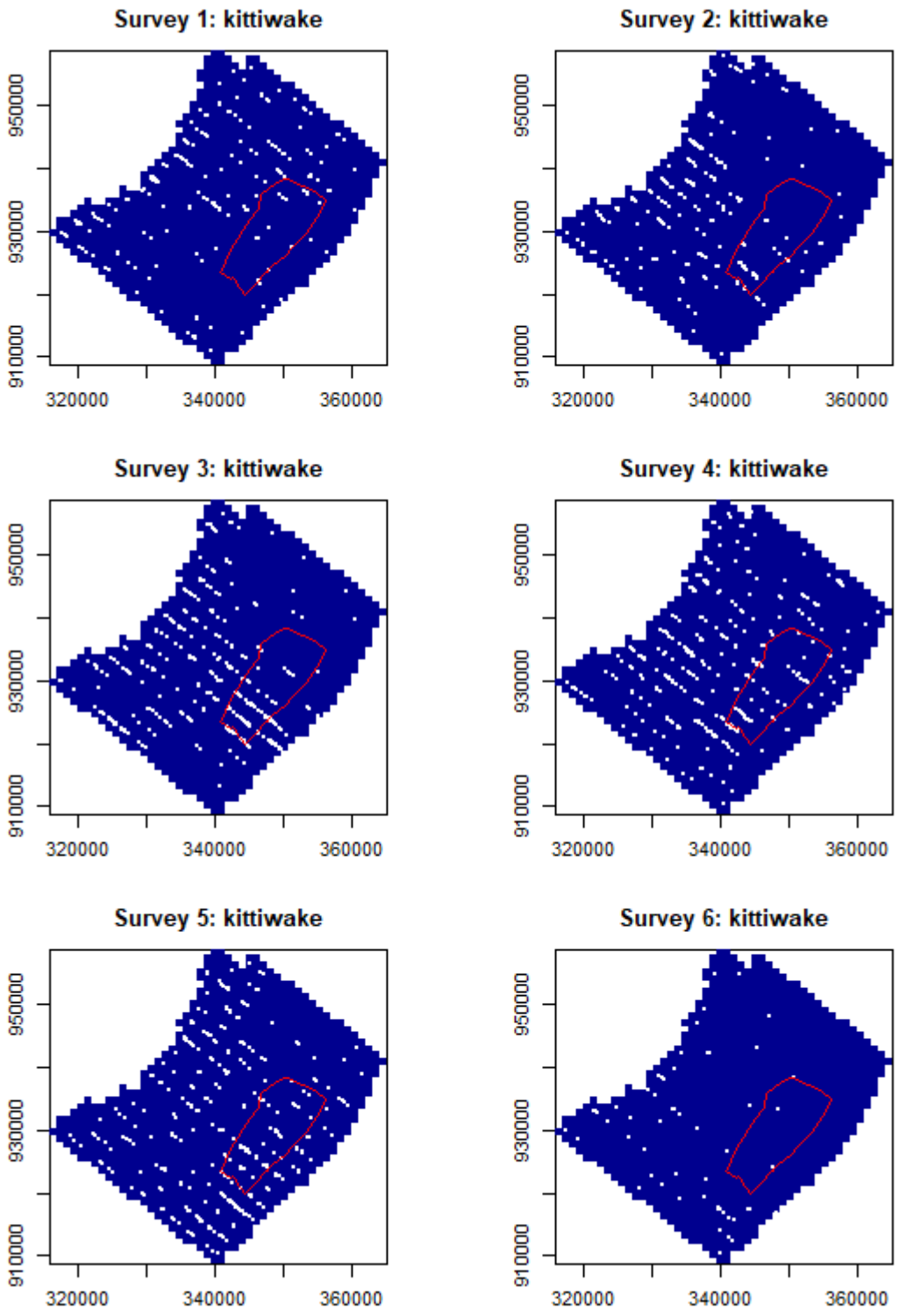

Figure B13. Locations of kittiwakes recorded in flight during 2015 surveys.

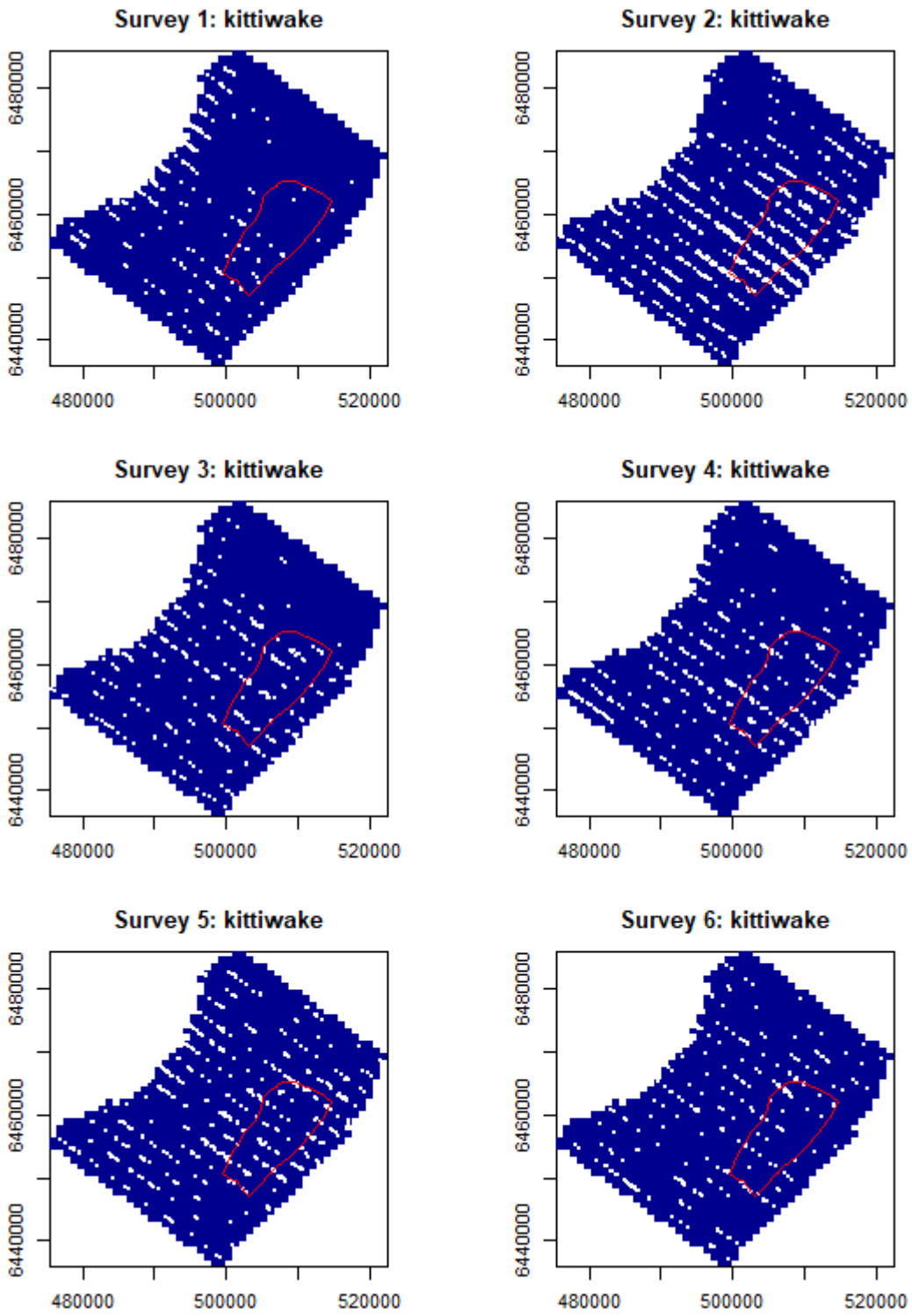

Figure B14. Locations of kittiwakes recorded in flight during 2019 surveys.

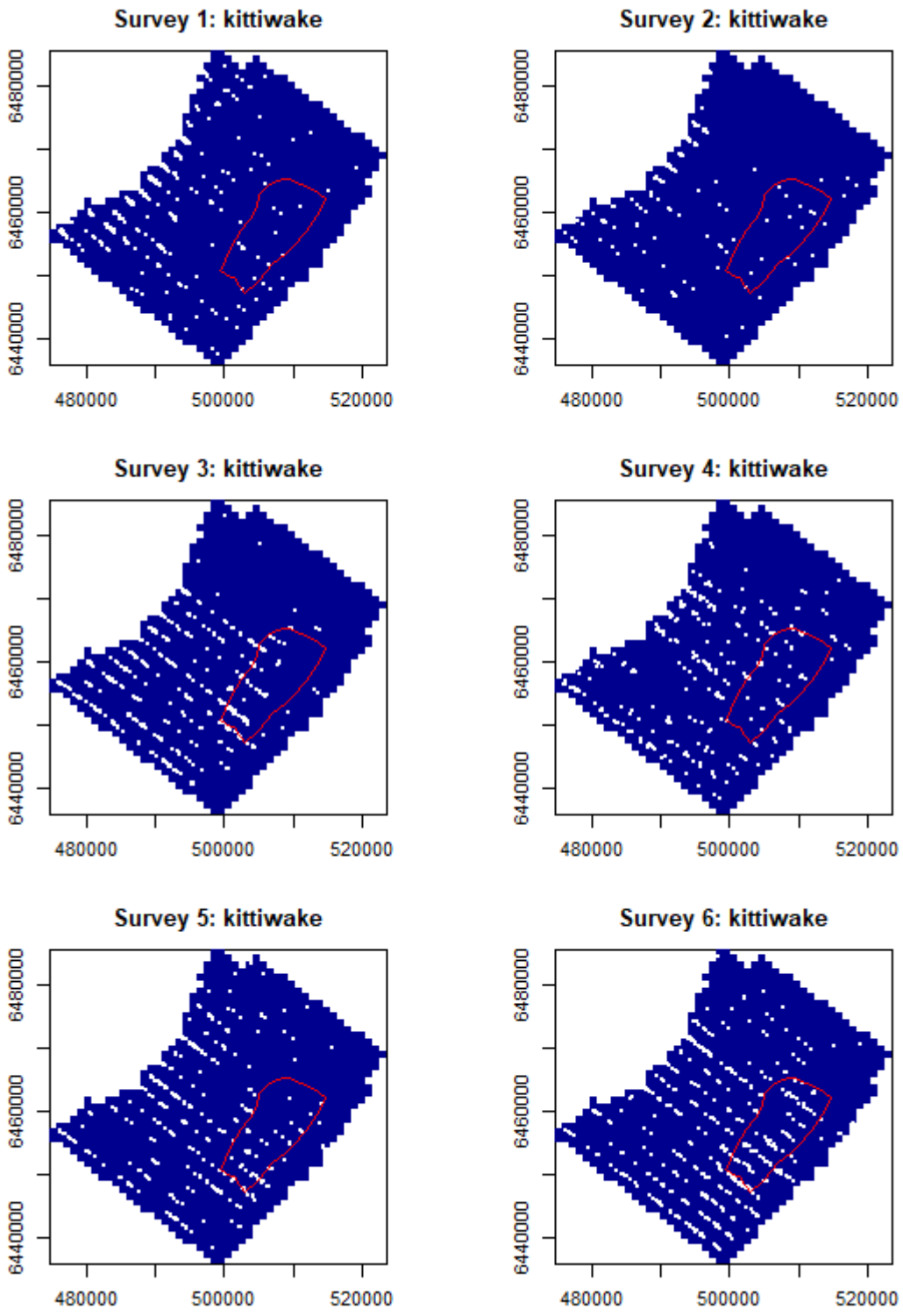

Figure B15. Locations of kittiwakes recorded in flight during 2021 surveys.

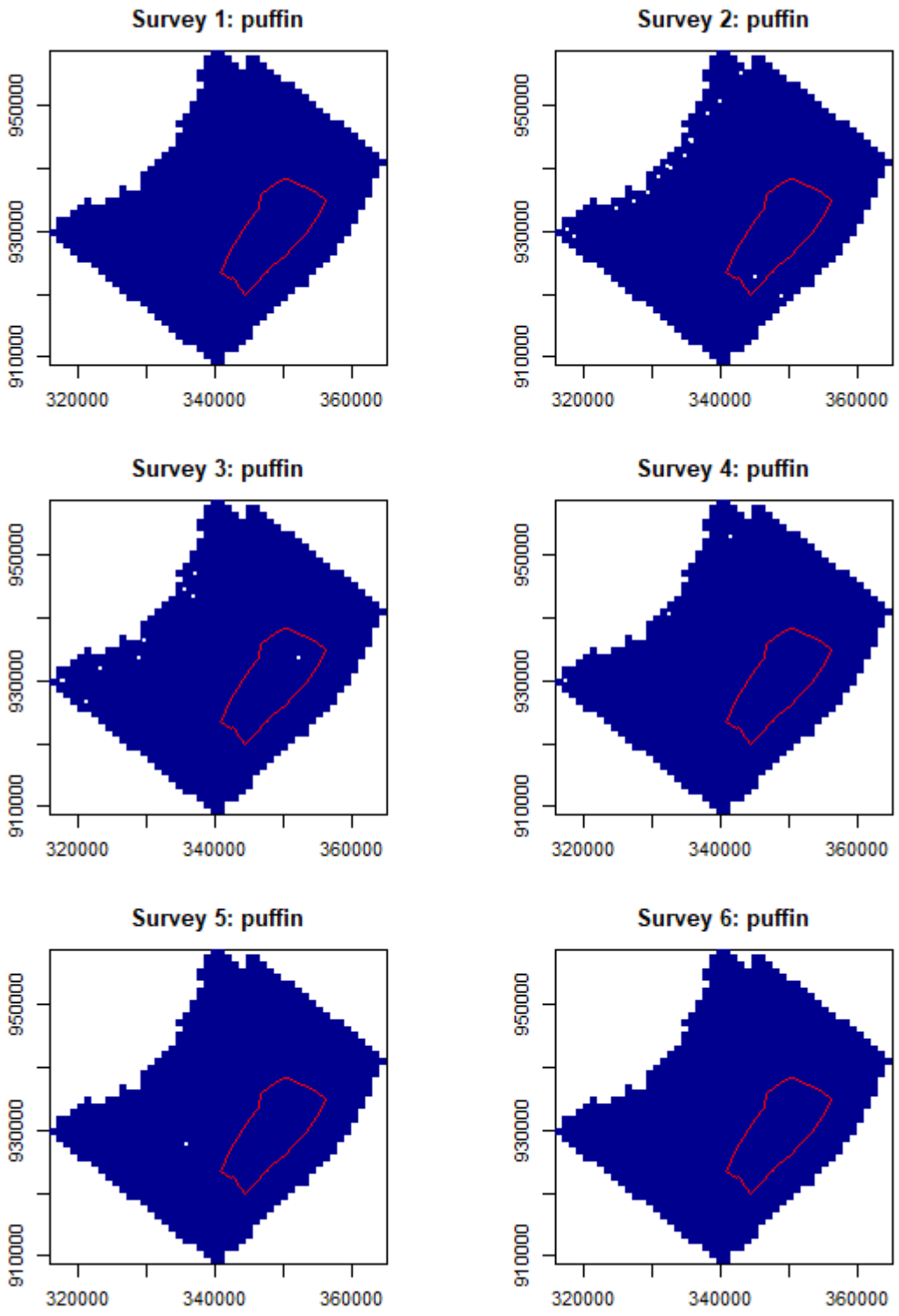

Figure B16. Locations of puffins recorded in flight during 2015 surveys.

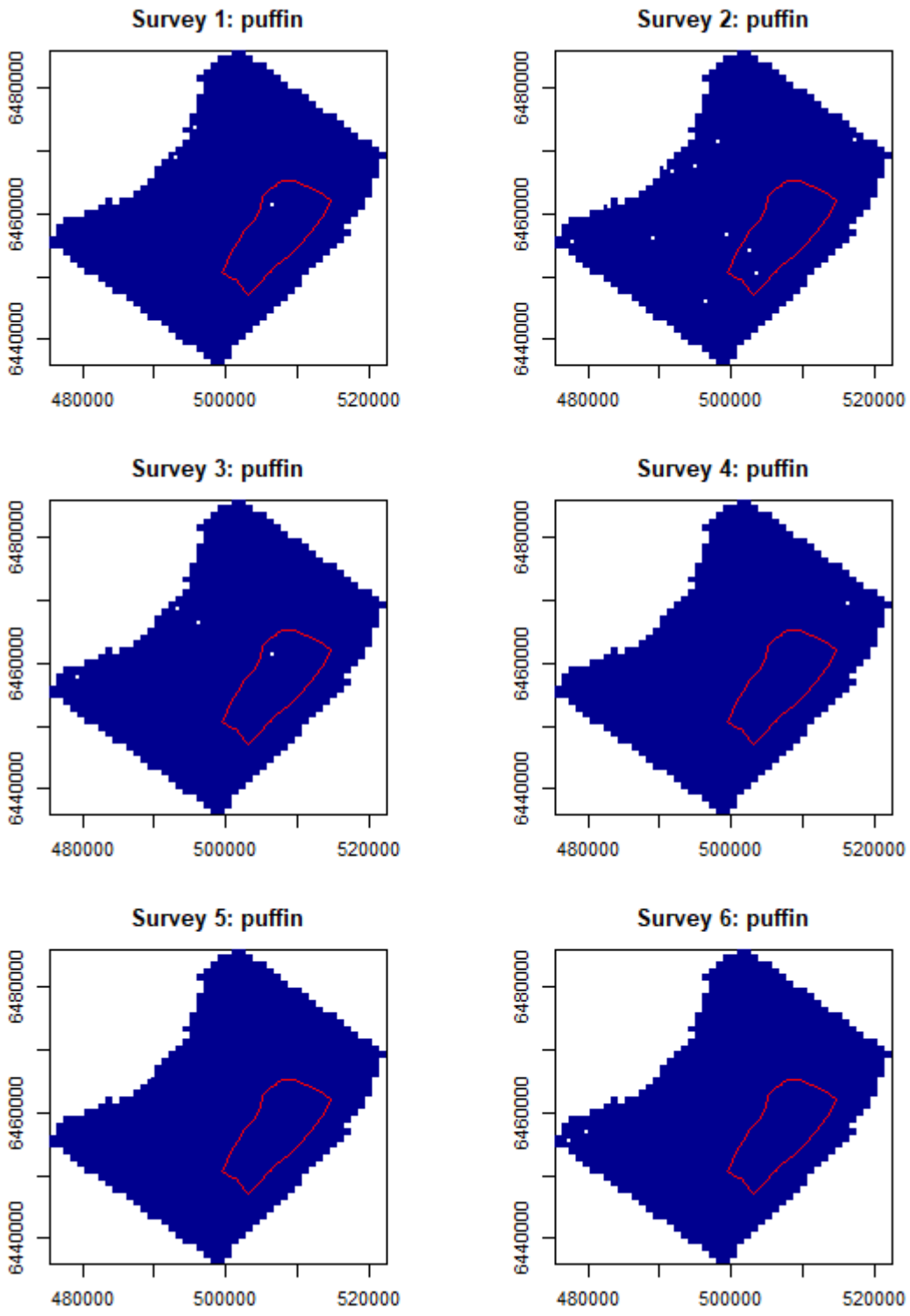

Figure B17. Locations of puffins recorded in flight during 2019 surveys.

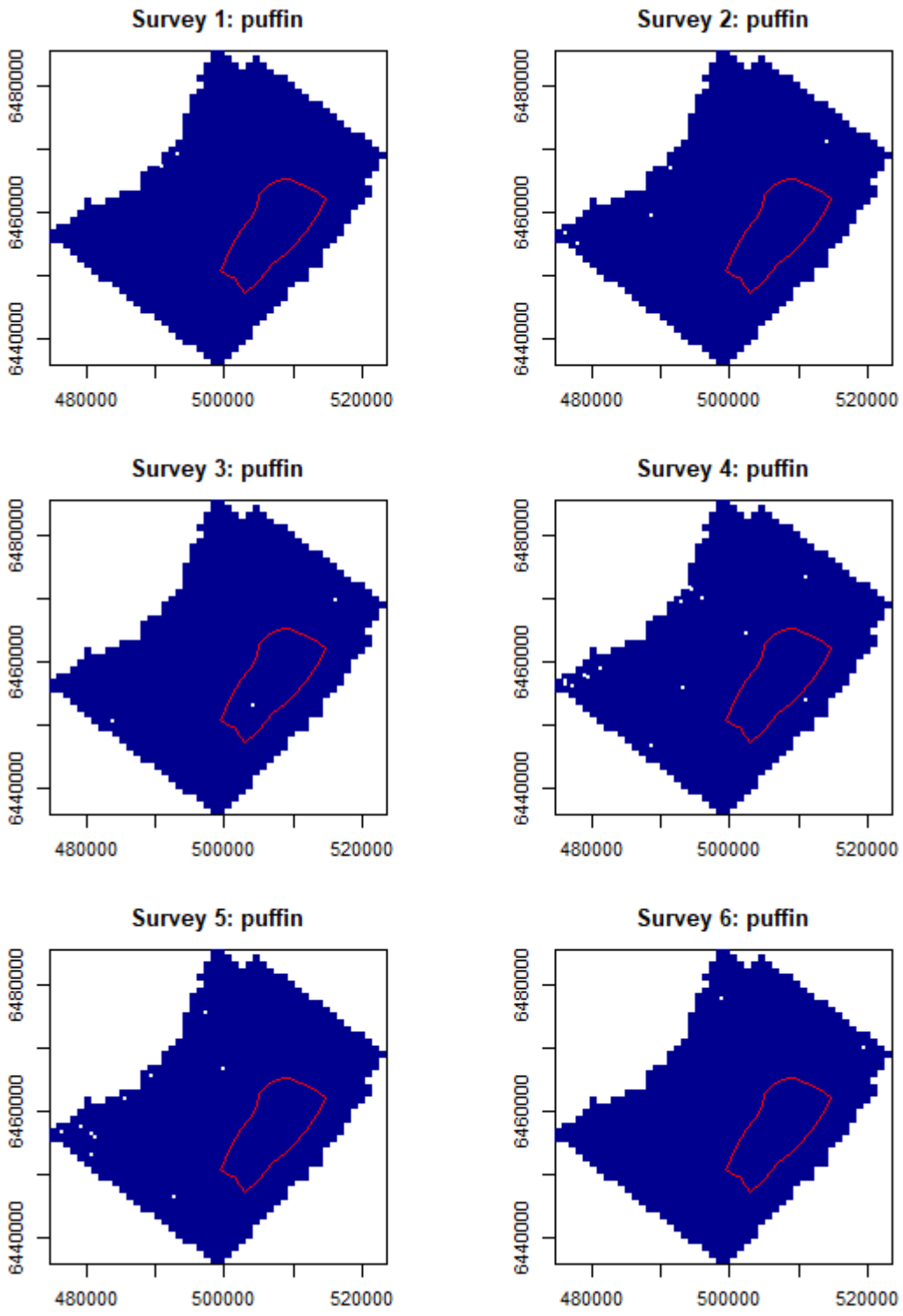

Figure B18. Locations of puffins recorded in flight during 2021 surveys.

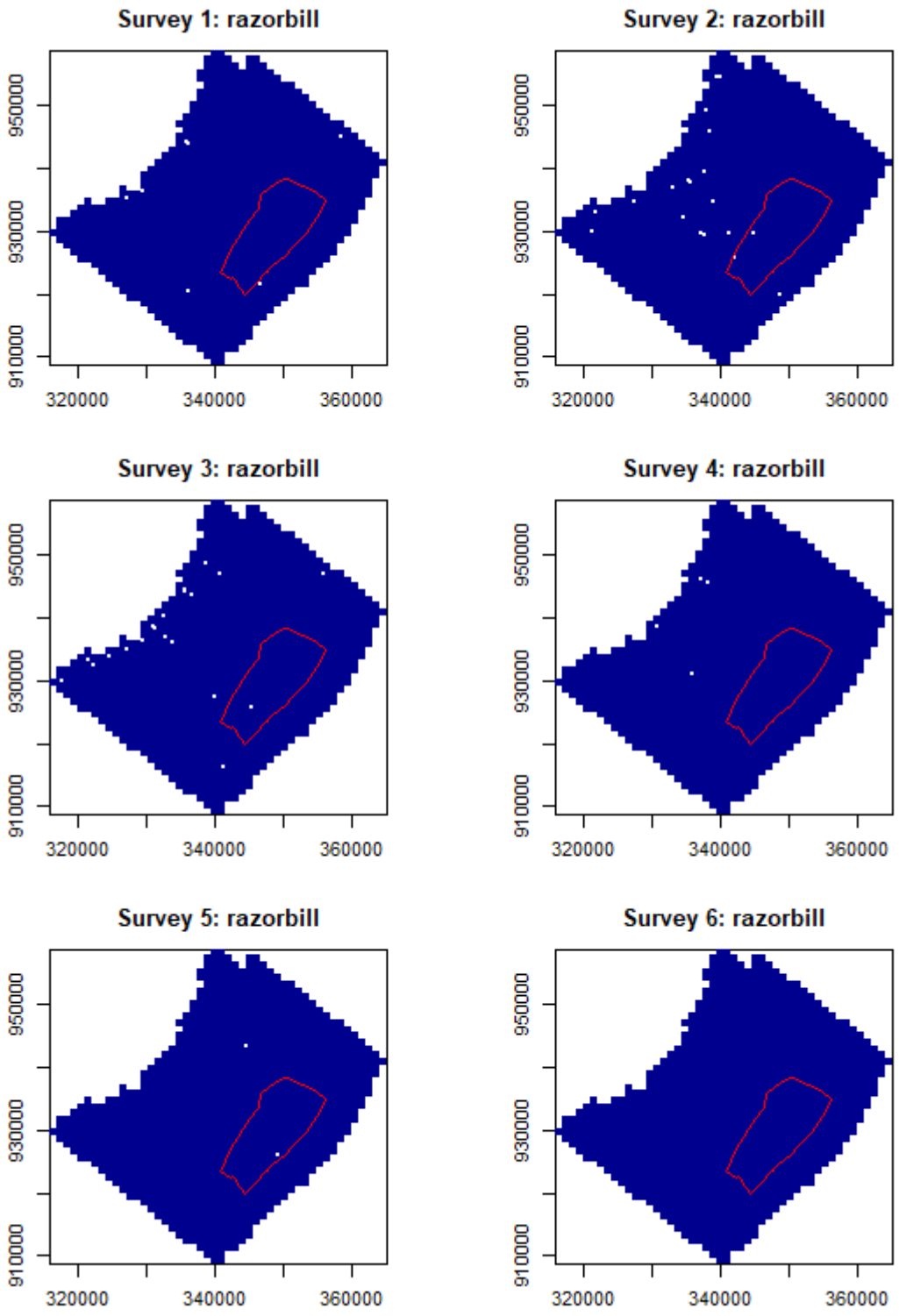

Figure B19. Locations of razorbills recorded in flight during 2015 surveys.

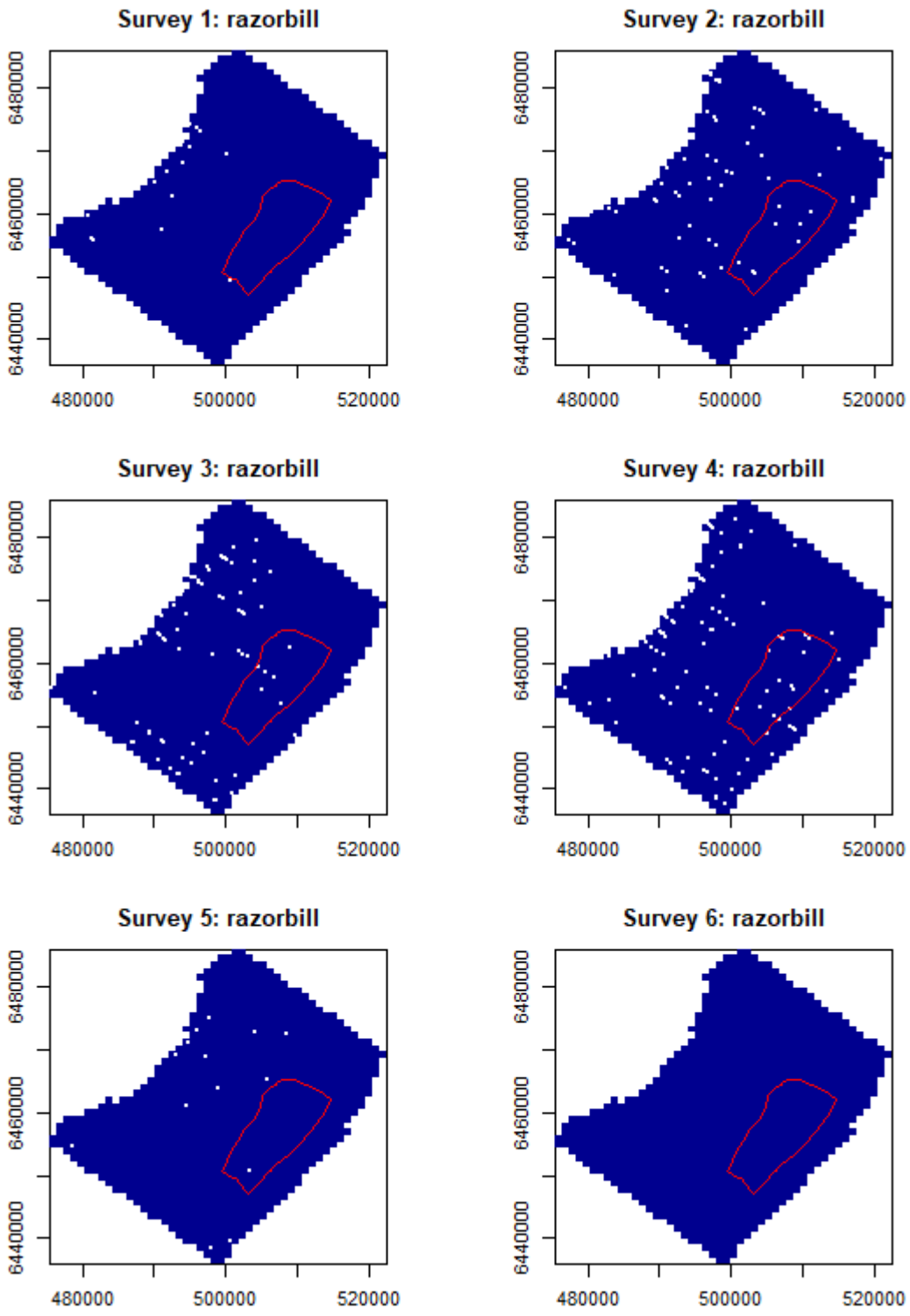

Figure B20. Locations of razorbills recorded in flight during 2019 surveys.

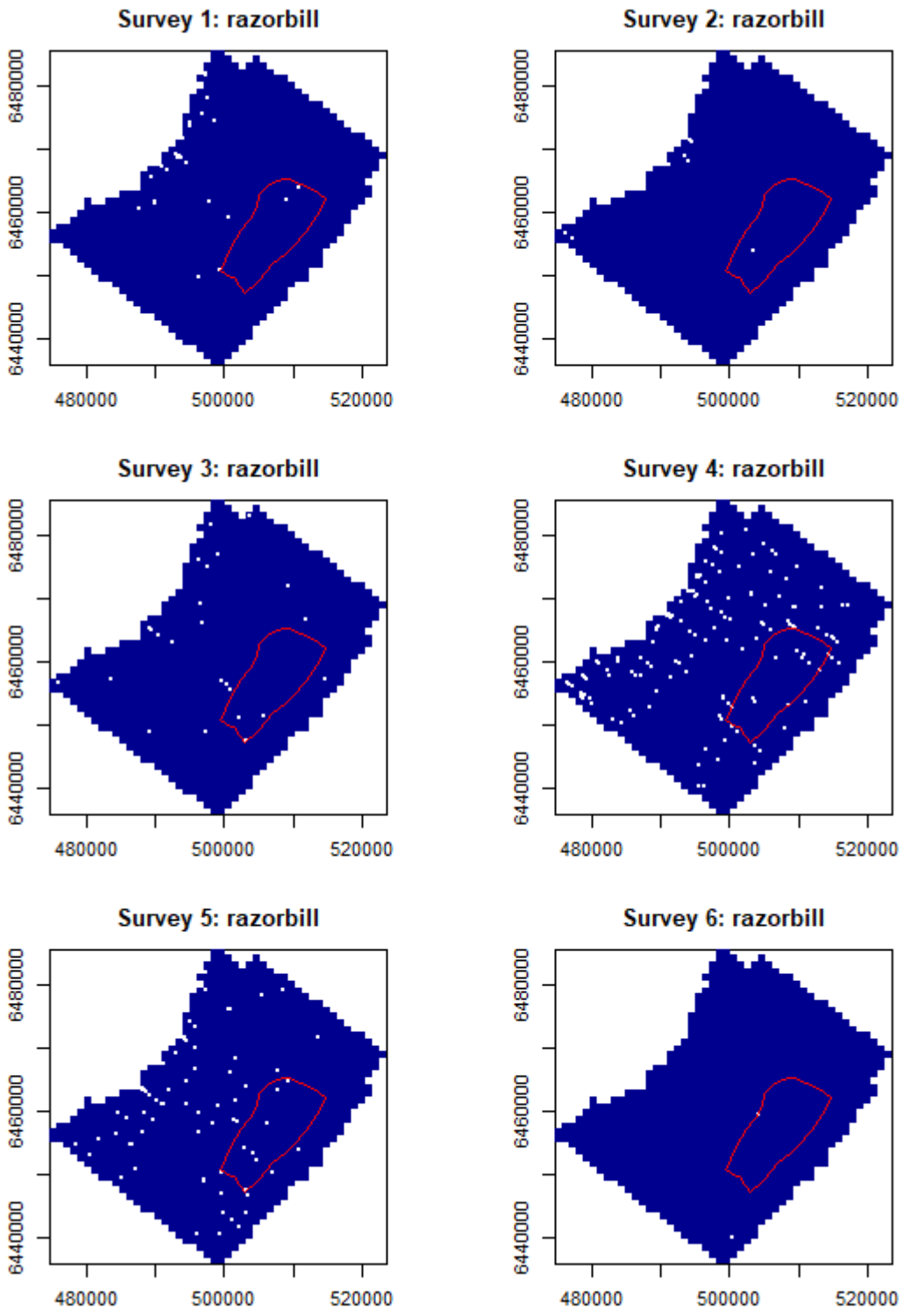

Figure B21. Locations of razorbills recorded in flight during 2021 surveys.

ANNEX C. SPATIAL MODEL COEFFICIENTS

Gannet

Gannet pre vs. post-1	Estimate	Std. Error	Robust S.E.	t value	Pr(>|t|)
(Intercept)	-23.003	6.187	6.741	-3.412	0.001
as.factor(impact)1	3.547	0.948	1.817	1.952	0.051
s(depth)1	12.436	6.921	8.209	1.515	0.130
s(depth)2	13.241	5.997	6.937	1.909	0.056
s(depth)3	13.884	6.779	7.544	1.840	0.066
s(cdist)1	-0.971	2.071	2.562	-0.379	0.705
s(cdist)2	-1.815	2.252	1.709	-1.062	0.288
s(cdist)3	-9.615	2.590	2.617	-3.674	0.000
s(x.pos, y.pos)b1	-5.566	2.121	1.790	-3.110	0.002
s(x.pos, y.pos)b2	-8.868	2.849	2.827	-3.137	0.002
s(x.pos, y.pos)b3	-4.860	1.867	2.099	-2.316	0.021
s(x.pos, y.pos)b4	4.289	3.637	3.257	1.317	0.188
s(x.pos, y.pos)b5	3.689	0.714	1.352	2.729	0.006
as.factor(impact)1:s(x.pos, y.pos)b1	-1.230	1.609	1.755	-0.701	0.483
as.factor(impact)1:s(x.pos, y.pos)b2	-6.624	3.469	5.071	-1.306	0.191
as.factor(impact)1:s(x.pos, y.pos)b3	-9.661	2.813	3.767	-2.564	0.010
as.factor(impact)1:s(x.pos, y.pos)b4	5.841	3.698	4.194	1.393	0.164
as.factor(impact)1:s(x.pos, y.pos)b5	-5.260	1.573	2.070	-2.541	0.011

Gannet pre vs. post-2	Estimate	Std. Error	Robust S.E.	t value	Pr(>|t|)
(Intercept)	-25.085	5.359	7.694	-3.260	0.001
as.factor(year)3	1.600	1.118	1.205	1.328	0.184
s(depth)1	14.036	6.562	9.471	1.482	0.138
s(depth)2	9.972	5.370	7.646	1.304	0.192
s(depth)3	11.792	6.583	9.115	1.294	0.196
s(cdist)1	0.602	2.137	1.847	0.326	0.744
s(cdist)2	0.123	1.598	1.166	0.106	0.916
s(cdist)3	-5.046	2.071	1.544	-3.269	0.001
s(x.pos, y.pos)b1	3.431	1.144	1.279	2.682	0.007
s(x.pos, y.pos)b2	-6.659	2.055	1.998	-3.332	0.001
s(x.pos, y.pos)b3	-4.139	1.922	2.110	-1.962	0.050
s(x.pos, y.pos)b4	6.076	2.142	1.873	3.244	0.001
as.factor(year)3:s(x.pos, y.pos)b1	-6.041	1.629	1.465	-4.123	0.000

Gannet pre vs. post-2	Estimate	Std. Error	Robust S.E.	t value	Pr(>|t|)
as.factor(year)3:s(x.pos, y.pos)b2	3.823	2.110	1.796	2.128	0.033
as.factor(year)3:s(x.pos, y.pos)b3	-2.968	2.576	3.081	-0.963	0.335
as.factor(year)3:s(x.pos, y.pos)b4	-1.463	2.385	2.030	-0.721	0.471

Gannet post-1 vs. post-2	Estimate	Std. Error	Robust S.E.	t value	Pr(>|t|)
(Intercept)	-18.129	3.247	2.437	-7.440	0.000
as.factor(year)3	0.838	0.585	0.921	0.910	0.363
s(depth)1	3.524	3.739	3.262	1.081	0.280
s(depth)2	8.011	3.400	3.607	2.221	0.026
s(depth)3	6.404	3.927	5.481	1.168	0.243
s(cdist)1	-3.079	1.407	1.700	-1.811	0.070
s(cdist)2	-1.313	1.131	1.426	-0.921	0.357
s(cdist)3	-3.626	1.565	1.454	-2.494	0.013
s(x.pos, y.pos)b1	65.835	21.964	32.718	2.012	0.044
s(x.pos, y.pos)b2	-65.501	21.445	33.058	-1.981	0.048
s(x.pos, y.pos)b3	-3.857	1.219	1.655	-2.331	0.020
s(x.pos, y.pos)b4	-6.020	3.992	4.195	-1.435	0.151
as.factor(year)3:s(x.pos, y.pos)b1	-16.690	21.721	27.319	-0.611	0.541
as.factor(year)3:s(x.pos, y.pos)b2	15.504	21.525	27.506	0.564	0.573
as.factor(year)3:s(x.pos, y.pos)b3	-1.659	1.385	1.128	-1.471	0.141
as.factor(year)3:s(x.pos, y.pos)b4	0.949	4.655	4.060	0.234	0.815

Guillemot

Guillemot pre vs. post-1	Estimate	Std. Error	Robust S.E.	t value	Pr(>|t|)
(Intercept)	-11.686	0.391	0.858	-13.613	0.000
as.factor(impact)1	2.893	0.387	0.635	4.554	0.000
s(depth)1	0.105	0.220	0.769	0.137	0.891
s(depth)2	-1.826	0.340	0.759	-2.405	0.016
s(depth)3	-1.262	0.383	0.964	-1.308	0.191
s(cdist)1	-3.644	0.344	0.536	-6.801	0.000
s(cdist)2	1.897	0.465	0.923	2.055	0.040
s(cdist)3	-0.644	0.522	0.999	-0.644	0.519
s(x.pos, y.pos)b1	2.434	0.378	1.138	2.138	0.033
s(x.pos, y.pos)b2	3.066	0.449	0.813	3.770	0.000
s(x.pos, y.pos)b3	-0.046	0.326	0.703	-0.066	0.947
s(x.pos, y.pos)b4	3.445	0.325	0.854	4.035	0.000
s(x.pos, y.pos)b5	0.924	0.419	0.608	1.520	0.128
as.factor(impact)1:s(x.pos, y.pos)b1	-3.466	0.486	1.194	-2.902	0.004
as.factor(impact)1:s(x.pos, y.pos)b2	-2.350	0.458	0.753	-3.119	0.002
as.factor(impact)1:s(x.pos, y.pos)b3	-2.353	0.381	0.853	-2.759	0.006
as.factor(impact)1:s(x.pos, y.pos)b4	-0.263	0.299	0.746	-0.353	0.724
as.factor(impact)1:s(x.pos, y.pos)b5	-2.646	0.438	0.757	-3.495	0.000

Guillemot pre vs. post-2	Estimate	Std. Error	Robust S.E.	t value	Pr(>|t|)
(Intercept)	-10.567	0.385	0.708	-14.930	0.000
as.factor(year)3	1.546	0.247	0.493	3.136	0.002
s(depth)1	0.805	0.220	0.487	1.655	0.098
s(depth)2	-2.686	0.305	0.686	-3.915	0.000
s(depth)3	-2.135	0.379	0.703	-3.039	0.002
s(cdist)1	0.803	0.212	0.513	1.564	0.118
s(cdist)2	-1.122	0.217	0.469	-2.389	0.017
s(cdist)3	3.605	0.507	1.144	3.150	0.002
s(cdist)4	-1.154	0.495	0.950	-1.215	0.224
s(x.pos, y.pos)b1	0.423	0.422	0.769	0.550	0.582
s(x.pos, y.pos)b2	11.194	1.893	4.547	2.462	0.014
s(x.pos, y.pos)b3	-9.282	1.938	4.501	-2.062	0.039
s(x.pos, y.pos)b4	-0.474	0.531	0.919	-0.516	0.606
as.factor(year)3:s(x.pos, y.pos)b1	-0.591	0.362	0.750	-0.789	0.430
as.factor(year)3:s(x.pos, y.pos)b2	14.314	2.104	5.388	2.657	0.008

Guillemot pre vs. post-2	Estimate	Std. Error	Robust S.E.	t value	Pr(>|t|)
as.factor(year)3:s(x.pos, y.pos)b3	-15.090	2.153	5.184	-2.911	0.004
as.factor(year)3:s(x.pos, y.pos)b4	-2.297	0.552	1.293	-1.776	0.076

Guillemot post-1 vs. post-2	Estimate	Std. Error	Robust S.E.	t value	Pr(>|t|)
(Intercept)	-8.154	0.137	0.277	-29.455	0.000
as.factor(year)3	0.430	0.149	0.356	1.208	0.227
s(cdist)1	-3.858	0.207	0.538	-7.171	0.000
s(cdist)2	-0.723	0.222	0.535	-1.352	0.176
s(cdist)3	-4.632	0.325	0.546	-8.479	0.000
s(cdist)4	-4.683	1.211	1.329	-3.524	0.000
s(x.pos, y.pos)b1	27.257	13.523	19.347	1.409	0.159
s(x.pos, y.pos)b2	-12.563	4.853	7.599	-1.653	0.098
s(x.pos, y.pos)b3	5.061	0.550	1.265	4.003	0.000
s(x.pos, y.pos)b4	-15.004	9.500	13.023	-1.152	0.249
s(x.pos, y.pos)b5	-5.192	0.564	1.209	-4.294	0.000
as.factor(year)3:s(x.pos, y.pos)b1	22.053	16.035	27.211	0.810	0.418
as.factor(year)3:s(x.pos, y.pos)b2	-11.930	5.878	10.582	-1.127	0.260
as.factor(year)3:s(x.pos, y.pos)b3	1.953	0.604	1.577	1.239	0.215
as.factor(year)3:s(x.pos, y.pos)b4	-10.863	11.073	18.068	-0.601	0.548
as.factor(year)3:s(x.pos, y.pos)b5	-1.649	0.642	1.545	-1.067	0.286

Kittiwake

Kittiwake pre vs. post-1	Estimate	Std. Error	Robust S.E.	t value	Pr(>|t|)
(Intercept)	-13.400	1.471	1.494	-8.972	0.000
as.factor(impact)1	3.124	1.485	1.695	1.843	0.065
s(depth)1	4.325	1.810	1.314	3.291	0.001
s(depth)2	-0.256	1.359	1.036	-0.247	0.805
s(depth)3	3.087	2.123	1.930	1.600	0.110
s(cdist)1	-1.016	1.348	1.550	-0.656	0.512
s(cdist)2	1.934	1.049	1.127	1.717	0.086
s(cdist)3	-0.715	1.180	1.200	-0.595	0.552
s(cdist)4	-1.947	1.454	1.757	-1.108	0.268
s(cdist)5	-3.335	1.631	1.665	-2.004	0.045
s(x.pos, y.pos)b1	1.083	1.395	1.584	0.684	0.494
s(x.pos, y.pos)b2	-1.498	1.462	1.622	-0.924	0.356
s(x.pos, y.pos)b3	-4.357	1.757	1.316	-3.311	0.001
s(x.pos, y.pos)b4	-5.554	2.699	2.928	-1.897	0.058
s(x.pos, y.pos)b5	6.620	3.333	3.496	1.894	0.058
as.factor(impact)1:s(x.pos, y.pos)b1	-5.575	1.595	1.899	-2.936	0.003
as.factor(impact)1:s(x.pos, y.pos)b2	-3.850	1.720	1.891	-2.037	0.042
as.factor(impact)1:s(x.pos, y.pos)b3	0.954	1.956	1.345	0.709	0.478
as.factor(impact)1:s(x.pos, y.pos)b4	5.838	2.707	3.007	1.942	0.052
as.factor(impact)1:s(x.pos, y.pos)b5	-9.278	3.666	4.054	-2.289	0.022

Kittiwake pre vs. post-2	Estimate	Std. Error	Robust S.E.	t value	Pr(>|t|)
(Intercept)	-14.502	1.016	1.163	-12.470	0.000
as.factor(year)3	1.197	0.434	0.640	1.869	0.062
s(depth)1	2.039	1.373	1.200	1.698	0.089
s(depth)2	-1.596	1.042	1.031	-1.548	0.122
s(depth)3	-0.311	1.131	0.891	-0.350	0.727
s(depth)4	-4.117	1.441	1.513	-2.720	0.007
s(depth)5	-0.600	1.938	1.588	-0.378	0.706
s(cdist)1	4.714	1.461	1.977	2.384	0.017
s(cdist)2	3.235	1.027	1.378	2.348	0.019
s(cdist)3	0.840	1.366	1.597	0.526	0.599
s(x.pos, y.pos)b1	5.579	1.643	2.332	2.392	0.017
s(x.pos, y.pos)b2	-2.984	1.596	1.577	-1.892	0.059
s(x.pos, y.pos)b3	-4.491	6.956	4.409	-1.018	0.308

Kittiwake pre vs. post-2	Estimate	Std. Error	Robust S.E.	t value	Pr(>|t|)
s(x.pos, y.pos)b4	1.291	7.315	4.599	0.281	0.779
as.factor(year)3:s(x.pos, y.pos)b1	1.114	1.376	1.691	0.659	0.510
as.factor(year)3:s(x.pos, y.pos)b2	-3.108	1.857	2.094	-1.484	0.138
as.factor(year)3:s(x.pos, y.pos)b3	8.687	9.612	7.169	1.212	0.226
as.factor(year)3:s(x.pos, y.pos)b4	-10.298	10.385	7.957	-1.294	0.196

Kittiwake post-1 vs. post-2	Estimate	Std. Error	Robust S.E.	t value	Pr(>|t|)
(Intercept)	-21.423	3.588	4.069	-5.266	0.000
as.factor(year)3	0.131	1.279	1.154	0.113	0.910
s(depth)1	-0.273	1.683	1.246	-0.219	0.827
s(depth)2	-0.688	1.521	1.186	-0.580	0.562
s(depth)3	-2.819	1.769	1.363	-2.069	0.039
s(depth)4	0.432	2.059	2.124	0.203	0.839
s(cdist)1	-0.259	1.635	1.225	-0.211	0.833
s(cdist)2	6.495	2.160	2.167	2.998	0.003
s(cdist)3	10.224	4.227	4.411	2.318	0.020
s(cdist)4	8.418	3.770	3.773	2.231	0.026
s(x.pos, y.pos)b1	7.195	3.448	3.597	2.000	0.046
s(x.pos, y.pos)b2	-0.259	1.351	1.233	-0.210	0.834
s(x.pos, y.pos)b3	5.502	2.745	3.173	1.734	0.083
s(x.pos, y.pos)b4	7.456	4.457	4.100	1.818	0.069
s(x.pos, y.pos)b5	-5.749	3.890	3.504	-1.641	0.101
as.factor(year)3:s(x.pos, y.pos)b1	2.106	1.896	1.960	1.074	0.283
as.factor(year)3:s(x.pos, y.pos)b2	0.069	1.839	1.632	0.042	0.966
as.factor(year)3:s(x.pos, y.pos)b3	-0.162	2.883	2.921	-0.055	0.956
as.factor(year)3:s(x.pos, y.pos)b4	5.784	2.761	2.712	2.132	0.033
as.factor(year)3:s(x.pos, y.pos)b5	-4.667	4.384	3.578	-1.305	0.192

Razorbill

Razorbill pre vs. post-1	Estimate	Std. Error	Robust S.E.	t value	Pr(>|t|)
(Intercept)	-11.018	0.500	0.805	-13.684	0.000
as.factor(impact)1	3.719	0.517	0.946	3.930	0.000
s(cdist)1	-1.802	0.290	0.371	-4.852	0.000
s(cdist)2	-1.026	0.301	0.410	-2.503	0.012
s(cdist)3	-5.327	0.420	0.719	-7.407	0.000
s(x.pos, y.pos)b1	-0.954	0.563	0.814	-1.171	0.242
s(x.pos, y.pos)b2	-0.971	0.704	1.223	-0.794	0.427
s(x.pos, y.pos)b3	-2.156	0.720	0.896	-2.407	0.016
s(x.pos, y.pos)b4	-0.735	0.508	0.662	-1.110	0.267
as.factor(impact)1:s(x.pos, y.pos)b1	-2.683	0.631	0.998	-2.687	0.007
as.factor(impact)1:s(x.pos, y.pos)b2	-3.184	0.676	1.356	-2.348	0.019
as.factor(impact)1:s(x.pos, y.pos)b3	-2.435	0.679	0.926	-2.629	0.009
as.factor(impact)1:s(x.pos, y.pos)b4	-1.048	0.491	0.707	-1.483	0.138

Razorbill pre vs. post-2	Estimate	Std. Error	Robust S.E.	t value	Pr(>|t|)
(Intercept)	-12.799	0.839	1.519	-8.427	0.000
as.factor(year)3	4.577	0.855	1.600	2.861	0.004
s(depth)1	2.621	0.463	0.639	4.101	0.000
s(depth)2	0.716	0.248	0.371	1.931	0.054
s(depth)3	1.344	0.401	0.554	2.426	0.015
s(depth)4	-1.173	0.413	0.604	-1.942	0.052
s(depth)5	-0.465	0.838	1.163	-0.400	0.689
s(depth)6	-1.581	1.606	1.837	-0.861	0.389
s(cdist)1	1.237	0.280	0.424	2.917	0.004
s(cdist)2	-1.732	0.396	0.551	-3.146	0.002
s(cdist)3	-0.762	0.442	0.798	-0.954	0.340
s(cdist)4	-4.386	0.572	1.055	-4.156	0.000
s(cdist)5	-6.082	0.842	1.391	-4.371	0.000
s(cdist)6	-6.743	0.736	1.024	-6.584	0.000
s(x.pos, y.pos)b1	3.506	0.905	1.747	2.007	0.045
s(x.pos, y.pos)b2	-1.733	0.756	1.361	-1.273	0.203
s(x.pos, y.pos)b3	2.177	0.961	1.838	1.184	0.236
s(x.pos, y.pos)b4	-3.514	3.354	4.939	-0.711	0.477
s(x.pos, y.pos)b5	2.560	3.310	4.407	0.581	0.561
as.factor(year)3:s(x.pos, y.pos)b1	-2.417	0.764	1.366	-1.769	0.077

Razorbill pre vs. post-2	Estimate	Std. Error	Robust S.E.	t value	Pr(>|t|)
as.factor(year)3:s(x.pos, y.pos)b2	-3.261	0.822	1.514	-2.154	0.031
as.factor(year)3:s(x.pos, y.pos)b3	-4.316	1.010	1.780	-2.425	0.015
as.factor(year)3:s(x.pos, y.pos)b4	-16.172	3.652	5.640	-2.867	0.004
as.factor(year)3:s(x.pos, y.pos)b5	13.980	3.529	4.810	2.906	0.004

Razorbill post-1 vs. post-2	Estimate	Std. Error	Robust S.E.	t value	Pr(>|t|)
(Intercept)	-4.990	0.482	0.958	-5.206	0.000
as.factor(year)3	-0.304	0.542	1.005	-0.302	0.762
s(cdist)1	-2.468	0.173	0.295	-8.367	0.000
s(cdist)2	-3.815	0.204	0.381	-10.020	0.000
s(cdist)3	-5.674	0.328	0.535	-10.604	0.000
s(x.pos, y.pos)b1	-2.668	0.288	0.494	-5.402	0.000
s(x.pos, y.pos)b2	1.247	0.345	0.497	2.507	0.012
s(x.pos, y.pos)b3	-5.021	0.521	1.082	-4.642	0.000
s(x.pos, y.pos)b4	-3.502	0.319	0.567	-6.172	0.000
as.factor(year)3:s(x.pos, y.pos)b1	0.198	0.316	0.493	0.402	0.688
as.factor(year)3:s(x.pos, y.pos)b2	-0.724	0.456	0.682	-1.062	0.288
as.factor(year)3:s(x.pos, y.pos)b3	0.238	0.614	1.202	0.198	0.843
as.factor(year)3:s(x.pos, y.pos)b4	0.249	0.381	0.631	0.395	0.693

Puffin

Puffin pre vs. post-1	Estimate	Std. Error	Robust S.E.	t value	Pr(>|t|)
(Intercept)	-6.003	0.443	1.252	-4.794	0.000
as.factor(impact)1	-0.835	0.588	0.883	-0.946	0.344
depth	-0.056	0.004	0.007	-8.525	0.000
cdist	-0.159	0.018	0.040	-3.936	0.000
s(x.pos, y.pos)b1	-5.565	0.446	1.144	-4.863	0.000
s(x.pos, y.pos)b2	-5.618	0.542	1.304	-4.307	0.000
s(x.pos, y.pos)b3	2.229	1.001	1.473	1.513	0.130
s(x.pos, y.pos)b4	-2.846	0.789	1.141	-2.493	0.013
s(x.pos, y.pos)b5	-1.509	0.648	1.102	-1.369	0.171
as.factor(impact)1:s(x.pos, y.pos)b1	1.135	0.665	0.870	1.304	0.192
as.factor(impact)1:s(x.pos, y.pos)b2	0.504	0.802	1.140	0.442	0.658
as.factor(impact)1:s(x.pos, y.pos)b3	5.129	1.555	1.919	2.672	0.008
as.factor(impact)1:s(x.pos, y.pos)b4	-2.433	1.336	1.653	-1.472	0.141
as.factor(impact)1:s(x.pos, y.pos)b5	-4.993	1.280	1.627	-3.069	0.002

Puffin pre vs. post-2	Estimate	Std. Error	Robust S.E.	t value	Pr(>|t|)
(Intercept)	-11.634	0.288	0.496	-23.442	0.000
as.factor(year)3	0.274	0.227	0.415	0.659	0.510
depth	-0.016	0.005	0.009	-1.909	0.056
s(cdist)1	-2.064	0.355	0.557	-3.709	0.000
s(cdist)2	-0.618	0.274	0.578	-1.069	0.285
s(cdist)3	-1.881	0.320	0.546	-3.448	0.001
s(cdist)4	-1.294	0.301	0.535	-2.419	0.016
s(cdist)5	-36.559	59.870	19.890	-1.838	0.066
s(cdist)6	-11.266	285.997	0.735	-15.325	0.000
s(x.pos, y.pos)b1	12.472	3.119	4.729	2.637	0.008
s(x.pos, y.pos)b2	-11.854	3.239	4.786	-2.477	0.013
s(x.pos, y.pos)b3	-2.036	1.333	2.276	-0.894	0.371
s(x.pos, y.pos)b4	0.817	0.569	1.096	0.746	0.456
s(x.pos, y.pos)b5	1.535	1.354	2.152	0.713	0.476
as.factor(year)3:s(x.pos, y.pos)b1	6.960	3.499	4.473	1.556	0.120
as.factor(year)3:s(x.pos, y.pos)b2	-6.985	3.580	4.497	-1.553	0.120
as.factor(year)3:s(x.pos, y.pos)b3	-4.560	1.372	2.211	-2.062	0.039
as.factor(year)3:s(x.pos, y.pos)b4	2.592	0.595	1.042	2.487	0.013
as.factor(year)3:s(x.pos, y.pos)b5	5.022	1.425	1.989	2.525	0.012

Puffin post-1 vs. post-2	Estimate	Std. Error	Robust S.E.	t value	Pr(>|t|)
(Intercept)	-11.105	0.458	0.982	-11.312	0.000
as.factor(year)3	3.456	0.340	0.560	6.173	0.000
s(depth)1	-0.567	0.519	0.645	-0.878	0.380
s(depth)2	-0.635	0.372	0.440	-1.442	0.149
s(depth)3	-0.102	0.405	0.528	-0.194	0.846
s(depth)4	-0.597	0.461	0.791	-0.755	0.450
s(depth)5	-0.020	0.546	0.721	-0.028	0.978
s(cdist)1	-1.806	0.489	0.931	-1.939	0.053
s(cdist)2	-4.239	0.618	1.066	-3.978	0.000
s(cdist)3	-4.220	0.596	0.993	-4.252	0.000
s(x.pos, y.pos)b1	12.416	10.734	12.323	1.008	0.314
s(x.pos, y.pos)b2	2.828	1.600	1.667	1.696	0.090
s(x.pos, y.pos)b3	-1.484	0.796	1.183	-1.255	0.210
s(x.pos, y.pos)b4	-13.099	11.336	13.089	-1.001	0.317
s(x.pos, y.pos)b5	-3.406	0.868	1.210	-2.814	0.005
as.factor(year)3:s(x.pos, y.pos)b1	32.447	11.008	15.373	2.111	0.035
as.factor(year)3:s(x.pos, y.pos)b2	1.081	1.671	2.058	0.525	0.599
as.factor(year)3:s(x.pos, y.pos)b3	-4.738	0.723	1.115	-4.251	0.000
as.factor(year)3:s(x.pos, y.pos)b4	-32.406	11.634	16.149	-2.007	0.045
as.factor(year)3:s(x.pos, y.pos)b5	0.172	0.806	1.014	0.169	0.866

ANNEX D. BEFORE:AFTER MODEL PARTIAL PLOTS

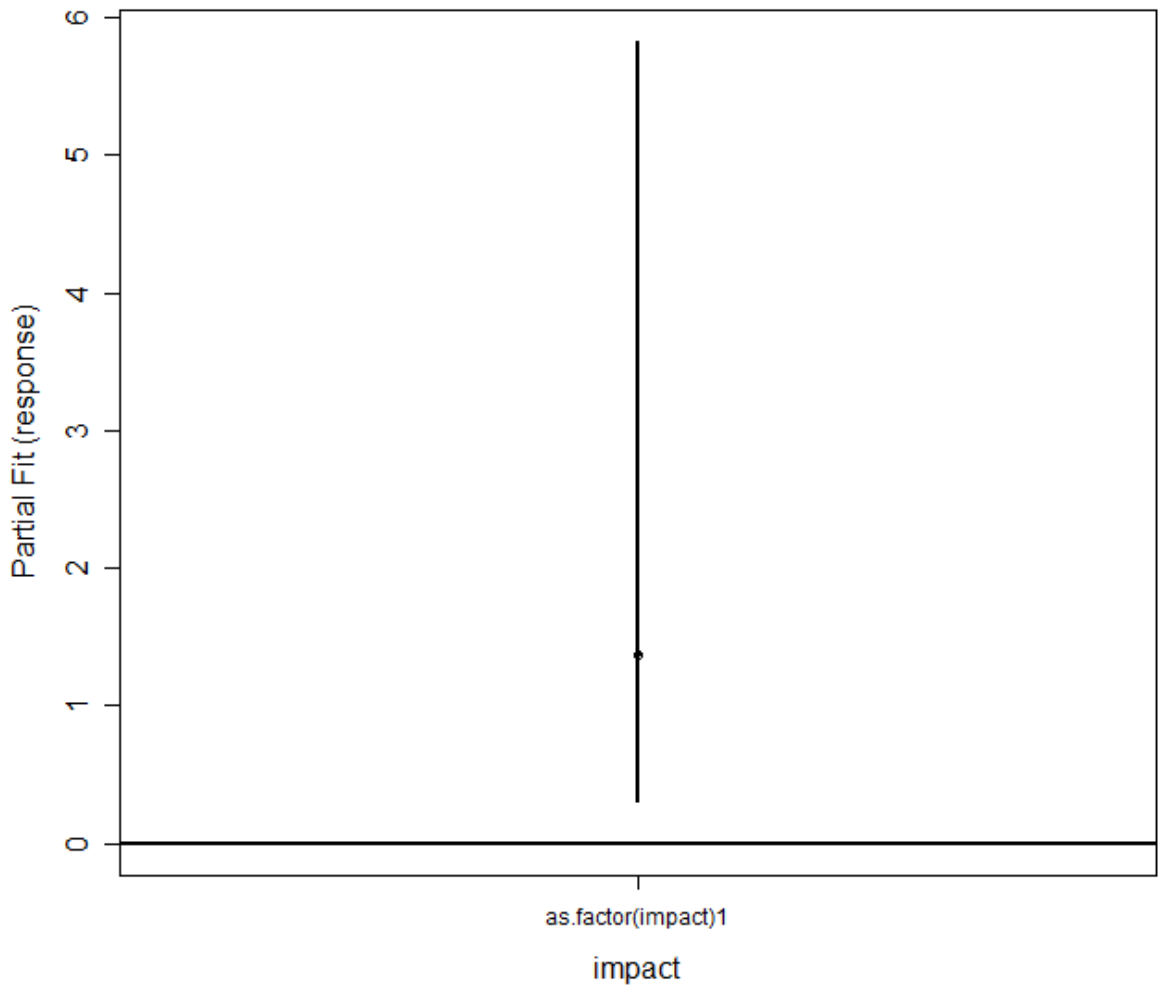

Figure D3.1 Gannet partial plot of impact

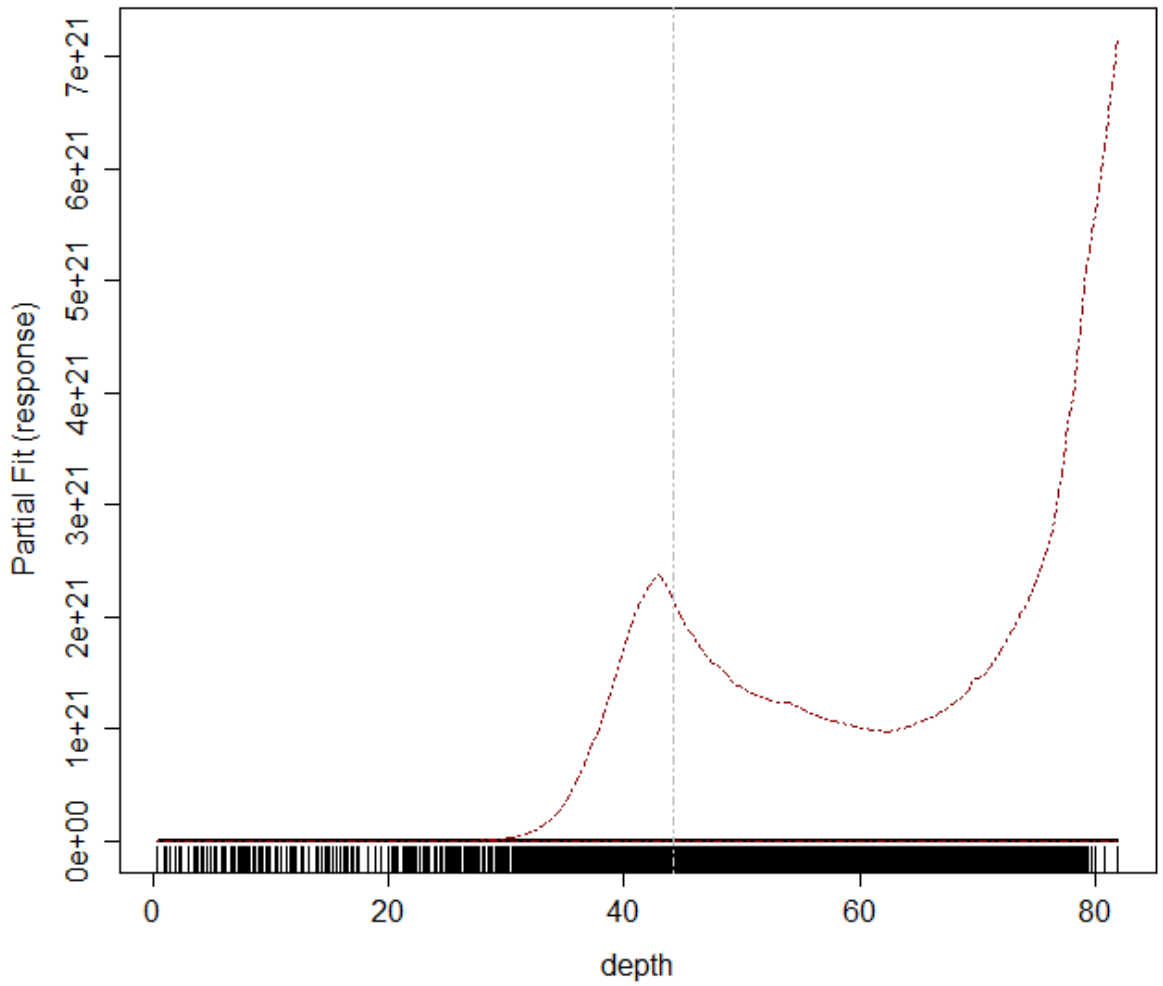

Figure D3.2 Gannet partial plot of depth

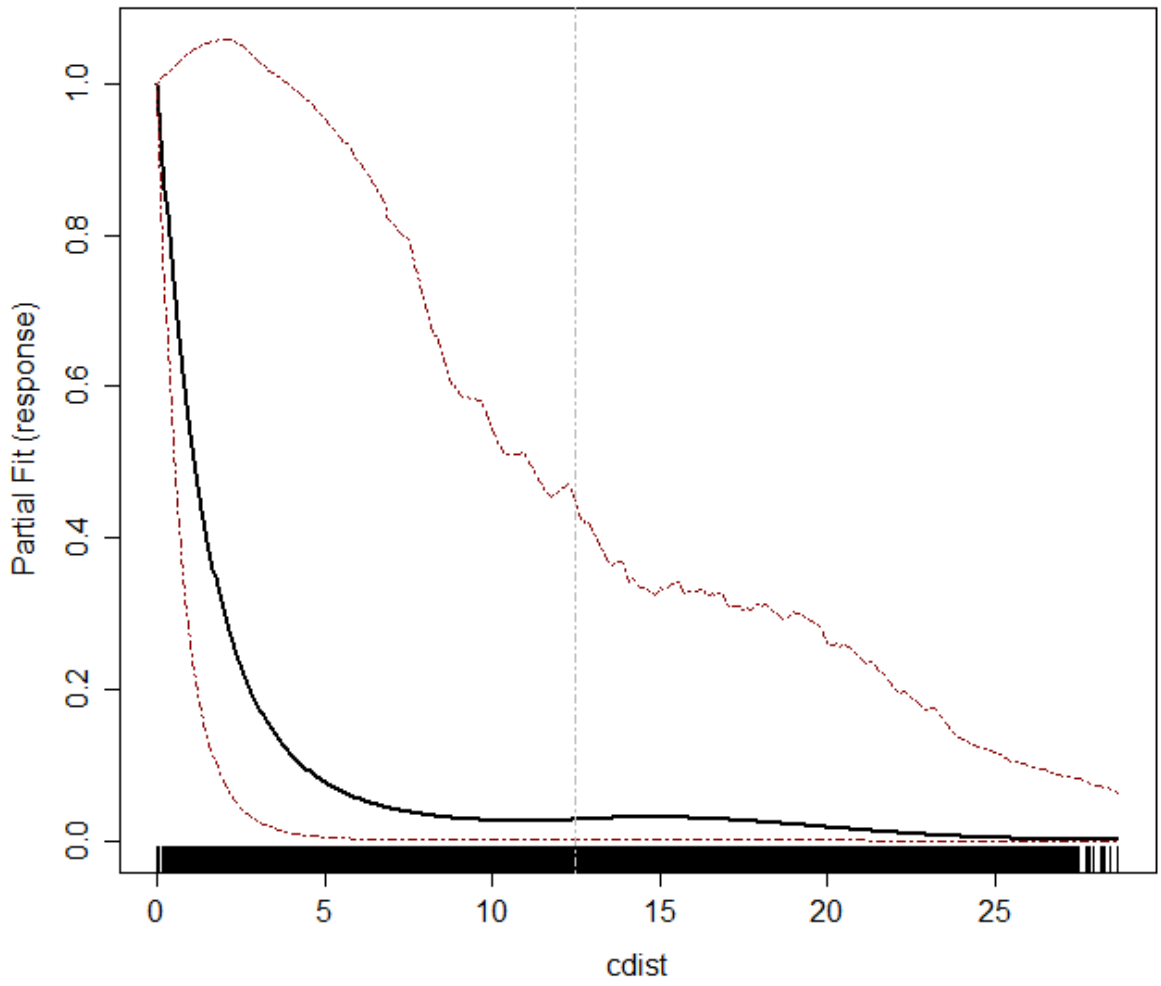

Figure D3.3. Gannet partial plot of distance to coast (cdist).

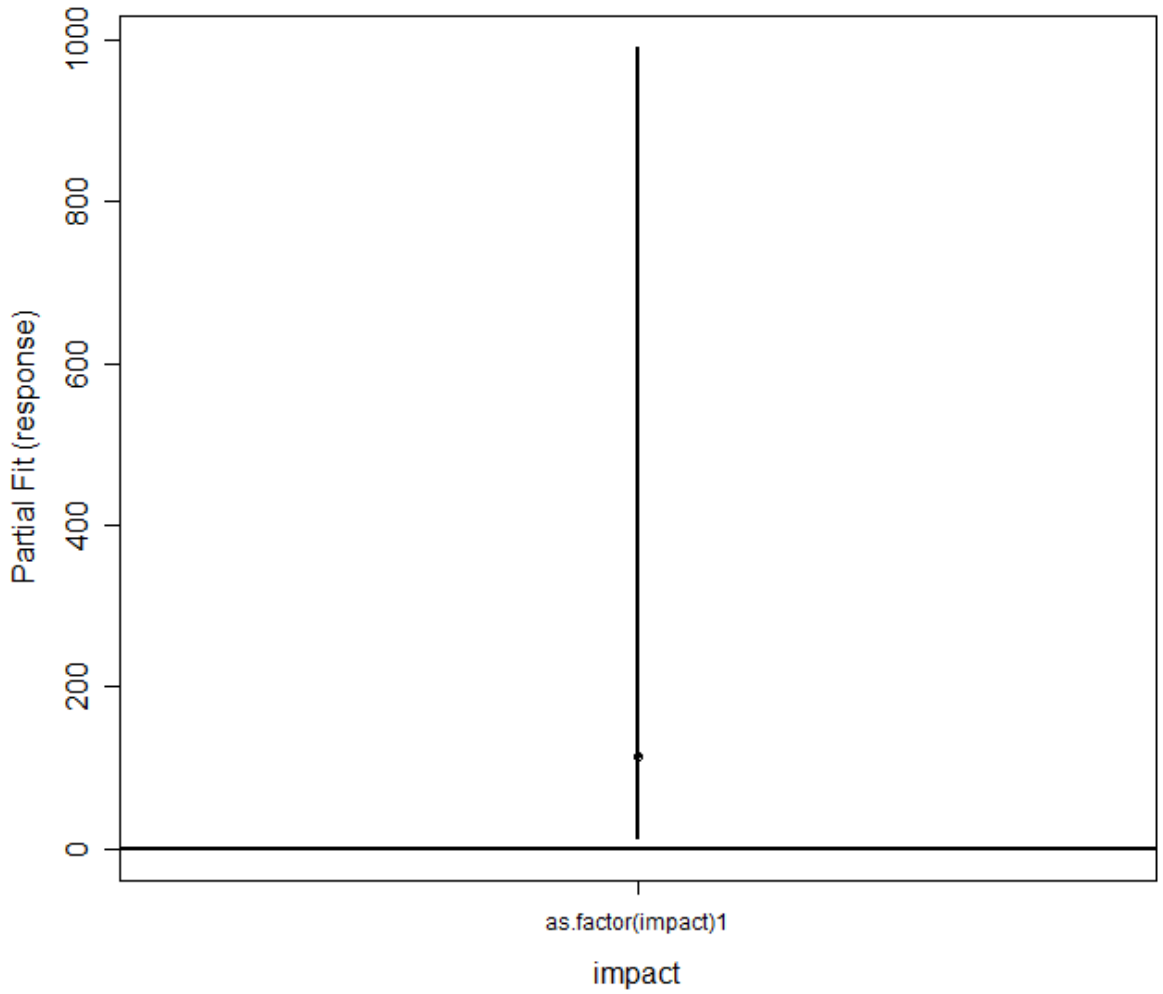

Figure D3.4. Guillemot partial plot of impact.

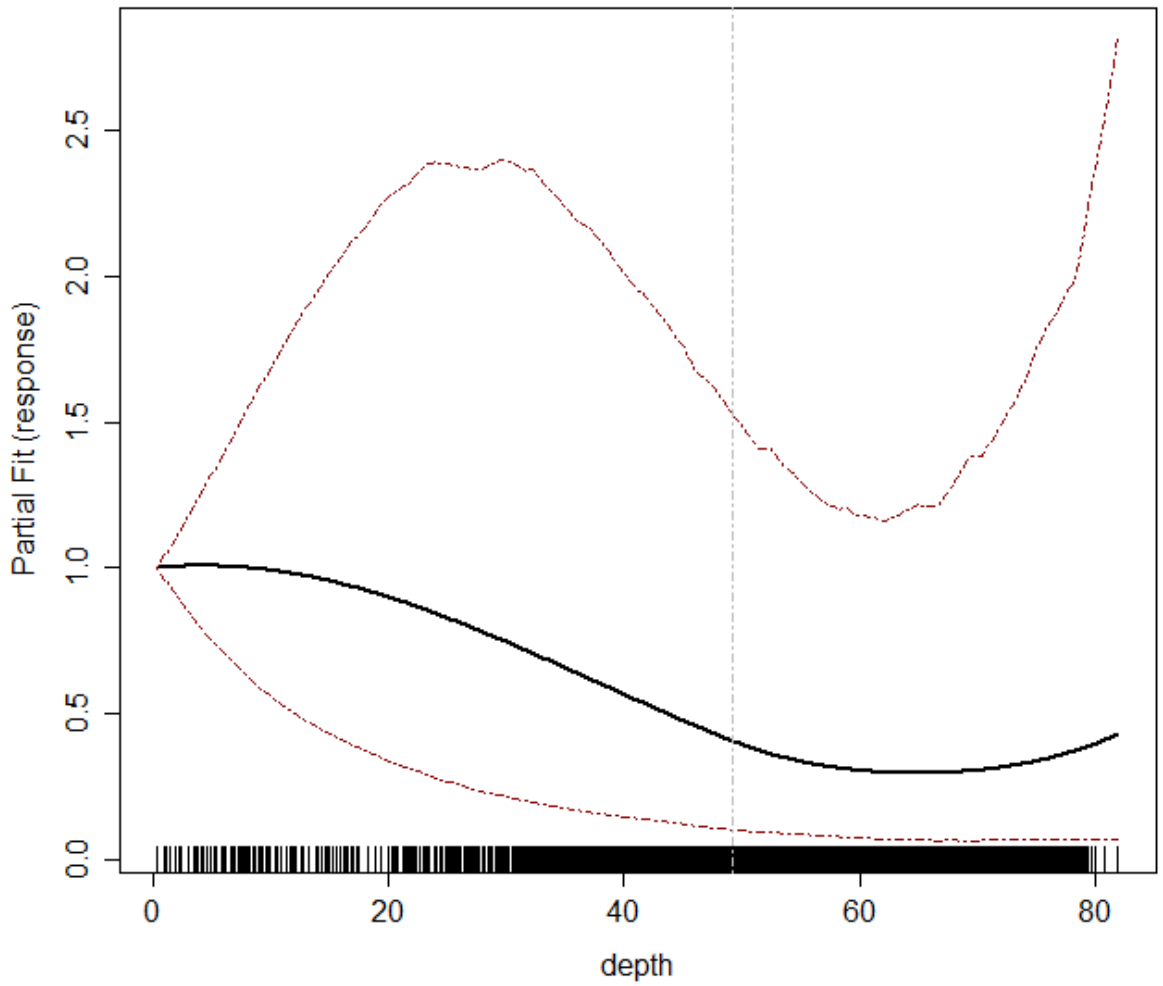

Figure D3.5. Guillemot partial plot of depth.

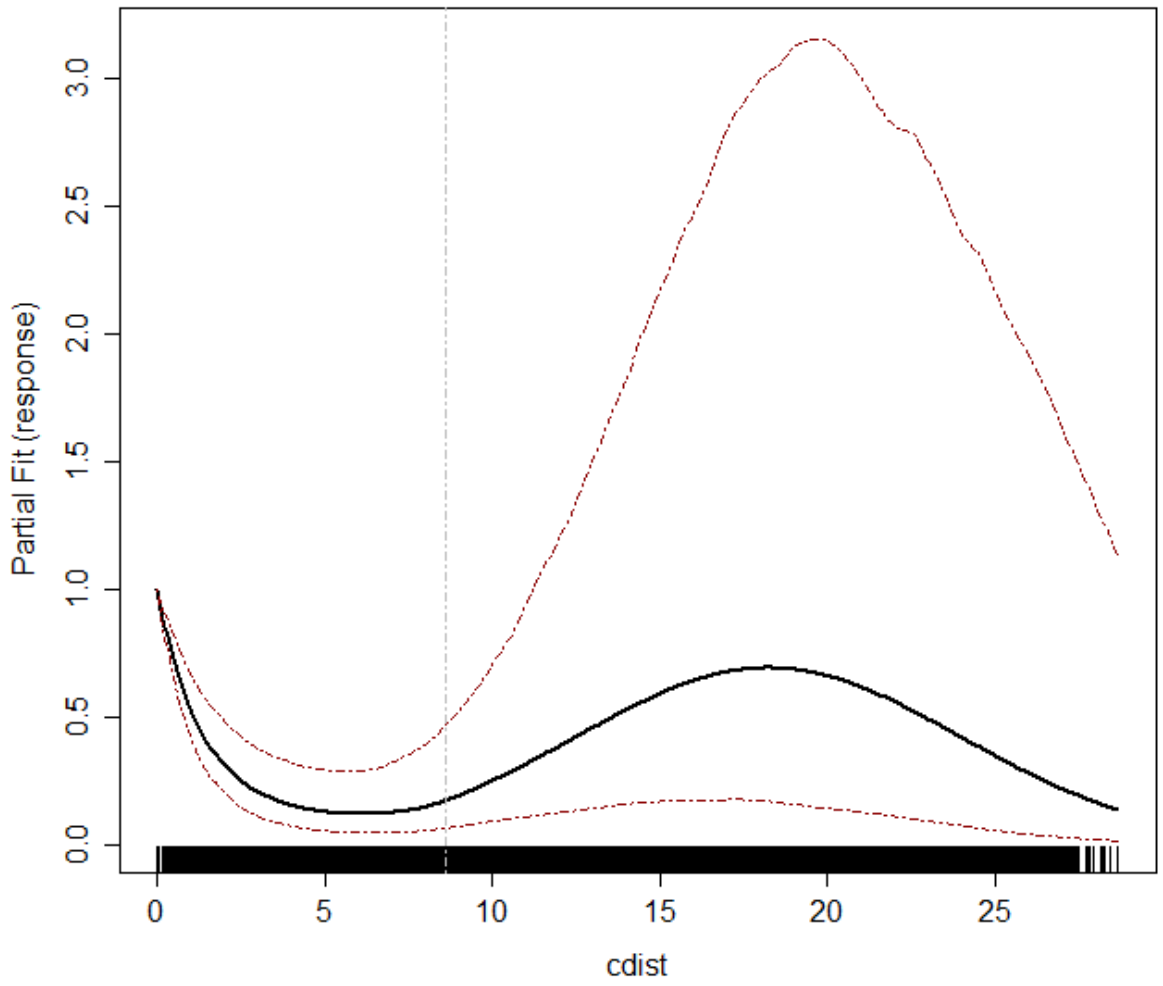

Figure D3.6. Guillemot partial plot of distance to coast (cdist).

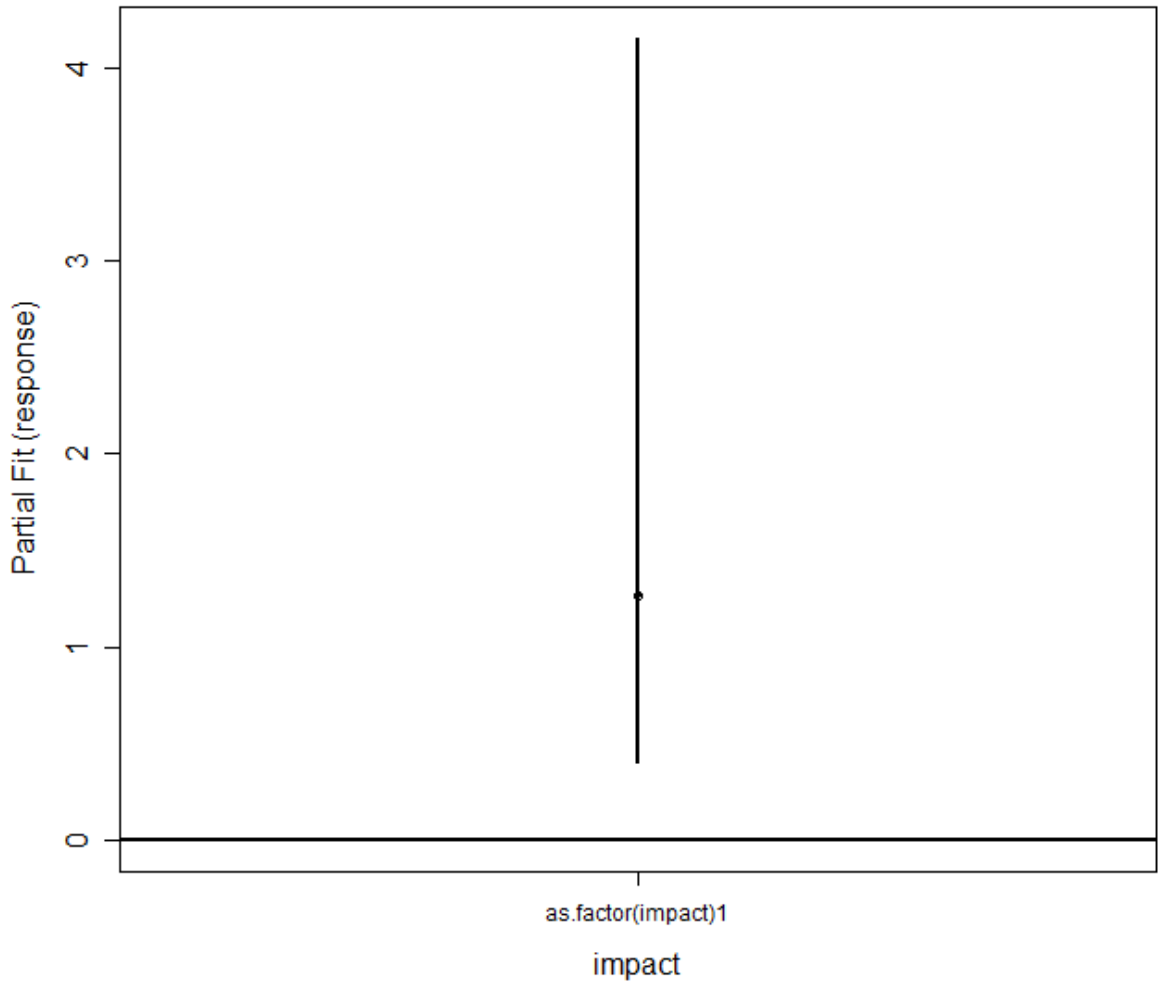

Figure D3.7 Kittiwake partial plot of impact.

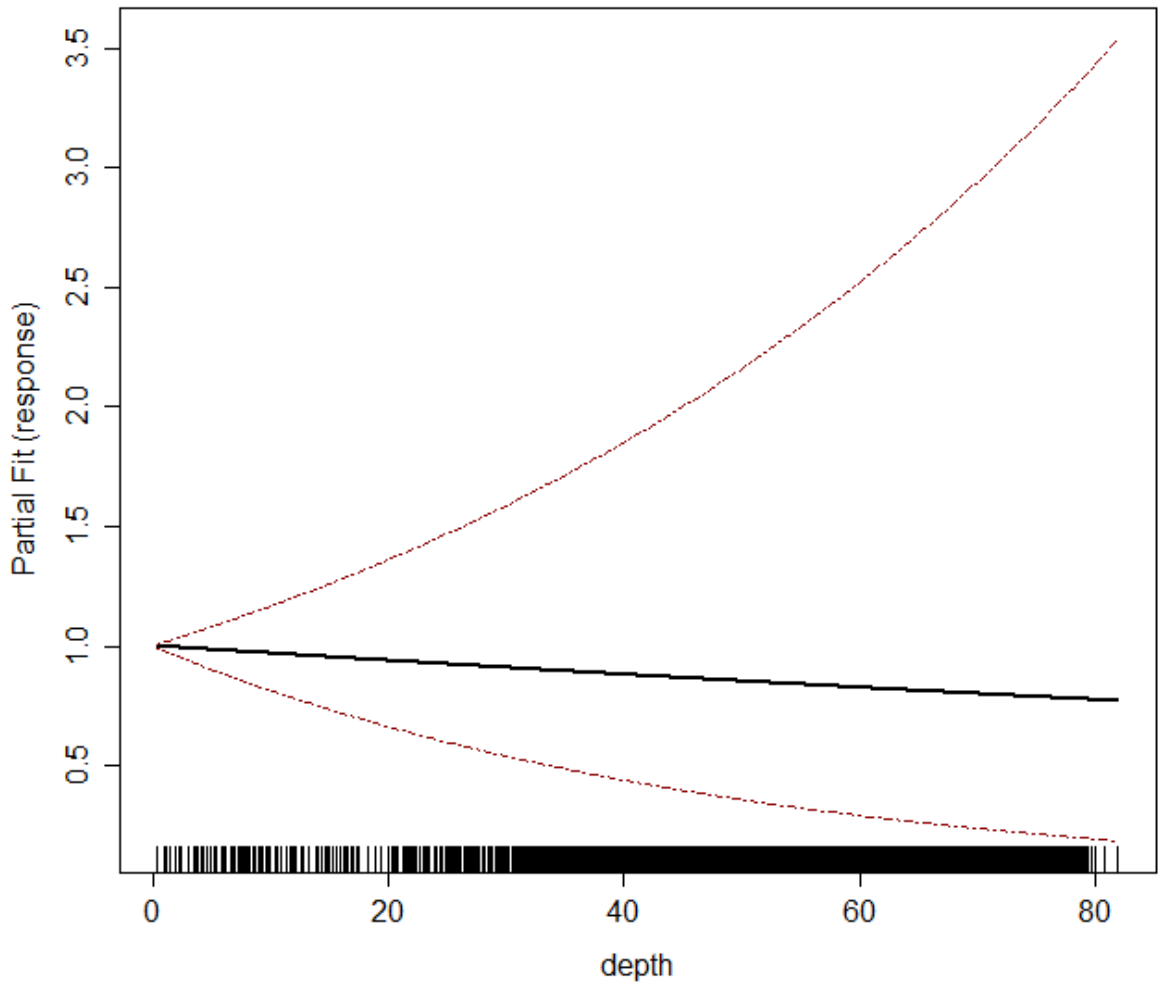

Figure D3.8. Kittiwake partial plot of depth.

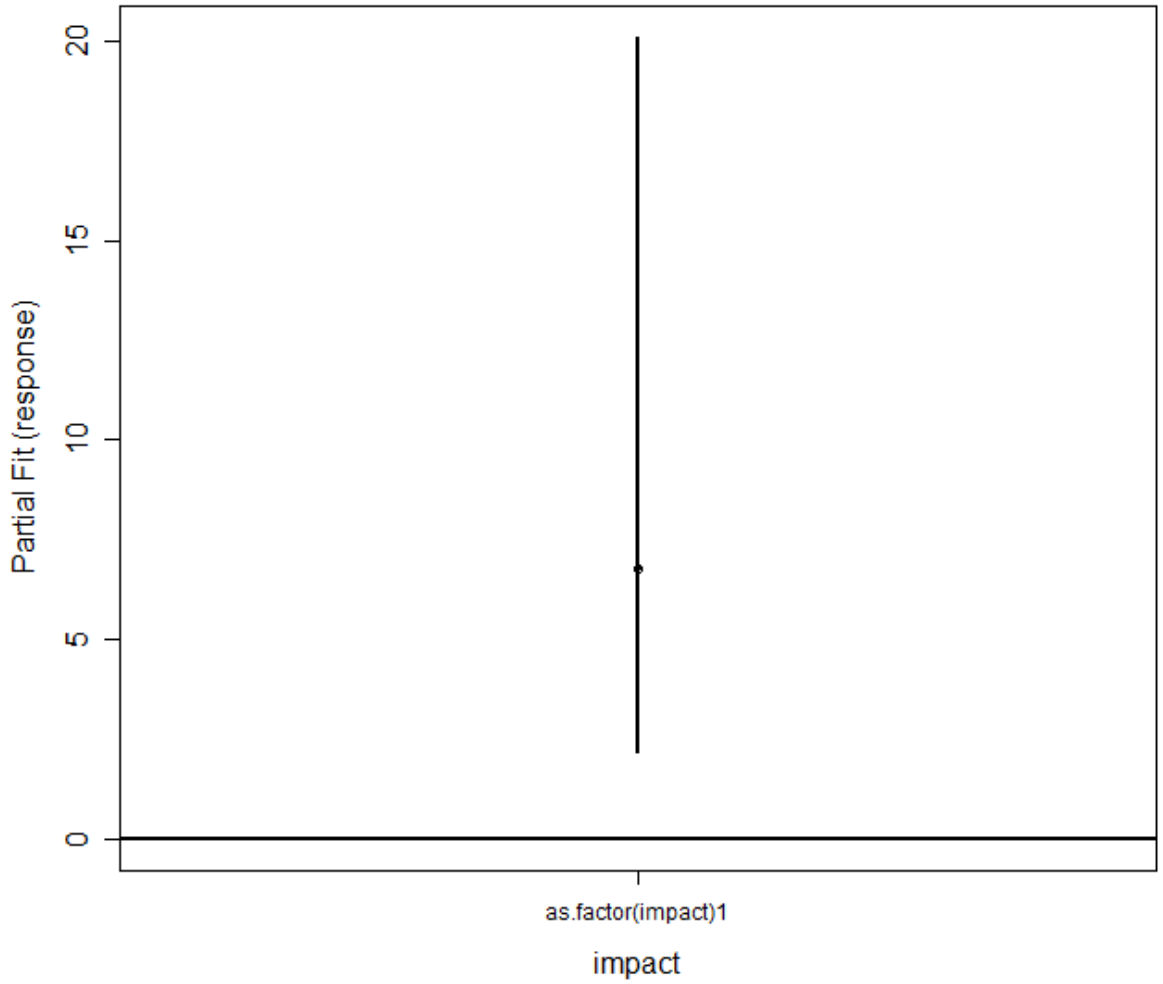

Figure D3.9. Razorbill partial plot of impact.

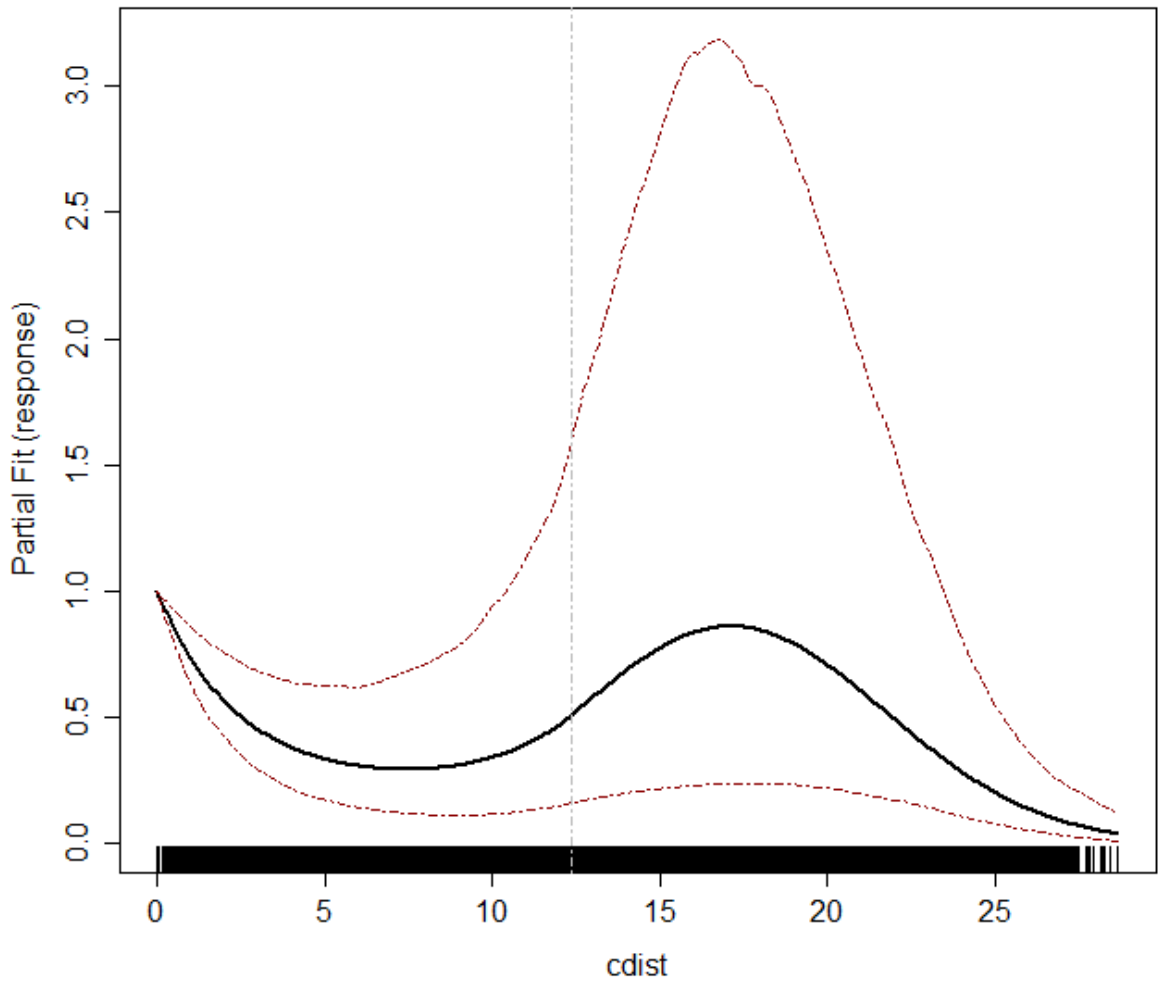

Figure D3.10. Razorbill partial plot of distance to coast (cdist).

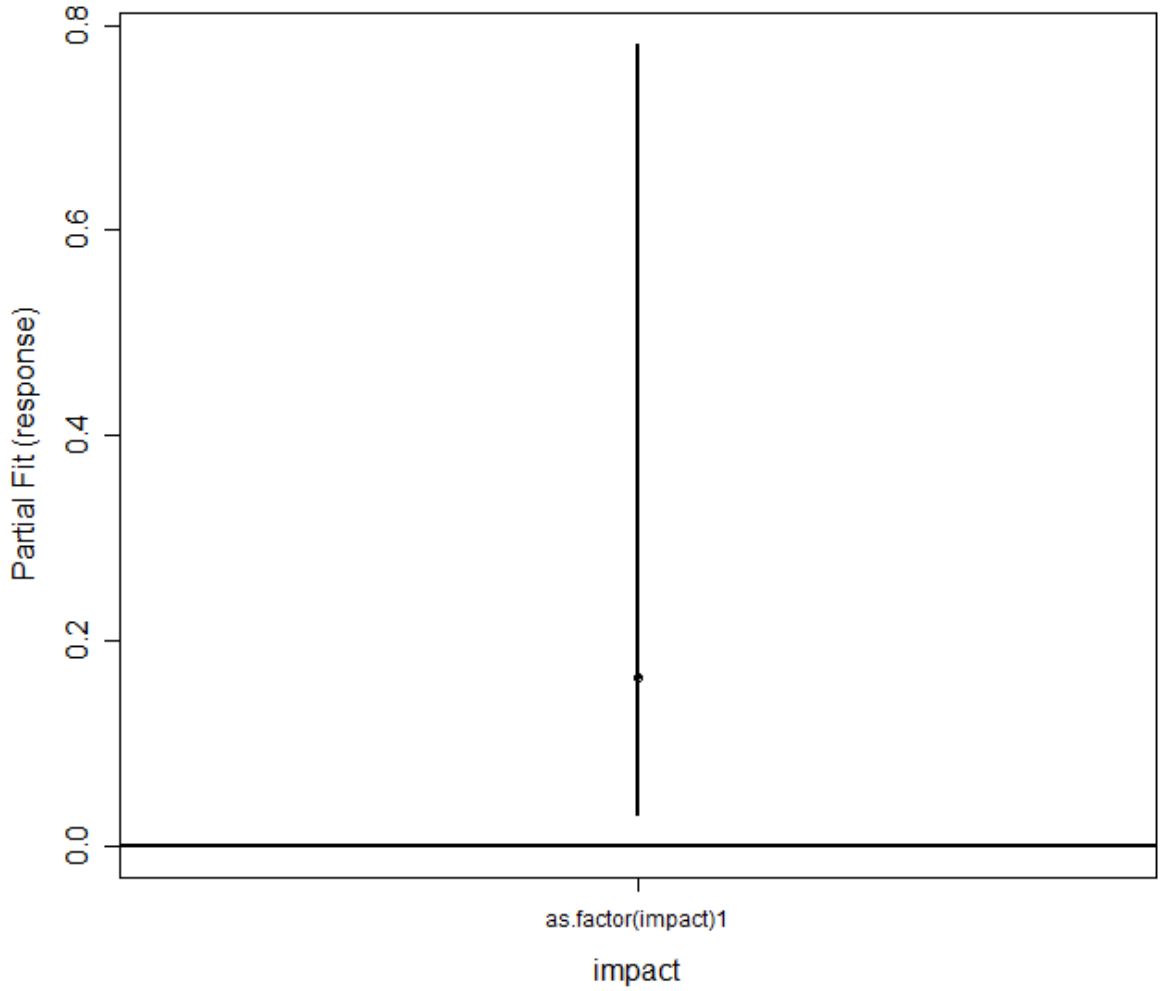

Figure D3.11 Puffin partial plot of impact.

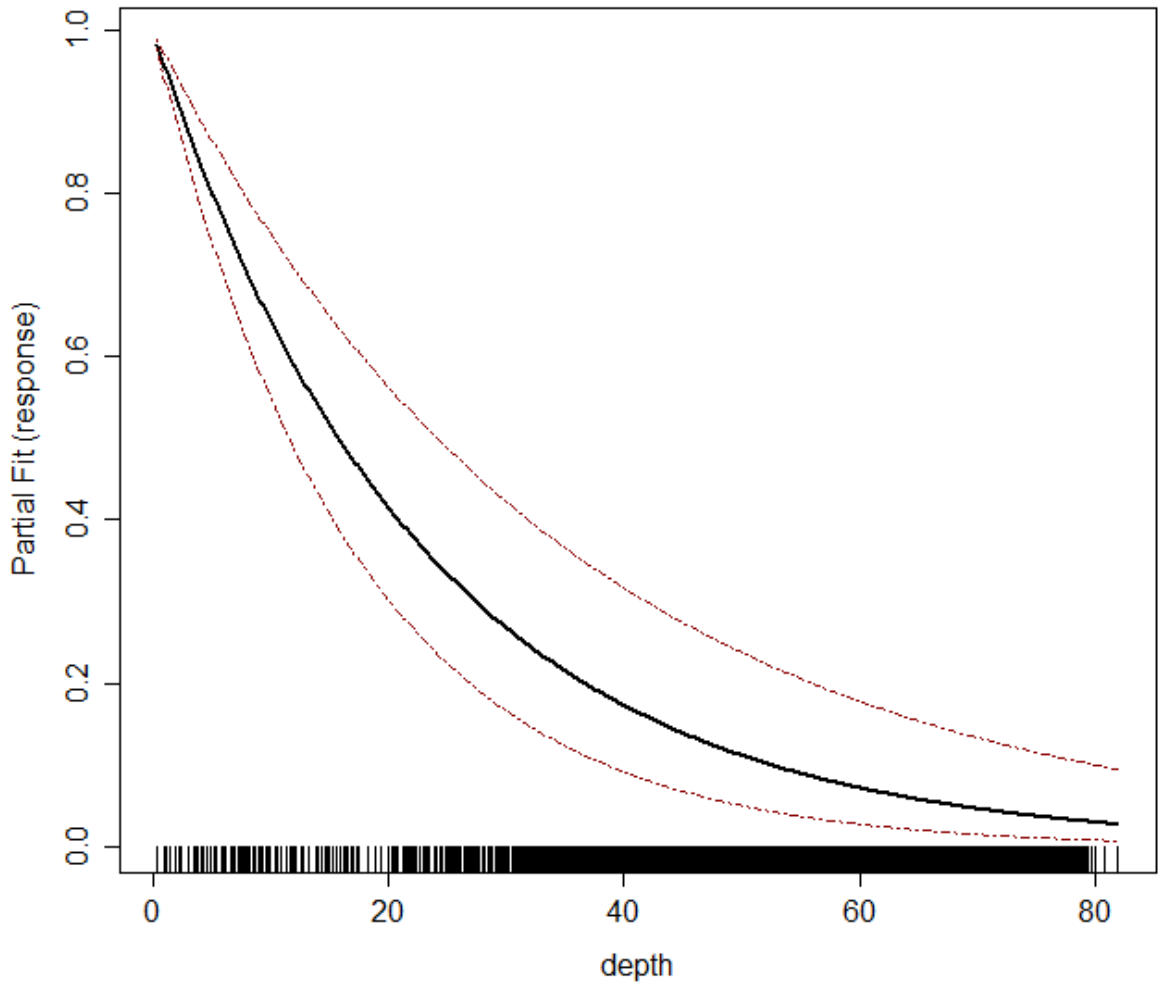

Figure D3.12. Puffin partial plot of depth.

ANNEX E. COVRATIO AND PRESS STATISTICS FOR THE BEFORE-AFTER MODELS

The MRSea function '*runInfluence*' provides two measures of the potential influence of individual blocks within the data. The covratio statistic indicates the change in the precision of the parameter estimates when each block is omitted, while the press statistic quantifies the sensitivity of the model predictions to removal of each block. Values of covratio >1 indicate inflation of model standard errors when the block is removed, and <1 indicate the opposite (reduction in standard errors). Relatively large values of the press statistic indicate the model is sensitive to the corresponding block. In both cases outputs are provided with 95% confidence intervals to assist identification of more influential blocks. It is important to bear in mind that, as stated in the MRSea guidance, there will always be values outside the 95% confidence intervals.

For the current pair-wise sets of comparisons (pre vs. post-1, pre vs. post-2 and post-1 vs. post-2): survey number (1-12) was used as the blocking structure, which permitted identification of surveys which had the potential to influence the overall results obtained.

Gannet

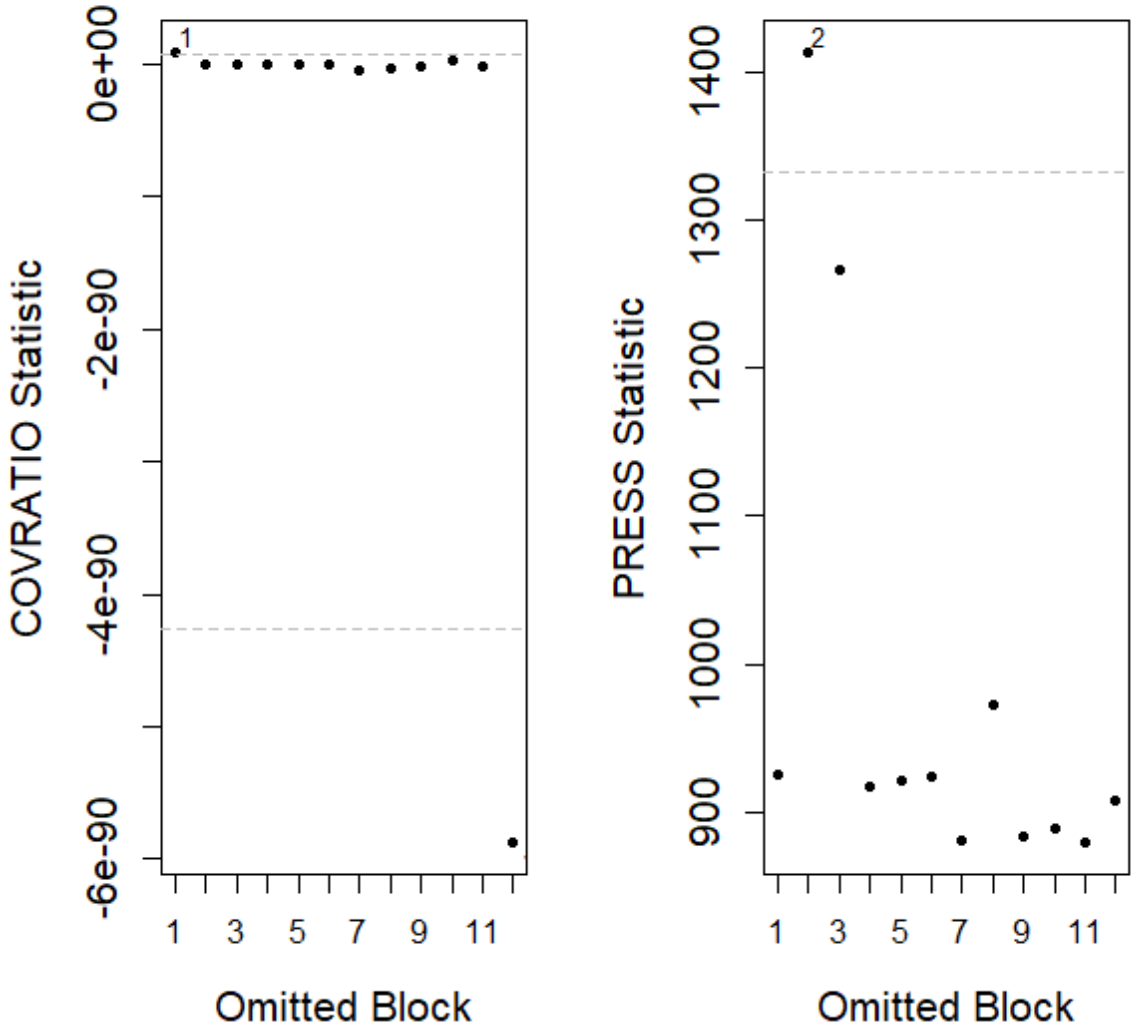

Figure E1. Gannet COVRATIO and PRESS statistic plots at the level of survey (pre vs. post-1).

Inclusion of survey 12 (survey 6 in 2019) in the results appeared to result in inflation of the standard errors (i.e. making detection of a significant impact less likely). This indicates the before-after impact result was precautionary.

Survey 2 (survey 2 in 2015) had a large press value indicating that the overall result was most sensitive to the data recorded on this survey. However, as this was a survey with a hotspot recorded within the wind farm, this is not an unexpected outcome.

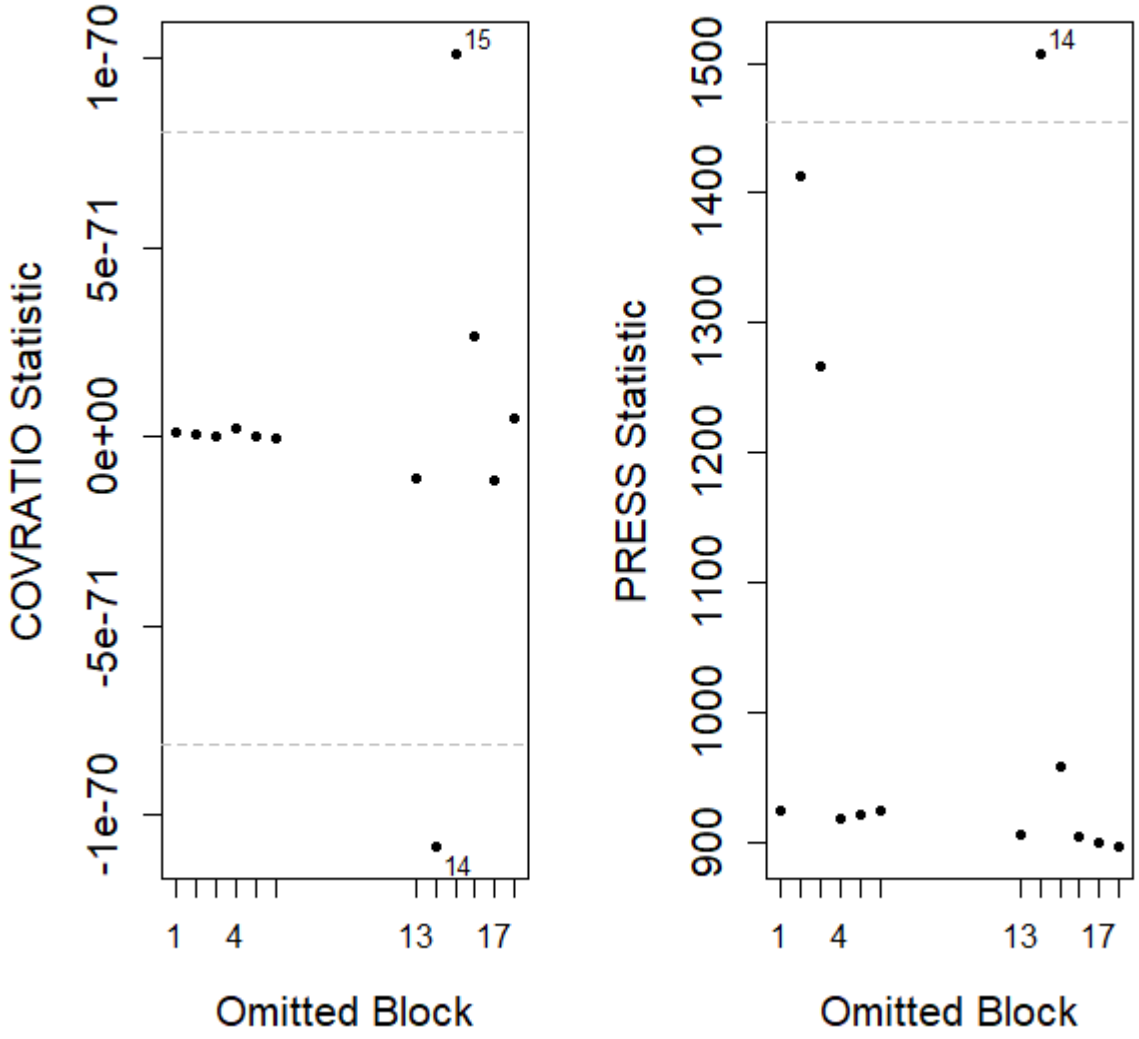

Figure E2. Gannet COVRATIO and PRESS statistic plots at the level of survey (pre vs. post-2).

Inclusion of survey 15 (survey 3 in 2021) in the results appeared to result in inflation of the standard errors (i.e. making detection of a significant impact less likely). This indicates the before-after impact result was precautionary.

Survey 14 (survey 4 in 2021) had a large press value indicating that the overall result was most sensitive to the data recorded on this survey.

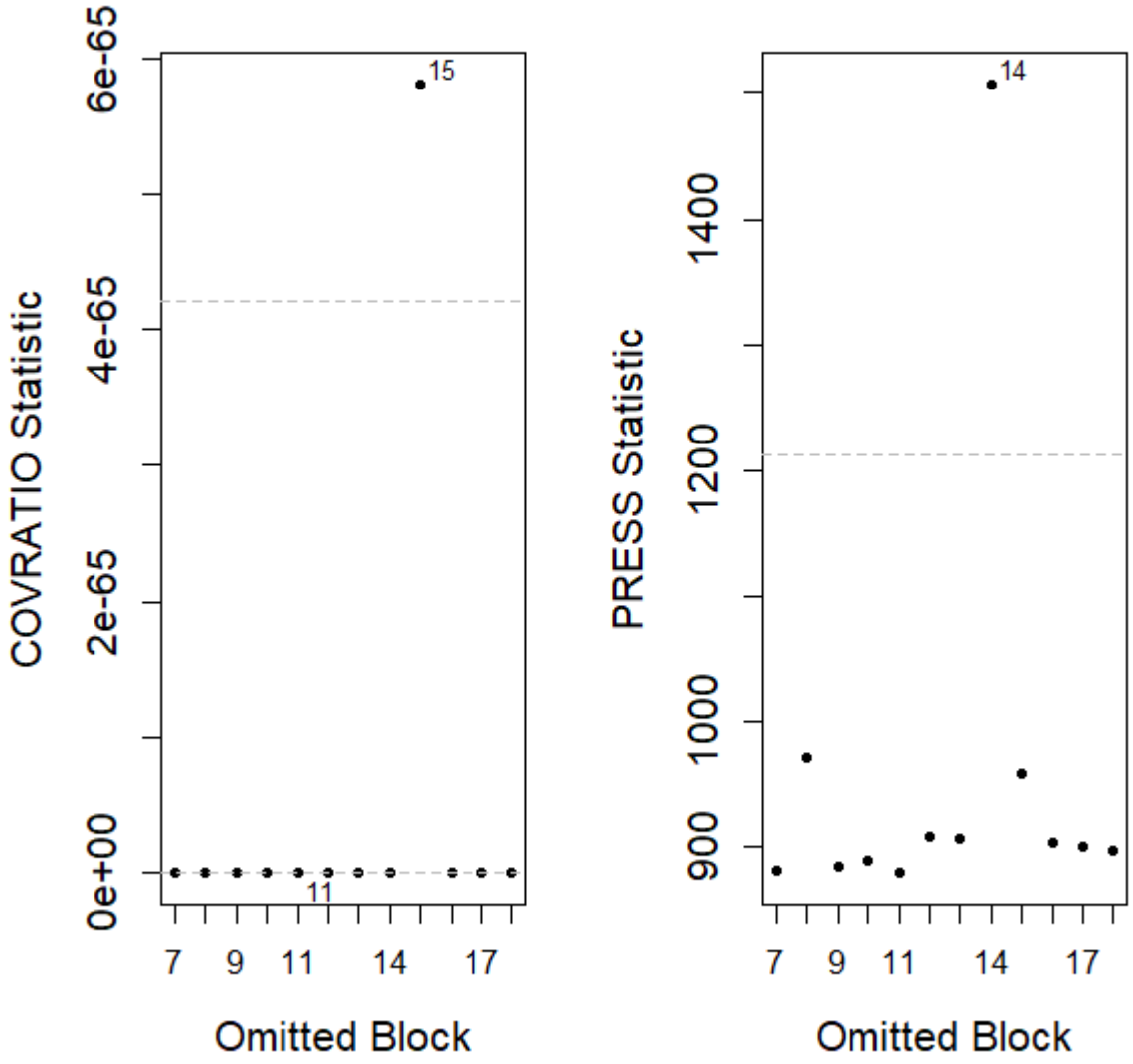

Figure E3. Gannet COVRATIO and PRESS statistic plots at the level of survey (post-1 vs. post-2).

Inclusion of survey 15 (survey 3 in 2021) in the results appeared to result in inflation of the standard errors (i.e. making detection of a significant impact less likely). This indicates the before-after impact result was precautionary.

Survey 14 (survey 4 in 2021) had a large press value indicating that the overall result was most sensitive to the data recorded on this survey.

Guillemot

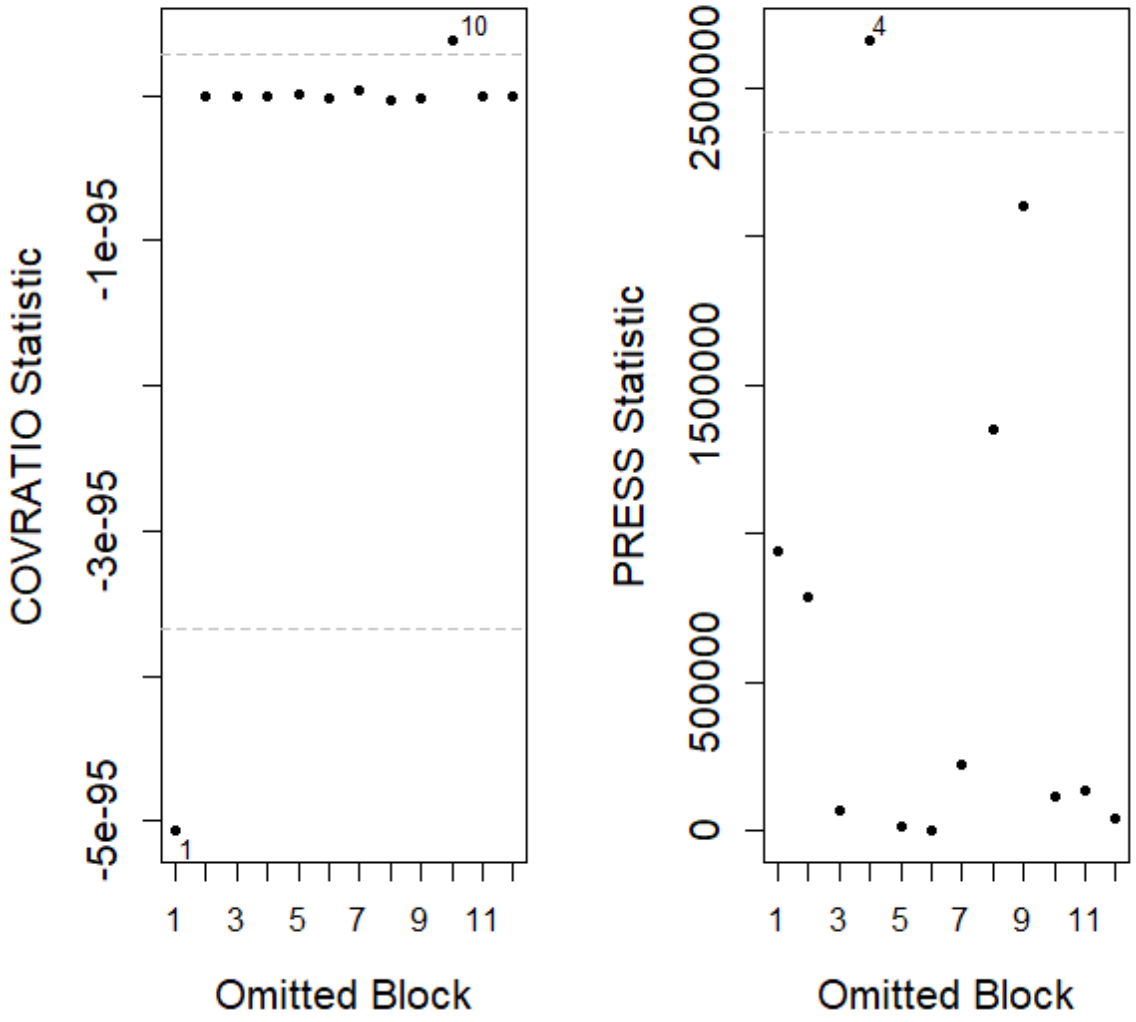

Figure E4. Guillemot COVRATIO and PRESS statistic plots at the level of survey (pre vs. post-1).

Inclusion of survey 1 (survey 1 in 2015) in the results appeared to result in inflation of the standard errors (i.e. making detection of a significant impact less likely), while survey 10 (survey 4 in 2019) was slightly above the 95% interval (i.e. slightly reducing standard errors). On balance, given the relative position of these outliers it appears that the before-after impact result was precautionary.

Survey 4 (survey 4 in 2015) had a large press value indicating that the overall result was most sensitive to the data recorded on this survey. However, this value is not far beyond the range of the other values and is not considered of concern.

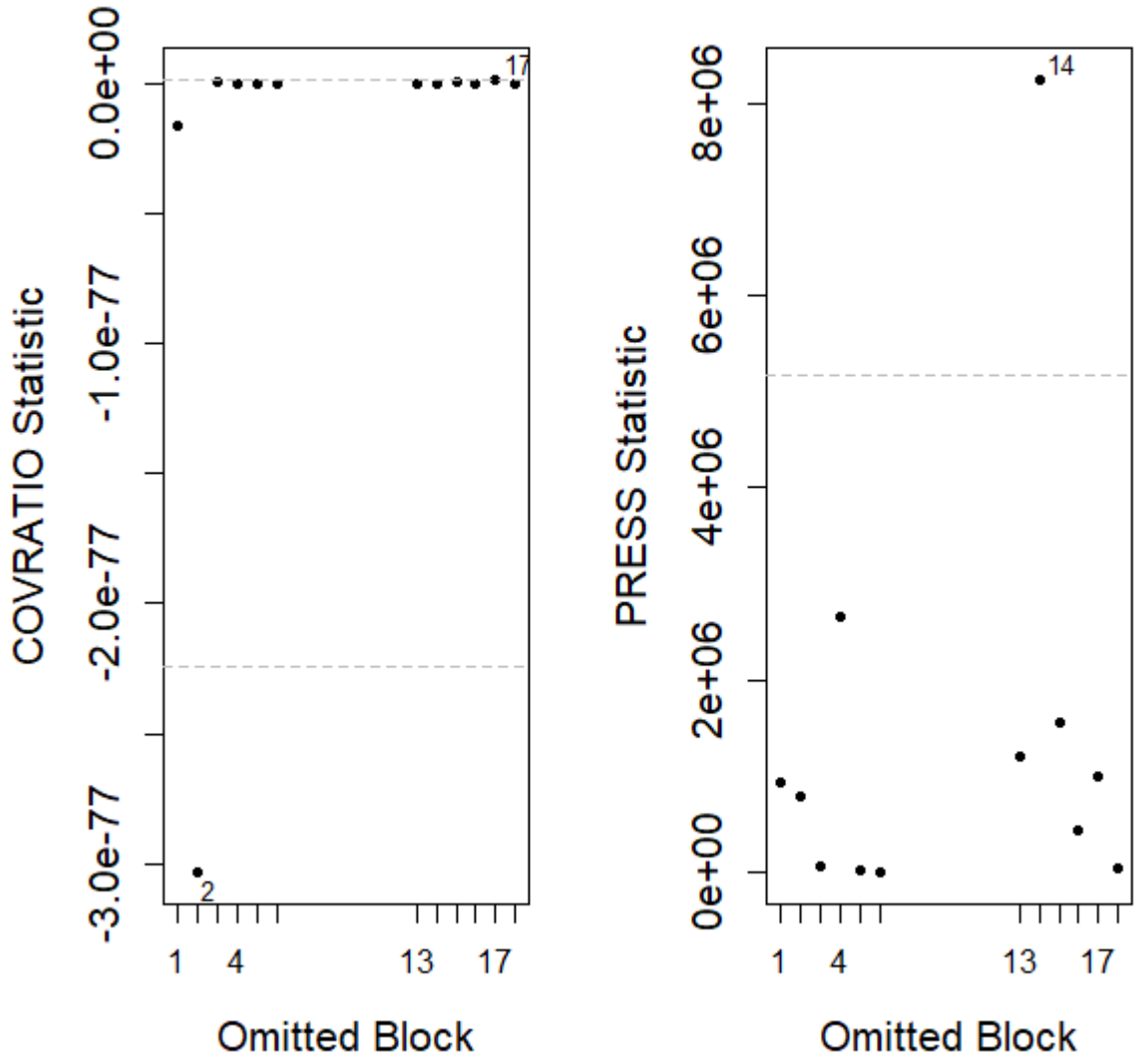

Figure E5. Guillemot COVRATIO and PRESS statistic plots at the level of survey (pre vs. post-2).

Inclusion of survey 17 (survey 5 in 2021) in the results appeared to result in inflation of the standard errors (i.e. making detection of a significant impact less likely), while survey 2 (survey 4 in 2019) was slightly above the 95% interval (i.e. slightly reducing standard errors). On balance, given the relative position of these outliers it appears that the before-after impact result was precautionary.

Survey 14 (survey 2 in 2021) had a large press value indicating that the overall result was most sensitive to the data recorded on this survey.

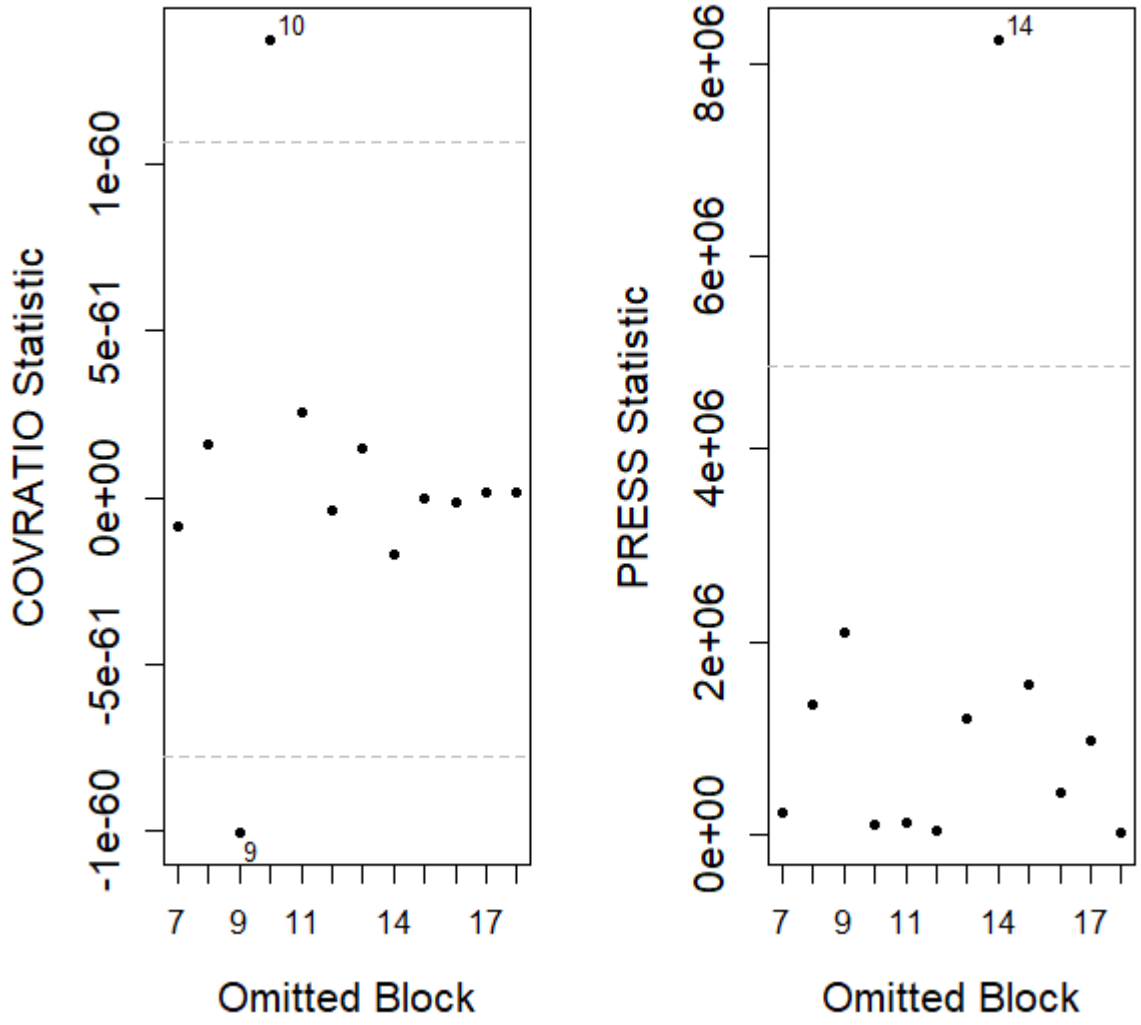

Figure E6. Guillemot COVRATIO and PRESS statistic plots at the level of survey (post-1 vs. post-2).

Inclusion of survey 9 (survey 3 in 2019) in the results appeared to result in inflation of the standard errors (i.e. making detection of a significant impact less likely), while survey 10 (survey 4 in 2019) was above the 95% interval (i.e. slightly reducing standard errors). On balance, given the relative position of these outliers it appears that the before-after impact result was precautionary.

Survey 14 (survey 2 in 2021) had a large press value indicating that the overall result was most sensitive to the data recorded on this survey.

Kittiwake

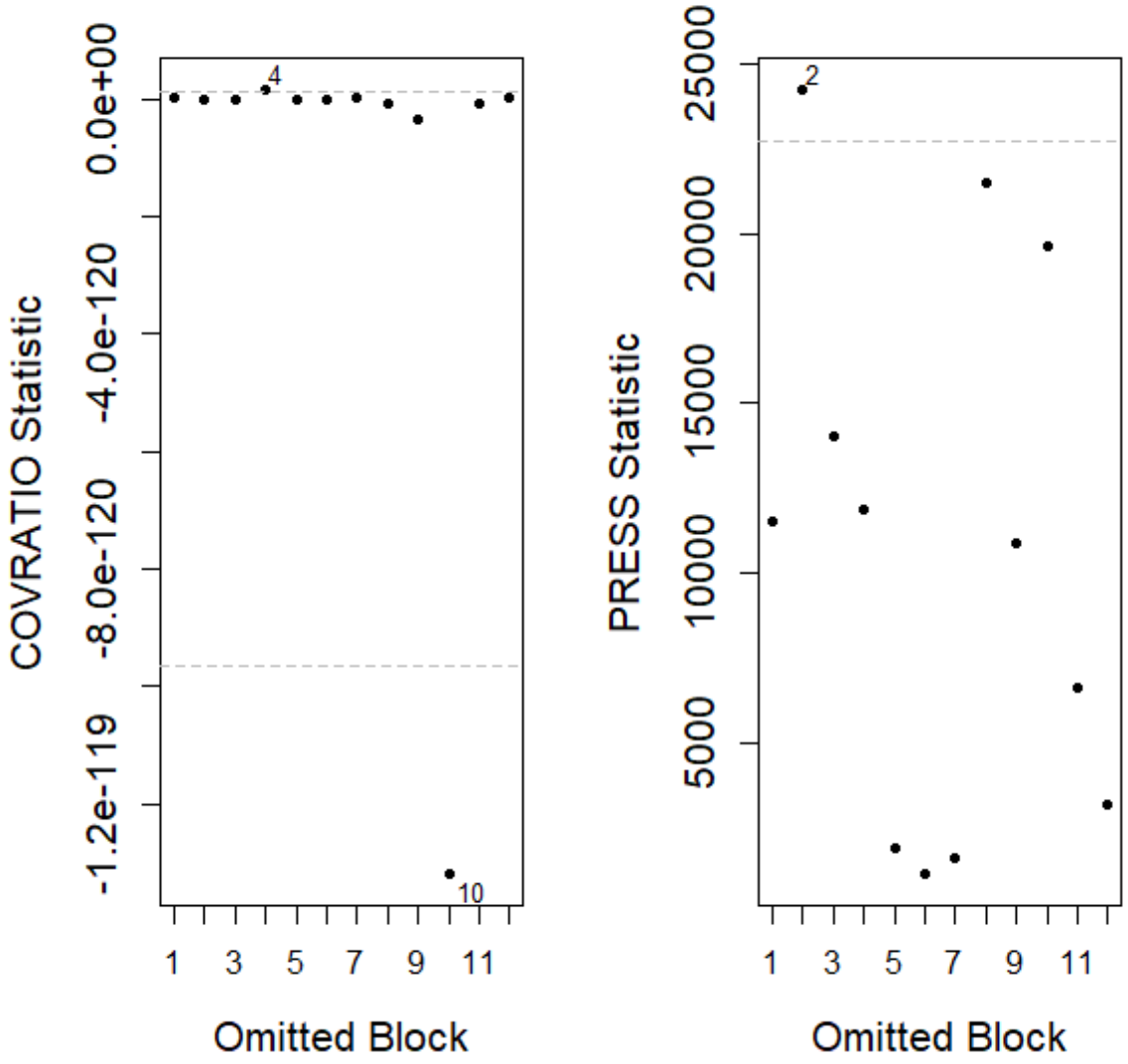

Figure E7. Kittiwake COVRATIO and PRESS statistic plots at the level of survey (pre vs. post-1).

Inclusion of survey 10 (survey 4 in 2019) in the results appeared to result in inflation of the standard errors (i.e. making detection of a significant impact less likely). On balance, given the relative position of these outliers it appears that the before-after impact result was little affected by these data.

Survey 2 (survey 2 in 2015) had a large press value indicating that the overall result was most sensitive to the data recorded on this survey. However, this value is not far beyond the range of the other values and is not considered of concern.

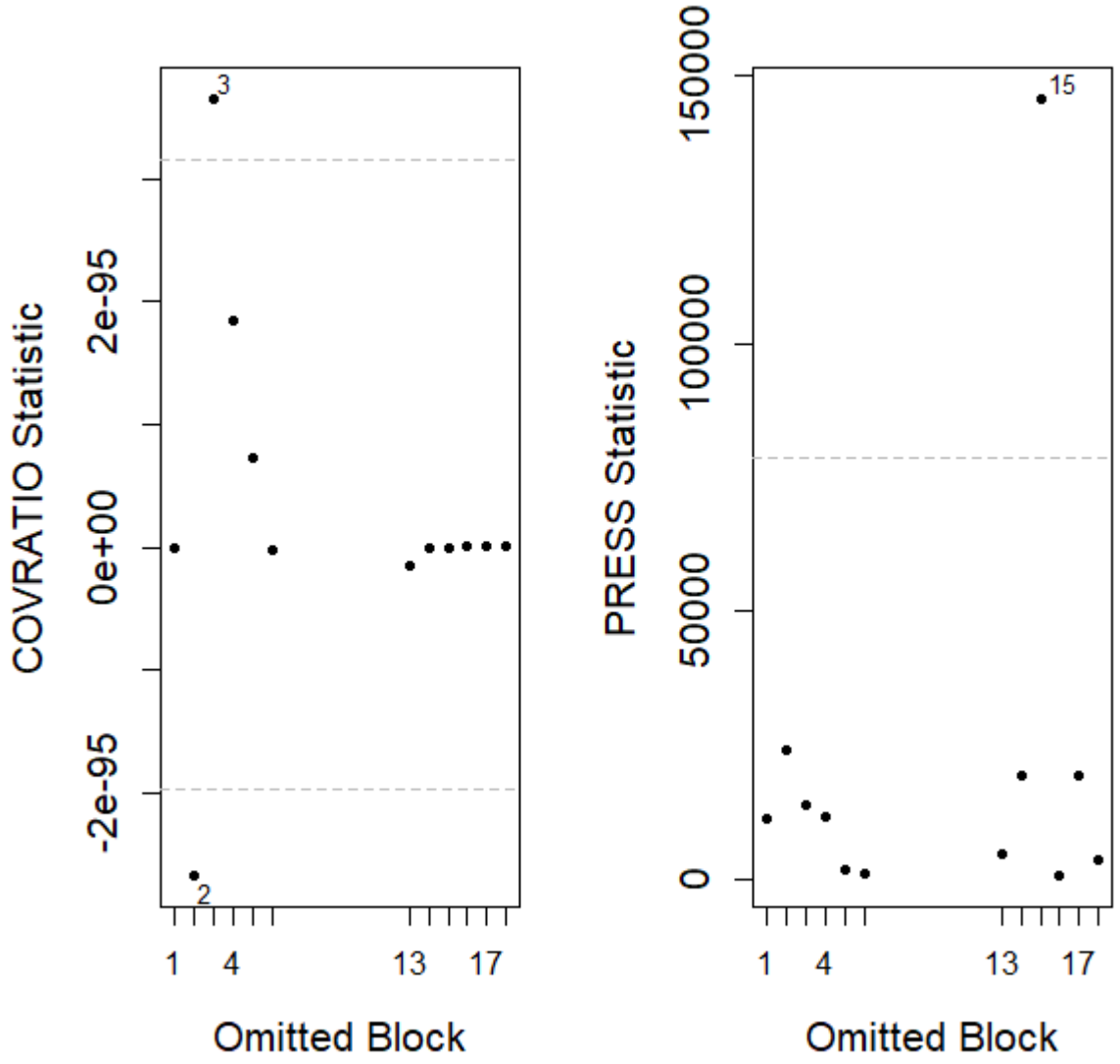

Figure E8. Kittiwake COVRATIO and PRESS statistic plots at the level of survey (pre vs. post-2).

Inclusion of survey 3 (survey 3 in 2015) in the results appeared to result in inflation of the standard errors (i.e. making detection of a significant impact less likely), while survey 2 (survey 2 in 2015) was below the 95% interval (i.e. its inclusion increases precision). On balance, given the relative position of these outliers it appears that the before-after impact result was precautionary.

Survey 15 (survey 3 in 2021) had a large press value indicating that the overall result was most sensitive to the data recorded on this survey.

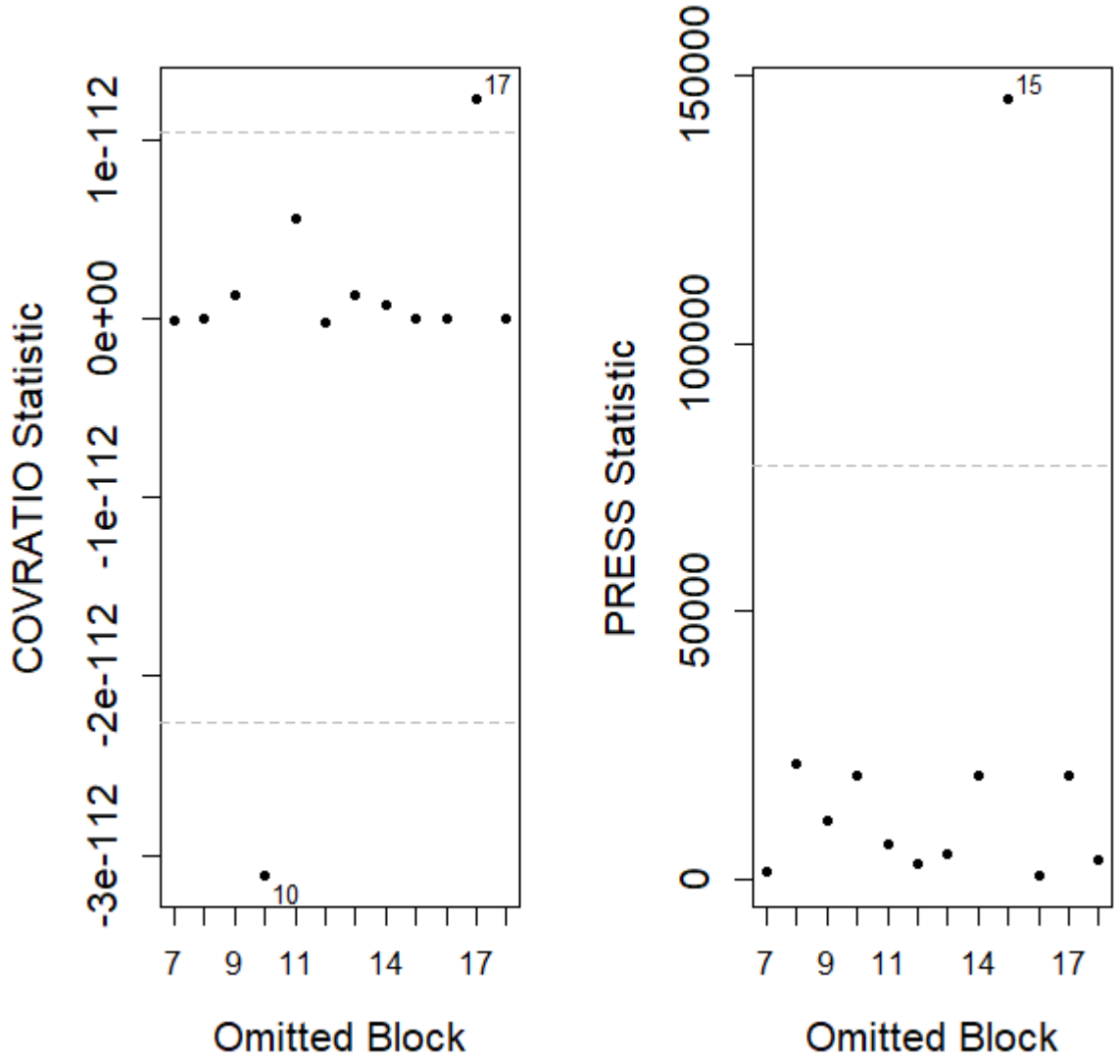

Figure E9. Kittiwake COVRATIO and PRESS statistic plots at the level of survey (post-1 vs. post-2).

Inclusion of survey 17 (survey 5 in 2021) in the results appeared to result in inflation of the standard errors (i.e. making detection of a significant impact less likely), while survey 10 (survey 5 in 2019) was below the 95% interval (i.e. its inclusion increases precision). On balance, given the relative position of these outliers it appears that the before-after impact result was precautionary.

Survey 15 (survey 3 in 2021) had a large press value indicating that the overall result was most sensitive to the data recorded on this survey.

Razorbill

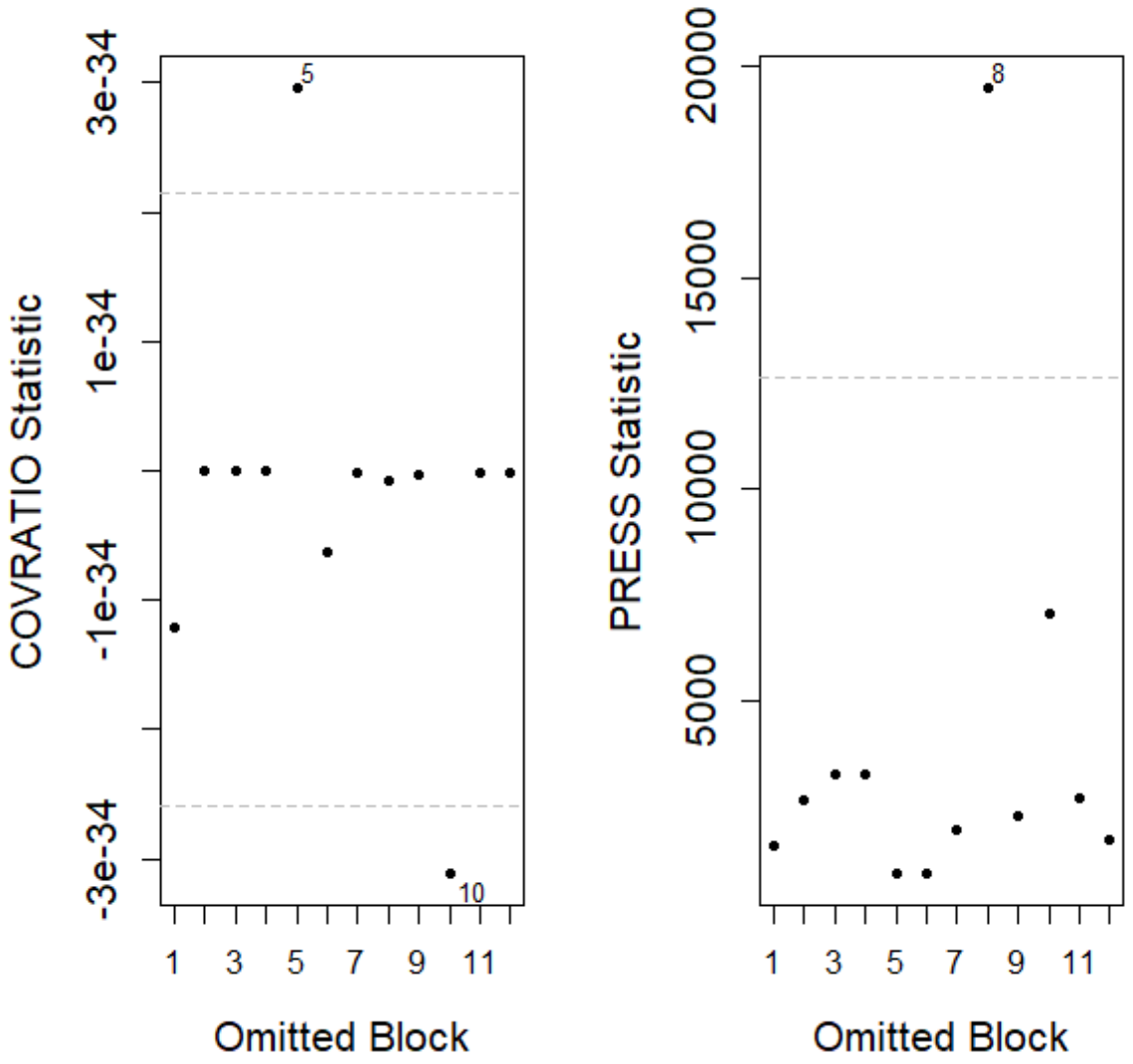

Figure E10. Razorbill COVRATIO and PRESS statistic plots at the level of survey (pre vs. post-1).

Inclusion of survey 10 (survey 5 in 2019) in the results appeared to result in inflation of the standard errors (i.e. making detection of a significant impact less likely), while survey 5 (survey 5 in 2015) was slightly above the 95% interval (i.e. slightly reducing standard errors). On balance, given the relative position of these outliers it appears that the before-after impact result was precautionary.

Survey 8 (survey 2 in 2019) had a large press value indicating that the overall result was most sensitive to the data recorded on this survey. However, this value is not far beyond the range of the other values and is not considered of concern.

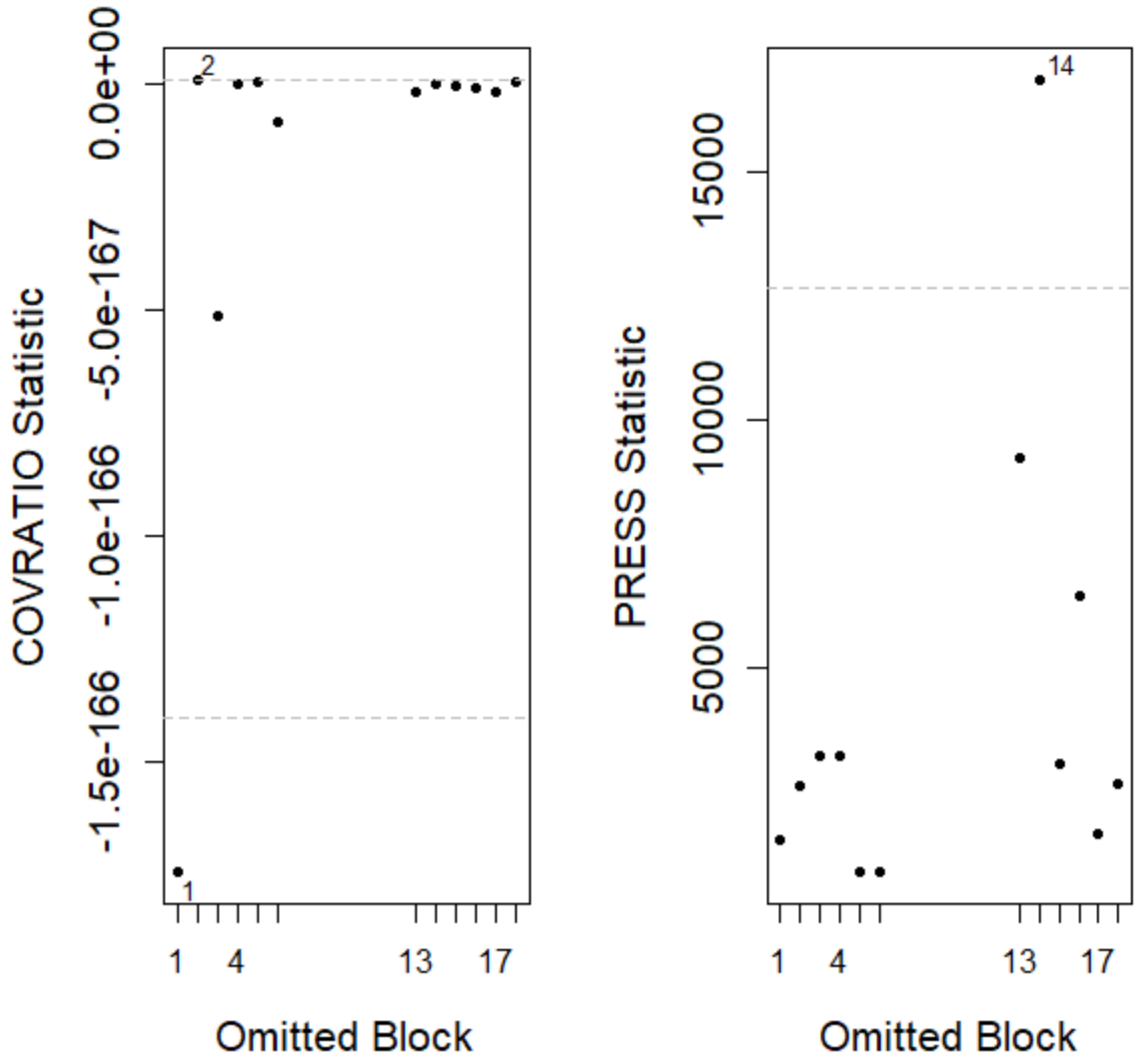

Figure E11. Razorbill COVRATIO and PRESS statistic plots at the level of survey (pre vs. post-2).

Inclusion of survey 2 (survey 2 in 2015) in the results appeared to result in inflation of the standard errors (i.e. making detection of a significant impact less likely), while survey 1 (survey 1 in 2015) was below the 95% interval (i.e. slightly reducing standard errors). On balance, given the relative position of these outliers it appears that the before-after impact result was precautionary.

Survey 14 (survey 2 in 2019) had a large press value indicating that the overall result was most sensitive to the data recorded on this survey. However, this value is not far beyond the range of the other values and is not considered of concern.

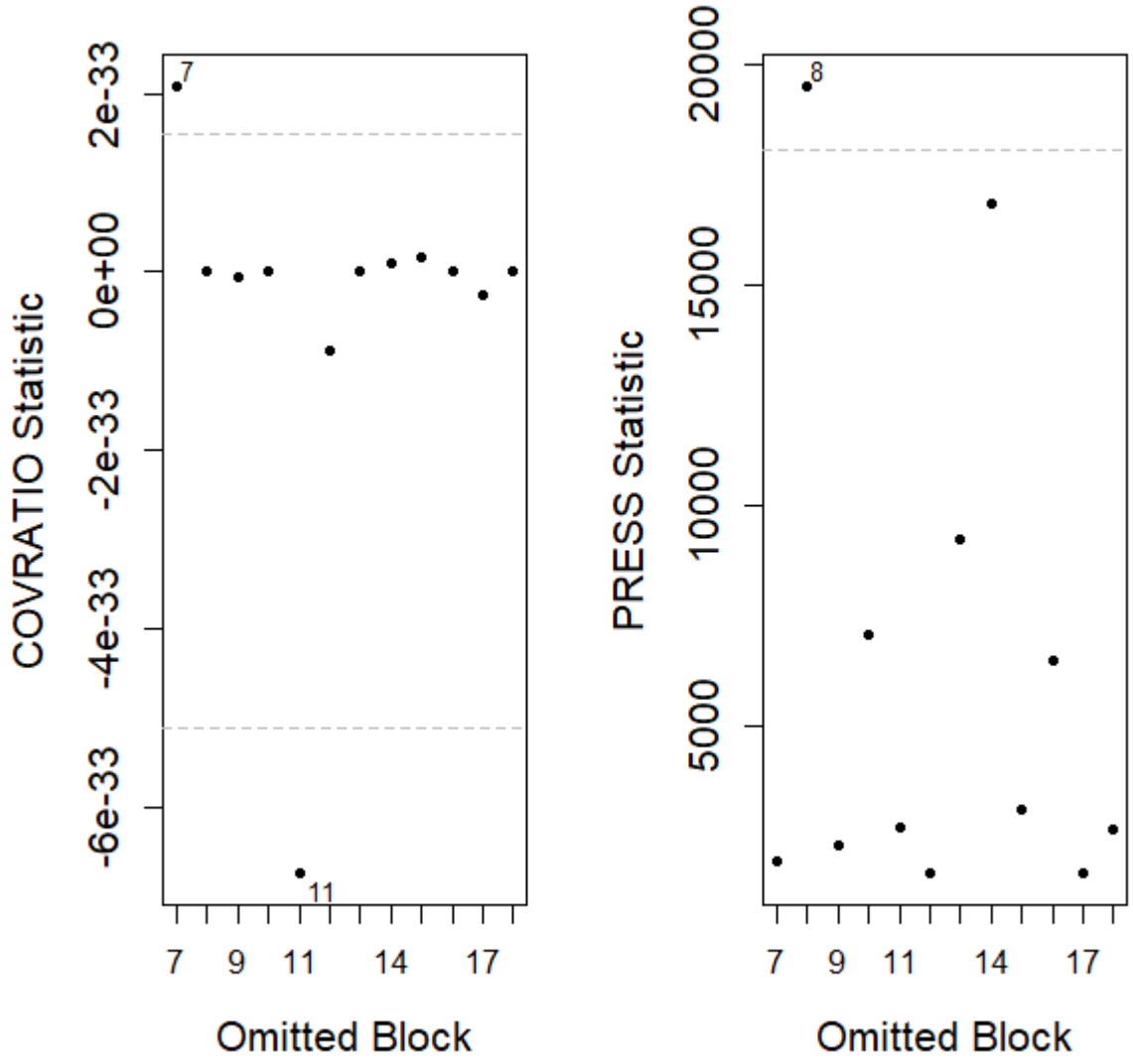

Figure E12. Razorbill COVRATIO and PRESS statistic plots at the level of survey (post-1 vs. post-2).

Inclusion of survey 7 (survey 2 in 2019) in the results appeared to result in inflation of the standard errors (i.e. making detection of a significant impact less likely), while survey 11 (survey 5 in 2019) was below the 95% interval (i.e. slightly reducing standard errors). On balance, given the relative position of these outliers it appears that the before-after impact result was precautionary.

Survey 8 (survey 2 in 2019) had a large press value indicating that the overall result was most sensitive to the data recorded on this survey. However, this value is not far beyond the range of the other values and is not considered of concern.

Puffin

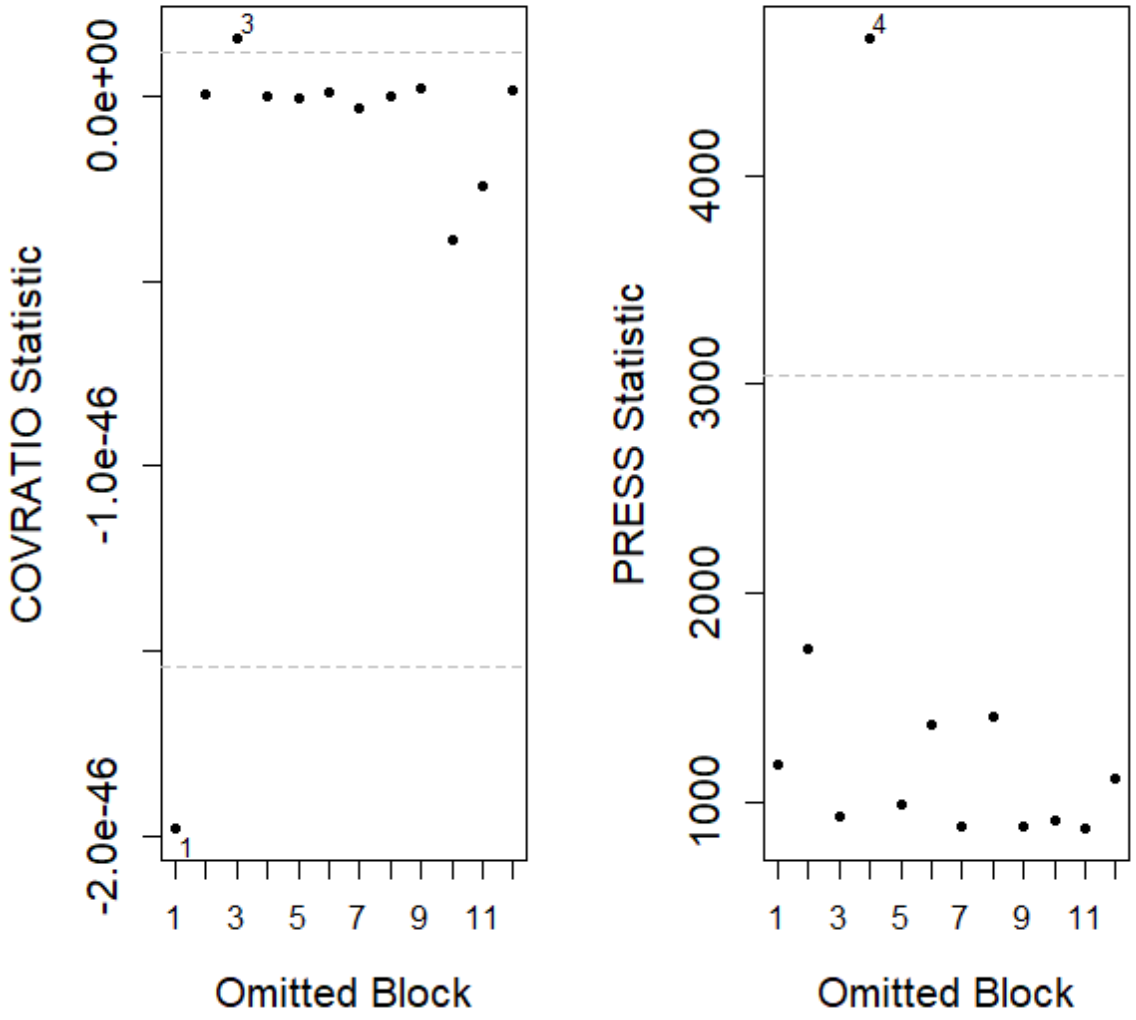

Figure E13. Puffin COVRATIO and PRESS statistic plots at the level of survey (pre vs. post-1).

Inclusion of survey 1 (survey 1 in 2015) in the results appeared to result in inflation of the standard errors (i.e. making detection of a significant impact less likely), while survey 3 (survey 3 in 2015) was slightly above the 95% interval (i.e. slightly reducing standard errors). On balance, given the relative position of these outliers it appears that the before-after impact result was precautionary.

Survey 4 (survey 4 in 2015) had a large press value indicating that the overall result was most sensitive to the data recorded on this survey. However, this value is not far beyond the range of the other values and is not considered of concern.

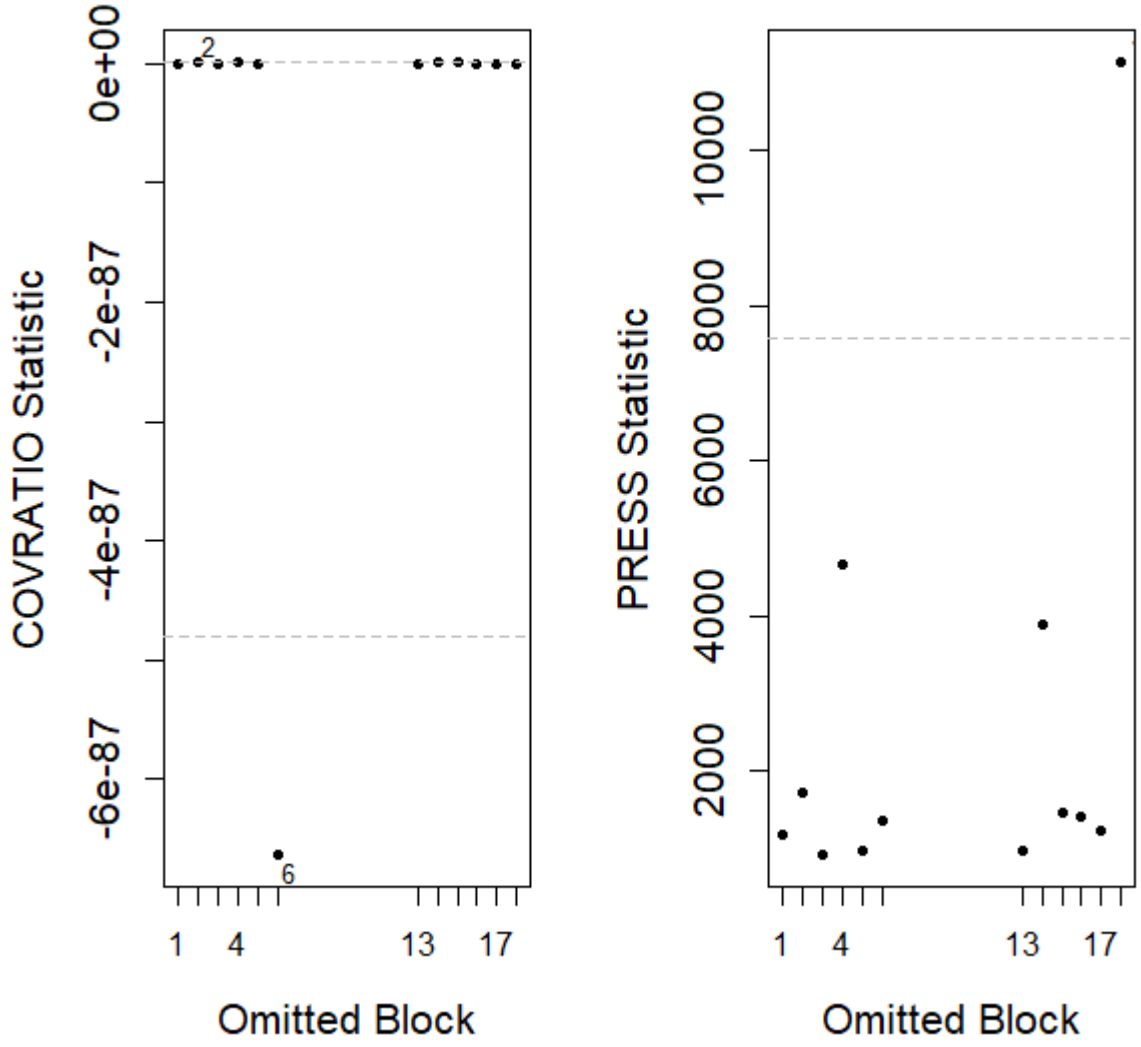

Figure E14. Puffin COVRATIO and PRESS statistic plots at the level of survey (pre vs. post-2).

Inclusion of survey 2 (survey 2 in 2015) in the results appeared to result in inflation of the standard errors (i.e. making detection of a significant impact less likely), while survey 6 (survey 6 in 2015) was slightly below the 95% interval (i.e. reducing standard errors). On balance, given the relative position of these outliers it appears that the before-after impact result was precautionary.

Survey 18 (survey 6 in 2021) had a large press value indicating that the overall result was most sensitive to the data recorded on this survey. However, this value is not far beyond the range of the other values and is not considered of concern.

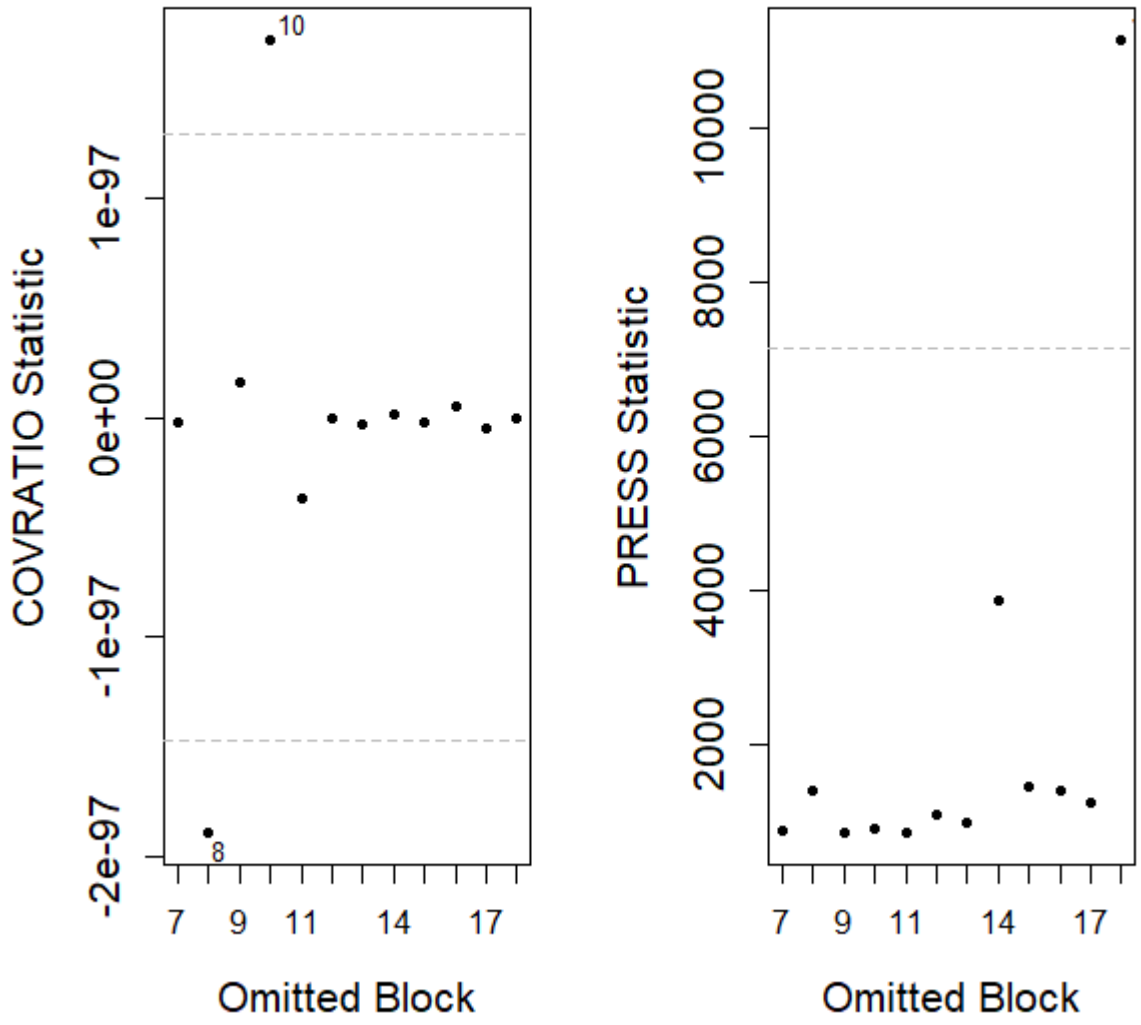

Figure E15. Puffin COVRATIO and PRESS statistic plots at the level of survey (post-1 vs. post-2).

Inclusion of survey 10 (survey 5 in 2019) in the results appeared to result in inflation of the standard errors (i.e. making detection of a significant impact less likely), while survey 8 (survey 3 in 2019) was slightly below the 95% interval (i.e. reducing standard errors). On balance, given the relative position of these outliers it appears that the before-after impact result was precautionary.

Survey 18 (survey 6 in 2021) had a large press value indicating that the overall result was most sensitive to the data recorded on this survey. However, this value is not far beyond the range of the other values and is not considered of concern.

ANNEX F. LOCATIONS OF CONSTRUCTION ACTIVITY IN MORAY EAST DURING 2021 SURVEY PERIOD

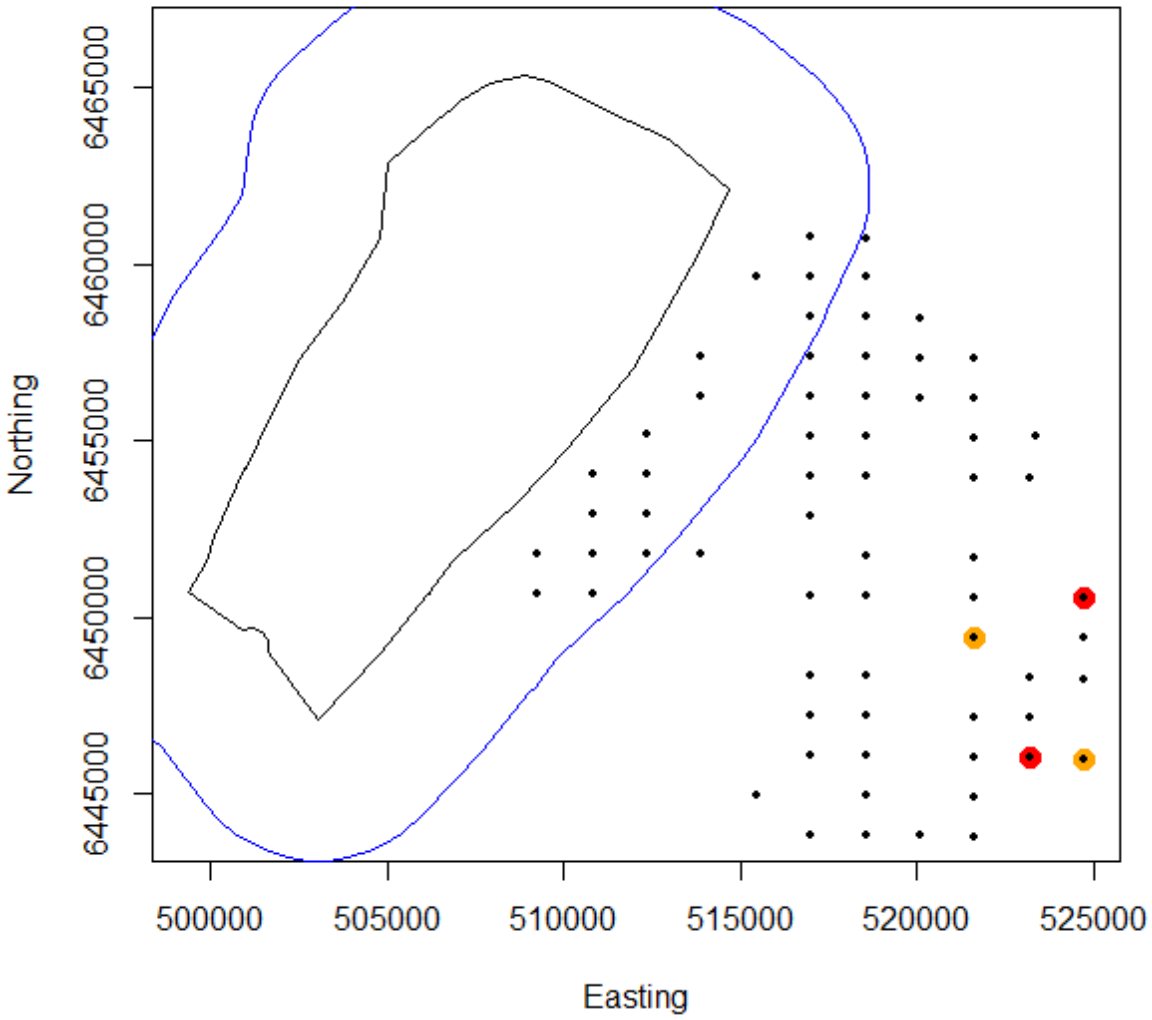

Figure F1. Locations of construction activity at the Moray East Wind Farm during the period of the 2021 surveys (May 22nd to August 4th, inclusive). The Beatrice Wind Farm (black line) and 4km buffer (blue line) are indicated. All turbine jackets in Moray East were installed during 2020 (i.e. the year before). The black dots indicate locations where turbines were installed between January and August 2021. Orange dots are turbines installed on the day prior to one of the 2021 surveys and red dots are turbines installed on the same day as one of the 2021 surveys. The closest installation activity was 8.3 km from the Beatrice 4km buffer (i.e. over 12km from the Beatrice wind farm itself).

ANNEX G. 2019 AND 2021 TURBINE AVOIDANCE PLOTS IN RELATION TO RPM

This annex provides revised plots of the turbine avoidance analysis for 2019, along with those for 2021 (the method for calculating the area of overlap between aerial transects and the radial buffers around turbines has been modified since the 2019 analysis, which has a small effect on the bird densities, so the earlier data has been reanalysed for presentation here).

To check whether the turbine avoidance results for 2021 presented in section 3.7 were influenced by turbine RPM the analysis was run on data subsets grouped using the average RPM for each turbine recorded during the surveys. Each bird observation had the average RPM (recorded during the 10 minute period corresponding to the bird time-stamps in the data) of the closest turbine appended to it.

Histograms for each species (guillemot, puffin, razorbill, kittiwake and herring gull) analysed for each RPM range (<2.5, >=2.5 & <5, >=5 & <7.5, >=7.5) are provided below, grouped by RPM. The results are summarised in section 3.7.

On each figure the vertical red line is the observed density within the relevant distance to turbines and the bars are the results of reanalysis of 1,000 re-runs of the analysis with randomised turbine positions (all turbines moved together to maintain their relative positions). If the red line is in the middle of the bar graph this indicates no difference in the distribution compared with that expected by chance. If the red line is to the left of the peak on the bar graph this indicates lower densities than expected by chance (consistent with avoidance), and if it is to the right this indicates higher densities than expected by chance (consistent with attraction).

RPM 0 – 2.5

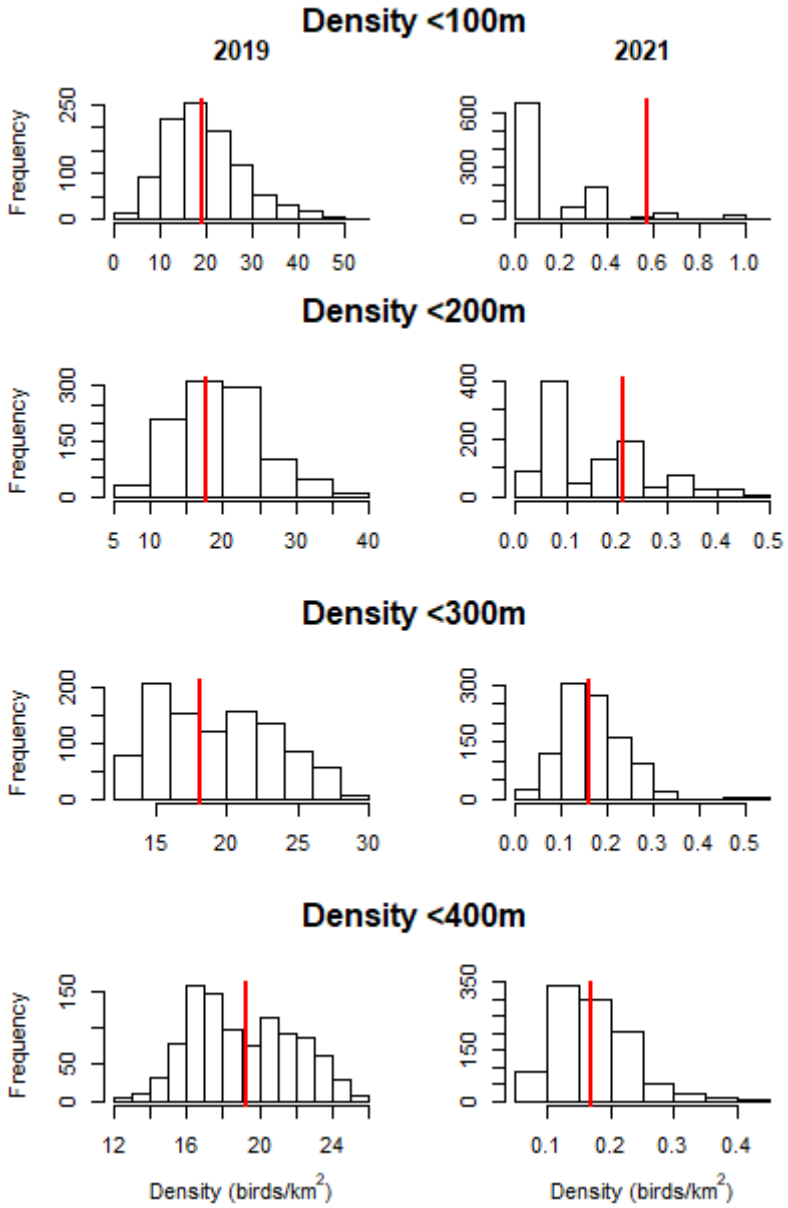

Figure G1. Guillemot densities in 2019 (left) and 2021 (right) within 100/200/300/400m of turbine locations (red lines) and distribution of densities estimated for 1,000 simulations with randomly re-positioned turbines (relative turbine positions maintained) at RPM <2.5.

RPM 0 – 2.5

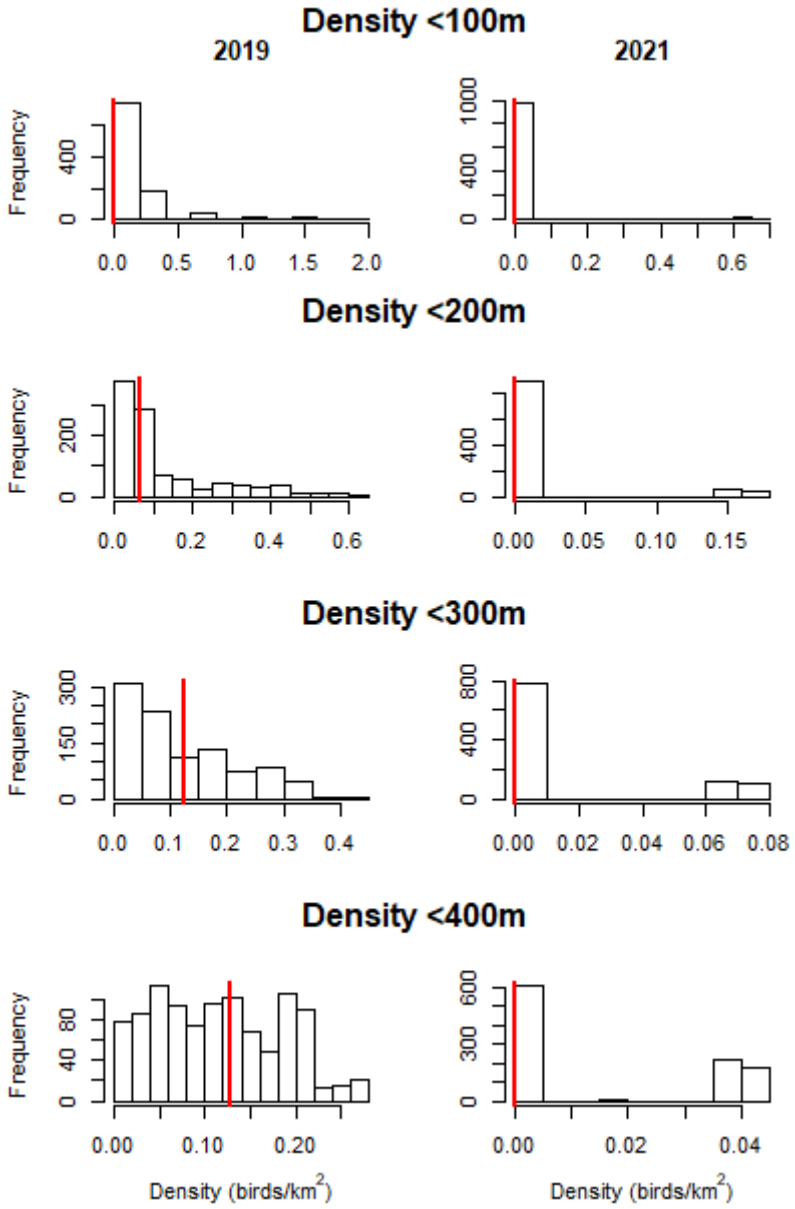

Figure G2. Puffin densities in 2019 (left) and 2021 (right) within 100/200/300/400m of turbine locations (red lines) and distribution of densities estimated for 1,000 simulations with randomly re-positioned turbines (relative turbine positions maintained) at RPM <2.5.

RPM 0 – 2.5

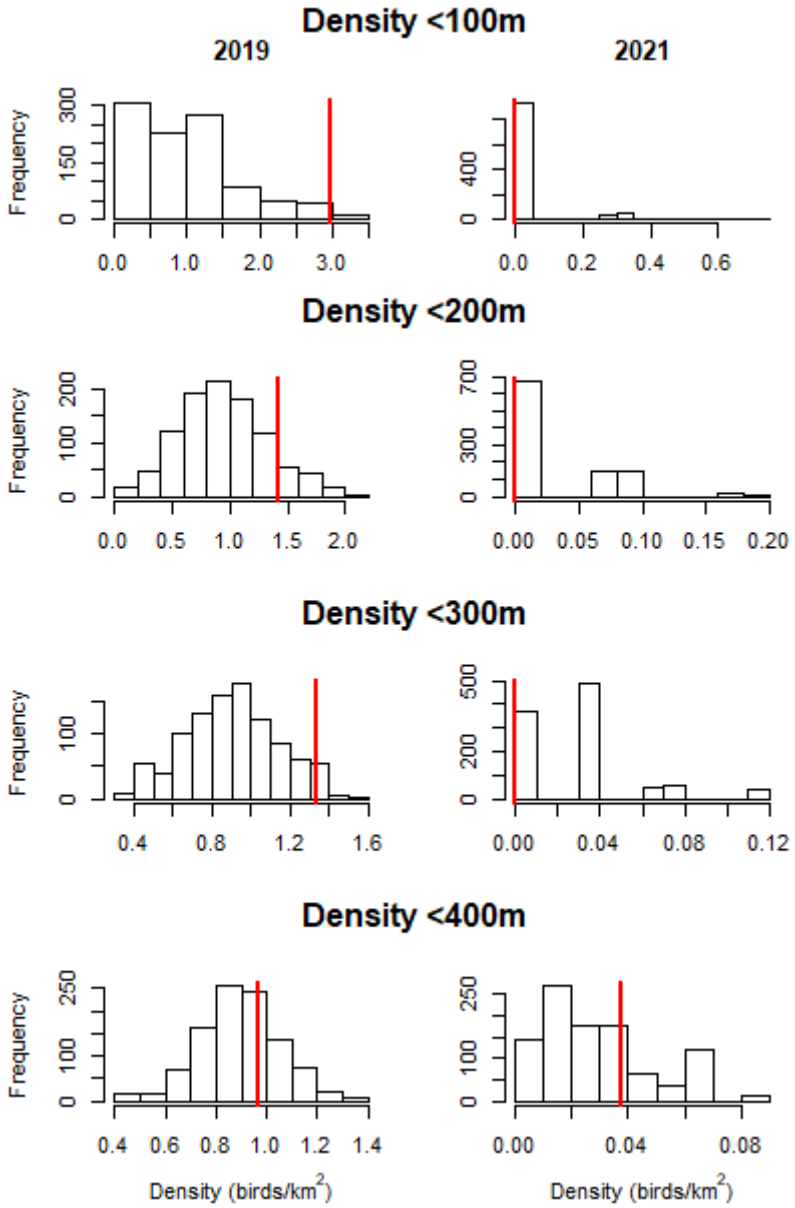

Figure G3. Razorbill densities in 2019 (left) and 2021 (right) within 100/200/300/400m of turbine locations (red lines) and distribution of densities estimated for 1,000 simulations with randomly re-positioned turbines (relative turbine positions maintained) at RPM <2.5.

RPM 0 – 2.5

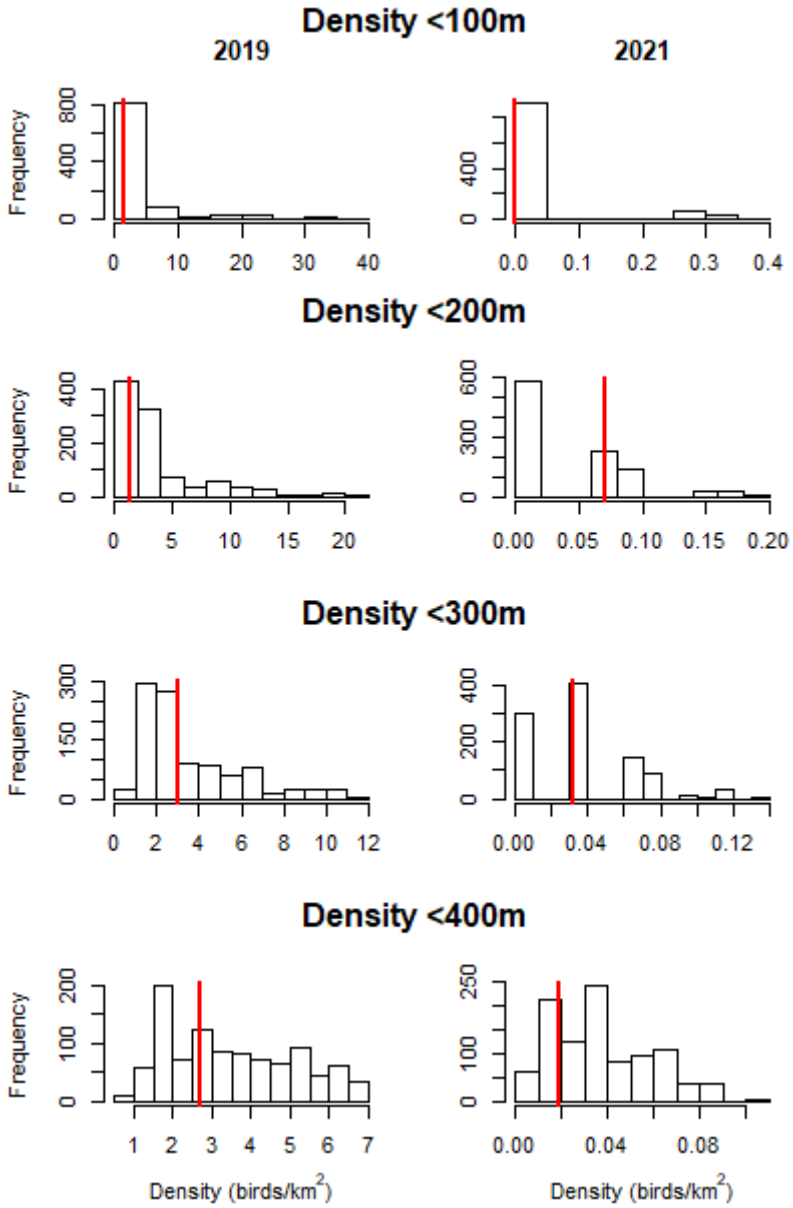

Figure G4. Kittiwake densities in 2019 (left) and 2021 (right) within 100/200/300/400m of turbine locations (red lines) and distribution of densities estimated for 1,000 simulations with randomly re-positioned turbines (relative turbine positions maintained) at RPM <2.5.

RPM 0 – 2.5

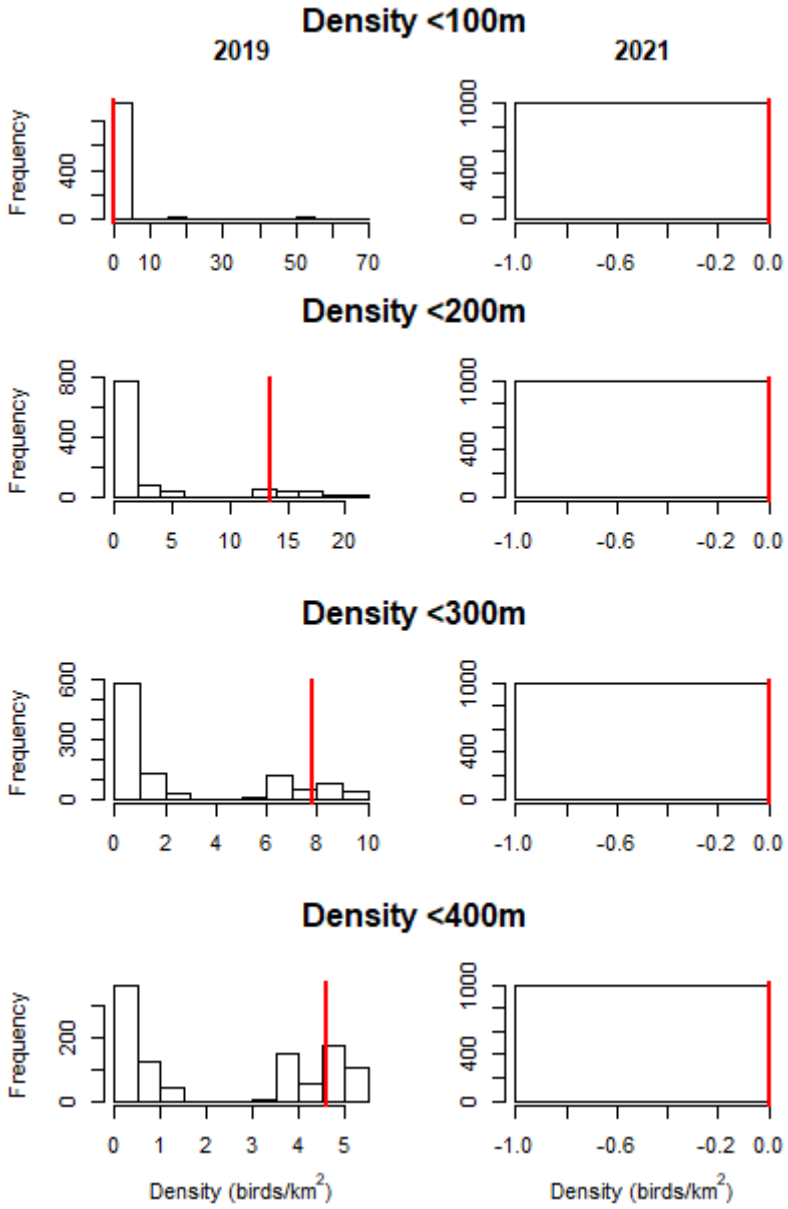

Figure G5. Herring gull densities in 2019 (left) and 2021 (right) within 100/200/300/400m of turbine locations (red lines) and distribution of densities estimated for 1,000 simulations with randomly re-positioned turbines (relative turbine positions maintained) at RPM <2.5 (no herring gull recorded in this data subset in 2021).

RPM 2.5 – 5.0

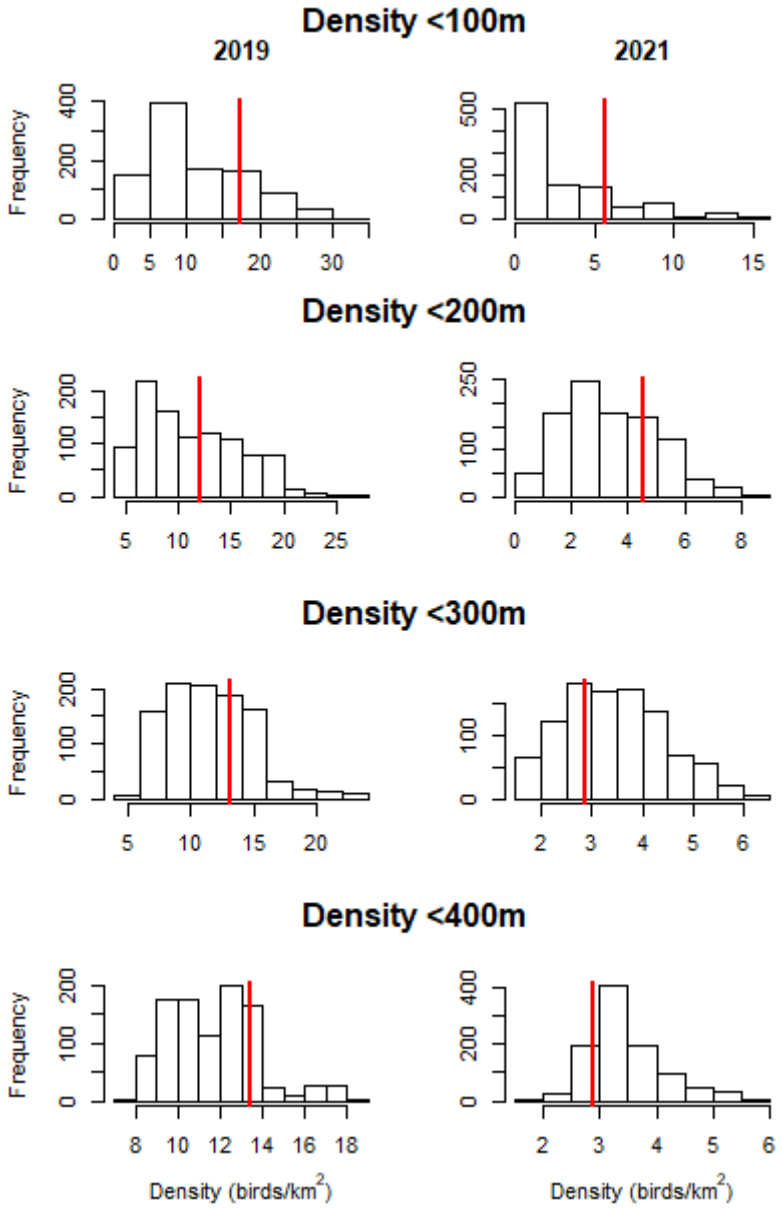

Figure G6. Guillemot densities in 2019 (left) and 2021 (right) within 100/200/300/400m of turbine locations (red lines) and distribution of densities estimated for 1,000 simulations with randomly re-positioned turbines (relative turbine positions maintained) at RPM >=2.5 and <5.0.

RPM 2.5 – 5.0

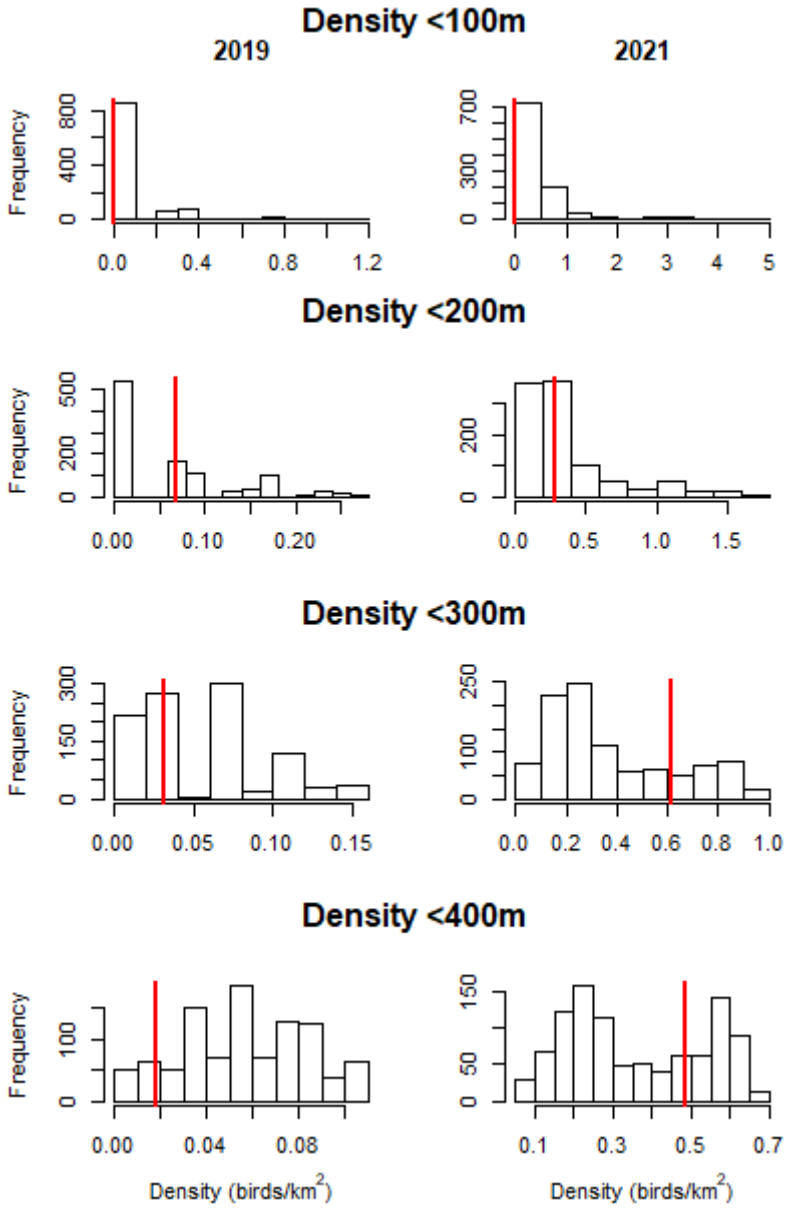

Figure G7. Puffin densities in 2019 (left) and 2021 (right) within 100/200/300/400m of turbine locations (red lines) and distribution of densities estimated for 1,000 simulations with randomly re-positioned turbines (relative turbine positions maintained) at RPM >=2.5 and <5.0.

RPM 2.5 – 5.0

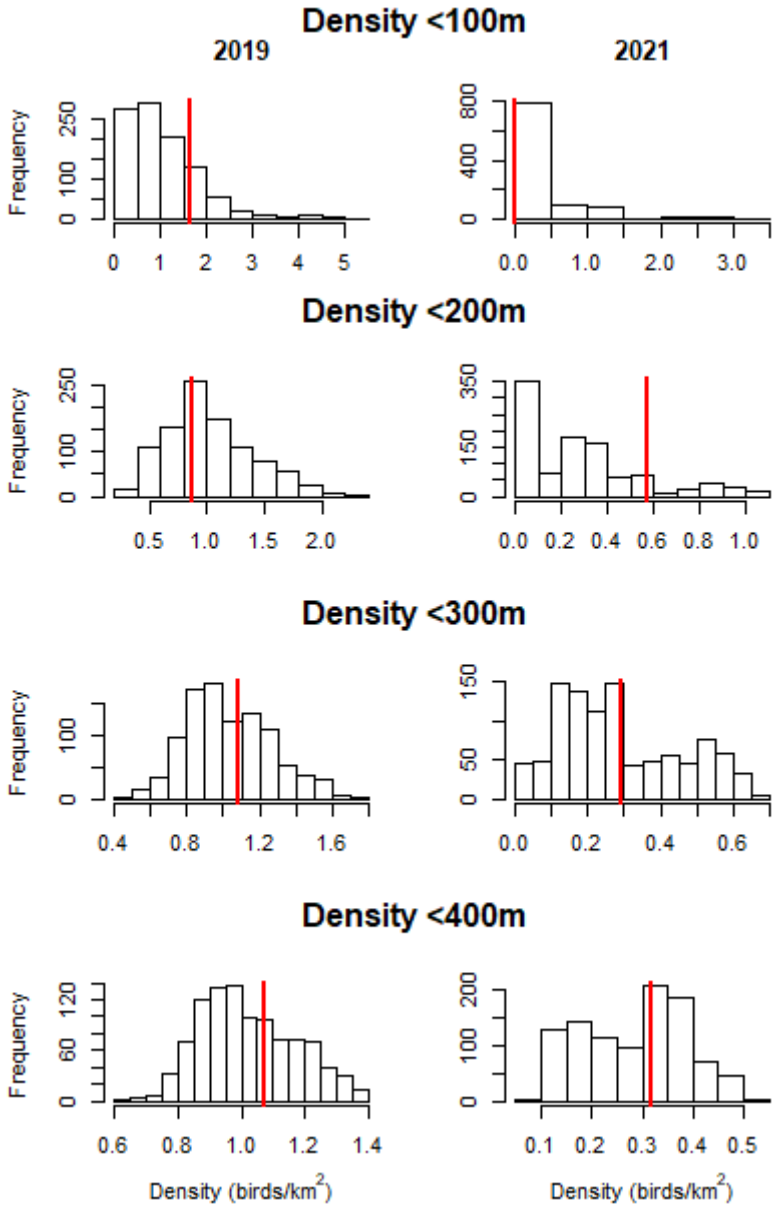

Figure G8. Razorbill densities in 2019 (left) and 2021 (right) within 100/200/300/400m of turbine locations (red lines) and distribution of densities estimated for 1,000 simulations with randomly re-positioned turbines (relative turbine positions maintained) at RPM >=2.5 and <5.0.

RPM 2.5 – 5.0

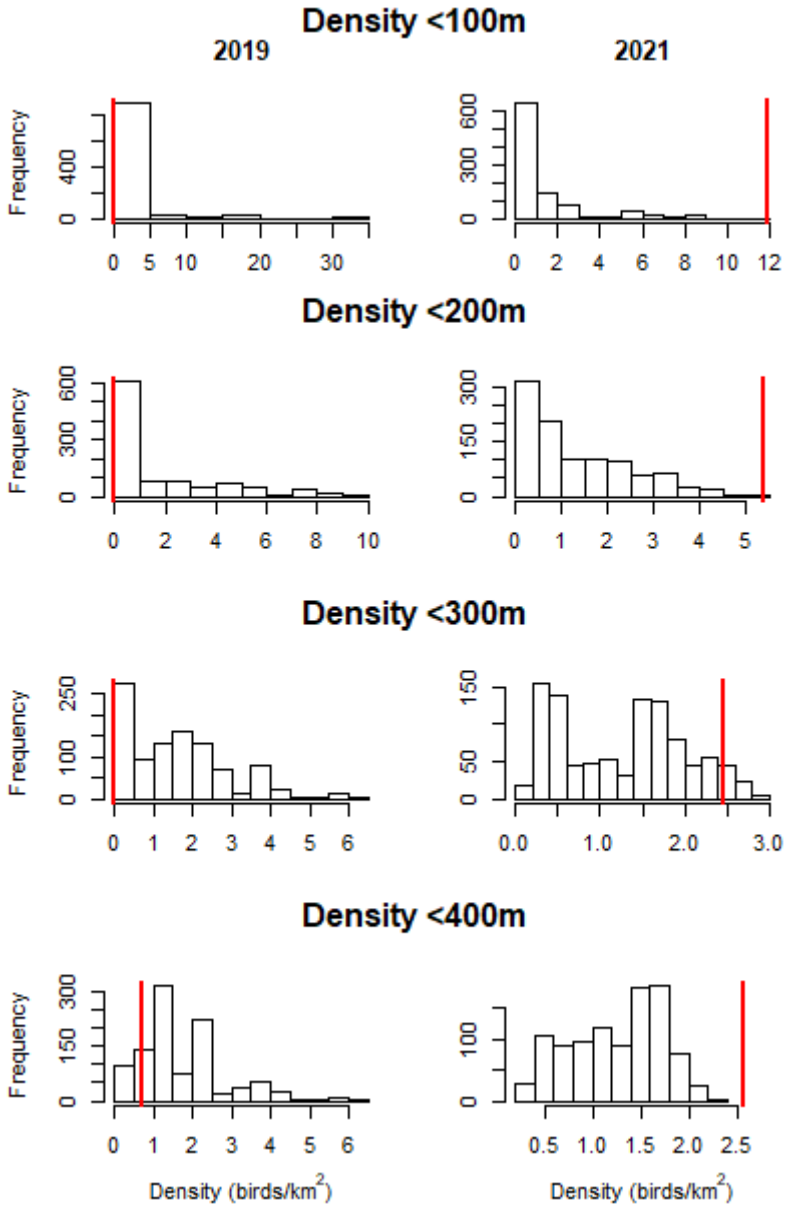

Figure G9. Kittiwake densities in 2019 (left) and 2021 (right) within 100/200/300/400m of turbine locations (red lines) and distribution of densities estimated for 1,000 simulations with randomly re-positioned turbines (relative turbine positions maintained) at RPM >=2.5 and <5.0.

RPM 2.5 – 5.0

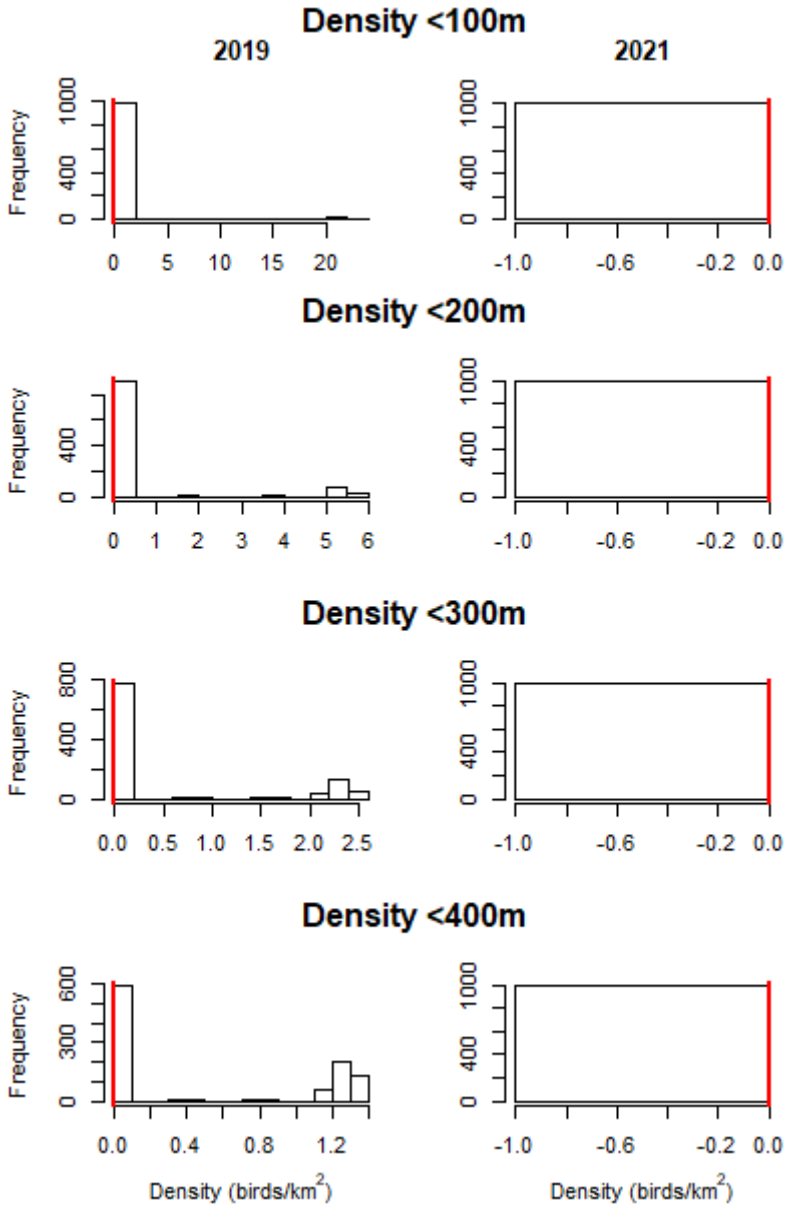

Figure G10. Herring gull densities in 2019 (left) and 2021 (right) within 100/200/300/400m of turbine locations (red lines) and distribution of densities estimated for 1,000 simulations with randomly re-positioned turbines (relative turbine positions maintained) at RPM >=2.5 and <5.0 (no herring gull were recorded in this data subset in 2021).

RPM 5.0 – 7.5

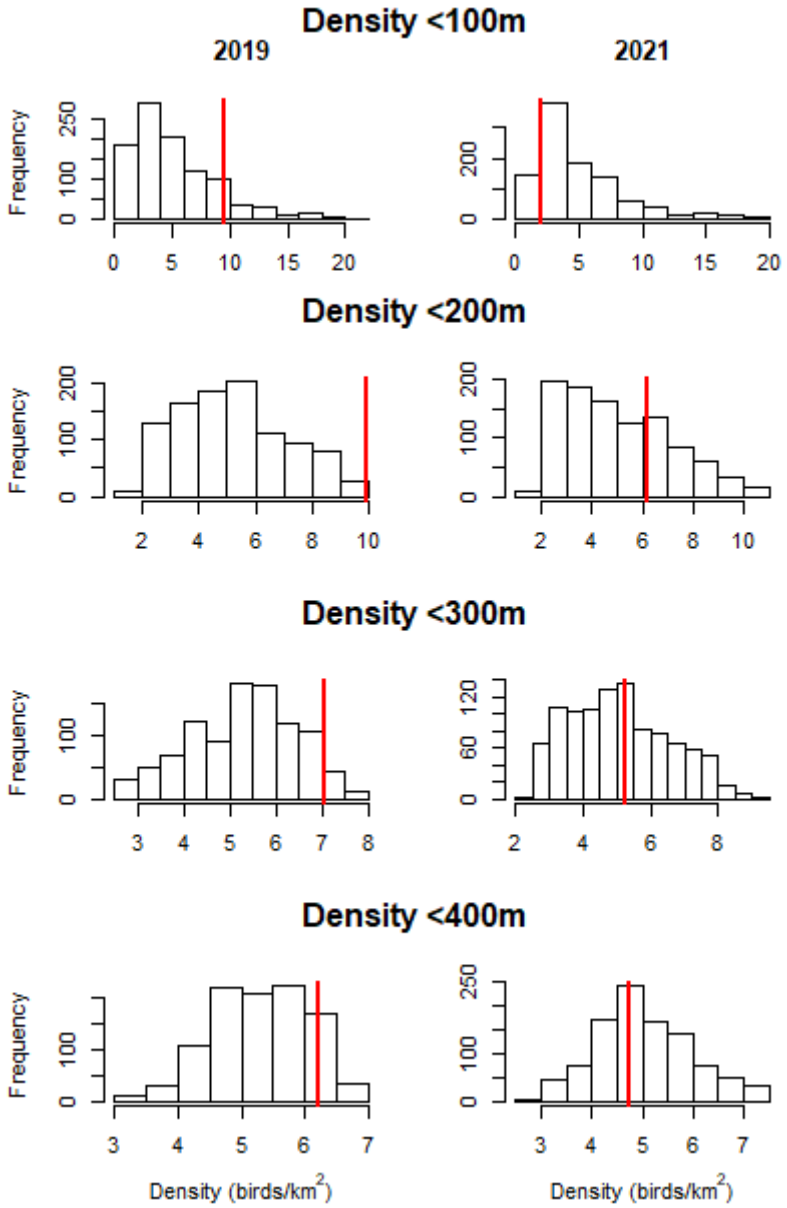

Figure G11. Guillemot densities in 2019 (left) and 2021 (right) within 100/200/300/400m of turbine locations (red lines) and distribution of densities estimated for 1,000 simulations with randomly re-positioned turbines (relative turbine positions maintained) at RPM >=5.0 and <7.5.

RPM 5.0 – 7.5

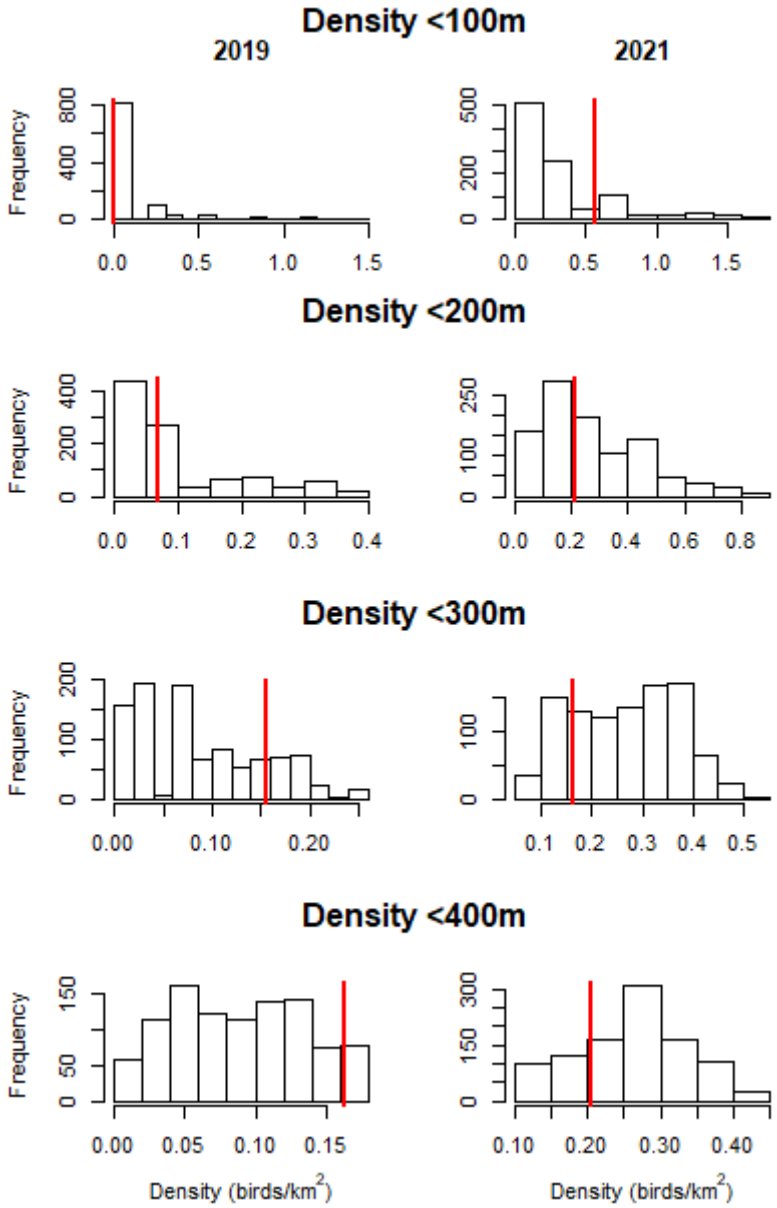

Figure G12. Puffin densities in 2019 (left) and 2021 (right) within 100/200/300/400m of turbine locations (red lines) and distribution of densities estimated for 1,000 simulations with randomly re-positioned turbines (relative turbine positions maintained) at RPM >=5.0 and <7.5.

RPM 5.0 – 7.5

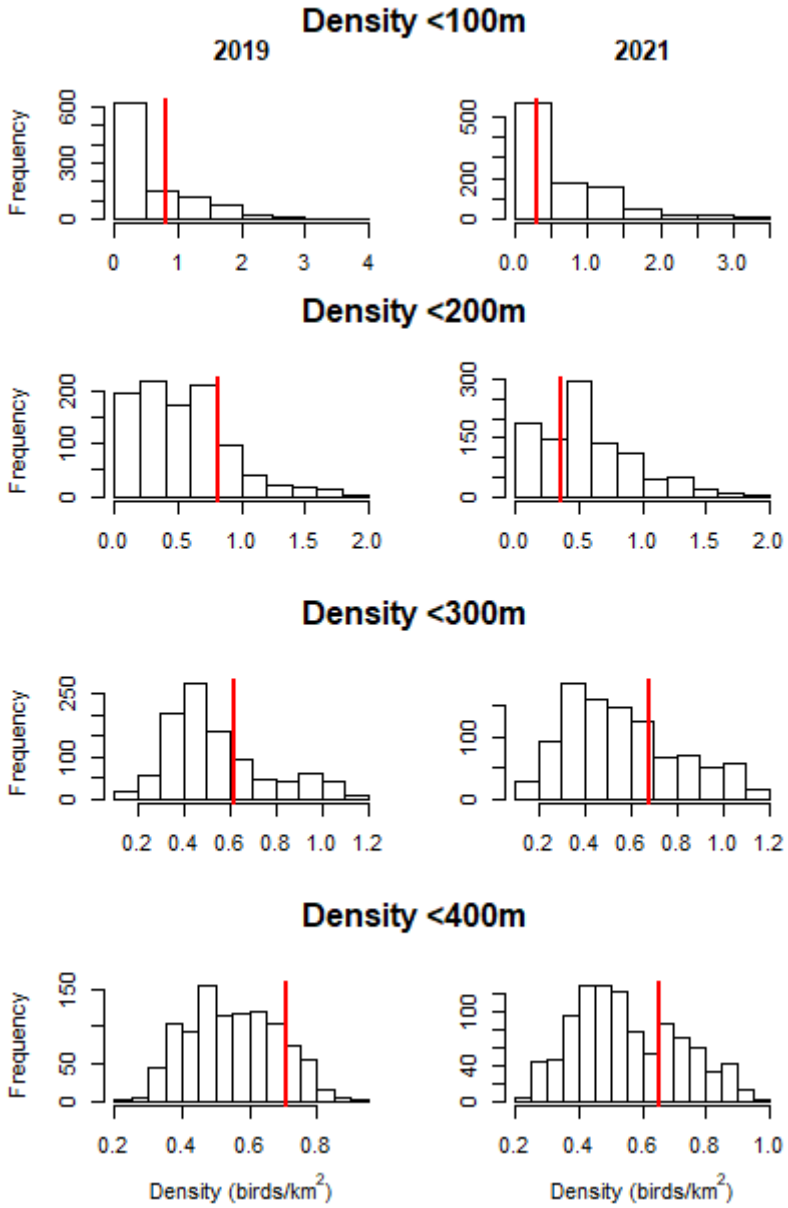

Figure G13. Razorbill densities in 2019 (left) and 2021 (right) within 100/200/300/400m of turbine locations (red lines) and distribution of densities estimated for 1,000 simulations with randomly re-positioned turbines (relative turbine positions maintained) at RPM >=5.0 and <7.5.

RPM 5.0 – 7.5

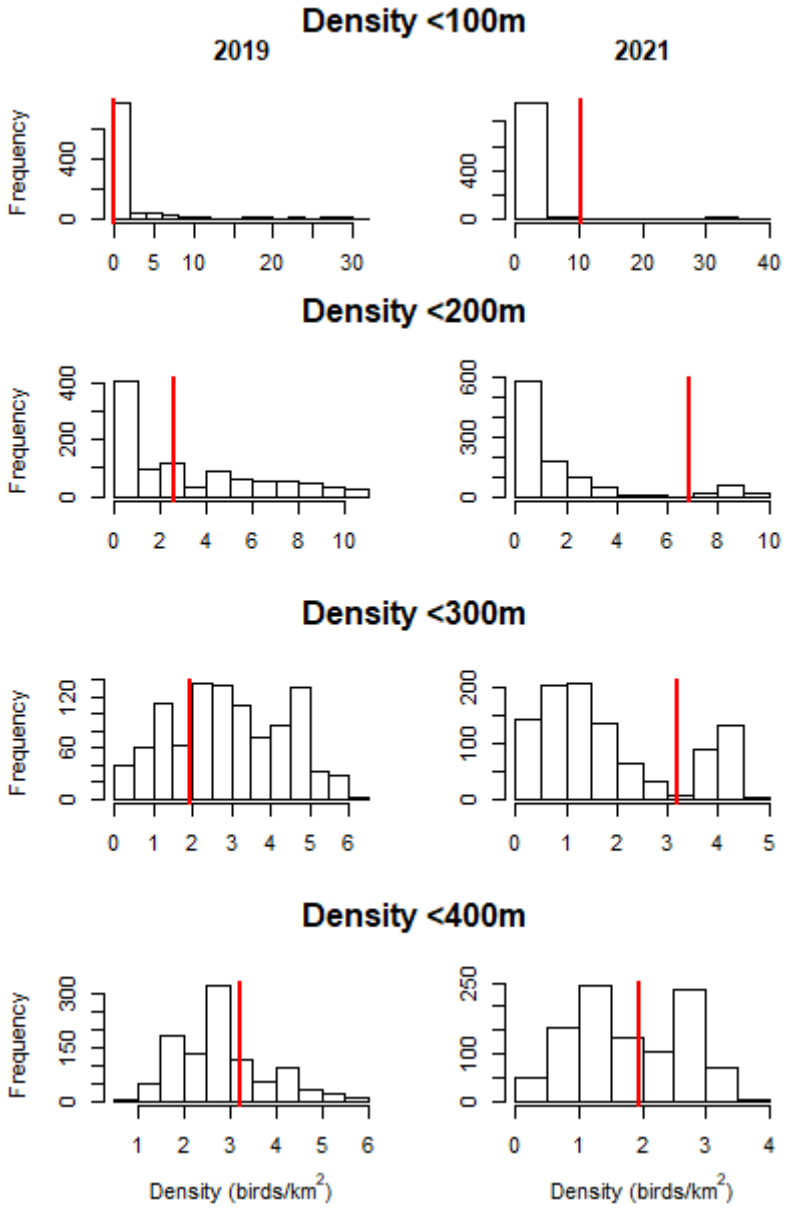

Figure G14. Kittiwake densities in 2019 (left) and 2021 (right) within 100/200/300/400m of turbine locations (red lines) and distribution of densities estimated for 1,000 simulations with randomly re-positioned turbines (relative turbine positions maintained) at RPM >=5.0 and <7.5.

RPM 5.0 – 7.5

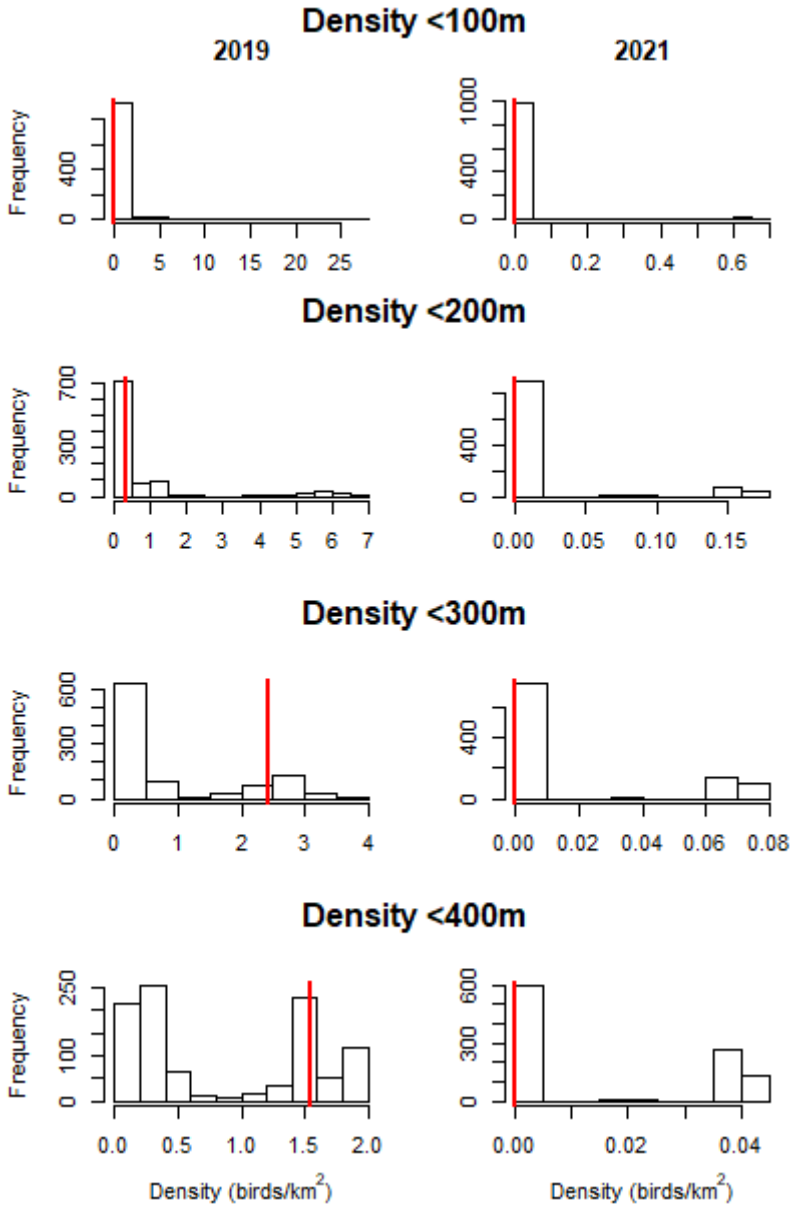

Figure G15. Herring gull densities in 2019 (left) and 2021 (right) within 100/200/300/400m of turbine locations (red lines) and distribution of densities estimated for 1,000 simulations with randomly re-positioned turbines (relative turbine positions maintained) at RPM >=5.0 and <7.5.

RPM 7.5+

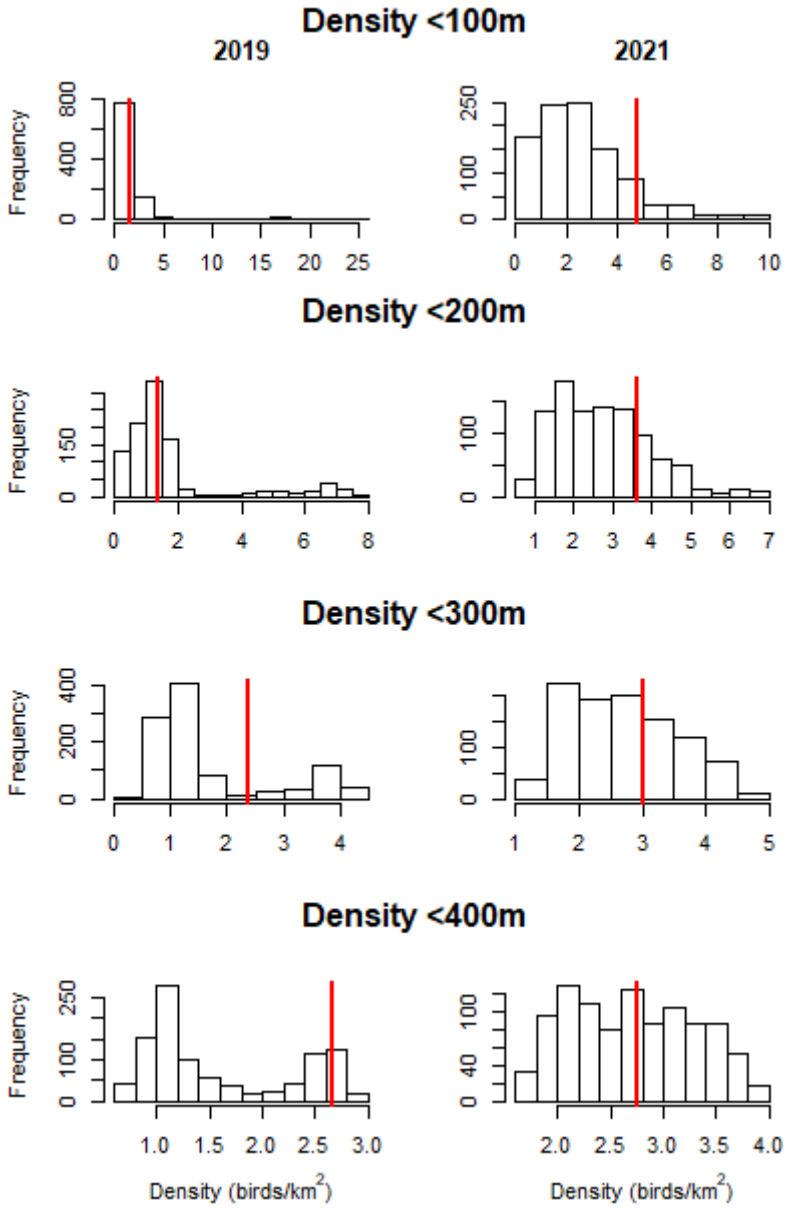

Figure G16. Guillemot densities in 2019 (left) and 2021 (right) within 100/200/300/400m of turbine locations (red lines) and distribution of densities estimated for 1,000 simulations with randomly re-positioned turbines (relative turbine positions maintained) at RPM >=7.5.

RPM 7.5+

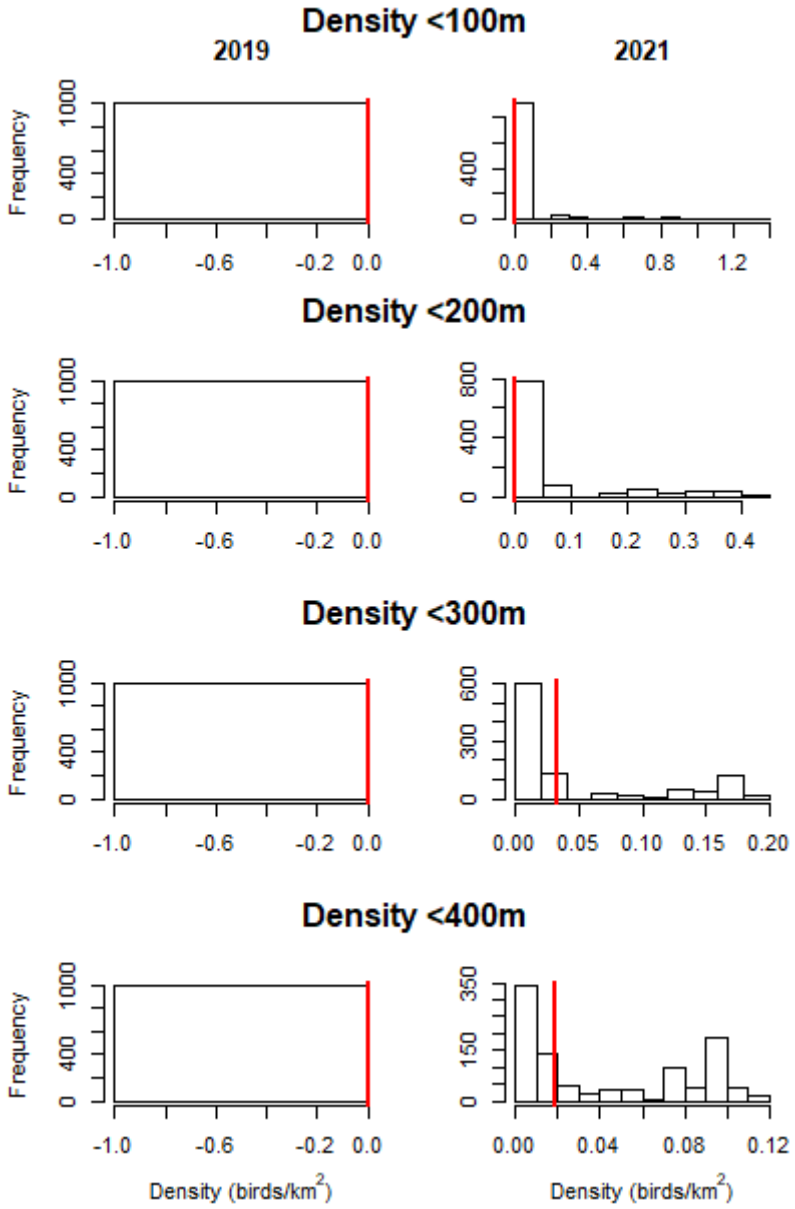

Figure G17. Puffin densities in 2019 (left) and 2021 (right) within 100/200/300/400m of turbine locations (red lines) and distribution of densities estimated for 1,000 simulations with randomly re-positioned turbines (relative turbine positions maintained) at RPM >=7.5 (no puffin records in 2019 in this data subset).

RPM 7.5+

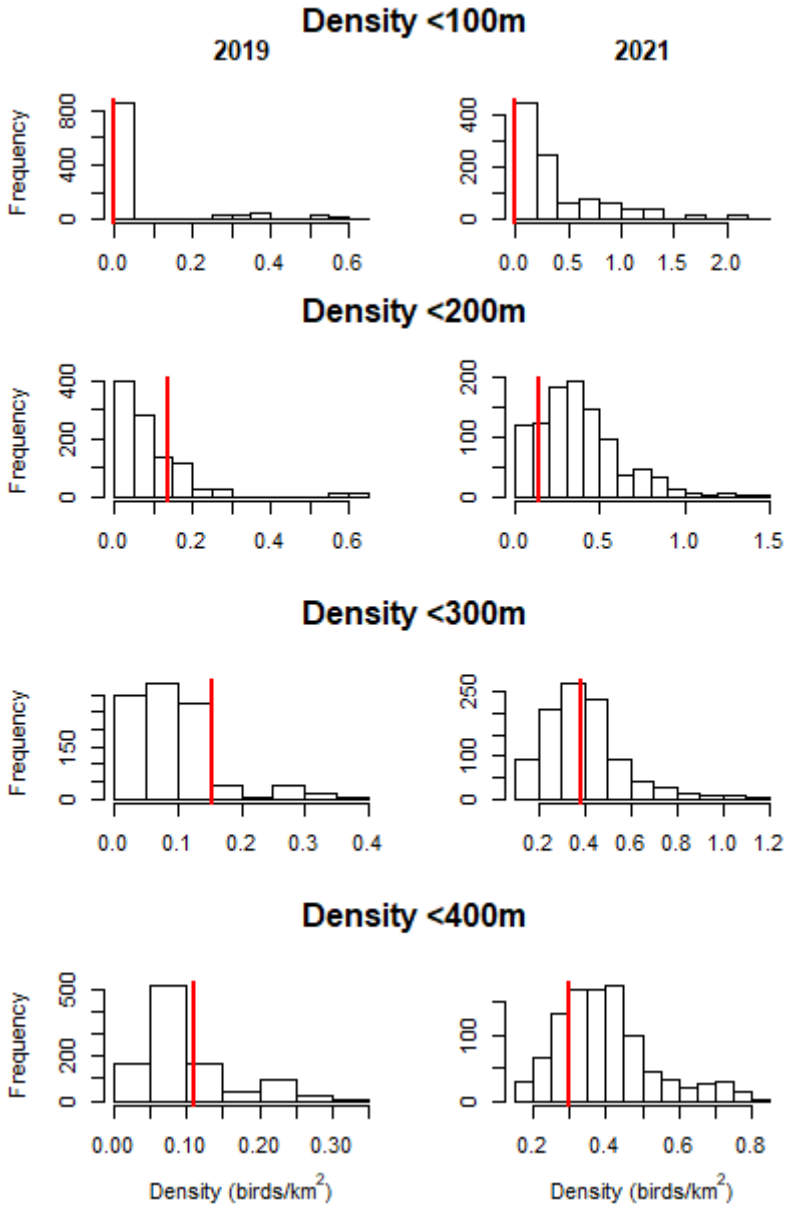

Figure G18. Razorbill densities in 2019 (left) and 2021 (right) within 100/200/300/400m of turbine locations (red lines) and distribution of densities estimated for 1,000 simulations with randomly re-positioned turbines (relative turbine positions maintained) at RPM >=7.5.

RPM 7.5+

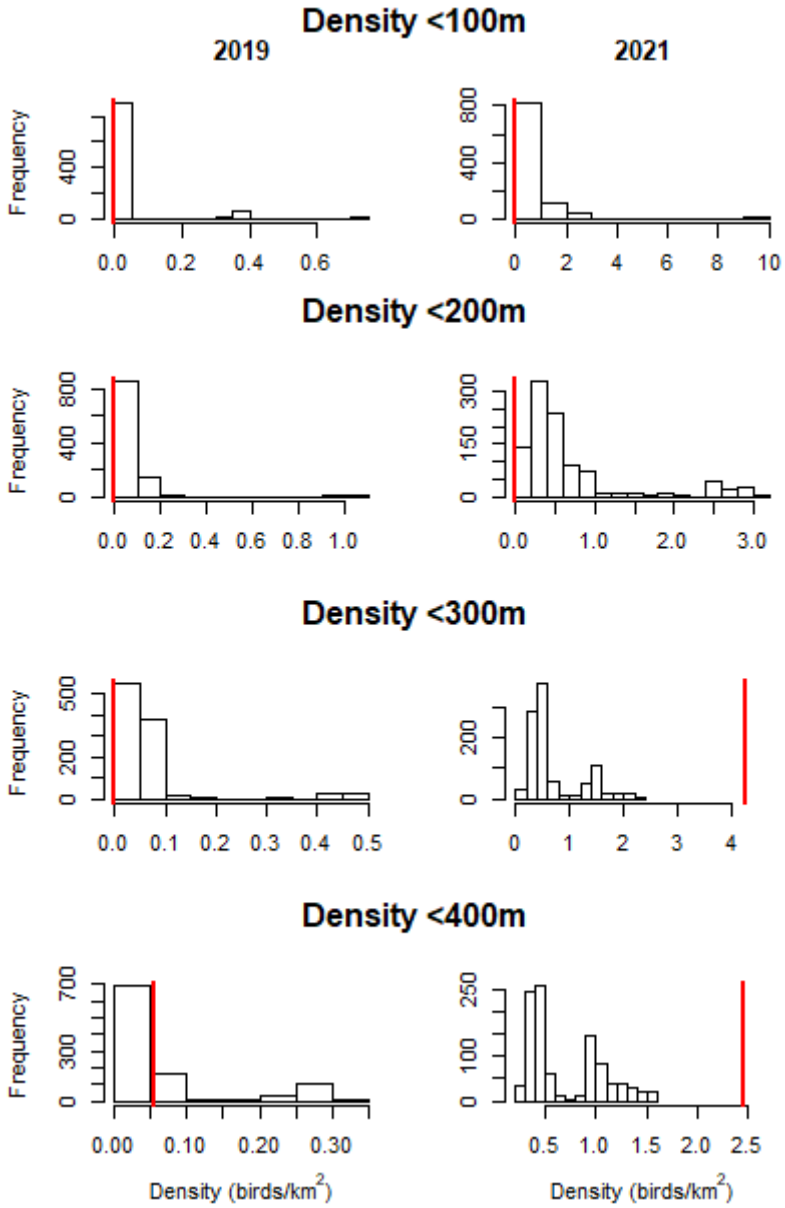

Figure G19. Kittiwake densities in 2019 (left) and 2021 (right) within 100/200/300/400m of turbine locations (red lines) and distribution of densities estimated for 1,000 simulations with randomly re-positioned turbines (relative turbine positions maintained) at RPM >=7.5.

RPM 7.5+

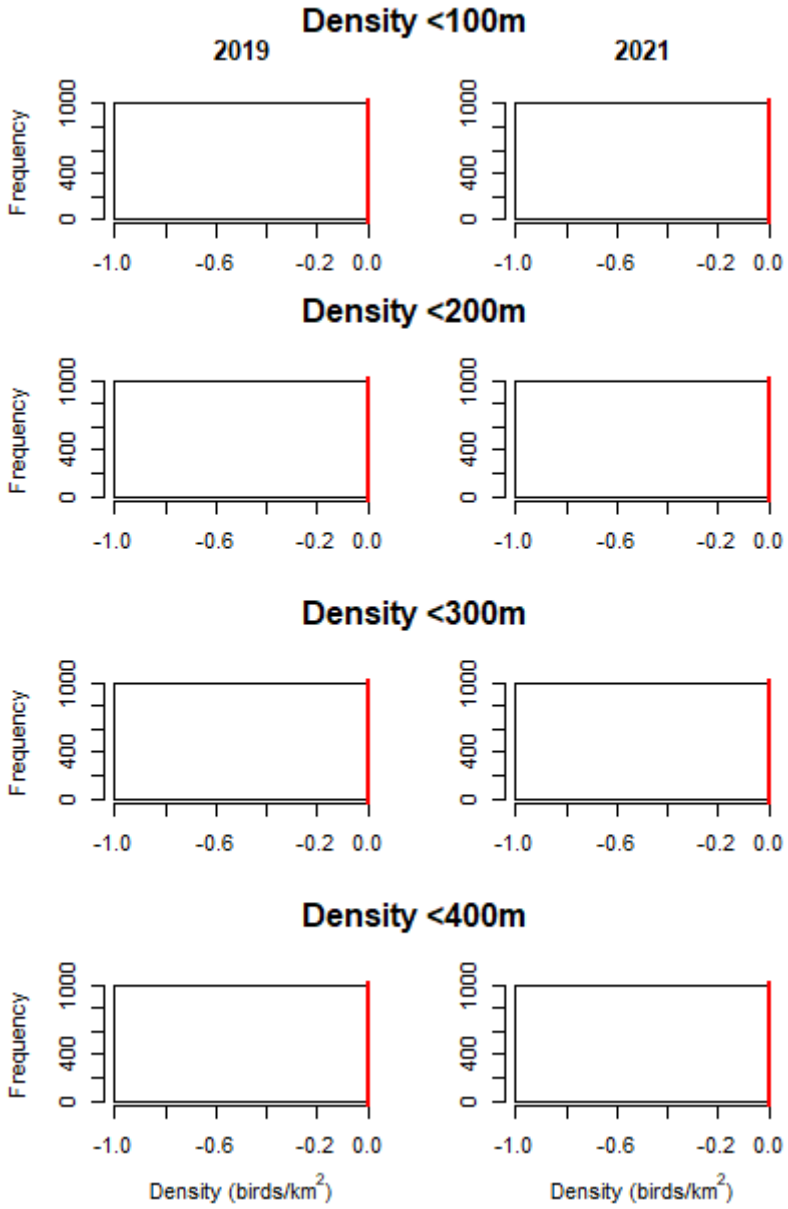

Figure G20. Herring gull densities in 2019 (left) and 2021 (right) within 100/200/300/400m of turbine locations (red lines) and distribution of densities estimated for 1,000 simulations with randomly re-positioned turbines (relative turbine positions maintained) at RPM>=7.5 (no herring gulls were recorded in this data subset in either year).